

Remediation of petroleum-contaminated Antarctic soil

BY

SUSAN HARRIET FERGUSON J.P.

B.App. Sci. – University of Canberra

B Ant. Stud. (Hons) – University of Tasmania

Submitted in fulfilment of the requirements for the Degree of
Doctor of Philosophy

University of Tasmania

November 2004

A thesis submitted in fulfilment of the requirements of Doctor of Philosophy

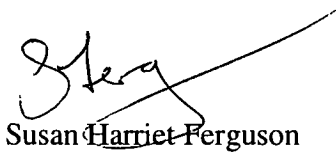
School of Geography and Environmental Studies

University of Tasmania

6 October 2004

Declaration

Except as stated herein, this thesis contains no material which has been accepted for the award of any other degree or diploma in a tertiary institution, and to the best of my knowledge and belief, contains no material previously published or written by another person, except when due reference is made.



Susan Harriet Ferguson

6 October 2004

for

All my wonderful family

**The love and support you have given me has allowed me to create wonderful
dreamsand then make them real
Thank you**

And

The Wombles - if we would only follow their lead

*Underground, overground, wombling free,
The Wombles of Wimbledon Common are we.
Making good use of the things that we find,
Things that the everyday folks leave behind.*

*Uncle Bulgaria,
He can remember the days when he wasn't behind the times,
With his map of the world.
Pick up the papers and take them to Tobermory!*

*Wombles are organised, work as a team.
Wombles are tidy and Wombles are clean.
Underground, overground, wombling free,
The Wombles of Wimbledon Common are we!*

*People don't notice us, they never see,
Under their noses a Womble may be.
We womble by night and we womble by day,
Looking for litter to trundle away.*

*We're so incredibly, utterly devious
Making the most of everything.
Even bottles and tins.
Pick up the pieces and make them into something new,
Is what we do!*

*Underground, overground, wombling free,
The Wombles of Wimbledon Common are we.
Making good use of the things that we find,
Things that the everyday folks leave behind.*

Acknowledgements

Acknowledgement for this study must go to my (cast of thousand) supervisors, Dr. Ian Snape, Dr. Peter Franzmann, Dr. Andrew Revill and Dr. Richard Coleman. As 'The Franzmann' liked to quote "without grit you can have no pearl"...you were all very (extremely) gritty.

During the time that it has taken me to complete this thesis, I've been fortunate to have many wondrous and amazing experience. Among the (too many to name) highlights - the best joy (ah-hem I mean maintenance) helicopter flight on my birthday in Antarctica – oh and all that diamond dust, waiting for a family of Emus on the Nullarbor, drinking warm ale with Jenny and Clare at a poky tavern in Cambridge (The Rat and Parrot), feeding the Archer fish on the Ord River and swimming in the (warm) Southern Ocean at Esperance. For these experiences I want to thank my family, friends and colleagues.

To all of the people who made the work more manageable: Dr. Michael Trefry, Dr. Ben Raymond, Rebecca Esmay, John Rayner, Dr. Steve Fisher, Dr. John Gibson, Andrei Woinarski, Shane Powell and Paul Harvey. The friends that where there even when they didn't quite understand why: Steven Whichelo, Richard Coleman, Shavawn Donoghue, Sandra Hodgson, Peter Deith and Mark Anderson to name just a few

The numerous and various housemates who had to put up with all the highs and lows: Gareth Stephenson, Scott Ayres, Dave Connell, Ben Fowler, Bronwen Butcher, Sean Westbrook, Alison McMorrow, Matt Paget, The Pink Room People and all the people who I "shared" with in Antarctica.

Special thanks to Brett Quinton, who may have joined the team in the final innings but made the last months very enjoyable.

For the cuddles when it was all too much or just because: Meg, Molly, Rama, and Tilda

Many thanks to the Antarctic Division (Kingston), CSIRO (Hobart and Perth) and ANARE for the use of their research facilities and field support in Antarctica. This research could not be completed without support from ASAC Grant No 1163

Thanks to you all

The following people and institutions contributed to the publication of the work undertaken as part of this thesis:

Ferguson, S. H., Franzmann, P. D., Snape, I., Revill, A. T., Trefry, M. G., Zappia, L. R., 2003. Effects of temperature on mineralisation of petroleum in contaminated Antarctic terrestrial sediments. *Chemosphere*. 52(6), 975-987.

Ferguson, S. H., Franzmann, P. D., Revill, A. T., Snape, I., Rayner, J. L., 2003. The effects of nitrogen and water on mineralisation of diesel-contaminated terrestrial Antarctic soils. *Cold Regions Science and Technology*. 37(2), 197-212.

Ferguson, S. H., Woinarski, A. Z., Snape, I., Morris, C. E., Revill, A. T., In Press. A field trial of In Situ Chemical Oxidation (ICO) to remediate long-term diesel contaminated Antarctic soil. *Cold Regions Science and Technology*.

Ferguson, S. H., Powell, S. M., Snape, I., Gibson, J. A. E. Franzmann P.D., Submitted. Effect of temperature on the microbial ecology of a hydrocarbon-contaminated Antarctic soil: Implications for high temperature remediation. *FEMS Microbial Ecology*.

Ferguson S. H., Franzmann P. D., Snape I, Zappia L. R. 2000. Determination of temperature effects on mineralisation of diesel-contaminated Antarctic sediments using ^{14}C -octadecane. 2nd International Conference on Contaminants in Freezing Ground, July 2-5, 2000, Cambridge, UK.

Ferguson S. H., Revill A. T., Snape I, Franzmann P. D. 2002. Comparison of microbial mineralisation of petroleum hydrocarbons in Antarctic sediments by radiometric experiments and gas chromatography. Proceedings of the Australian Organic Geochemistry Conference. 12-15 February 2002, Hobart, Australia.

Ferguson S. H., Franzmann P. D., Snape I, Revill A. T., Zappia LR. 2002. The effect of nutrients and water availability on mineralisation of diesel-contaminated Antarctic sediments as determined by ^{14}C -octadecane microcosm experiments. Proceedings of the 3rd International Conference on Contaminants in Freezing Ground, 14-18 April 2002, Hobart, Australia.

Snape, I., Ferguson, S. H., Harvey, P., Revill, A. T., Submitted. Chemical constraints on natural attenuation of fuel spills at Casey Station, Antarctica. *Chemosphere*.

Snape, I., Ferguson, S. H., Revill, A. T., 2003. Constraints on rates of natural attenuation and *in situ* bioremediation of petroleum spills in Antarctica. In: Nahir, M., Bigger, K. Cotta, G (Eds.) *Assessment and remediation of contaminated sites in Arctic and cold climates (ARCSACC)* Edmonton, Canada, May 4-6.

Snape I, Ferguson S. H., Cole C. M., Morris C. E., Revill A. T. 2000. *In situ* bioremediation as a management strategy for petroleum-contaminated sediments in Antarctica. 2nd International Conference on Contaminants in Freezing Ground, July 2-5, 2000, Cambridge, UK.

Snape I, Ferguson S. H., Franzmann P. D., Morris C. E., Revill A. T. 2000. Contaminants in the Antarctic Environment VII: Remediation of petroleum hydrocarbons. In: Hughson T., Ruckstuhl C. (Eds.). *Proceedings of the 6th International Symposium on Cold Region Development (ISCORD)*: 148-150.

- I. Snape, P. Franzmann and A. Revill assisted with guidance and general supervision in all aspects of producing publishable quality manuscripts
- Molecular biology (DGGE and 16S rRNA gene sequencing) by S. Powell
- J. Gibson assisted in phospholipid interpretation and re-analysis of isolate signatures
- Soil nitrogen and phosphorous concentrations conducted by CSL laboratories.
- Soil pH was measured by A. Woinarski
- Three half order modelling performed by M. Trefry
- L. Zappia offered general and radiometric laboratory assistance
- Field implementation experimental design and field sampling (ICO) by C. Morris and A. Woinarski
- NMR analysis and evaporation experiment of SAB performed by P. Harvey

We the undersigned agree with the above stated “proportion of work undertaken” for each of the above published (or submitted) peer-reviewed manuscripts contributing to this thesis:

I Snape	
P. D. Franzmann	
A. T. Revill	
C. E. Morris	
L. R. Zappia	
M. G. Trefry	
J. L. Rayner	
S. M. Powell	
J. A. E. Gibson	
A. Z. Woinarski	
P. Harvey	

Abstract

Remediation of petroleum hydrocarbons in polar environments is more costly and logistically and technically more difficult than corresponding temperate and tropical contaminated sites. Bioremediation and *in-situ* chemical oxidation (ICO) are possible strategies which may overcome the financial and technical challenges associated with polar-region site remediation. ICO involves introducing reactive chemicals to contaminated soils so that organic contaminants such as petroleum hydrocarbons are oxidised to environmentally innocuous compounds, while bioremediation relies on microbial activity to achieve this.

At Old Casey Station, East Antarctica (66°17'S, 110°32'E) more than 20 000 L of Special Antarctic Blend (SAB) diesel fuel was spilt over 15 years ago. Concentrations in the spill zone are still about 20 000 ppm and the rates of natural attenuation are relatively slow. The application of oxidative chemicals to the site did not significantly reduce petroleum hydrocarbon concentrations and would likely hinder biodegradation through the destruction of the subsurface microbial communities to below the level of detection for over 2 years. Bioremediation is considered the only likely viable alternative to natural attenuation or dig-and-haul procedures.

The factors which were suspected of limiting microbial degradation of petroleum contaminants were temperature, nutrients and water availability. Their potential limitations were investigated with a series of radiometric treatability (microcosm) studies. A positive correlation between temperatures (between -2 and 42°C) and the rate of ¹⁴C-octadecane mineralisation was found. The high rate of mineralisation at 37 and 42°C was surprising, as most continental Antarctic microorganisms have an optimal temperature between 20 and 30°C and a maximal growth temperature of less than 37°C.

^{14}C -octadecane mineralisation at nine different inorganic nitrogen concentrations (ranging from 85 to over 27 000 mg N kg-soil- H_2O^{-1}) was monitored. Total mineralisation increased with increasing nutrient concentration peaking in the range 1000-1600 mg N kg-soil- H_2O^{-1} . Higher N concentrations reduced the rate of mineralisation, highlighting the importance of avoiding over-fertilisation. Gas chromatographic analysis of the aliphatic components of the SAB diesel in the contaminated soil showed good agreement with the radiometric microcosm outcomes. Ratios of $n\text{-C}_{17}$: pristane and $n\text{-C}_{18}$: phytane indicated that low nutrient concentrations rather than water were the main limiting factor for biodegradation of hydrocarbons in the soil collected from Old Casey Station when incubated at 10°C . The high rate of mineralisation at 42°C and the microbial population dynamics were also investigated in a series of non-radiometric microcosm studies. Denaturing gradient gel electrophoresis of nutrient-amended contaminated soil after 40 days incubation at 4, 10 and 42°C indicated significant differences between the microbial communities at each of the incubation temperatures. 16S rRNA gene sequences and fatty acid methyl ester analysis indicate that the dominant hydrocarbon degrading bacteria at 4 and 10°C are *Pseudomonas spp.*, while *Paenibacillus spp.* are likely to be the dominant hydrocarbon degrading bacteria at 42°C . The main implication for bioremediation in Antarctica from this study is that a high-temperature treatment would yield the most rapid biodegradation of the contaminant. *In situ* biodegradation using nutrients and other amendments is still possible at soil temperatures that occur naturally during summer in Antarctica. However, because the soils from this site are characterised by low water holding capacities, it would be difficult to maintain optimal nutrient concentrations during full scale

treatment, and thus the use of a controlled release nutrient should be considered for full scale remediation of petroleum contaminated soil in Antarctica.

Table of Contents

Acknowledgements	v
Abstract	viii
List of Tables, Figures and Equations	xvi
Acronyms	xxvii
Chapter 1 Petroleum products in Antarctica	1
1.1 Introduction	1
1.2 History of petroleum spills in Antarctica	2
1.3 Old Casey Station and surrounds	3
1.4 Physical characterisation of the Casey region	5
1.5 The Old Casey petroleum plume	6
1.6 Objectives and thesis outline	7
Chapter 2 Characterisation of the petroleum hydrocarbon contaminants at Old Casey Station	11
2.1 Introduction	11
2.2 Petroleum products at Australian Antarctic Stations	12
2.3 Precedence for use of diagnostic ratios	18
2.3.1 Source identification	19
2.3.2 Biodegradation	19
2.3.3 Abiotic weathering	20
2.4 Source signatures of fuels at Old Casey Station	20
2.5 Experimental verification of diagnostic ratios in SAB; effect of abiotic weathering	21
2.5.1 Theoretical weathering model	22

2.5.2	Empirical determination of the effect of evaporation on diagnostic ratios	22
2.5.3	Conclusions	27
2.6	Experimental verification of diagnostic ratios in SAB; effect of biological mineralisation	27
2.6.1	Introduction	27
2.6.2	Methods	28
2.6.3	Results and discussion	29
2.6.4	Conclusions	34
2.7	Application of diagnostic ratios	35
2.7.1	The use of diagnostic ratios in treatability studies	37
2.7.2	The use of diagnostic ratios at Old Casey Station	37
2.7.3	Limitations	39
2.8	Conclusions	41
Chapter 3 Effects of temperature on the mineralisation of petroleum-hydrocarbons ..		42
3.1	Introduction	42
3.2	Methods	43
3.2.1	Temperature regime of Old Casey Station	43
3.2.2	Soils, contaminants and microorganisms	44
3.2.3	Microcosm preparations	44
3.2.4	Hydrocarbon analysis of the soil	47
3.3	Results and discussion	48
3.3.1	Soil thermal regime at Old Casey Station	48
3.3.2	Mineralisation of the ¹⁴ C-octadecane	49

3.3.3	Post incubation analysis	53
3.4	Conclusions	55
Chapter 4 The effects of nitrogen and water on the mineralisation of petroleum-hydrocarbons		
		57
4.1	Introduction	57
4.2	Methods	60
4.2.1	Rationale	60
4.2.2	Site characterization	62
4.2.3	Hydraulic properties of the soil	63
4.2.4	Microcosm preparation	64
4.2.5	Hydrocarbon analysis of the soil	65
4.3	Results	66
4.3.1	Control microcosms	66
4.3.2	Repeat microcosm experiment using soil I after 2 years storage	69
4.3.3	Differences between soil I and soil II	70
4.3.4	Unamended soil	71
4.3.5	Water amended treatments with constant nutrient-soil ratio	71
4.3.6	Nutrient amended treatments with constant water-soil ratio	72
4.4	Discussion	73
4.4.1	Nutrients, water and biodegradation	73
4.4.2	Strengths and weaknesses of the microcosm approach to site assessment	74
4.4.3	Implication for nutrient amended remediation at Old Casey Station ...	76
4.5	Conclusions	79

Chapter 5 Numerical modelling of ^{14}C mineralisation data.....	82
5.1 Introduction.....	82
5.1.1 Microbial kinetic rate equations.....	82
5.1.2 Temperature- dependent rate models	85
5.2 Results and discussion	87
5.2.1 Modelling the effect of temperature on microbial mineralisation of ^{14}C -octadecane	87
5.2.2 Modelling the effect of nitrogen and water on microbial mineralisation of ^{14}C -octadecane	99
5.3 Conclusion	100
Chapter 6 Effect of temperature on the soil microbial ecology: implications of high-temperature remediation	102
6.1 Introduction.....	102
6.2 Methods.....	105
6.2.1 Site history, contaminants, experimental rationale and set-up.....	105
6.2.2 Hydrocarbon analysis.....	106
6.2.3 Microbial population enumeration and isolation	107
6.2.4 Soil microbial community composition	108
6.2.5 Identification of hydrocarbon degrading isolates.....	108
6.2.6 Extraction and identification of fatty acids from pure cultures.....	109
6.3 Results and discussion	111
6.3.1 Hydrocarbon concentrations throughout the experiment.....	111
6.3.2 Bacterial abundance	113
6.3.3 Microbial community structure.....	115

6.3.4	Dominant hydrocarbon degrading isolates.....	119
6.3.5	Implications.....	124
6.4	Conclusions.....	126
Chapter 7 <i>In situ</i> Chemical Oxidation (ICO)		128
7.1	Introduction.....	128
7.2	Materials and methods	132
7.2.1	Field trials	132
7.2.2	Chemical analysis.....	135
7.2.3	Microbial measurements	136
7.3	Results.....	136
7.3.1	Open plot small-scale field trial	136
7.3.2	Semi-enclosed box-plot.....	140
7.4	Discussion	143
7.4.1	Chemical penetration and subsurface transport	143
7.4.2	Limitations and implication of ICO treatment of hydrocarbon contaminated soil in polar-regions	145
7.5	Conclusions.....	148
Chapter 8 Conclusions		150
Chapter 9 References		155
Chapter 10 Appendix		173
10.1	Structure of several hydrocarbons present in SAB or used as standards ...	173
10.2	Chemical composition of SAB – historical data	174
10.3	Soil temperature profiles from Old Casey Station	175

List of Tables, Figures and Equations

Table 2.1 U.S. Environmental Protection Agency (EPA) test methods for determining petroleum hydrocarbons (reproduced from Anon, 1997). Numbers refer to EPA method numbers. Several types of analyses do not have established water/wastewater methods (n/a – not available).	12
Table 2.2 Resolved components of the diesel-ranged fuels commonly used by the Australian Antarctic Program.	16
Table 2.3 Summary of diagnostic ratios (source, biodegradation and abiotic) as outlined in Sections 2.3.1 – 2.3.3 for the fuels shown in the reference chromatograms (Figure 2.3) of the petroleum products used within the Casey region. Isoprenoid pristane and phytane are abbreviated to pr and ph respectively.....	21
Table 2.4 Summary of the diagnostic ratios in Sections 2.3.1 – 2.3.3 for SAB as it is lost through evaporation at -20°C. Isoprenoid pristane and phytane abbreviated as pr and ph respectively. Light <i>n</i> -alkanes: heavy <i>n</i> -alkanes represents the sum of <i>n</i> -alkanes between <i>n</i> -C ₉ – <i>n</i> -C ₁₈ : sum of <i>n</i> -C ₁₇ and <i>n</i> -C ₁₈	25
Table 2.5 Summary of diagnostic ratios in Sections 2.3.1 – 2.3.3 for SAB as it is lost through biodegradation at 4°C. Isoprenoid pristane and phytane abbreviated as pr and ph respectively. Light <i>n</i> -alkanes: heavy <i>n</i> -alkanes represents the sum of <i>n</i> -alkanes between <i>n</i> -C ₉ – <i>n</i> -C ₁₈ : sum of <i>n</i> -C ₁₇ and <i>n</i> -C ₁₈ as there was insignificant quantities of fuel components with ECNs > 18.5 in the neat SAB.....	34
Table 2.6 Summary of diagnostic ratios in Sections 2.3.1 – 2.3.3 for neat SAB and the petroleum hydrocarbon contamination at Old Casey Station. Light <i>n</i> -alkanes: heavy <i>n</i> -alkanes represents the sum of <i>n</i> -alkanes between <i>n</i> -C ₉ – <i>n</i> -C ₂₃ : sum of <i>n</i> -C ₁₇ – <i>n</i> -C ₂₃ . Error bars (1s) are shown for the field samples (n=6).....	39

Table 3.1 Hourly averaged <i>in situ</i> soil temperatures during summer at Old Casey station, Antarctica at two sites, a relatively dry and wet site. Maximum and minimum temperatures represent the hourly averaged temperatures.	49
Table 4.1 Microcosm conditions used to test the effects of water and nutrient additions on the mineralisation of ¹⁴ C-octadecane and degradation of the aliphatic components of SAB at 10°C. Nitrogen concentration was estimated by summing natural and added N. The C:N ratio was calculated from an initial hydrocarbon concentration of 15 000 ppm. Repeat microcosm data are from Chapter 3; A sub-sample of soil I was incubated as part of the previous study for 45 days and a different sub sample was incubated as part of these experiments for 95 days. Treatments indicated with an asterisk are shown twice on the table.	62
Table 4.2 Gas chromatography results for pre and post incubation (95 days at 10°C) microcosm soils. Soil I did not contain squalane and thus these indices can not be calculated. Results are the average values and 1s of replicates shown in Table 4.1. Isoprenoids are abbreviated as pristane, pr; phytane, ph and squalane, sq.	67
Table 4.3 First order mineralisation rate half-lives T _{1/2} , and zeroth order mineralisation rates of ¹⁴ C-octadecane to ¹⁴ CO ₂ in soil microcosms at different N loadings between the time intervals indicated. The lag was estimated from the time delay required for the best-fit zeroth order function. The microcosms indicated by an asterisk did not exhibit a plateau phase of ¹⁴ C-octadecane mineralisation. At these concentrations, first order rates were calculated as the average time for the evolution from 10 % to 100 % of the total ¹⁴ CO ₂	69
Table 5.1 Results of nonlinear regressions on the production curves for different temperatures, with ideal linear microbial growth ($\lambda = 0$) and non-ideal (Gaussian)	

mineralisation. S_0 and the root-mean-square regression residual R are expressed in units of $\text{mg } ^{14}\text{C-octadecane}/(\text{kg soil})$ converted to $^{14}\text{CO}_2$, k_0 in units of $\text{mmol } ^{14}\text{C-octadecane}/(\text{g soil})/\text{day}$, k_2 in units of d^{-2} , and v in units of days. Confidence intervals are expressed at the 95% level.	92
Table 5.2 Results of non-linear regressions on the production curves for different temperatures, with ideal exponential microbial growth ($\lambda = 0$) and non-ideal (Gaussian) mineralisation. S_0 and the root-mean-square regression residual R are expressed in units of $\text{mg } ^{14}\text{C-octadecane}/(\text{kg soil})$ converted to $^{14}\text{CO}_2$, k_0 in units of $\text{mmol } ^{14}\text{C-octadecane}/(\text{g soil})/\text{day}$, E_0 and μ in units of d^{-1} , and v in units of days. Confidence intervals are expressed at the 95% level. ^a Estimated value.	93
Table 5.3 Temperature dependence of the total $^{14}\text{CO}_2$ production from the highly bioavailable fraction.....	98
Table 5.4 Results of nonlinear regression on the production curves for different nutrient concentrations, with ideal exponential microbial growth ($\lambda=350$ or 0) and non-ideal (Gaussian) mineralisation. S_o are expressed in units of $\text{mg } ^{14}\text{C-octadecane kg soil}^{-1}$ converted to $^{14}\text{CO}_2$, k_o in units of $^{14}\text{C-octadecane kg-soil}^{-1} \text{ d}^{-1}$, E_o and μ are in units of d^{-1} and v in units of days.	100
Table 6.1 Numbers of heterotrophic and hydrocarbon degrading bacterial numbers as determined by MPN ($\text{cells per g dry soil}^{-1}$). Mean and standard deviation (1s) are shown. NG is no cells recovered in the MPN medium.	114
Table 6.2 Pair-wise ANOSIM of the DGGE banding patterns with initial control and test soil combined but excluding the 42°C controls. R statistic is a measure of similarity (0 is maximum similarly while 1 is maximum dissimilarly) while the significance level is the percent of instances the observed pattern occurs during random	

permutations. Each treatment and control consisted of three replicates, while the initial soil represents four treatments. Ten and 2.9 % are the best achievable statistic level with 3 x 3 or 3 x 4 replicates compared respectively. 119

Table 6.3. Whole-cell fatty acid compositions (% of total) of the dominant hydrocarbon degrading bacteria isolated from each microcosm. Isolates are labelled according to incubation temperature, microcosm replicate and isolate. All isolates were grown on TSA Individual fatty acids which comprised less than 0.1% of the totals were combined into the other acid column, which includes: 12:0, 14:0 3OH, *i*16:1 ω 10c, 17:0, *i*17:1 ω 11c, *a*17:1 ω 11c, 17:1 ω 12c..... 122

Table 6.4. Pair-wise ANOSIM of the isolated FAME composition including FAME composition of mucoid and non-mucoid isolates from Danne *et al.* (2002). Groups indicate the temperature the bacteria were isolated at (or colony morphology). R statistic is a measure of similarity (0 is maximum similarity while 1 is maximum dissimilarity) while the significance level is the percent of instances the observed pattern occurs during random permutations..... 123

Table 6.5. Pair-wise ANOSIM of the isolated FAME composition including FAME composition of mucoid and non-mucoid isolates from Danne *et al.* (2002) grown at 28°C. Groups indicate the temperature the isolates were grown at before phospholipid extraction. R statistic is a measure of similarity (0 is maximum similarity while 1 is maximum dissimilarity) while the significance level is the percent of instances the observed pattern occurs during random permutations..... 124

Table 7.1 Summary of the chemical treatments applied to the soil from the semi-enclosed box-plot and open-plot small-scale implementation ICO field trials. The semi-enclosed box-plot experiment was established in duplicate, composites

<p>samples from 4 separate locations within each plot in the open-plot small-scale field trial was taken at each time Asterisks indicate where only single samples were obtained. Treatments were applied in the open-plot small-scale field trial on days 1 and 14.</p>	133
<p>Table 7.2 Soil parameters and chemical results for the open-plot small-scale trial. Arrows indicate before and after oxidant treatment. Unk represented unknown values as the samples were lost in transit. Air and soil temperature at time of samplings varied between -3.8 and -0.5°C and 1.8 and 13°C respectively.</p>	138
<p>Table 7.3 Average results for the geochemical and microbial analysis of the soil from the semi-enclosed box-plot ICO trial. Pr is pristane. MPNs are in most probable number of microbes per g dry soil⁻¹. Percentage hydrocarbon degrading bacteria of total heterotrophic bacteria are shown in parenthesis in the hydrocarbon degraders column. Some samples were not collected because the soil was frozen. ND is Not Detected, detection limit of MPN method was 0.03 x 10³ microbes g⁻¹. Standard deviation (1s) are shown (n=2). Biodegradation data from Snape <i>et al.</i> (2003) are shown for comparison (n=4).</p>	141
<p>Figure 1.1 Panel a is a map of Antarctica with the Windmill Islands indicated by a circle. Panel b is a more detailed map or the Windmill Islands region and Panel c shows the location of both the New and Old Casey Stations.....</p>	4
<p>Figure 2.1 Gas chromatography traces of the total and aliphatic fractions of SAB. Panel A shows the entire trace. Panels B-E are detailed locations of Panel A. Identification of the naphthalene, 1-methyl, 2-methyl naphthalene and the di-methyl naphthalene hydrocarbons were by spikes of known structures. Identification of the</p>	

substituted benzenes are tentatively based on literature data (Gustafson <i>et al.</i> , 1997).	14
Figure 2.2 60 MHz- ¹ H-nuclear magnetic resonance spectrum of neat SAB in <i>d</i> -chloroform (CDCl ₃), residual CHCl ₃ appears at 7.3 ppm, internal standard (IS) is tetramethylsilane (Si(CH ₃) ₄). Side chains (R) are of undetermined structure.	15
Figure 2.3 Reference chromatograms of the main fuels known to have been spilled in the Casey region (SAB = Special Antarctic Blend, ‘Bergen’ = arctic blend diesel, MGO = marine gas oil, Jet-A1 = ATK or aviation turbine kerosene). Isoprenoids are shown by *. An expansion of the <i>n</i> -C ₁₇ – phytane region of each trace is included to show the relative concentration of these compounds.....	17
Figure 2.4 Gas chromatography traces of SAB with varying degrees of abiotic weather (-20°C). Panel A shows the entire envelope of GC-FID detectable compounds present in neat SAB (<i>cf.</i> Figure 2.1). Panels B-E are expansions of Panel A; panel B also shows cyclo-octane which was used as a quality control standard. Methyl- and ethyl- groups are abbreviated to Me and Et respectively. Structures of the isoprenoids are shown in Appendix 10.1	24
Figure 2.5 Snape <i>et al.</i> (Submitted) and experimentally derived changes in the abiotic weathering diagnostic ratios for SAB. Panel A shows the predicted change in the light to heavy isoprenoid diagnostic ratios and a source (pristane: phytane) ratio. Panel B is the change in both the experimentally and modelled change in the <i>i</i> -C ₁₃ : pristane ratio at both -20 and 20°C. Isoprenoids pristane and phytane abbreviated to pr and ph respectively.	26
Figure 2.6 Gas chromatography traces of SAB with varying degrees of biodegradation in liquid-phase microcosms. Panel A shows the entire envelope of GC-FID detectable	

compounds present in neat SAB (<i>cf.</i> Figure 2.1). Panels B-E are expansions of Panel A; panel B also shows adamantane which was used as an internal standard, squalane was also used as an internal standard but is not shown in the figure. Note the extra peaks in Panel E (red and green lines), these peaks are likely to be polar compounds, but were not identified. Methyl- and ethyl- groups are abbreviated to Me and Et respectively. Structures of the isoprenoids are shown in Appendix 10.1	32
Figure 2.7 Biodegradation diagnostic ratio ($n\text{-C}_{12}$: $i\text{-C}_{13}$) over the 146 days incubation at 4°C. Error bars (1s) are also shown.	33
Figure 2.8 Chromatogram of the fuel contamination at Old Casey Station (Panel A) and neat SAB (Panel B). Isoprenoids are shown by *.	38
Figure 3.1 Design of the microcosms used in the experiments to measure mineralisation of ^{14}C -octadecane to $^{14}\text{CO}_2$.	46
Figure 3.2 Recovery of $^{14}\text{CO}_2$ from ^{14}C -octadecane in microcosm experiments. The different symbols identify replicates. The best-fit production curves from the Trefry and Franzmann (2003) (exponential growth rate) are also plotted (see Chapter 5).	51
Figure 3.3 Gas chromatography results showing total aliphatic hydrocarbons in the pre- and final microcosm soils in panel A; and percentage change from the pre-treated soil for $n\text{-C}_{17}$: pristane and $n\text{-C}_{18}$: phytane in panel B. Control data is from the 15°C microcosms. Error bars (2s) are shown.	54
Figure 4.1 Panel A- percentage of ^{14}C -octadecane mineralised to $^{14}\text{CO}_2$ in Antarctic soils treated with <i>ca</i> 500 mg N kg-soil- H_2O^{-1} incubated at 10°C for 95 days. The 420 mg N kg-soil- H_2O^{-1} microcosms (diamond symbols) is reproduced from Chapter 3. Control data represents the average of both heat killed and chemically inhibited	

(sterile) control microcosms (closed circle symbols) and unamended controls (closed square symbols). All symbols represent the average of the number of replicates shown in Table 4.1 and error bars represent 1s. Panel B- total aliphatic hydrocarbon concentration, normalised to squalane, in the pre-treatment, and after 95 days incubation at 10°C for the control and treatment microcosm soils. Points are an average of data from microcosms in each treatment. Error bars (1s) are shown, data also present in Table 4.2. Panel C- percentage change from pre-treatment soil of two common biodegradation ratios (*n*-C₁₇: pristane and *n*-C₁₈: phytane). Error bars (1s) are shown, data also present in Table 4.2. Panel D- percentage change from pre-treatment soil of an evaporation ratio (*i*-C₁₃: squalane). Note that the 420 mg N kg-soil-H₂O⁻¹ microcosm data are not present as these microcosms did not contain squalane. Error bars (1s) are shown, data also present in Table 4.2.....68

Figure 5.1 Arrhenius plot of the natural log of the first order rate co-efficient (k_1 , Equation 5.5) for ¹⁴CO₂ production from ¹⁴C-octadecane in the microcosms presented in Chapter 3. Mineralisation rates were calculated from the exponential phase of growth except for the 28°C microcosms which is shown twice (lag and exponential mineralisation rates are shown). Microcosms grown from -2 to 28°C are nominally labelled as psychrotrophic, while mesophilic microcosms are from 28 to 42°C. Error bars (2s) are shown.....89

Figure 5.2 Ratkowsky (1983) plot and best-fit estimates when applied to the ¹⁴C-octadecane mineralisation rates (-2°C to 28°C) from Chapter 3.....90

Figure 5.3 Temperature dependence of the exponential growth rate model parameters. Best-fit estimates are shown, together with standard errors92

Figure 5.4 Production rate curves calculated using best-fit parameters for the two growth models, based on the highly bioavailable fraction of the label.....	99
Figure 6.1 Total aliphatic hydrocarbon concentration (Panel A) and the change from the initial (pre-treatment) for both evaporation (Panel B; <i>i</i> -C ₁₃ : pristane) and biodegradation (Panel C; <i>n</i> -C ₁₇ : pristane). Square symbols represent the data from this experiment; data from Chapter 3 are shown for comparison (diamond symbols). Error bars in panels A-C represent one standard deviation of the microcosm replicates at each time point, and the change required for statistical differences according to student t-test are indicated by a broken line on these panels.....	112
Figure 6.2 Photographs of the DGGE gels from the analysis of the triplicate soil microcosms. The outside lanes (unlabelled) on each gel are a standard DNA control mix used within our laboratory. The DNA from the initial soil (T _{zero}) and after 40 days incubation; lanes are labelled with the incubation temperature.....	116
Figure 6.3 Panels A and B are MDS ordination plots showing the relative similarities in the DGGE banding pattern between initial soil, incubated treatment and control microcosms. Panel A is the complete data set, while Panel B has the 42°C control microcosms removed as they contained only one band and were completely dissimilar to all of the other patterns. The initial soil with and without HgCl ₂ exhibited the same banding pattern and thus were combined for further statistical analysis. Panel C and D show the MDS ordination plots of the relative similarity of the FAME data. In Panel C mucoid and non-mucoid isolates are from Daane <i>et al.</i> (2002). The acids identified in this study and not by the MIDI system as used by Daane <i>et al.</i> (2002) have been grouped to form ‘other’ in the multivariate statistical	

analysis. Panel D is the MDS based the temperature the isolates were incubated at before FAME analysis.....118

Figure 6.4 Panel A shows the similarities between the isolates FAME. The tree was constructed after square-root Bray-Curtis transformation and cluster analysis (group-average linkages). Temperatures indicated after the isolate designations specify the temperature at which the isolates were regrown to investigate the effect of temperature on FAME composition. Panel B is a phylogenetic tree based on partial 16S rRNA gene sequences. Isolates are designated according to incubation temperature and isolate designation, (e.g. 4°C isolate b is 4(b)). Reference sequences are shown with GenBank accession numbers. Isolates indicated by an asterisk were isolated by Daane *et al.* (2002) and isolates with a cross were from Antarctica (Christner *et al.*, 2001).....120

Figure 7.1 Photographs of the Casey region and experimental plots. Panel A is the small-scale open-plot field trial. Plots are 1 high NaHOCl; 2 Control; 3 low NaHOCl; 4 Fentons and 5 H₂O₂. Soil for the semi-enclosed box-plot was collected from the lower right hand corner of the insert (circled) and panel B shows the semi-enclosed box-plots.....134

Figure 7.2 GC trace of the aliphatic fraction of neat SAB with normal and isoprenoid alkanes labelled. Insert A and B is the GC trace extracted from the control tins pre and post 15 months respectively. The remain aliphatic contamination 2 years after treatment with 6.25% NaHOCl and Fentons are shown in Insert C and Insert D respectively. Insert E shows the remaining aliphatic hydrocarbon contamination 15 months after treatment with hydrogen peroxide, while Insert F shows the

contamination after 3 years of bioremediation treatment (Snape *et al.*, 2003).

Acyclic isoprenoids are indicated with an asterisk.	147
Equation 5.1 Brunner and Focht (1984) three-half order linear growth model.	83
Equation 5.2 Brunner and Focht (1984) three-half order exponential growth model.....	83
Equation 5.3 Trefry and Franzmann (2003) model with linear biomass growth.	84
Equation 5.4 Trefry and Franzmann (2003) model with exponential biomass growth. ..	84
Equation 5.5 First-order rate kinetics (k_1)	86
Equation 5.6 Arrhenius (1889) equation	86
Equation 5.7 Ratkowsky (1983) bacterial growth rate model.....	87
Equation 7.1-7.4 Stoichiometric reactions involved in the Fenton's Process.....	129

Acronyms

ATK	Aviation Turbine Kerosene
CPI	Carbon Preference Index
C:N:P	Carbon: Nitrogen: Phosphorous
CRN	Control Release Nutrients
DGGE	Denaturing Gradient Gel Electrophoresis
ECN	Effective Carbon Number
EPA	Environmental Protection Agency (USA)
FID	Flame Ionisation Detector
GC	Gas Chromatography
HP	Hewlard Packard
HPLC	High Performance Liquid Chromatography
ICO	<i>In situ</i> Chemical Oxidation
IR	Infra Red
K _{sat}	Saturated hydraulic Conductivity
MGO	Marine Grade Oil
MPN	Most Probable Number
MS	Mass Spectrometry
NMR	Nuclear Magnetic Resonance
PAH	Poly Aromatic Hydrocarbons
Ph	Phytane
PHC	Petroleum Hydrocarbons
PID	Photo Ionisation Detector
Pr	Pristane
r	Pearson product moment correlation coefficient
SAB	Special Antarctic Blend
TCE	Trichloroethylene
TLC	Thin Layer Chromatography
TPH	Total Petroleum Hydrocarbon
T _{max}	Maximum growth temperature
T _{min}	Minimum growth temperature
T _{opt}	Optimum growth temperature
TSB	Tryptone Soya Broth
T _{1/2}	Half life
Sq	Squalane
SFC	Supercritical Fluid Chromatography
UCM	Unresolved Complex Mixture

Chapter 1

Petroleum products in Antarctica

1.1 Introduction

The Antarctic can no longer be considered a pristine environment as contamination from waste disposal sites and petroleum spills has affected many terrestrial and coastal marine areas. Of all the different types of contamination reported on the continent, petroleum has been identified as one of the most significant problems (Snape *et al.*, 2000). Once a spill has occurred it is particularly problematic to recover or remediate, as many techniques employed in temperate regions are either unsuitable or difficult to implement in Antarctica. Moreover, the environmental impacts of contamination in Antarctica are also likely to be more detrimental than elsewhere because of the relative rarity of ice free Antarctic coastal habitats, the slow rates of chemical breakdown and ecological recovery from perturbation, and the wilderness values that may be compromised (Manzoni, 1992; Gore *et al.*, 1999; Poland *et al.*, 2004).

The 'do nothing' or natural attenuation approach to remediation of petroleum contaminated soils in Antarctica is not effective, with numerous sites still highly contaminated many years after spills have occurred. Therefore, active remediation will need to be undertaken, provided cost-effective management options can be identified. A number of remediation strategies have been considered for petroleum spills in Antarctica, but bioremediation has been proposed as the only viable management option that can be implemented on a large scale (Snape *et al.*, 2001). On a smaller scale, *in situ* chemical oxidation (ICO) has been identified as a complementary remediation strategy that could deliver fast-acting results for highly contaminated soils and avoid many of the shortcomings of bioremediation.

Bioremediation of petroleum-contaminated soils requires an understanding of the processes that limit degradation, especially in remote cold regions where operational costs are high and site conditions are very different to those found in temperate and tropical regions. Although many full-scale bioremediation applications have been undertaken for petroleum spills in the Arctic, trials in Antarctica have been limited to small-scale controlled-spill experiments (Kerry, 1993; Delille, 2000). Little or no remediation work has been undertaken on contaminated sites in Antarctica using indigenous microbial communities in weathered spills in which the petroleum contamination still resides long after the initial period of downward migration and evaporation.

1.2 History of petroleum spills in Antarctica

Perhaps the most famous fuel spill in Antarctica was the *Bahia Paraiso* incident, in which an Argentine tourist ship sank near Palmer station in 1982 releasing more than 680 000 L of diesel into Arthur Harbour (Karl, 1989; Wilkniss and Chiang, 1990; Kennicutt II *et al.*, 1991; Karl, 1992). Marine spills of this type are often highly visible and are regarded as being ecologically most damaging because their impact is immediate at many trophic levels (Kennicutt II, 1990). However, many substantial spills also occur on land where the immediate environmental impacts are often not so apparent. For example, 760 000 L of fuel was spilled at McMurdo Station between 1980 and 1989, with a further 380 000 L spilled at the runway area in three separate incidents (Tumeo and Wolk, 1994). There is a similar unfortunate history of accidental spills around Australia's Casey Station, with 38 000 L spilled in the 1980s (Reid, 1999); 91 000 L in 1990 (ANARE news, 1990), 16 000 L in 1991 (Melick, 1991) and between 2000 and 10 000 L spilled in 1999. Many of these spills occurred on land where they percolated

into porous soils or dispersed along impermeable frozen ground or ice before passing through catchments into the near-shore marine environment. Of the 73 reported petroleum spill incidents recorded by COMNAP in 1999, 59 spills were on land (COMNAP, 1999). Many of these petroleum plumes will continue to slowly migrate for decades after the initial accident, often releasing a pulse of contaminants each season with the summer snowmelt (Tumeo and Cummings, 1996; Snape *et al.*, 2001).

Given the high frequency and large volumes of petroleum products spilt into the fragile Antarctic environment, it is perhaps surprising that very little remedial action has occurred. In response to the ratification of the Madrid Protocol in 1998, the Australian Antarctic Division instigated a multidisciplinary investigation into the origin, distribution and fate of contaminants at its stations and bases in Antarctica (Snape *et al.*, 2001). Of the many potentially contaminated sites identified in the Casey region, two sites were identified as a priority for remediation based on contaminant loading and the potential for ecological damage associated with persistent discharge into the near-shore marine ecosystem. The highest priority is the Thala Valley tip site, which is contaminated with high levels of cadmium, copper, lead and zinc, and is currently the focus of a major clean-up effort. The second highest priority is the site of the former workshop-powerhouse at Old Casey Station, which has very high levels of diesel-range petroleum hydrocarbons (Snape *et al.*, 2001; Snape *et al.*, Submitted). This study focuses on the workshop-powerhouse contaminated site and is an integral part of Australian Antarctic Divisions' investigation into the contaminated sites in the Casey region.

1.3 Old Casey Station and surrounds

Old Casey Station is located in the Windmill Islands on the coast of east Antarctica at approximately 66°17' S, 110°32' E (Figure 1.1). In common with many stations in

Antarctica, Old Casey Station is located on a coastal ice-free rock and gravel peninsula. Sea ice is usually present in the winter months but melts or is blown out each summer (Snape *et al.*, 2001). Mean annual air temperature is -9.3°C , with summer air temperatures slightly above freezing, and winter temperatures averaging about -20°C . Mean wind speed averages are about 18 and 31 km hr^{-1} for summer and winter respectively. Annual precipitation is about 180 mm and occurs mostly as snow (Shepherd, 1999).

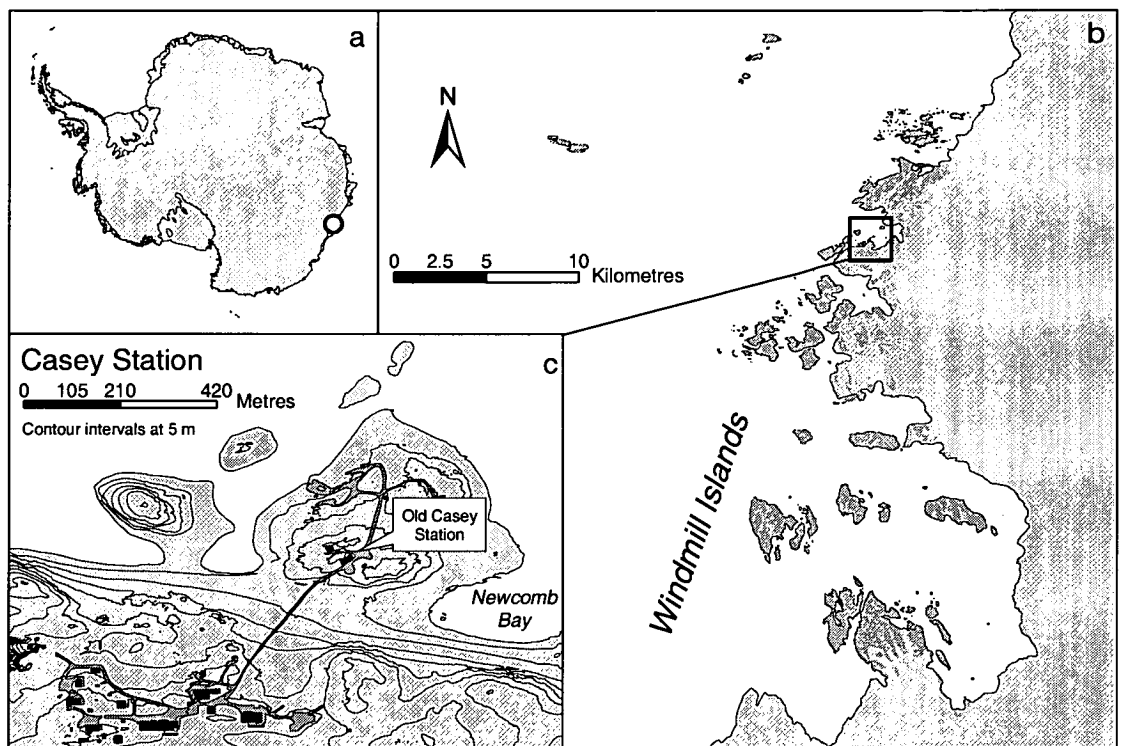


Figure 1.1 Panel a is a map of Antarctica with the Windmill Islands indicated by a circle. Panel b is a more detailed map of the Windmill Islands region and Panel c shows the location of both the New and Old Casey Stations.

The Casey region contains some of the most developed and extensive flora communities on continental Antarctica and thus several areas have been designated as Sites of Special Interest (ATCM, 1985). This region has unusually extensive bryophyte vegetation that is probably a result of favourable environmental (chemical and climatic)

conditions (Smith, 1990). The nearby marine ecosystem is also diverse and shallow waters, away from the impacts of abandoned waste sites and petroleum spills, support communities of algae, invertebrates and fish. The Windmill Islands are also breeding grounds for seals, penguins and flying birds.

1.4 Physical characterisation of the Casey region

The distribution and nature of soils is highly variable on local scales of tens to hundreds of metres. Loamy fine earth is separated from sand, gravel and larger clasts by extensive cryoturbation (Blume *et al.*, 1997). However, soil development is generally poor in the immediate vicinity of the station and has been extensively modified by human activities. In particular, many areas have been covered in coarse aggregate, and nearby accumulation of fine-grained soils deposited by runoff and wind deposition is common. Organic matter in the soils is initially derived from either dead moss (Beyer *et al.*, 1995) or more locally through the input of penguin guano (Beyer *et al.*, 1997). Carbon (C) concentrations vary from <0.5 - 10 wt %, total nitrogen (N) is relatively high, typically <0.3 wt % and C:N ratios are generally low, with C:N generally <30, possibly indicating high availability of humic matter. Availability of micronutrients, such as phosphate (P) and potassium (K), is also considered to be relatively high (Beyer and Bölter, 1998).

Soil moisture is highly variable laterally, vertically and seasonally. During the winter months there is no free water or associated runoff. As the summer thaw progresses, snow melt initially ponds within the snow profile or more commonly at the interface between snow and the frozen active layer. The first melt pulse then disperses largely by overland flow in channels. As the thaw continues, surface water tends to migrate downwards and subsurface water movement becomes dominant (Snape *et al.*, 2002).

The locus of this movement tends to occur at the base of the advancing active layer and soil moisture gradients can develop between only a few weight percent soil-moisture near the surface down to saturation and about 40-50 % water by weight, just above the base of the active layer. In detail, however, the soil water regime around Casey is highly site dependant.

1.5 The Old Casey petroleum plume

The contaminated site selected for this study was from a large spill that accumulated in front of the mechanical workshop-powerhouse at Old Casey Station. This site, used for parking and as a refuelling area for station vehicles, was subjected to chronic small-scale contamination while the station was operational (1969-1989). The most extensive contamination occurred in 1988 when approximately 38 000 L of Special Antarctic Blend (SAB) was spilled (Reid, 1999). Unfortunately, there are no official records of the spill or the action taken in response to the spill, but the site was recognised as being highly contaminated by Deprez *et al.* (1994) in their 1993-94 survey of the region. Deprez *et al.* (1994) identified an old plume that contained total petroleum hydrocarbon (TPH) concentrations $> 10\,000\text{ mg kg}^{-1}$ in several samples, and one sample with $47\,631\text{ mg TPH kg}^{-1}$. The workshop-powerhouse site is denoted by Deprez *et al.* (1994) as WS6 and WS7. Snape *et al.* (2001) also described the petroleum contamination at this site, noting that some intrinsic remediation has taken place.

The workshop-powerhouse is located on a rocky promontory 18 m above sea level. Petroleum-contaminated soils occur throughout the catchment from the site of the old powerhouse, down gradient through to Newcomb Bay. Soils at the spill site are mostly coarse aggregates, with a grain size of *ca* 50% $> 5\text{ mm}$. Fines washed from these aggregates have been transported downstream and deposited throughout the catchment.

Soil in the immediate study area consists of fluvial modified glacial deposits that are equally well described as mineral sediments (Snape *et al.*, 2001). The main spill zone comprises poorly developed soil and an aggregate road. Relatively undegraded SAB still leaches into Newcomb Bay during the annual summer melt (Revill *et al.*, 1998). The site is locally heterogenous in terms of contaminant concentration, grain size and wetness (Revill *et al.*, 1998). Because of the high contaminant concentration, and its relatively fast flow rate into the near-shore marine ecosystem, soils in the vicinity of the Old Casey Station workshop-powerhouse have been identified as a priority for remedial clean-up (Snape *et al.*, 2001).

1.6 Objectives and thesis outline

The overall objective of this study was to evaluate *in situ* bioremediation and ICO as remediation options for the contaminated soils at Old Casey Station, with the hope of using research from this site as a case study to be applied to other contaminated sites throughout Antarctica and other cold regions. The general approach adopted in this study is similar to many other treatability studies. Typically, a treatability study first consists of site and spill characterization, primarily to identify to what extent natural attenuation processes have degraded the plume (e.g. Yang *et al.*, 1997; Margesin and Schinner, 2001; Delille and Pelletier, 2002). In such studies, field sites are often characterised by a variety of techniques and methods including photo-ionisation detection (PID) of the volatile hydrocarbons (e.g. Clark, 2003), soil pH analysis (e.g. Filler and Barnes, 2003; Fiore *et al.*, 2003), gravimetric soil moisture (e.g. Grundy *et al.*, 1996; Cho *et al.*, 2000), hydraulic conductivity (e.g. White and Williams, 1999) and the measurement of soil temperature (e.g. Mohn *et al.*, 2001).

There are a number of possible analytical methods for the investigation of petroleum hydrocarbon contamination, for example infra-red (IR) spectrophotometry (e.g. EPA method 418.8) and high performance liquid chromatography (HPLC) (e.g. EPA 8325 and ASTM D-6379). However, for diesel range organics, the method of choice is gas chromatography-flame ionising detector (GC-FID) as it enables detailed characterisation of constituent components of petroleum products and offers a good compromise between selectivity, sensitivity and cost (e.g. Wang *et al.*, 1995; Wang and Fingas, 1997; Wang and Fingas, 2003a). The characterisation of the aliphatic fraction of fuels provides evidence of biotic and abiotic mechanisms responsible for hydrocarbon removal which is discussed in Chapter 2. The unambiguous characterization of evaporation and biodegradation processes based on alkanes within a spill are extremely useful parameters from which remediation efforts can be gauged (e.g. Bragg *et al.*, 1994; Bonham, 2002; Prince *et al.*, 2002).

For ICO, the key issues relate to whether the treatment removes the hydrocarbon contamination, and what damage it does to the soil and micro-fauna in the process (Watts and Dilly, 1996; Zappi *et al.*, 2000; Chen *et al.*, 2001; Yeh *et al.*, 2003). In other assessments of ICO efficacy, contaminant removal was monitored using combined field and laboratory analyses including soil pH and temperature measurement (e.g. Yeh *et al.*, 2002), PID and GC-FID analyses of the soil contaminant concentration (e.g. Watts *et al.*, 2000). Damage to the soil microbiota can be assessed with a variety of methods, but the most probable number (MPN) estimations is perhaps the simplest measure of microbial community health (discussed in Chapter 7).

To quantify biodegradation in the soil through successive manipulations, radiometric microcosm studies were identified as the safest and most cost effective way of

constraining rate processes (e.g. Whyte *et al.*, 1999; Mohn and Stewart, 2000; Whyte *et al.*, 2001). For any biodegradation treatability study, the main objective is to quantify the rate of biodegradation under various environmental restraints which can be precisely controlled. By isolating the effects of one variable, it is possible to establish what the limitations of bioremediation are and how these restraints can be favourably managed. Previous investigations into temperature, nutrients and water have used soil from the Arctic and Sub-Antarctic regions, which have fundamentally different physical and biological characteristics and are under contrasting climatic conditions (e.g. Loynachan, 1978; Walworth *et al.*, 1997; Macnaughton *et al.*, 1999; Mohn and Stewart, 2000; Brook *et al.*, 2001; Eriksson *et al.*, 2001). The effects of temperature (Chapter 3), nutrients and water (Chapter 4) on biodegradation of petroleum hydrocarbons in Antarctic contaminated soils are investigated in this study.

Empirical fitting of the microcosm mineralisation results, such as from Chapter 3 and Chapter 4, to the various kinetic models provides useful estimates of the dependence of key microbial population parameters (Arrhenius, 1889; Ratkowsky *et al.*, 1983; Brunner and Focht, 1984; Trefry and Franzmann, 2003). The availability of these functions raises the possibility of applying the radio-isotope mineralisation curves to obtain quantitative estimates of *in situ* remediation efficiencies under the seasonal thermal cycles and nutrient concentration manipulations at Old Casey Station.

The only way to validate such treatability studies is to adopt an interdisciplinary approach focused with careful confirmation of successful treatments (Watanabe, 2002; Watanabe and Hamamura, 2003; Wellington *et al.*, 2003). A variety of chemical and biological tracers can be used to quantify or qualitatively describe the response of the soil microbial ecology with remediation manipulation, such as denaturing gradient gel

electrophoresis (DGGE) (Powell *et al.*, 2003), phospholipid fatty acids composition (Nichols *et al.*, 1986) microarrays (Zhou, 2003), functional gene expression (Watanabe and Hamamura, 2003), and stable isotope (Pelz *et al.*, 2001; Manefield *et al.*, 2002; Pombo *et al.*, 2002; Adamczyk *et al.*, 2003). No one technique allows for the identification and characterisation of the key microbial elements within a contaminated site; scientists are reliant on a combination of culture-dependent, molecular, chemical and physiological approaches. To gain an insight into the population dynamics within microcosm studies and to determine the bacteria responsible for petroleum-hydrocarbon degradation under psychrotrophic and mesophilic conditions, soil microbial populations were characterised by MPN estimation of heterotrophic and hydrocarbon degrading bacteria, microbial communities were characterised by denaturing gradient gel electrophoresis, and individual cultures of numerically-dominant hydrocarbon degrading bacteria were characterised by 16S rRNA gene sequencing and fatty acid methyl ester (FAME) analysis.

Ultimately, no single technique can provide an unequivocal measure of all the processes occurring in contaminated soil undergoing remediation, and the results of several techniques used in combination offer the best chance of identifying suitable treatment options.

Chapter 2

Characterisation of the petroleum hydrocarbon contaminants at Old Casey Station

2.1 Introduction

There are numerous techniques and analytical procedures used in the characterisation of crude oil and its' refined products. The concentration of total petroleum hydrocarbons (TPH) in environmental samples can be determined by non-specific methods such as infra-red (IR) spectrophotometry (EPA method 418.8, Table 2.1) or gravimetrically (EPA method 9071B, Anon, 2003). Detailed characterisation of the individual components of petroleum occurred as early as 1857 with the identification of several aromatic hydrocarbons (Speight, 2001 and references therein). More recently, detailed characterisation of petroleum hydrocarbons is usually performed with chromatography methods. There is an extensive choice of analytical methods including, but not restricted too, gas chromatography-flame ionization detection (GC-FID) (eg. EPA method 8015B (Anon, 2003)), GC mass spectrophotometry (MS) (eg. EPA method 8270C and ASTM D-2425 (Nadkarni, 2000)), photo ionization detection (PID) (eg. EPA method 8021B), high performance liquid chromatography (HPLC) (eg. EPA 8325; ASTM D-6379), thin layer chromatography (TLC) (eg. Cavanagh *et al.*, 1995; Watson *et al.*, 2002), supercritical fluid chromatography (SFC) (eg. EPA 3560) and nuclear magnetic resonance (NMR) (eg. ASTM 5292).

The choice of an analytical procedure is largely determined by factors such as speed, selectivity, sensitivity, cost and the objective of the analysis. In environmental matrices, Wang *et al.* (1997) considered the main objectives of petroleum analysis to include the quantification of the major constituents to facilitate the study of the fate (and behaviour) of the oil in the environment, the identification of the environmentally hazardous

constitutes, and also the characterisation of the biomarkers used to indicate the source, nature and type of spilt petroleum products.

Table 2.1 U.S. Environmental Protection Agency (EPA) test methods for determining petroleum hydrocarbons (reproduced from Anon, 1997). Numbers refer to EPA method numbers. Several types of analyses do not have established water/ wastewater methods (n/a – not available).

SW-846 Method	Water/ Wastewater Method	Analyte	Primary Equipment	Sample Preparation
4030	n/a	TPH	Immunoassay	Included in kit
4035	n/a	PAH	Immunoassay	Included in kit
8015	n/a	Aliphatic and aromatic hydrocarbons; Nonhalogenated volatile organic compounds	GC/FID	Extraction (semi-volatile organic compounds) Purge-and-Trap and Headspace (volatile organic compounds), Azeotropic Distillation (Nonhalogenated volatile organic compounds)
8021	502.2/602	Aromatic volatile organic compounds (not ethers or alcohols)	GC/PID	Purge-and-Trap
8100	n/a	PAH	GC/FID	Extraction
8260	524.2/624	Volatile organic compounds	GC/MS	Purge-and-Trap; Static Headspace; Azeotropic Distillation
8270	525/625	Semi-volatile organic compounds	GC/MS	Extraction
8310	610	PAH	HPLC	Extraction
8440	418.1	TPH	IR Spectrophotometer	SFE from soils

2.2 Petroleum products at Australian Antarctic Stations

A wide variety of petroleum products have been used at the Australian Antarctic Stations, including mineral and synthetic lubrication oil, marine gas oil (MGO), light diesel, kerosene, and petrol. The most common product used by Australia is MGO, a heavy marine diesel, although this is largely limited to use on resupply ships. The most commonly used product on the continent is a light diesel fuel, Special Antarctic Blend (SAB), which is used extensively at Australian Antarctic stations for power generation

and heavy vehicle transport. Aviation turbine kerosene (ATK) and petrol are used to a much lesser extent for helicopters, light aircraft and for vehicles that travel off station to the interior of the continent.

As most refined petroleum products are manufactured for performance rather than for specific composition, some degree of compositional variation (Appendix 10.2) within one product is likely and is influenced by the availability and composition of the parent material (Gill and Robotham, 1989). The chemical compositions detailed below are based on samples obtained from the manufacturer in 2002-03.

SAB is specially refined by BP Australia for use in cold climates and a summary of the historical chemical composition as supplied from BP is shown in Appendix 10.2. SAB is the main soil contaminant at Old Casey Station, and thus it has been characterised in more detail than the other petroleum products used by the Australian Antarctic Program. While there is batch to batch variability, generally SAB is primarily comprised of aliphatic hydrocarbons with *n*-alkanes in the range nonane (*n*-C₉) to tricosane (*n*-C₂₃) with concentrations peaking around dodecane (*n*-C₁₂) (Figure 2.1). It also contains several acyclic isoprenoids, such as those shown in Appendix 10.1. Figure 2.1 shows the differences in neat SAB when the aromatic hydrocarbons are removed with silica-alumina chromatographic cleanup (Section 3.2.4). Silica-alumina cleanup removes up to *ca* 19% of the total hydrocarbons. ¹H-NMR analysis of neat SAB indicates that only *ca* 4% of the protons are bound directly to an aromatic ring (Figure 2.2). Biomarkers such as the pentacyclic hopanes and the C₂₇ to C₂₉ steranes, having effective carbon numbers (ECN) >27 (Gustafson *et al.*, 1997), can not be detected in significant quantities in SAB by GC-FID analysis. Fresh SAB has a relatively high proportion of resolved compounds, with a resolved proportion from *n*-C₉ to hexadecane (*n*-C₁₆) of about 70% (Table 2.2).

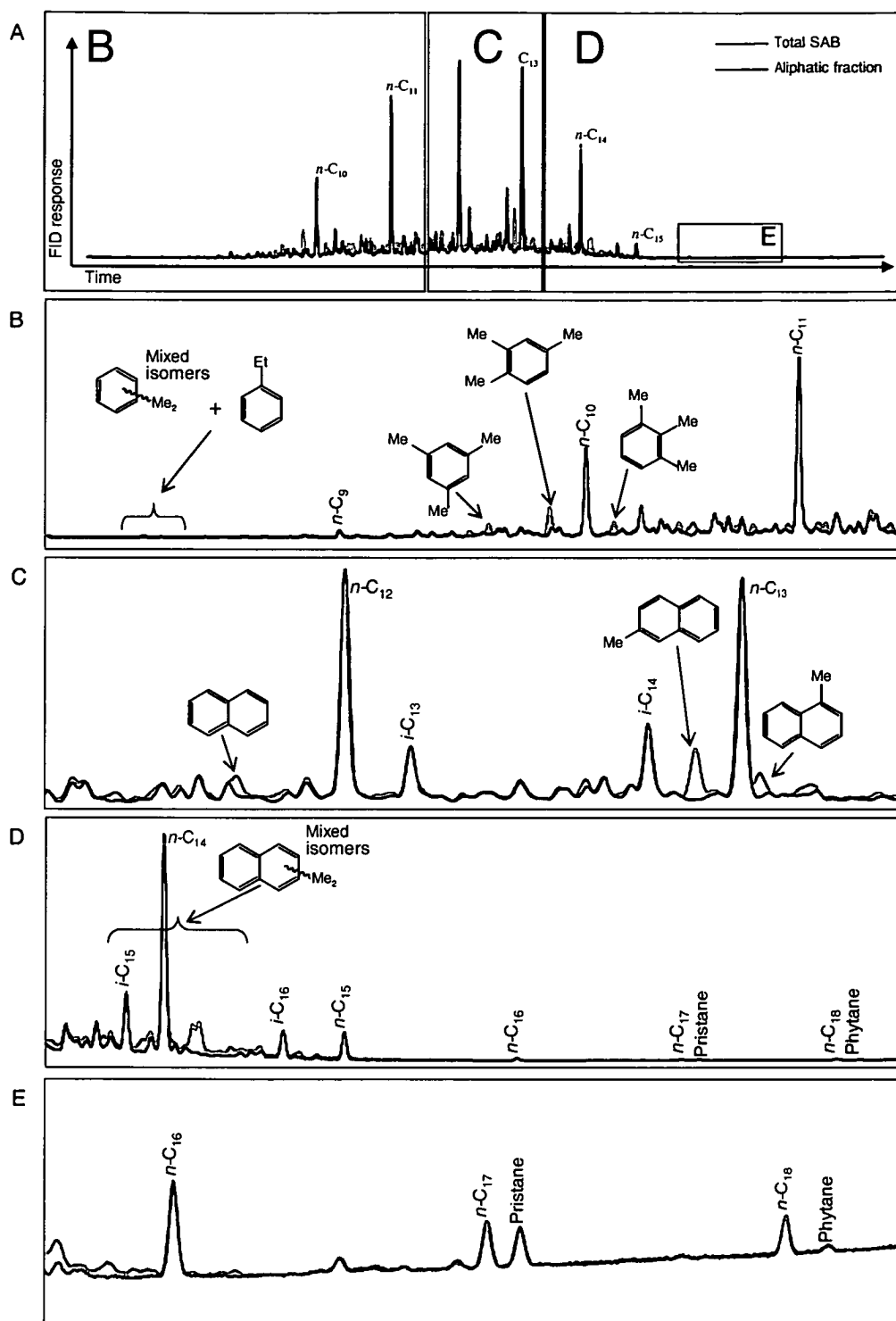


Figure 2.1 Gas chromatography traces of the total and aliphatic fractions of SAB. Panel A shows the entire trace. Panels B-E are detailed locations of Panel A. Identification of the naphthalene, 1-methyl, 2-methyl naphthalene and the di-methyl naphthalene hydrocarbons were by spikes of known structures. Identification of the substituted benzenes are tentatively based on literature data (Gustafson *et al.*, 1997).

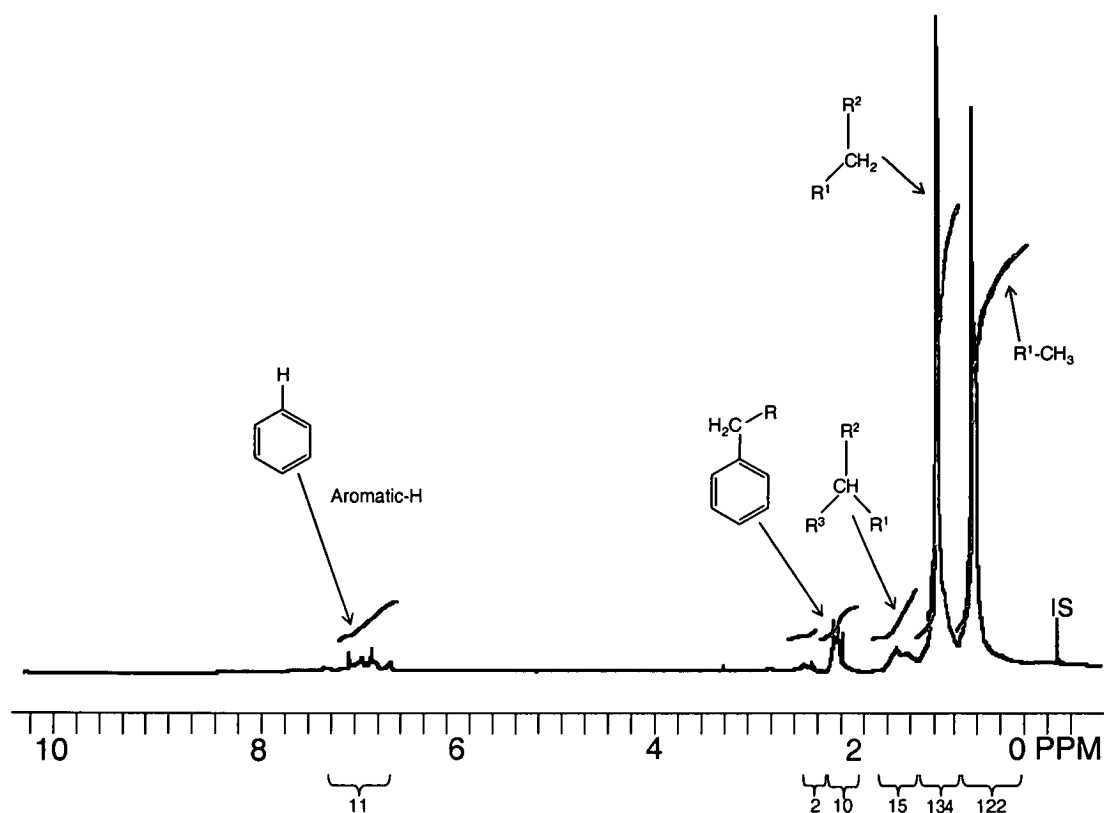


Figure 2.2 60 MHz- ^1H -nuclear magnetic resonance spectrum of neat SAB in d -chloroform (CDCl_3), residual CHCl_3 appears at 7.3 ppm, internal standard (IS) is tetramethylsilane ($\text{Si}(\text{CH}_3)_4$). Side chains (R) are of undetermined structure.

Both ATK and Jet-A1 have very similar aliphatic component as SAB (Figure 2.3); they are slightly more volatile peaking at undecane ($n\text{-C}_{11}$). The resolved component of these fuels is *ca* 75% (Table 2.2). While MGO also peaks at $n\text{-C}_{11}$, it has a higher concentration of the heavier alkanes and is the heaviest fuel used by the Australian Antarctic Program. The resolved component of MGO is similar to SAB, with a resolved component between $n\text{-C}_9$ to $n\text{-C}_{23}$ constituting *ca* 71% of the fuel, but with a greater proportion in the $n\text{-C}_{18}$ - $n\text{-C}_{23}$ range.

Table 2.2 Resolved components of the diesel-ranged fuels commonly used by the Australian Antarctic Program.

Component	Jet-A1 (%)	ATK (%)	SAB 2003 (%)	SAB 2002 (%)	SAB 2002 (%)	Bergen (%)	MGO (%)
<i>n-alkanes</i>							
<i>n</i> -C ₉	2.0	1.5	0.1	0.2	0.2	0.3	1.3
<i>n</i> -C ₁₀	4.6	3.7	1.8	2.3	2.1	1.1	3.0
<i>n</i> -C ₁₁	5.3	4.4	3.6	4.7	3.5	1.7	3.6
<i>n</i> -C ₁₂	4.4	3.6	4.4	4.8	4.8	1.8	3.1
<i>n</i> -C ₁₃	2.8	2.6	4.4	3.7	4.9	1.6	2.2
<i>n</i> -C ₁₄	1.1	1.6	2.8	1.4	3.0	1.0	1.4
<i>n</i> -C ₁₅	0.2	0.4	0.4	0.1	0.8	0.8	0.8
<i>n</i> -C ₁₆	0.02	0.1	0.03	0.05	0.3	0.6	0.7
<i>n</i> -C ₁₇		0.01	0.02	0.05	0.1	0.5	0.7
<i>n</i> -C ₁₈		0.01	0.01	0.04	0.1	0.3	0.6
<i>n</i> -C ₁₉		0.01	0.01	0.04	0.02	0.3	0.6
<i>n</i> -C ₂₀			0.01	0.03		0.2	0.5
<i>n</i> -C ₂₁			0.01	0.02		0.1	0.4
<i>n</i> -C ₂₂			0.01	0.02		0.1	0.2
<i>n</i> -C ₂₃			0.01	0.01		0.02	0.1
<i>n</i> -C ₂₄				0.01		0.01	0.05
<i>n</i> -C ₂₅						0.01	0.02
<i>n</i> -C ₂₆							0.01
<i>isoprenoids</i>							
<i>i</i> -C ₁₃	1.0	0.9	1.2	1.3	1.1	0.6	0.6
<i>i</i> -C ₁₄	0.9	0.9	1.5	1.2	1.2	0.6	1.3
<i>i</i> -C ₁₅	0.3	0.4	0.6	0.3	0.6	0.3	0.3
<i>i</i> -C ₁₆	0.2	0.3	0.3	0.1	0.5	0.4	0.4
Pristane		0.01	0.02	0.04	0.07	0.5	0.5
Phytane			0.01	0.01	0.01	0.2	0.1
Resolved	75.3	73.6	70.0	71.0	72.8	64.9	71.3

Arctic blend diesel obtained from Bergen, Norway has occasionally been used as an alternative to SAB (Figure 2.3). While the aliphatic fraction of ‘Bergen’ fuel also peaks at *n*-C₁₂, the same as SAB, the fuel is slightly heavier than SAB as it contains higher concentrations of the alkanes from tetradecane (*n*-C₁₄) to docosane (*n*-C₂₂). ‘Bergen’ fuel has the least resolved component of the diesel-range fuel used by the Australian Antarctic Program; between *n*-C₉ to *n*-C₂₂ only *ca* 65% of ‘Bergen’ is resolved.

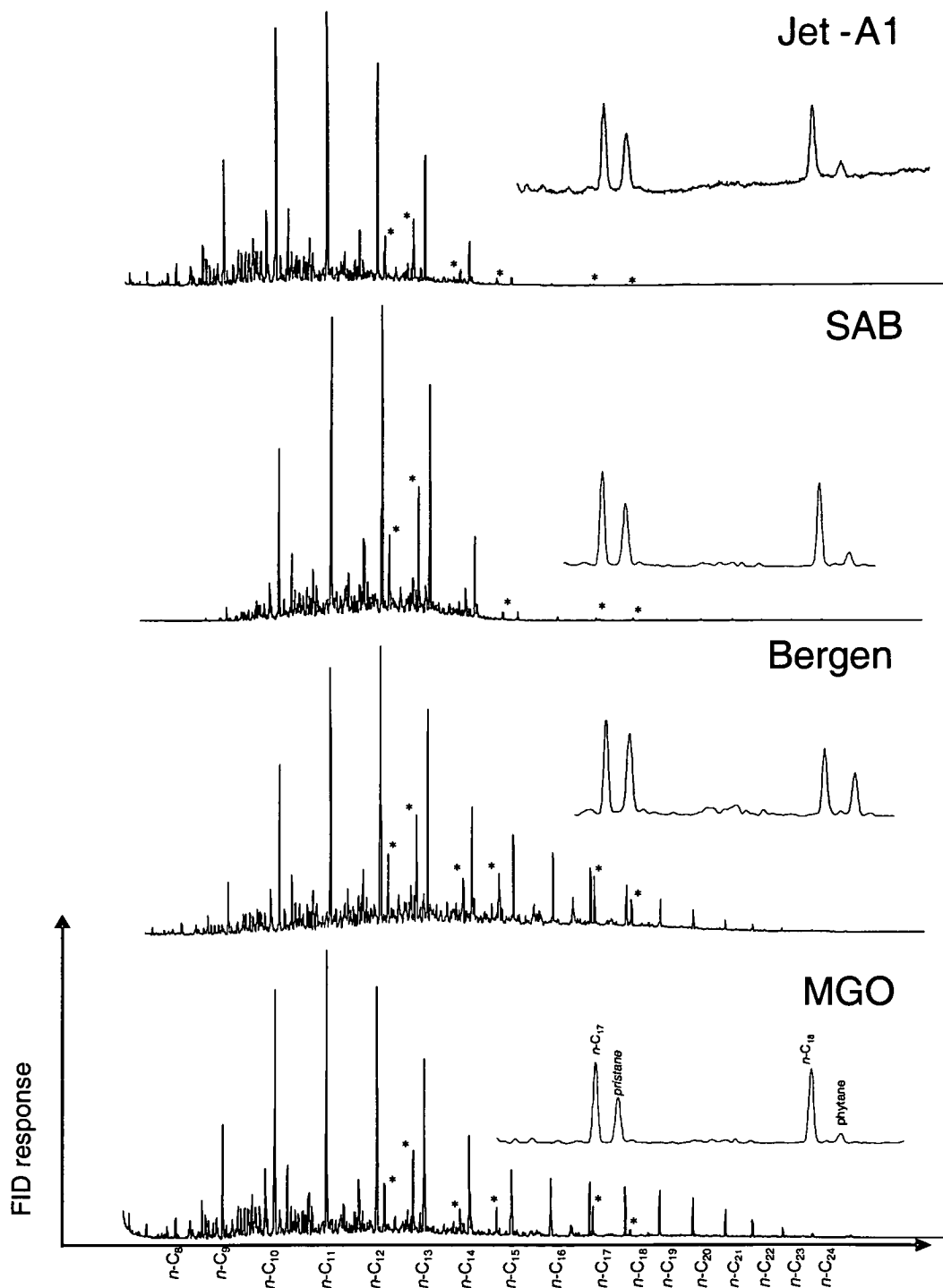


Figure 2.3 Reference chromatograms of the main fuels known to have been spilled in the Casey region (SAB = Special Antarctic Blend, 'Bergen' = arctic blend diesel, MGO = marine gas oil, Jet-A1 = ATK or aviation turbine kerosene). Isoprenoids are shown by *. An expansion of the $n\text{-C}_{17}$ – phytane region of each trace is included to show the relative concentration of these compounds.

2.3 Precedence for use of diagnostic ratios

GC-FID analysis of petroleum hydrocarbons offers a good compromise between selectivity, sensitivity and cost; although a more detailed characterisation of the constituents of petroleum requires GC-MS. Analysis of contaminated soils and waters by GC-FID and GC-MS provides a fingerprint of the petroleum hydrocarbons present. Hydrocarbon fingerprints can be useful for identifying the source of petroleum hydrocarbons in the environment and monitoring its subsequent breakdown. At the simplest level, TPH analysis can be used to measure concentrations and monitor decreases with time. One of the problems with TPH measurements is that many of the compounds found in petroleum hydrocarbons either occur naturally in the environment or fractionate on a GC at the same time as natural organic material, and it is sometimes difficult to assess at a spill site how much of the petroleum is anthropogenic (e.g. Woolard *et al.*, 1999; Wang and Fingas, 2003b). It is also difficult to assess how much petroleum has migrated vertically or laterally from the site, how much has been diluted, or how much has been lost through evaporation or biodegradation. More detailed fingerprinting techniques aim to identify and quantify a range of organic compounds. These can be used to define source signatures, differentiate between contaminant sources that might have similar chain length molecules, and provide estimates of changes associated with dilution, evaporation or biodegradation (e.g. Gill and Robotham, 1989; Wigger and Torkelson, 1997; Whittaker *et al.*, 1999; Wang and Fingas, 2003b). The differentiation of biotic (e.g. biodegradation) and abiotic (e.g. volatilisation) weathering processes, determining the biodegradability of any spilled petroleum products, and evaluating the efficiency of any remedial activity undertaken, is extremely important in the management of a contaminated site.

Of the numerous diagnostic ratios outlined in the literature (e.g. Humphrey *et al.*, 1987; Wang *et al.*, 1995; Wang and Fingas, 2003a), very few can be used at the Old Casey Station contaminated site. Typical ratios often utilise hopanoid compounds, such as C₃₀-17 α (H),21 β (H)-hopane (ECN *ca* 27) (Bence *et al.*, 1996); SAB generally contains insignificant concentration of any compounds with ECNs >20.

Of the ratios identified in the literature the following can be used at the Old Casey Station contaminated site to identify the source of the petroleum contamination (Section 2.3.1), the degree of biological (Section 2.3.2) and abiotic (Section 2.3.3) loss of the light diesel products used by the Australian Antarctic Program.

2.3.1 Source identification

- Pristane: phytane (Gill and Robotham, 1989; Wang *et al.*, 1998 and references therein)
- Heptadecane (*n*-C₁₇): pristane (Wang *et al.*, 1999)
- Carbon preference index (CPI), ratio of odd-carbon *n*-alkanes: even-carbon *n*-alkanes, used to identify biogenic or petrogenic hydrocarbons – biogenic *n*-alkanes tend to have odd number of carbon atoms (Boehm *et al.*, 1987; Humphrey *et al.*, 1987; Gill and Robotham, 1989 and references therein)

2.3.2 Biodegradation

- *n*-alkane: matching isoprenoid such as (*n*-C₁₇: pristane and octadecane (*n*-C₁₈): phytane) (Boehm *et al.*, 1987; Wang and Fingas, 1997; Wang *et al.*, 1998)

- R: UCM or percent of the fuel which is resolved (Gill and Robotham, 1989 and references therein; Bence *et al.*, 1996; Wang *et al.*, 1998; Snape *et al.*, Submitted)
- Sum *n*-alkanes: sum of isoprenoids (Atlas *et al.*, 1981; Boehm *et al.*, 1987; Humphrey *et al.*, 1987; Wang and Fingas, 1997 and references therein; Wang *et al.*, 1998)

2.3.3 Abiotic weathering

- Sum of *n*-alkanes decane (*n*-C₁₀) to pentacosane (*n*-C₂₅): sum of *n*-alkanes *n*-C₁₇ to *n*-C₂₅ (Gill and Robotham, 1989 and references therein; Humphrey *et al.*, 1992)
- Light isoprenoid, such as 2,6-dimethyl undecane (*i*-C₁₃): pristane (Guille *et al.*, 1997; Ferguson *et al.*, Submitted; Snape *et al.*, Submitted)

2.4 Source signatures of fuels at Old Casey Station

Although there is a comprehensive database of chemical compositions of common crude oil products (NOSID, 2001), there is not a similar resource for the more refined fuels and oils commonly used in Antarctica. One of the objectives of this study was to provide a chemical reference for the fuels most commonly used by the Australian Antarctic Program between 1999 and 2003. It is important to note that small changes are likely to have occurred over time in products that have the same common name (*cf.* Table 2.2; Appendix 10.2). This limits the certainty of quantifying subsequent changes to old spills where reference chemical signatures have not been recorded, and a degree of caution should be applied to such extrapolations. The diagnostic ratios from neat fuel obtained in 2002-03 are shown in Table 2.3.

Table 2.3 Summary of diagnostic ratios (source, biodegradation and abiotic) as outlined in Sections 2.3.1 – 2.3.3 for the fuels shown in the reference chromatograms (Figure 2.3) of the petroleum products used within the Casey region. Isoprenoid pristane and phytane are abbreviated to pr and ph respectively.

	Jet-A1	ATK	SAB 2003	SAB 2002	SAB 2002	Bergen
Source						
pr: ph	4.4	8.7	5.0	4.4	8.1	1.9
CPI	1.03	0.99	0.95	1.03	0.95	1.05
Biodegradation						
<i>n</i> -C ₁₂ : <i>i</i> -C ₁₃	4.28	3.88	3.52	3.74	4.49	3.02
<i>n</i> -C ₁₃ : <i>i</i> -C ₁₄	2.97	2.84	3.00	2.98	4.05	2.83
<i>n</i> -C ₁₄ : <i>i</i> -C ₁₅	4.06	4.33	4.35	3.87	4.73	3.53
<i>n</i> -C ₁₅ : <i>i</i> -C ₁₆	1.20	1.35	1.09	1.27	1.77	1.86
<i>n</i> -C ₁₇ : pr	1.47	1.55	1.12	1.27	1.70	0.99
<i>n</i> -C ₁₈ : ph	2.6	6.4	4.6	4.8	5.41	1.3
<i>n</i> -alkane: isoprenoid	8.6	7.0	4.7	5.7	5.7	4.0
Abiotic weathering						
<i>i</i> -C ₁₃ : pr	287.6	96.6	79.2	32.5	15.2	1.24
<i>i</i> -C ₁₄ : pr	263	96.8	94.5	31.7	17.3	1.17
<i>i</i> -C ₁₅ : pr	75.1	39.4	40.8	8.90	8.92	0.60
<i>i</i> -C ₁₆ : pr	43.9	35.0	20.9	2.78	6.87	0.85
sum <i>n</i> -alkane (C ₁₀ – C ₂₅):	>1000	585	204	76	108	7.1
sum <i>n</i> -alkane (C ₁₇ – C ₂₅)						

2.5 Experimental verification of diagnostic ratios in SAB; effect of abiotic weathering

To quantify how fuel might weather through evaporation in the Antarctic environment two evaporation experiments were undertaken. The aim of the experiments was to verify the use of the abiotic weathering indexes in Section 2.3.3 for SAB at two temperatures (-20 and 20°C). The experimentally derived abiotic weathering ratios were then matched to those predicted by a theoretical model developed to determine the fractionation of SAB at different temperatures (Snape *et al.*, Submitted).

2.5.1 Theoretical weathering model

The Snape *et al.* (Submitted) fuel evaporation model divides the fuel into a number of fractions by grouping the UCM and resolved components into 0.5 ECN ranges. The model then combines several factors for each fuel-group including vapour pressure (literature values), mole fraction (based on Raoult's Law), and the effect of temperature (Antoine's Equation) to predict the fractionation of the fuel into the vapour phase. The model is a simple approximation for direct evaporation of a surface spill with no account taken for chemical gradients associated with boundary layer effects, sorption or soil covering.

Snape *et al.* (Submitted) list several limitations of this approach, including limited availability of vapour pressure data and thus the need to use estimates for some classes of compounds and grouping compounds with different structure and chemical characteristics but with similar GC retention times.

2.5.2 Empirical determination of the effect of evaporation on diagnostic ratios

2.5.2.1 Methods

To determine the effect of abiotic weathering on SAB, two experiments were conducted at 20°C and at -20°C. Neat fuel (SAB), between 200 and 500 µL in 40 mL vials, was slowly evaporated under a stream of air (BOC). The flasks were rotated at 75 rpm to avoid chemical gradients between the surface and the bulk of the sample. Evaporative loss was calculated from the mass loss. For GC analysis, the SAB in each flask was diluted with hexane (between 2 and 5 mL depending on the amount of fuel lost) and cyclo-octane was added as a quality assurance standard. The fuel samples were analysed using a Varian 3410 gas chromatograph fitted with a septum-equipped programmable injector and flame ionisation detector. Analyses were performed using a

50 m non-polar methyl-silicone-fused silica capillary column (HP-1, 0.32 mm internal diameter, 0.23 μm film thickness) with helium as the carrier gas. GC conditions were 35°C for 1 min then ramped to 120°C at 30°C min⁻¹ then ramped to 310°C at 4°C min⁻¹ and then held for 15 min. The observed fractionation trends were then compared with the Snape *et al.* (Submitted) evaporation model.

2.5.2.2 Results and discussion

The evaporation rates varied considerably between the two experiments. At 20°C more than 99% the fuel evaporated from the flasks in 3 days, whereas it took 10 days to evaporate *ca* 45% of the fuel at -20°C.

A similar pattern of fuel fractionation was observed at -20°C as at 20°C; the chromatogram (Figure 2.4) and diagnostic ratios (Table 2.3) described below are based on the -20°C experiment. As expected, the aliphatic fuel components were lost in order of GC elution and there were no preferential losses between the *n*-alkane peaks and components with similar retention time. The dominant peak in the fuel migrated from *n*-C₁₂ to *n*-C₁₃ after 45% loss of the fuel. There was complete loss of all of the fuel components up to *n*-C₁₁, and with *ca* 66 and 25 % loss of *n*-C₁₁ and *n*-C₁₂ respectively.

Evaporation resulted in significant fractionation of the ratios of *n*-alkanes and isoprenoids with very different volatilities. Although there was a marked difference in the rate of evaporation at -20 and 20°C, the differences in the degree of fractionation of the *n*-alkanes and isoprenoids were insignificant. It is reassuring to note that there were no significant changes in any of the diagnostic ratios indicative of biodegradation (i.e. those listed in Section 2.3.2; Table 2.4).

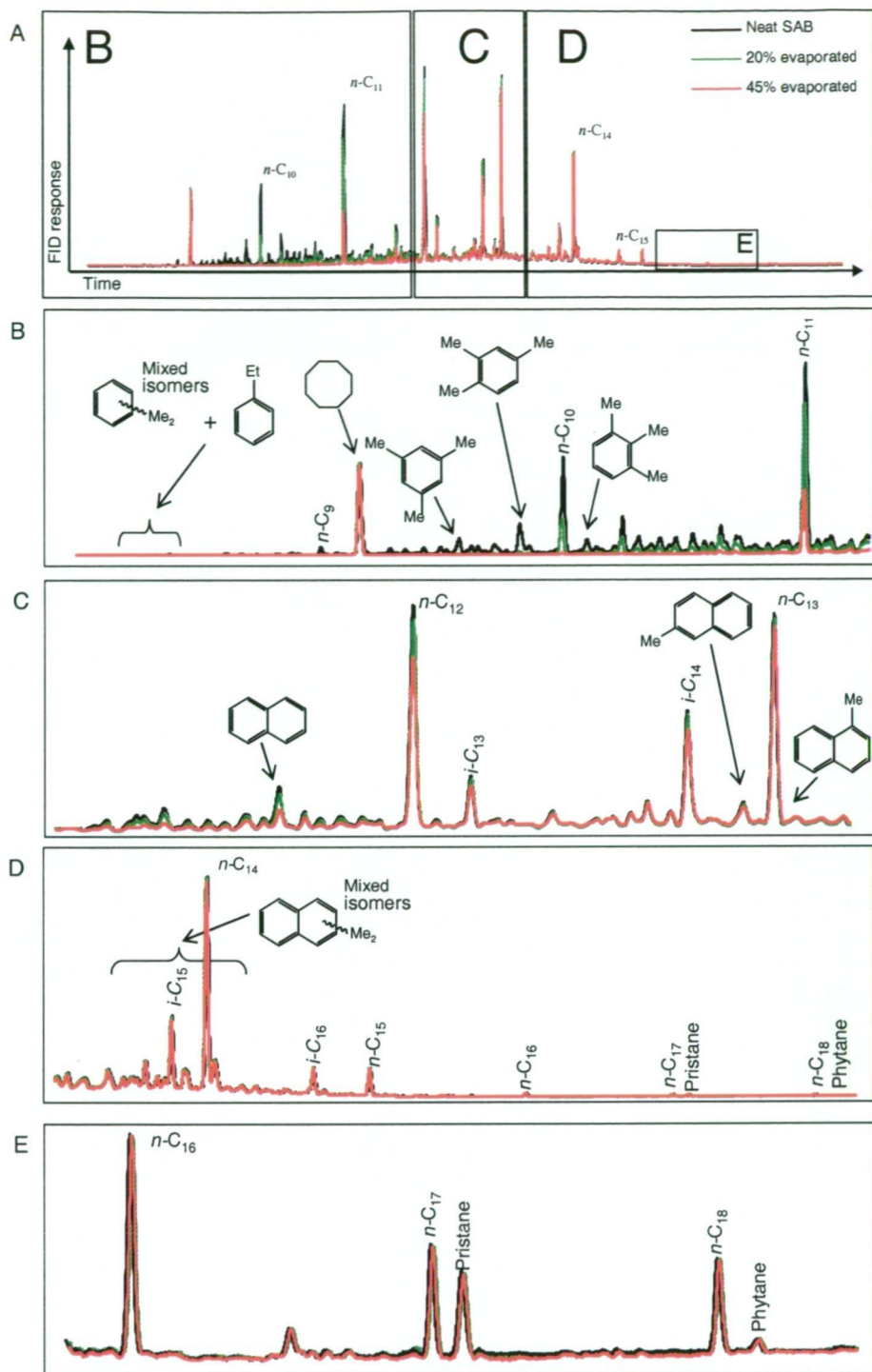


Figure 2.4 Gas chromatography traces of SAB with varying degrees of abiotic weather (-20°C). Panel A shows the entire envelope of GC-FID detectable compounds present in neat SAB (*cf.* Figure 2.1). Panels B-E are expansions of Panel A; panel B also shows cyclo-octane which was used as a quality control standard. Methyl- and ethyl- groups are abbreviated to Me and Et respectively. Structures of the isoprenoids are shown in Appendix 10.1

Table 2.4 Summary of the diagnostic ratios in Sections 2.3.1 – 2.3.3 for SAB as it is lost through evaporation at -20°C. Isoprenoid pristane and phytane abbreviated as pr and ph respectively. Light *n*-alkanes: heavy *n*-alkanes represents the sum of *n*-alkanes between *n*-C₉ – *n*-C₁₈; sum of *n*-C₁₇ and *n*-C₁₈.

	Mass lost (%)												
	0	1.9	7.7	7.8	17.5	21.1	21.2	21.8	25.1	29.2	32.4	34.7	42.8
Source													
pr: ph	5.68	5.4	5.45	5.56	6.07	5.14	4.95	5.7	5.66	5.88	5.16	6.13	4.90
CPI	0.93	0.93	0.94	0.94	0.96	0.97	0.97	0.97	0.97	0.97	0.95	0.94	0.90
Biodegradation													
<i>n</i> -C ₁₂ : <i>i</i> -C ₁₃	4.46	4.45	4.49	4.47	4.43	4.47	4.7	4.45	4.39	4.35	4.35	4.38	4.84
<i>n</i> -C ₁₃ : <i>i</i> -C ₁₄	1.77	1.75	1.8	1.88	1.84	1.93	1.98	1.78	1.93	1.89	1.91	1.9	2.12
<i>n</i> -C ₁₄ : <i>i</i> -C ₁₅	3.10	3.05	3.04	3.10	3.24	3.05	3.03	3.37	3.13	4.20	3.06	3.06	3.04
<i>n</i> -C ₁₅ : <i>i</i> -C ₁₆	0.95	0.94	0.94	0.94	0.91	0.96	0.93	0.94	0.93	0.95	0.93	0.93	0.96
<i>n</i> -C ₁₇ : pr	1.13	1.11	1.14	1.12	1.13	1.14	1.14	1.13	1.12	1.13	1.14	1.12	1.14
<i>n</i> -C ₁₈ : ph	5.57	5.17	5.29	5.39	5.81	5.09	4.92	5.51	5.54	5.67	5.04	5.86	4.86
<i>n</i> -alkanes: isoprenoids resolved	3.74	3.67	3.61	3.72	3.47	3.45	3.51	3.34	3.32	3.36	3.08	3.03	3.06
(%)	75	75	75	75	75	75	75	74	74	74	74	74	74
Abiotic weathering													
<i>i</i> -C ₁₃ : pr	68.3	67.2	66.0	66.5	64.5	64.9	63.5	63.6	63.7	63.8	61.7	59.0	47.4
<i>i</i> -C ₁₄ : pr	161	160	157	149	150	146	147	155	145	148	146	144	126
<i>i</i> -C ₁₅ : pr	56.9	57.1	57.8	56.3	53.3	58.0	59.7	51.5	56.2	41.8	57.8	56.8	56.5
<i>i</i> -C ₁₆ : pr	22.8	22.6	23.0	22.7	23.3	22.7	23.7	22.6	23.2	22.7	23.5	22.9	22.4
light <i>n</i> -alkanes:													
heavy	546	543	519	525	484	475	484	468	456	445	424	414	363
<i>n</i> -alkanes													

The Snape *et al.* (Submitted) evaporation model neatly depicted the fractionation of the abiotic diagnostic ratios, such as *i*-C₁₃: pristane, over a range of temperatures. Furthermore, the model predicted that low temperatures would result in a more selective progression of the compounds being evaporated, which largely reflects a more efficient removal of the more volatile component in each ratio at low temperatures (Figure 2.5A). For example, in Figure 2.5 there is initially little change in the *i*-C₁₃: pristane ratio, the ratio then undergoes a period of high change as *i*-C₁₃ is lost. When the majority of the *i*-C₁₃ has been lost, the ratio starts to asymptote towards zero. It is during the period of

high $i\text{-C}_{13}$ loss, i.e. when the ratio is rapidly changing, that this abiotic weathering ratio is useful.

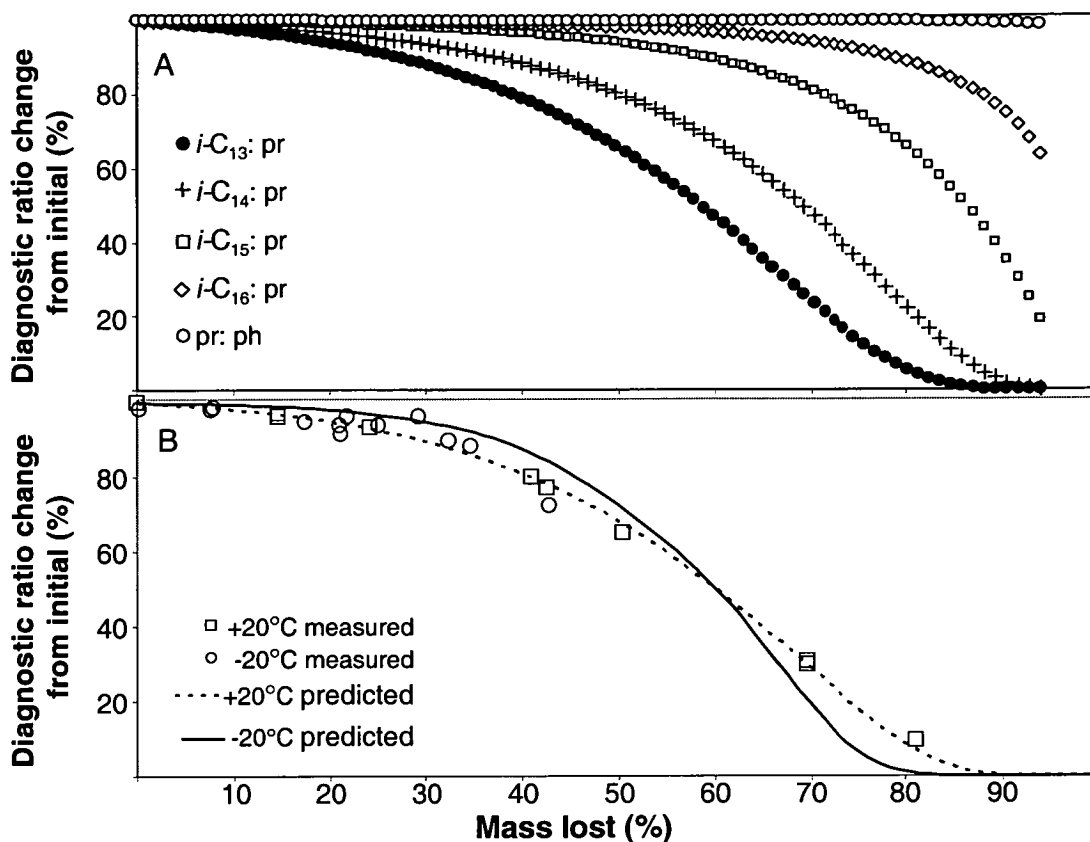


Figure 2.5 Snape *et al.* (Submitted) and experimentally derived changes in the abiotic weathering diagnostic ratios for SAB. Panel A shows the predicted change in the light to heavy isoprenoid diagnostic ratios and a source (pristane: phytane) ratio. Panel B is the change in both the experimentally and modelled change in the $i\text{-C}_{13}$: pristane ratio at both -20 and 20°C. Isoprenoids pristane and phytane abbreviated to pr and ph respectively.

Agreement between the theoretical model and the observed data were very good for the 20°C experiment. While the experimental data also confirmed that fractionation was more selective at -20°C, the agreement between the experiment and model was not as good (Figure 2.5B). This discrepancy probably reflects the extrapolation of limited vapour pressure data to low temperatures, possibly coupled to experimental issues such as a viscosity change as the SAB residue approached its waxing point and the problems associated with accounting for condensation at -20°C when weighing the vials.

2.5.3 Conclusions

The rate of SAB volatilisation at -20°C was significantly slower than at 20°C, but the pattern of compound fractionation at the two temperatures was not significantly different. As expected, volatilisation of alkanes was in order of their vapour pressures; decreasing the temperature to -20°C caused a small increase in the degree of fractionation. While good agreement was found between experimental results and a numerical evaporation model, temperature played less of a role in fuel fractionation than predicted by the evaporation model. The abiotic weathering ratios in Section 2.3.3, in particular the ratio of light to heavy isoprenoid were good indices of evaporation; the biodegradation ratios (Section 2.3.2) were not altered during evaporative fuel loss.

2.6 Experimental verification of diagnostic ratios in SAB; effect of biological mineralisation

2.6.1 Introduction

Although the initial investigations of hydrocarbon degradation under cold polar conditions occurred over 30 years ago (Atlas and Bartha, 1972; ZoBell, 1973; Westlake *et al.*, 1974), there still remains a need for precise information pertaining to the biodegradability of the constituents of crude oils and their refined products at low temperatures (e.g. Foght *et al.*, 1999). It has been generally believed that chemical structure is the primary determining factor for biodegradation; biodegradation of petroleum is thought to occur in the order of *n*-alkanes > branched and cyclic alkanes > aromatics > polar compounds and with alkyl branching and substitution increasing the compounds resistance to biomineralisation (Atlas, 1981). While the above simplification

is still a commonly held axiom today, there are many examples of exception to this 'rule' (e.g. Olson *et al.*, 1999; Watson *et al.*, 2002).

The utility of the biodegradation diagnostic ratios in Section 2.3.2 are based upon the general perception of light *n*-alkanes biodegrading before heavier more complex compounds. Not only is the microbial degradation of petroleum hydrocarbons dependent on the chemical structure of the individual compound, but other factors such as matrix-pH (Foght *et al.*, 1999), microbial consortia (Wang *et al.*, 1998) and the total chemical composition of the crude oil (Westlake *et al.*, 1974) are also important in the order of breakdown.

Since, by at least the time of Jesus Christ, we have been introducing petroleum hydrocarbons into our environment (Speight, 2001 and references therein), with microbes evolving since at least that time to utilise them as a carbon source. Indeed, microbes are capable of utilising most, if not all, of the hydrocarbons contained in petroleum, including isoprenoids such as pristane, and phytane (Robson and Rowland, 1988), hopanes (Watson *et al.*, 2002), and the compounds within the UCM (Gough *et al.*, 1992). Nevertheless, with the proviso of eventual mineralisation of the nominally 'recalcitrant' compounds, the use of diagnostic ratios provides an indication of bioremediation in the early and mid stages of petroleum breakdown. The effect of biodegradation of SAB, and the selective degradation of alkanes by an Antarctic consortium was investigated with a series of microcosm experiments.

2.6.2 Methods

Screw capped amber glass bottles (250 mL, I-Chem) with Teflon septa containing 170 mL Bushnell-Haas mineral salt broth (Difco) were autoclaved at 121°C for 20 minutes. After cooling, 250 µL of a filter sterilised SAB standard with squalane and

adamantane (2,6,10,15,19,23-hexamethyltetracosane and $C_{10}H_{16}$ respectively, Appendix 10.1), acting as conservative internal standards, was added to each microcosm. Squalane and adamantane are known to be resistant to microbial degradation but have very different volatilities (Watkinson and Morgan, 1990; Bagrii, 1995; Berekaa and Steinbuchel, 2000; Grice *et al.*, 2000), and were therefore used to gauge abiotic losses from the microcosms. An actively growing mixed-microbial inoculation of psychrotrophic hydrocarbon degrading soil bacteria (1.58×10^8 total cells) from Old Casey Station (equal quantities of isolates 4(b), 10(d), 10(e) and 10(f), see Chapter 6) was added. To ensure aerobic metabolism, all microcosms were aseptically flushed with *ca* 50 mL of O_2 (BOC) at 4°C when sufficient hydrocarbon degradation for oxygen depletion was indicated by GC-FID analysis. Abiotic flasks were prepared in a similar manner except without the addition of the bacterial consortia. All microcosms were rotated, on their sides to increase the interface available for gas exchange, at 12 rpm in the dark at 4°C. Hydrocarbon disappearance was determined by sacrificial sampling on days 0, 21, 55, 71, 105 and 146.

The flasks were extracted with the addition of 10 mL hexane. Extracts were analysed using a Varian 3800 GC-FID fitted with a 30 m non-polar methyl-silicone-fused capillary column (BP-1(SGE), 0.32 internal diameter, 0.25 μ m film thickness), and with helium as the carrier gas. The injector temperature was set at 270°C and 0.6 μ L was injected with a 20:1 split. GC conditions were 35°C for 2.5 min then ramped to 310°C at 25°C min⁻¹ and held for 1.5 min.

2.6.3 Results and discussion

Evidence of biodegradation was seen at the first sampling (21 days), with naphthalene, methyl-naphthalenes, *n*-C₉ and *n*-C₁₀ clearly degraded relative to the

control microcosms (Figure 2.6). Naphthalene, methyl-naphthalenes and *n*-C₉ were largely indistinguishable from the UCM after 55 days. It is interesting to note that relatively insoluble dimethyl-naphthalenes were not degraded even after 146 days of incubation. Likewise, Wang *et al.* (1998) found increasing recalcitrance to biodegradation with increasing alkylation in the naphthalene family. Watson *et al.* (2002) also found concurrent *n*-alkane, naphthalene and methyl-naphthalenes biodegradation in liquid phase microcosm studies. The early mineralization of naphthalene and the methyl-naphthalenes in microcosm studies, before extensive degradation of the *n*-alkane series is attributed to the higher water solubilities of naphthalene and methyl-naphthalene (Weast, 1995), as it is well established that contaminants are more bioavailable in a soluble form (Wodzinski and Coyle, 1974).

Apparent *n*-alkane degradation occurred by day 55, with a significant reduction of *ca* 60 and 25 % of *n*-C₁₀ and *n*-C₁₁ respectively. Unfortunately, there were variable losses in the abiotic control flasks from day 71 onwards. These losses were probably due to a combination of leaking and diffusion through the rubber backed Teflon septa after re-oxygenation; there was little change in either the biodegradation or abiotic weathering diagnostic ratios (discussed below) in the control flasks as compared to the neat fuel standard (Figures 2.7, Table 2.5). Furthermore, the control flasks remained clear, while increased turbidity indicated biological growth in the test microcosms. By the end of the experiment (day 146) *n*-C₁₂ and *n*-C₁₃ were significantly degraded, and *n*-C₁₄ had also begun to degrade. Importantly, *i*-C₁₃, *i*-C₁₄ and *i*-C₁₅ were not overly reduced throughout the experiment.

There was an increase in several unidentified compounds which eluted in the *n*-C₁₆ to *n*-C₁₈ range (ECN ~ 15.8 – 16.7) (Figure 2.6E). These compounds are likely to be polar organic compounds (Oudot *et al.*, 1998). The biodegradation of *n*-alkanes involves the

terminal oxidation of the methyl groups, with the formation of alcohols. Carboxylic acids, via aldehydes, are then formed by dehydrogenation of the alcohol (Riser-Roberts, 1998). Watson *et al.* (2002) found the production of medium molecular weight ($<C_{20}$) carboxylic acids during the biodegradation of a weathered (up to $n-C_{10}$) light Arabian crude oil. As these medium molecular weight carboxylic acids were degraded only after extensive degradation of the crude oil (including the majority of the three-ring aromatic hydrocarbons), they may be useful as additional biomarkers in heavily degraded environmental samples, though their utility has not been studied here.

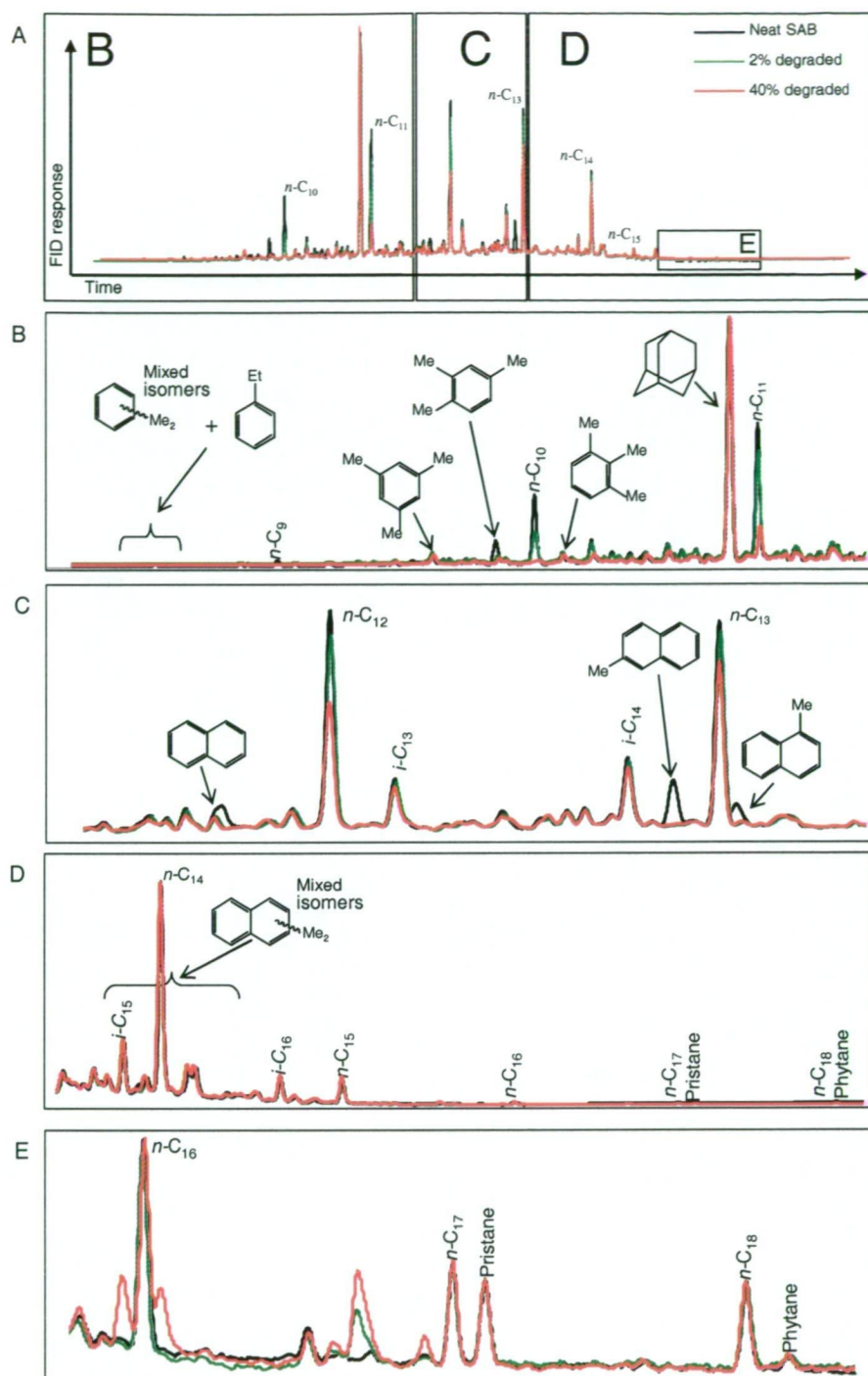


Figure 2.6 Gas chromatography traces of SAB with varying degrees of biodegradation in liquid-phase microcosms incubated at 4°C. Panel A shows the entire envelope of GC-FID detectable compounds present in neat SAB (*cf.* Figure 2.1). Panels B-E are expansions of Panel A; panel B also shows adamantane which was used as an internal standard, squalane was also used as an internal standard but is not shown in the figure. Note the extra peaks in Panel E (red and green lines), these peaks are likely to be polar compounds, but were not identified. Methyl- and ethyl- groups are abbreviated to Me and Et respectively. Structures of the isoprenoids are shown in Appendix 10.1

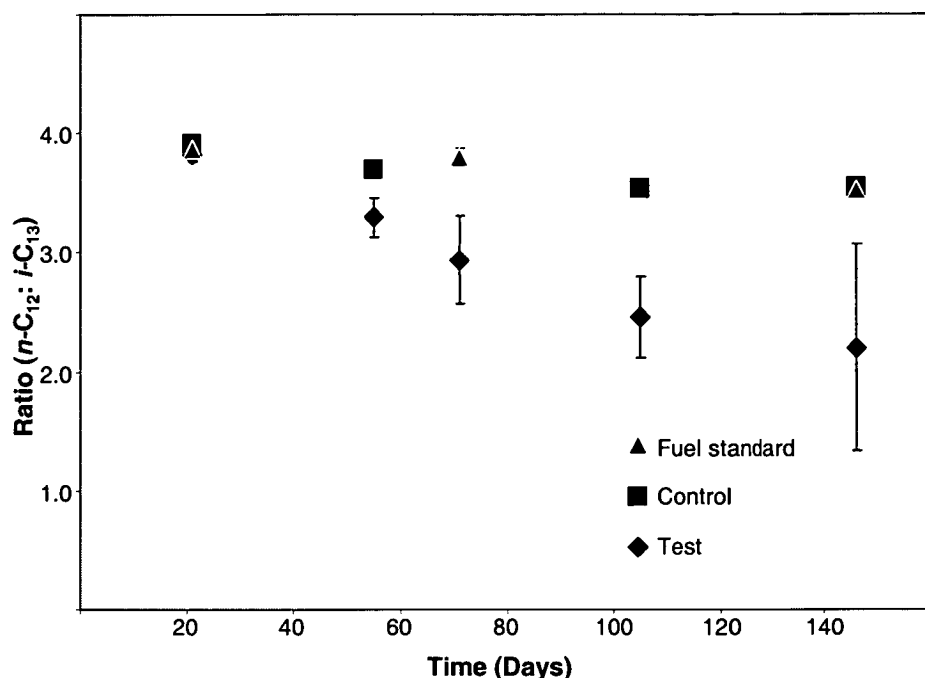


Figure 2.7 Biodegradation diagnostic ratio ($n\text{-C}_{12}$: $i\text{-C}_{13}$) over the 146 days incubation at 4°C. Error bars (1s) are also shown.

As there was a significant reduction in the C_{12} and C_{13} n -alkanes, and little reduction in the matched isoprenoids of similar volatilities, the n -alkane: matched isoprenoid biodegradation ratios (Section 2.3.2) changed significantly as biodegradation proceeded (Figure 2.7, Table 2.5). By comparing the inoculated microcosms and controls at each time interval, it is apparent that the dominant process occurring was of biotic origin, and biodegradation of the light alkanes accounts for most of the total mass losses.

No significant reduction was found in the resolved component in this biodegradation experiment, although the extent of biodegradation was not comprehensive and would thus indicate extensive biodegradation is required before the proportion of resolved compounds can be used in field samples. One reason for the lack of biological degradation of the petroleum hydrocarbons in these microcosms could relate to the isolates used in these experiments. The strains, putatively identified as psychrotrophic

Pseudomonas spp., were cultured from hydrocarbon-contaminated soil (Chapter 6). As the vast majority of soil bacteria are associated with particles, the lack of attachment sites within the microcosm may have inhibited their growth (Franzmann *et al.*, 1996).

Quantification of the abiotic diagnostic ratios which are dependent upon pristane resulted in large standard errors; there are difficulties in the integration of relatively minor component of SAB (*cf.* Figure 2.1).

Table 2.5 Summary of diagnostic ratios in Sections 2.3.1 – 2.3.3 for SAB as it is lost through biodegradation at 4°C. Isoprenoid pristane and phytane abbreviated as pr and ph respectively. Light *n*-alkanes: heavy *n*-alkanes represents the sum of *n*-alkanes between *n*-C₉ – *n*-C₁₈: sum of *n*-C₁₇ and *n*-C₁₈ as there was insignificant quantities of fuel components with ECNs > 18.5 in the neat SAB.

	Inoculated microcosms (day)						Control (day 146)	Standard (day 146)
	0	21	55	71	105	146		
Source								
pr: ph	5.79 ± 0.80	5.52 ± 0.40	3.96 ± 0.95	5.28 ± 0.55	4.44 ± 0.77	3.54 ± 0.85	3.28 ± 0.59	5.53 ± 0.20
CPI	0.92 ± 0.00	0.94 ± 0.01	0.97 ± 0.02	0.96 ± 0.03	0.91 ± 0.04	0.91 ± 0.04	0.93 ± 0.00	0.94 ± 0.00
Biodegradation								
<i>n</i> -C ₁₂ : <i>i</i> -C ₁₃	3.87 ± 0.05	3.81 ± 0.05	3.32 ± 0.14	2.99 ± 0.28	2.46 ± 0.32	2.20 ± 0.80	3.55 ± 0.02	3.53 ± 0.01
<i>n</i> -C ₁₃ : <i>i</i> -C ₁₄	2.78 ± 0.01	2.70 ± 0.01	2.69 ± 0.03	2.66 ± 0.03	2.53 ± 0.10	2.37 ± 0.28	2.90 ± 0.02	2.96 ± 0.01
<i>n</i> -C ₁₄ : <i>i</i> -C ₁₅	4.24 ± 0.02	4.25 ± 0.03	4.35 ± 0.13	4.40 ± 0.13	4.47 ± 0.11	4.25 ± 0.03	4.39 ± 0.02	4.37 ± 0.02
<i>n</i> -C ₁₅ : <i>i</i> -C ₁₆	1.06 ± 0.01	1.05 ± 0.01	1.10 ± 0.02	1.11 ± 0.03	1.15 ± 0.03	1.10 ± 0.01	1.08 ± 0.03	1.10 ± 0.01
<i>n</i> -C ₁₇ : pr	1.11 ± 0.02	1.15 ± 0.01	1.18 ± 0.06	1.15 ± 0.02	1.19 ± 0.05	1.28 ± 0.20	1.24 ± 0.10	1.14 ± 0.01
<i>n</i> -C ₁₈ : ph	5.17 ± 0.63	5.17 ± 0.32	4.14 ± 0.69	5.13 ± 0.44	4.67 ± 0.57	3.93 ± 0.69	3.49 ± 0.58	5.19 ± 0.16
<i>n</i> -alkanes: isoprenoids	2.97 ± 0.02	2.79 ± 0.03	2.43 ± 0.10	2.17 ± 0.17	1.89 ± 0.15	1.78 ± 0.32	2.84 ± 0.01	2.85 ± 0.01
resolved (%)	73 ± 0	72 ± 0	73 ± 1	72 ± 0	71 ± 0	71 ± 1	73 ± 0	73 ± 0
Abiotic weathering								
<i>i</i> -C ₁₃ : pr	84.5 ± 2.58	87.7 ± 1.58	77.5 ± 18.8	81.5 ± 2.53	73.2 ± 4.15	62.9 ± 7.14	65.0 ± 5.48	80.5 ± 3.41
<i>i</i> -C ₁₄ : pr	112 ± 3.51	121 ± 1.61	97.9 ± 22.5	103 ± 3.39	92.3 ± 5.11	85.6 ± 7.31	80.7 ± 6.82	95.7 ± 3.43
<i>i</i> -C ₁₅ : pr	46.3 ± 1.48	48.4 ± 0.50	39.4 ± 8.07	42.2 ± 0.89	38.5 ± 1.49	35.8 ± 2.92	34.9 ± 3.02	40.5 ± 0.98
<i>i</i> -C ₁₆ : pr	22.0 ± 0.67	23.1 ± 0.36	19.4 ± 3.47	20.7 ± 0.35	19.5 ± 0.75	18.2 ± 1.52	18.5 ± 1.51	20.7 ± 0.39
light <i>n</i> -alkanes:								
heavy	637 ± 9.5	608 ± 12.8	429 ± 122	424 ± 54.2	314 ± 5.7	253 ± 81.6	403 ± 23.4	543 ± 18.4
<i>n</i> -alkanes								

2.6.4 Conclusions

While the extent of fuel mineralisation was not extensive in the biodegradation experiment described here, the biological fractionation of normal and branched alkanes

within SAB supports the use of matched *n*-alkane: isoprenoid diagnostic ratios for use within a SAB contaminated site. Although the biodegradation of pristane and phytane has previously been noted by many authors, diagnostic ratios utilising these compounds is justified as SAB lacks hopanoid or other biomarker compounds.

2.7 Application of diagnostic ratios

From the experimental and theoretical results presented in Sections 2.5 and 2.6 it is possible to identify which ratios will be most useful for constraining petroleum-hydrocarbon losses through evaporation and biodegradation for SAB. However, the application of these diagnostic ratios is complex as several mechanisms may be involved in the loss of compounds resulting in concurrent alterations of the diagnostic ratios. Furthermore, for assessing historic spills, another major limitation concerns accurate characterisation of the source. Even when only one fuel source is suspected, such as at the contaminated site at Old Casey Station, there are significant variations in the refined fuel.

Nevertheless, where a fresh fuel source can be accurately determined, or for a bioremediation treatment where the starting composition is well known, successive changes can be quantitatively ascribed to abiotic and or biotic processes. To do this, it is useful to consider plume degradation in three phases – as early (0-25% losses), middle (25-75% losses) and late (75-100% losses). Using the experimental evaporation of SAB at -20°C as an example, the early stages of evaporative loss are most easily detected by changes in the *i*-C₁₃: pristane ratio. However, during the early stages, quantitative extrapolation from diagnostic ratios to the proportion of mass loss is strongly limited by the analytical precision, as relatively small uncertainties (as in the integration of minor GC-FID peaks - such as pristane) propagate to relatively large uncertainties in the

estimate of mass loss (Figure 2.5). Furthermore, loss of the more volatile components ($n\text{-C}_9$ to $n\text{-C}_{12}$) might indicate extensive evaporative loss, but in the natural environment it will be difficult to distinguish evaporative losses from those produced by biodegradation. During both the early and middle stages of fuel loss, the $i\text{-C}_{13}$: pristane ratio will yield the best overall measure of evaporation. In the late stages $i\text{-C}_{15}$: pristane or $i\text{-C}_{16}$: pristane would provide a better estimate of abiotic loss as the diagnostic ratios involving isoprenoids smaller than $i\text{-C}_{15}$ become asymptotic. However, the use of pristane in diagnostic ratios can be complicated by concurrent biological production of pristane (Raoux *et al.*, 1999) and the difficulties involved in quantifying compounds at low concentrations.

For the early stages of loss through biodegradation, the $n\text{-C}_{12}$: $i\text{-C}_{13}$ ratio would give the best unequivocal measure of biomineralisation. In the natural environment, biological degradation of the most bioavailable components ($n\text{-C}_9$, $n\text{-C}_{10}$, $n\text{-C}_{11}$, naphthalenes and methyl-naphthalenes) would be difficult to distinguish from losses caused by evaporation and dissolution. Although the low-temperature biodegradation experiment using SAB and an Antarctic consortium did not progress beyond the early stage of fuel degradation, other studies have shown that the middle stages of degradation are characterised by complete loss of alkanes, followed by progressive loss of the isoprenoids. The final stage of biodegradation is characterised by near total loss of the isoprenoids leaving little more than the highly recalcitrant UCM (e.g. Westlake *et al.*, 1974; Oudot *et al.*, 1998).

2.7.1 The use of diagnostic ratios in treatability studies

Biodegradation treatability studies are often undertaken as part of the site characterisation phase of a remediation project. These treatability studies can provide an indication of the possible rate of biodegradation under differing treatment strategies by using replicated microcosms and radiolabelled substrates (*cf.* Chapter 3 and Chapter 4). Microcosm studies allow an indirect measurement of contaminant degradation through the use of a proxy hydrocarbon, the relevance of this proxy to the rest of the *in situ* contaminant has to be then assessed. By undertaking both GC-FID analysis and microcosm studies it is possible to assess the contribution of both biodegradation and evaporation. GC-FID analysis provides information on a broader range of contaminants, and assesses the contribution of both biological and abiotic weathering processes within the entire fuel fraction. Unfortunately, GC-FID analysis is destructive and is difficult to use in time course laboratory investigations.

2.7.2 The use of diagnostic ratios at Old Casey Station

The workshop-power house contaminated site at Old Casey Station is contaminated with *ca* 20 000 ppm of petroleum hydrocarbons. A typical GC-FID chromatogram of the hexane-isopropanol soil extract from the contaminated zone is shown in Figure 2.8A and the diagnostic ratios for the field contamination are compared to a neat SAB sample in Table 2.8. The contamination present at the field site contains alkanes in the range of *n*-C₁₁ to *n*-C₂₃, and does not contain significant quantities of any of the naphthalenes. It also has a high pristane: phytane ratio (*ca* 9.9, Table 2.8). Although there is significant batch variation in the pristane: phytane ratio in neat SAB, it is the only diesel fuel which has such a high pristane: phytane ratio and thus the contamination at Old Casey Station is most likely to be SAB.

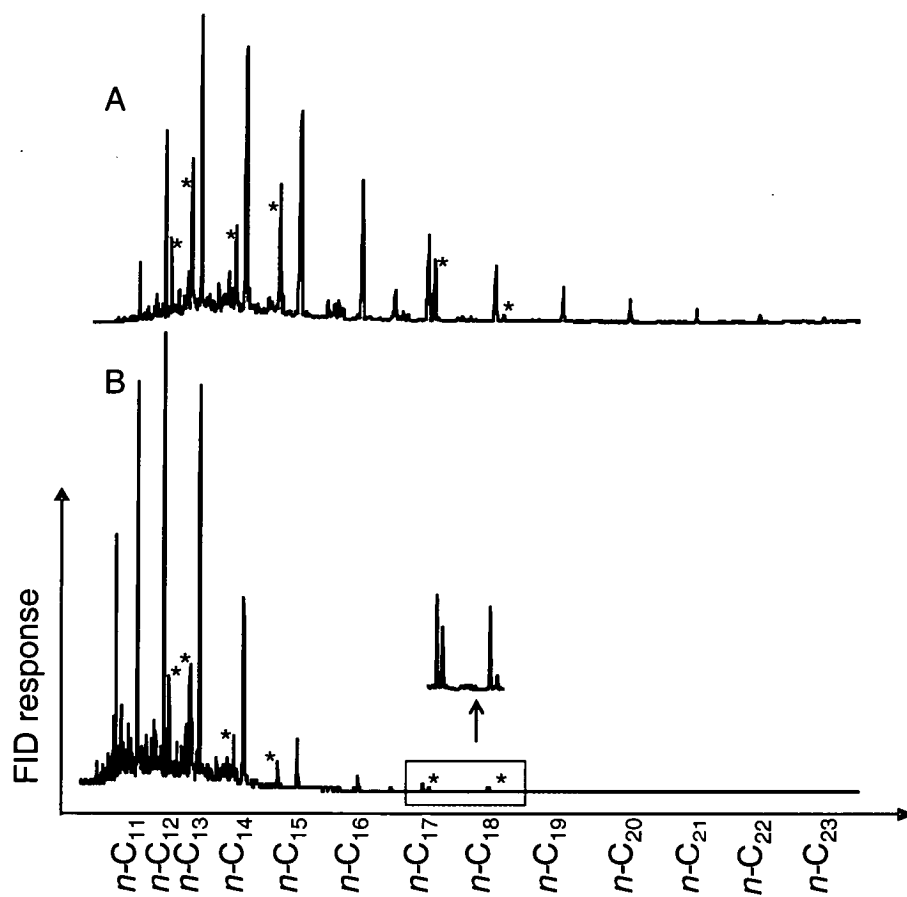


Figure 2.8 Chromatogram of the fuel contamination at Old Casey Station (Panel A) and neat SAB (Panel B). Isoprenoids are shown by *.

It is not possible to gauge how much contamination has been lost in the 15 years since it was spilt; the diagnostic ratios for the spilt fuel were not calculated. As the SAB present within the soil contains significant quantities of $n\text{-C}_{12}$ and $i\text{-C}_{13}$ it is probable that very little of the fuel has been lost through either evaporation or biodegradation.

Table 2.6 Summary of diagnostic ratios in Sections 2.3.1 – 2.3.3 for neat SAB and the petroleum hydrocarbon contamination at Old Casey Station. Light *n*-alkanes: heavy *n*-alkanes represents the sum of *n*-alkanes between *n*-C₉ – *n*-C₂₃: sum of *n*-C₁₇ – *n*-C₂₃. Error bars (1s) are shown for the field samples (n=6).

	SAB 2002	Field site
Source		
pristane: phytane	8.93	9.93 ± 0.19
CPI	0.95	0.97 ± 0.08
Biodegradation		
<i>n</i> -C ₁₂ : <i>i</i> -C ₁₃	4.92	2.73 ± 0.21
<i>n</i> -C ₁₃ : <i>i</i> -C ₁₄	4.05	1.80 ± 0.42
<i>n</i> -C ₁₄ : <i>i</i> -C ₁₅	5.04	3.33 ± 1.36
<i>n</i> -C ₁₅ : <i>i</i> -C ₁₆	1.87	1.81 ± 0.28
<i>n</i> -C ₁₇ : pristane	1.76	1.11 ± 0.03
<i>n</i> -C ₁₈ : phytane	7.2	5.96 ± 0.10
<i>n</i> -alkanes: isoprenoids	5.7	2.49 ± 0.29
resolved (%)	56.4	54.2 ± 5.85
Abiotic weathering		
<i>i</i> -C ₁₃ : pristane	14.5	0.96 ± 0.20
<i>i</i> -C ₁₄ : pristane	18.2	2.80 ± 0.68
<i>i</i> -C ₁₅ : pristane	8.43	2.08 ± 0.66
<i>i</i> -C ₁₆ : pristane	6.3	2.93 ± 0.48
light <i>n</i> -alkanes: heavy <i>n</i> -alkanes	108	8.73 ± 2.19

2.7.3 Limitations

Unfortunately geochemical fingerprinting to identify contaminant sources and subsequent plume evolution is not a precise tool; as Wigger and Torkelson (1997) noted, hydrocarbon fingerprinting is largely a qualitative practice. Slight changes in extraction and/ or sample clean-up methods, GC operating conditions, or integration of chromatograms can have significant effects on the results obtained. Furthermore, a lack of commercial standards and quality control/ assurance practices in commercial and research laboratories increase the variability of results and thus decrease their practicality when comparing different sites, different time within the same site or different remediation strategies.

Variations in the feed stock for the refining process for fuels specially designed for use in cold climates, such as SAB and Jet-A1, has resulted in significant changes within the chemical composition of these fuels, thus limiting the use of diagnostic ratios. A slight change in the concentration of pristane and phytane results in very different ratio based of these constituents (e.g., the pristane: phytane ratio is *ca* 9 in the evaporation experiment in Section 2.6 while it is *ca* 5 in the fuel-standard used for the biodegradation experiment in Section 2.7). Both fuels were obtained from the manufacturer within a twelve month period, and thus the diagnostic ratios can not be used as a true global indicator of biodegradation and evaporation for unknown source spills. Although, it is still possible to compare changes within an experiment or spill site if the source-fuel can be clearly identified, and no additional fuel contamination occurs at the site, or after an initial characterisation has been undertaken.

Another very important limitation with the use of paired compound ratios to indicate evaporation and biodegradation, is that these indices do not work in sites with highly degraded signatures (Prince, 1993). As the fuel becomes progressively more biodegraded, microbes will start degrading the less bioavailable compounds such as the isoprenoids, cyclic aliphatics, hopanes and aromatics. Biodegradation of pristane in SAB at *in situ* soil temperatures is unlikely until extensive fuel loss, and thus ratios relating to pristane are regarded as robust even quite large amounts of evaporation and biodegradation. Unfortunately, the biodegradation microcosm experiments did not proceed to the point where the highly recalcitrant compounds such as pristane began to significantly degrade, even after 5 months incubation.

It should be also be noted that incomplete oxidation of a compound will still result in a decrease in the peak area according to GC-FID – resulting in an overestimation of the amount of biomineralisation of that compound and any diagnostic ratio based on it.

Further work to determine the effects of water washing, sorption, and biodegradation in solid-phase microcosm studies is required for complete understanding of the mechanisms of cold-region fuel attenuation at field sites, but the results determined here validate the use of the matched isoprenoid: *n*-alkane and light: heavy isoprenoid ratios to indicate biodegradation and evaporation respectively.

2.8 Conclusions

Petroleum products are an integral part of human habitation of Antarctica. Our survival on the frozen continent is dependent on the use of low-wax point fuels for transport, heating and power generation. While every effort is made, the harsh environmental conditions of Antarctica mean that petroleum products will be spilt. The Australian Antarctic Program utilizes several light-diesel range fuels to maintain and operate its stations on the continent. These fuels generally contain aliphatic hydrocarbons in the range of *n*-C₉ to *n*-C₁₈, but may also contain *n*-alkanes up to *n*-C₂₆, as well as several acyclic isoprenoids, and trace amounts of aromatic compounds.

The effective management of petroleum-contaminated sites requires the use of indicator or diagnostic ratios. While these diagnostic ratios are commonly used in the management of crude-oil remediation, their use in Antarctic is complicated as many of the recalcitrant compounds contained in crude oil are insignificant components of cold-region fuels. Furthermore, minor alterations in the refining of these fuels can result in large shift in the diagnostic ratios. With characterization of the fuels, and contaminated sites, it is still possible to utilize diagnostic ratios in Antarctica. In fact, diagnostic ratios are an important tool for the optimisation of Antarctic fuel-spill remediation strategies.

Chapter 3

Effects of temperature on the mineralisation of petroleum-hydrocarbons

3.1 Introduction

In temperate and tropical regions, the availability of nutrients, water and oxygen are usually the most important limiting factors for hydrocarbon biodegradation, but in polar environments, low temperature is commonly assumed to be the most significant factor, as cold temperature slows microbial activity (Morita, 1992; Nedwell, 1999). The effects of temperature on biodegradation rates of hydrocarbons in soil from a long-lived plume at Old Casey Station were examined using a series of microcosm experiments. The rates of hydrocarbon mineralisation were determined for a range of temperatures between -2 and 42°C by monitoring the mineralisation of added ^{14}C -octadecane and the disappearance of aliphatic petroleum hydrocarbons in nutrient-amended microcosms.

^{14}C -octadecane was chosen as a proxy molecule for the *in situ* hydrocarbon contamination for several reasons. Firstly, octadecane is at the higher molecular weight range of SAB and thus it will be one of the last alkanes to be biodegraded or volatilised (Chapter 2: Atlas, 1981; Deprez *et al.*, 1999). Secondly, as the ^{14}C -octadecane represented a relatively very small amount of the total *in situ* hydrocarbon contamination (~0.3%), the recovery of $^{14}\text{CO}_2$ from the mineralisation of ^{14}C -octadecane will provide a conservative estimation of the total biodegradation potential. Lastly, the ratio of *n*-C₁₈ to phytane as determined by gas chromatography is often used as a marker of biodegradation (Chapter 2).

Gas chromatography can be used to determine the loss of contaminants from the soil. It is also possible to distinguish between the degree of degradation due to microbial

activity and abiotic loss. This is done by comparing changes in the relative concentrations of a straight chain alkane to the relative concentration of an isoprenoid with a similar vapour point. Both molecules undergo similar abiotic weathering such as evaporation, but the straight chain alkanes are more biodegradable (Chapter 2: Atlas, 1981). Unfortunately, highly recalcitrant molecules, such as hopanes, are not present in SAB. However, the ratio of *n*-alkane: isoprenoid provides a means of monitoring the extent of biological mineralisation (Humphrey *et al.*, 1987). Although microbes have been shown to degrade isoprenoids (Prince, 1993; Bej *et al.*, 2000), the ratio of *n*-C₁₇: pristane and *n*-C₁₈: phytane can be used in the early to middle stages of bioremediation, and with caution, in the very late stages.

3.2 Methods

3.2.1 *Temperature regime of Old Casey Station*

To measure the *in-situ* temperature regime at the Old Casey Station workshop-powerhouse site, a data logger (Prologger, Unidata Australia) with 8 15-Ω resistor thermistors was installed at the site. Two holes within the area of contamination were excavated to the bedrock at a dry and a wet site. Temperature thermistors were placed at depths of 560, 280, 110 mm and just below the surface at the dry site, and depths of 410, 250, 110 mm and just below the surface at the wet site. The data logger and thermistors were installed 10 months prior to the commencement of recording to allow the site to settle. Temperature was measured over the summers 2000/01 and 2001/02 every 5 minutes, and hourly average and actual temperature on the hour was recorded.

3.2.2 *Soils, contaminants and microorganisms*

The contaminated soil used in the microcosm experiments was collected between locations WS6 and WS7 as shown by Deprez *et al.* (1994; 1999). Surface soils with heavy oil stains were not collected.

Approximately 70 kg of highly contaminated soil from a depth of 100-200 mm was collected, sieved to 5 mm grain size, and homogenised. A sub-sample of the material, stored in pre-cleaned glass jars, was frozen and transported to Australia for the experiment. Freezing the sample at -18°C effectively halted microbial activity and thus biodegradation, but was not expected to be detrimental to the microbiota. It was expected that the sampling regime would not substantially change the geochemical characteristics or the microbial community as the site undergoes seasonal and diurnal freeze-thaw cycles.

3.2.3 *Microcosm preparations*

Approximately 800 g of soil was thawed at 4°C, homogenised and kept on ice while each microcosm was prepared. ^{14}C -octadecane (Octadecane-1- ^{14}C 100 μCi , >99% radiometrically pure, Sigma St Louis) was dissolved in 0.86 mL pentane. One hundred microlitres of this solution was added to a further 4.9 mL of pentane, which was added dropwise to the soil while the soil was actively mixed. Thus the 800 g of soil received 0.25 mg (12.5 μCi) of ^{14}C -octadecane, or 36 350 dpm g^{-1} of soil. The soil was left on ice for *ca* 30 minutes to allow evaporation of the pentane prior to further processing. The aliphatic hydrocarbon concentration in the soil was previously measured at *ca* 15 000 mg kg^{-1} . If all of the SAB in the 800 g of soil was to provide carbon for building biomass, about 540 mg NH_4Cl and 100 mg K_2HPO_4 would be required in the soil (based

on carbon (C): phosphorous (P): nitrogen (N) ratio of 106: 16: 1 in biomass (Redfield *et al.*, 1963). For more details pertaining to soil-nutrient requirements refer to Chapter 3). However, because of the potential toxicity of nutrient additions at high concentrations (Walworth *et al.*, 1997), and the expectation that probably only 10-30% of SAB carbon would be used to make biomass (McFarland and Sims, 1991), only one third of the potential fertiliser demand was added (i.e., 178 mg NH_4Cl and 35 mg K_2HPO_4 dissolved in 26.7 mL distilled water was added dropwise to the 800 g of soil, raising the water content from 10.7% to 13.6%). Sub-samples were taken for the determination of dry weight, petroleum hydrocarbon concentration and the solvent-extractable isotope concentration in the soil. Approximately 20 g sub-samples of the prepared soil were added to biometer flasks (Bellco, New Jersey) and 10 mL of 1 M NaOH was added to the trap of each flask. The flasks were sealed and placed in a purging system that allowed controlled replacement of the air and periodic sampling of the NaOH (Figure 3.1). To ensure that the biometer flasks did not become anoxic, they were flushed with *ca* 2 L of air once a week. The air was bubbled through water in an impinger in order to supply humidified air to each microcosm and to minimise water loss during purging. A dreschel bottle filled with 1M NaOH was used on the air outlet to trap expired $^{14}\text{CO}_2$.

Microcosms were incubated at 0, 4, 10, 15, 20, 28 and 37°C in triplicate, and in duplicate at -2 and 42°C. Several sterile controls were prepared to account for abiotic loss of the SAB and ^{14}C -octadecane. Chemically inhibited controls were prepared with the addition of 0.05 g sodium azide to the soil. Heat-killed controls were prepared with *ca* 3 mL saturated HgCl solution per microcosm and then autoclaved at 121°C for 20 min. The chemically inhibited controls were incubated in duplicate at 10 and 37°C and singularly at 15°C. Four heat-killed controls were incubated at 10°C.

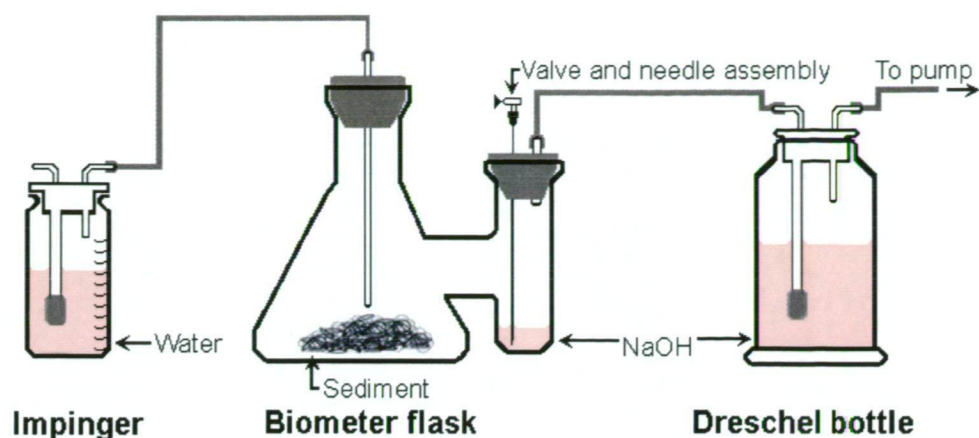


Figure 3.1 Design of the microcosms used in the experiments to measure mineralisation of ^{14}C -octadecane to $^{14}\text{CO}_2$.

The microcosm CO_2 traps were sampled once a day for the first week, then three times a week for the next three weeks and twice weekly for a further two weeks.

To measure the amount of ^{14}C -octadecane mineralised in each biometer flask, the isotope converted to $^{14}\text{CO}_2$ was measured by removing *ca* 1 mL NaOH from each trap and replacing it with 1 mL of fresh NaOH. The removed NaOH was mixed with 9 mL scintillant (Starscinttm, Packard) and allowed to equilibrate for at least 24 hours. Radioactivity was measured on a 2250CA Tri-carb Packard Liquid Scintillation Analyser. Quench was accounted for by the Automatic Efficiency Control-quench curve; generated for quenched ^{14}C -standards (Amersham). The radioactivity in the trap at each time was calculated by multiplying the radioactivity in each *ca* 1 mL sample by the ratio of volume of sample removed to total trap volume. Tracer recovery (and thus percentage octadecane mineralised) at each time was calculated by the addition of the trap radioactivity with all prior sample (disregarded) radioactivities.

3.2.4. *Hydrocarbon analysis of the soil*

At the end of the experiment, 50 µg of squalane (Sigma, >98% pure) dissolved in hexane was added to 5 g of soil from each microcosm. Hydrocarbon extractions were performed with the addition of *ca* 35 mL of isopropanol: hexane (2:1). The samples were sonicated in a bath at 150 Hz for 10 min and then centrifuged at 25 000 x *g* for 5 minutes. The supernatant was then collected. The extraction procedure was repeated and the two supernatants combined in a separation funnel. Hexane and water were added to the combined supernatants to a final ratio of water: isopropanol: hexane (1:1:1). The combined supernatants were shaken and allowed to settle for at least 30 minutes, after which the hydrocarbon fraction was collected and concentrated by rotary evaporation to a final sample volume of *ca* 1.5 mL.

The aliphatic fraction from 1 mL of the concentrated hydrocarbon extracts were separated by column chromatography. The columns consisted of 1 g alumina (Ajax (Lab Chem) neutral, activity 1) on top of 2 g silica gel (Mallinckrodt, 100-200 mesh 60Å). Both silica and alumina were soxhlet cleaned and heat-activated at 60°C for at least 24 hours before use. The aliphatic fractions were eluted from the columns with 12 mL of hexane. The fractions were then concentrated to *ca* 1.5 mL by rotary evaporation and stored at -20°C until analysed.

The aliphatic fractions were analysed using a Varian 3410 gas chromatograph fitted with a septum-equipped programmable injector and flame ionisation detector. Analyses were performed using a 50 m non-polar methyl-silicone-fused silica capillary column (HP-1, 0.32 mm internal diameter, 0.23 µm film thickness) with helium as the carrier gas. GC conditions were 35°C for 1 min then ramped to 120°C at 30°C min⁻¹ then to 310°C at 4°C min⁻¹ and then held for 15 min. Reported aliphatic hydrocarbon values

were approximated by the sum of all the GC-resolved peak areas and the area of the unresolved complex mixture in the aliphatic fraction normalised to the added squalane standard.

3.3 Results and discussion

3.3.1 Soil thermal regime at Old Casey Station

The *in situ* soil temperatures for Old Casey Station during summer are shown in Table 3.1 (with the raw data shown in Appendix 10.2). The maximum soil temperature recorded was 28.2°C at the surface of the dry site at midday on the 27th December 2000. The average surface temperature over the summer period, at both sites, was *ca* 4°C. Unsurprisingly, soil moisture content acted as a thermal buffer with surface soil temperatures fluctuating more within the dry site. Previously it has been found that minimum surface soil temperatures correlate with ambient air temperatures (Beyer *et al.*, 2000). To investigate factors affecting soil temperature, ambient air temperature (Shepherd, 1999) and incoming solar radiation (Guichard, 1999) data between 12th December 2000 and 26th January 2001 were obtained and Pearson product moment correlation coefficients (*r*) were derived. In this study, no significant correlations between ambient air and surface soil temperatures at either of the sites studied were found. The highest correlation with ambient temperature was between daily minimum ambient and maximum soil temperatures at the wet site (*r* = 0.25, but this was not statistically significant). Conversely, daily maximum soil temperatures and averaged incoming solar radiation were strongly correlated at both the wet and dry sites, *r* = 0.74 (*p*<0.05) and *r* = 0.79 (*p*<0.05) respectively.

Table 3.1 Hourly averaged *in situ* soil temperatures during summer at Old Casey station, Antarctica at two sites, a relatively dry and wet site. Maximum and minimum temperatures represent the hourly averaged temperatures.

Date	Max Temp (°C)	Min Temp (°C)	Mean \pm 1s (°C)	Max Temp (°C)	Min Temp (°C)	Mean \pm 1s (°C)
Surface						
	Wet			Dry		
Dec-00	23.2	-0.8	6.6 \pm 6.2	27.7	-4.2	6.6 \pm 7.8
Jan-01	20.9	-1.3	5.4 \pm 5.0	24.7	-3.4	4.9 \pm 6.2
Nov-01	12.2	-10.8	-1.9 \pm 4.8	13.8	-12.8	-1.4 \pm 6.1
Dec-01	21.2	-2.7	4.4 \pm 6.2	25.5	-6.6	4.4 \pm 7.6
110 mm						
	Wet			Dry		
Dec-00	13.7	-0.1	5.3 \pm 3.5	15.7	0.0	5.0 \pm 4.3
Jan-01	12.4	0.9	4.9 \pm 3.0	14.4	0.6	4.1 \pm 3.2
Nov-01	-0.1	-8.0	-2.8 \pm 1.8	1.9	-9.1	-2.7 \pm 2.5
Dec-01	12.3	0.1	3.3 \pm 3.0	14.6	-0.3	3.6 \pm 4.1
250/ 280 mm						
	Wet			Dry		
Dec-00	9.0	-0.1	4.5 \pm 2.3	7.6	0.0	2.5 \pm 2.3
Jan-01	8.0	1.3	4.3 \pm 1.8	7.8	1.1	3.6 \pm 1.6
Nov-01	-1.6	-6.1	-3.0 \pm 1.2	-1.5	-7.0	-3.3 \pm 1.5
Dec-01	7.3	0.3	2.7 \pm 1.5	6.3	0.0	1.4 \pm 1.5
Bed rock						
	Wet			Dry		
Dec-00	7.2	-0.1	3.9 \pm 2.0	3.5	-0.6	0.4 \pm 1.3
Jan-01	6.8	1.6	4.0 \pm 1.3	4.9	1.3	3.0 \pm 0.9
Nov-01	-1.9	-5.5	-3.2 \pm 1.0	-2.7	-6.4	-4.1 \pm 1.3
Dec-01	5.0	-0.3	2.1 \pm 1.1	1.0	-0.6	-0.2 \pm 0.3

3.3.2 Mineralisation of the ^{14}C -octadecane

Mineralisation of ^{14}C -octadecane confirmed that SAB in nutrient-amended contaminated soils from Old Casey Station can be biodegraded under a wide range of temperatures (Figure 3.2) without microbial augmentation. The amount of ^{14}C -octadecane mineralised after 40-48 days increased with increasing temperatures. Less than 0.2% of the ^{14}C -octadecane was recovered as $^{14}\text{CO}_2$ over 40 days at -2°C , while *ca* 35% was recovered as $^{14}\text{CO}_2$ after 48 days at 42°C . Apparent abiotic mineralisation of the ^{14}C -octadecane was minimal, with an average of only 0.3% isotope recovery in the sodium hydroxide traps of the sterile controls. Only very small amounts

of mineralization occurred in the -2°C microcosm. The mineralisation at -2°C is not significantly different from the abiotic controls and indicates that insignificant mineralisation occurs without free water in the bulk soil. For temperatures at and above 0°C, three distinct types of mineralization profile occurred, that could be assigned to low (0 and 4°C) medium (10, 15, 20 and 28°C) and high (37 and 42°C) incubation temperatures. These profiles were distinguished by mineralisation rate and the length of the initial lag phase.

In the lower temperature microcosms (0 and 4°C), the lag phase lasted six or more days. The ^{14}C -octadecane was then slowly mineralised with only 6% recovered as $^{14}\text{CO}_2$ after 43 days at 4°C. Little or no mineralisation at 0°C was expected as free water is required to provide a milieu for microbial growth. Appreciable mineralisation of alkanes in the environment at these temperatures is not expected in the short term; octadecane had an estimated half-life of 359 days at 4°C in these experiments. Although the 4°C microcosms were slow to initiate mineralisation, the final recovery of the isotope in the NaOH (5.8%) was similar to the recovery at 10°C (6.0%). The longer lag phase at 4°C compared to 10°C was expected; the similar $^{14}\text{CO}_2$ recovery in both microcosms over 40 days was not as low temperatures slow the rate of microbial activity (Morita, 1992). The similar isotope recoveries at 4 and 10°C indicate that the microbes responsible for hydrocarbon degradation at these temperatures have similar biodegradation potentials but are capable of faster reproduction at 10°C.

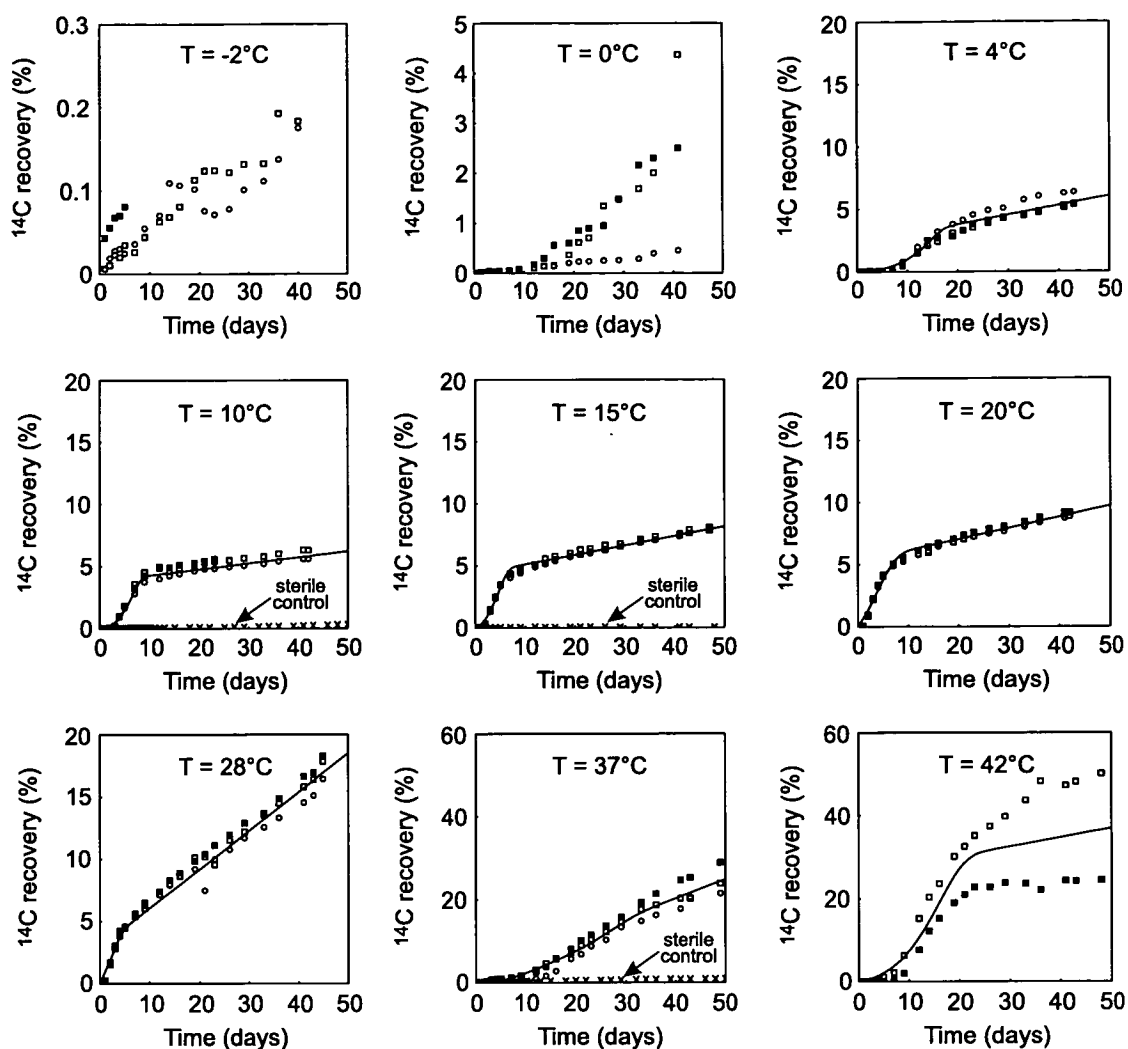


Figure 3.2 Recovery of $^{14}\text{CO}_2$ from ^{14}C -octadecane in microcosm experiments. The different symbols identify replicates. The best-fit production curves from the Trefry and Franzmann (2003) (exponential growth rate) are also plotted (see Chapter 5).

In the mid range temperature microcosms (10 to 28°C) the lag phase was short (< 3 days), and mineralisation commenced almost immediately. The main difference between the low and the mid temperatures was the lack of initial lag phase in the mid range temperature microcosms. This overall lack of a lag phase might be a physiological response to the temperature fluctuations normally experienced at Old Casey Station. The microbiota is presumably well adapted to respond quickly to a rapidly changing thermal

regime to take full advantage of the *in situ* diurnal warm periods. The actual soil temperature between 4th December 2000 and 27th January 2001 fluctuated between -4.1 and 28.2°C (Appendix 10.3), with the wet site fluctuating less, presumably due to thermal buffering by water. A rapid response by cold-region microbiota incubated in this temperature range is well documented (Whyte *et al.*, 1996; Aislabie *et al.*, 1998; Whyte *et al.*, 1998; Mohn and Stewart, 2000).

In the higher temperature microcosms (37 and 42°C) there was a pronounced lag phase (approximately 9 days), followed by a sharp increase in mineralisation rate that remained high even after 40 days of incubation. The incubation temperatures chosen for these microcosms were intended to bracket the expected temperature range for growth of Antarctic microbes. Antarctic microbes tend to be psychrotrophic (Franzmann, 1996; McCammon *et al.*, 1998; Smith *et al.*, 2000), and generally have an optimum growth temperature (T_{opt}) of around 25°C and a maximum growth temperature (T_{max}) below *ca* 37°C (Morita, 1992). Hence, the experiments were limited to the range -2 to 42°C. However, it was found that the high temperature microcosms, at 37 and 42°C, mineralised the most ¹⁴C-octadecane. One possible explanation is that the autochthonous microbiota may contain low numbers of mesophilic species, as they may experience brief periods of surface soil temperatures of up to 38°C (Beyer and Bölder, 1999). Vincent and Quesada (1997) suggested that a 'perfect fit' of a microorganism to its environment in all niche dimensions is neither likely, nor a strategy for long-term evolutionary survival. Alternatively, mesophilic hydrocarbon-degrading organisms may have been introduced to the soil with the contaminating fuel, where they remained in low numbers until warmed in the nutrient-rich microcosms. Initially, the psychrotrophic species in the population would have been unable to mineralise hydrocarbons at the

higher temperatures experienced in the microcosms, and it would have taken several days for the mesophilic microbes to reach adequate numbers for measurable mineralisation to occur. This is consistent with the outcomes of the mineralisation experiment. Mohn and Stewart (2000) found that the mineralisation of ^{14}C -dodecane in contaminated Arctic soils increased with increasing temperature, from 7 to 30°C. Above 22°C temperature increases had little effect on the mineralisation rate. Many Antarctic species have an optimal temperature for growth near 23°C with no growth occurring in these species at 30°C (Franzmann, 1996), so the results were feasible, but somewhat surprising, although not so if the organisms were introduced from temperate or tropical environments with the hydrocarbon contamination.

3.3.3 *Post incubation analysis*

At the end of the incubation periods, the contaminated soils from the microcosms were analysed by GC-FID to investigate the fate of the non-radiolabeled aliphatic hydrocarbons in the soil. The soil used in this experiment had residual contamination of *ca* 15 000 mg aliphatic hydrocarbons kg^{-1} . The final concentration at each temperature is shown in Figure 3.3A. The difference in aliphatic concentration in the heat-killed and chemically inhibited controls is presumably due to loss of hydrocarbons during the heat sterilisation procedure. For microcosms incubated in the range of 10 - 42°C there is a general linear trend of decreasing hydrocarbon concentration with increasing temperature.

Two biodegradation ratios commonly used to indicate biodegradation are shown in Figure 3.3B. These ratios have been plotted as percent change from the pre-treatment ratio to allow both ratios to be shown on one graph.

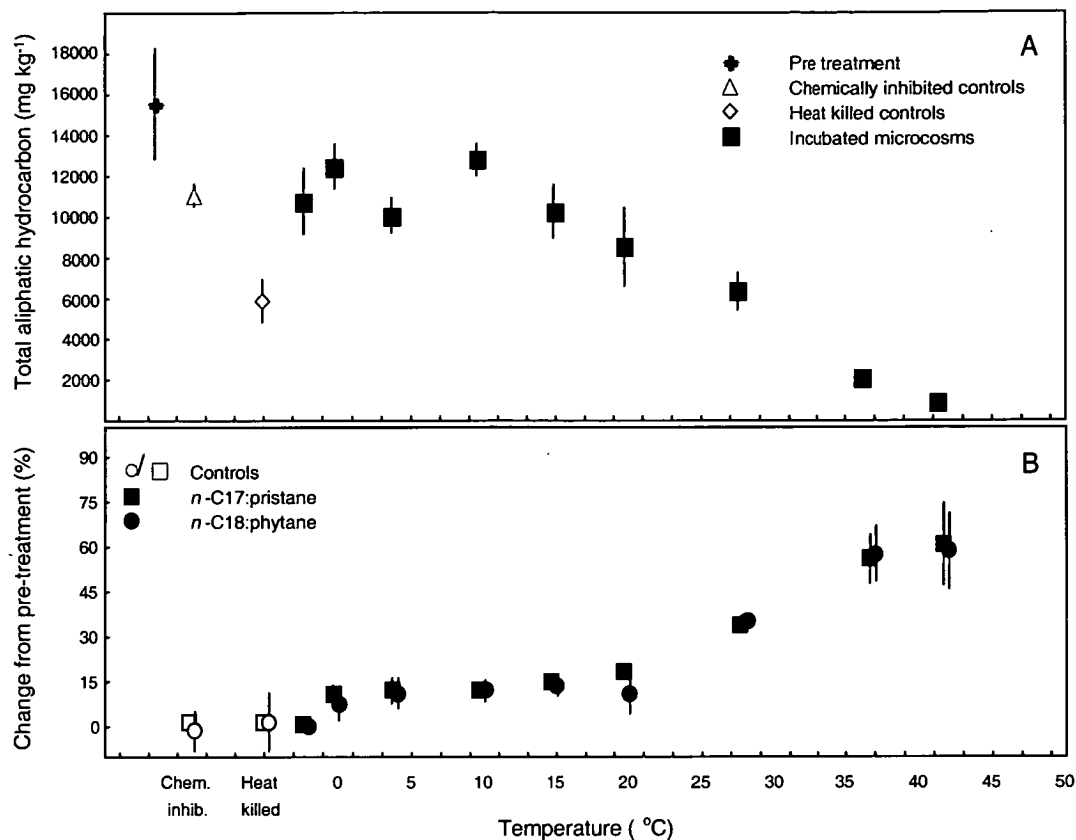


Figure 3.3 Gas chromatography results showing total aliphatic hydrocarbons in the pre- and final microcosm soils in panel A; and percentage change from the pre-treated soil for *n*-C₁₇: pristane and *n*-C₁₈: phytane in panel B. Control data is from the 15°C microcosms. Error bars (2s) are shown.

Gas chromatography showed that the total aliphatic hydrocarbon concentration in the heat-killed controls was greatly reduced (Figure 3.3A), while the biodegradation ratios were unchanged (Figure 3.3B). As *n*-C₁₇: pristane and *n*-C₁₈: phytane have similar vapour pressures they are equally affected by evaporation, confirming that the hydrocarbon loss in these controls occurred during sterilisation (*cf.* Figure 3.3A) The two biodegradation ratios followed a similar trend, a slight increase from -2 to 0°C, constant between 0 and 20°C and then increasing with increasing temperature. The increase at 0°C is presumably due to water availability, while the increase at

temperatures at and above 28°C may be due to increased bioavailability of the alkanes, and of course the faster rate of mineralisation achieved at higher temperatures (see Figure 3.2)

3.4 Conclusions

The clear conclusion from these results is that increasing the soil temperature, in the presence of nutrients and water is likely to yield appreciably better bioremediation of petroleum spills at Old Casey Station. Introduction of exogenic organisms is not needed and should not be undertaken because of the risks associated with introduced species into Antarctica (Manzoni, 1992; Smith, 1996). It is also likely that bioaugmentation is not required in the Arctic (Filler *et al.*, 2001).

The main implication for remediation of the petroleum-contaminated site at Old Casey Station from this study is that a high temperature (42°C or higher) bioreactor-type system would yield the most rapid biodegradation. The technical difficulties and expenses associated with contaminated site management will always incorporate value judgements on the tolerance of risk and costs, which incorporates economic and political information (NEPC, 1999). *In situ* biodegradation using nutrients and other amendments is still possible at soil temperatures that occur naturally in summer at Old Casey Station. The average soil temperature measured during December-January 2000-01 at 250 mm was *ca* 4°C. Based on the radiometric results presented here, 4°C should be sufficient for significant *in-situ* mineralisation of the petroleum hydrocarbon contamination at this site. The paucity of *in situ* degradation at this site, even after 15 years since the contaminating activities ceased, must be due to environmental factors other than temperature. Beyer *et al.* (2000) suggested that free water availability may be the primary determining factor to microbial growth in soil around Old Casey Station.

Treatments involving nutrient and water amendments, without heating, might ultimately deliver comparable levels of contaminant reduction, at much lower costs, but remediation will take appreciably longer. Further work into quantifying the effects of limited nutrients and water and also the effect of freeze-thaw cycles is required before an informed decision regarding the most appropriate remediation strategy on the basis of cost-benefit-risk analysis can be made (Chapter 4).

Chapter 4

The effects of nitrogen and water on the mineralisation of petroleum-hydrocarbons

4.1 Introduction

In Chapter 3 it was established that low temperatures inhibit microbial activity and there is generally a positive correlation between temperature and biodegradation through the range of -2 to 42°C for soils around Old Casey Station. Although, the average summer air temperature is only *ca* 4°C at Casey Station (Shepherd, 1999), daily surface soil temperatures in summer commonly exceed 20°C and maximum temperatures have been recorded above 28°C (Appendix 10.3). Even at relatively low soil temperatures of 10°C, microcosm experiments predict that *in situ* degradation is possible (Chapter 3), although rates were slower than at higher temperatures. However, an understanding of the other factors that limit biodegradation, such as nutrients and water availability, are also required to design a bioremediation strategy that is suitable for petroleum contaminated sites in Antarctica.

The importance of nutrients to microbial processes has long been known. Nitrogen is required in amino acids, and phosphorous is involved in energy transport as adenosine triphosphate and also occurs in nucleic acids and lipids. Compositional analysis of microbial biomass indicates that C, N and P occur roughly in the ratio of *ca* 106:16:1 respectively (Redfield *et al.*, 1963). Contaminated soils that have intrinsically low N and P will require nutrient additions to allow a sufficient increase in biomass for environmentally significant hydrocarbon degradation to occur. To estimate how much nutrient amendment is required, the so called Redfield ratio (106:16:1) is commonly cited as an optimal C: N: P target. This theoretically determines the nutrients required

for total hydrocarbon conversion to biomass, although the application of the Redfield ratio to mineralisation experiments does not consider that the majority of the carbon that is mineralised is generally converted to CO₂ and is then lost from the system. Also, inorganic species of nitrogen can be lost from the system through nitrification-denitrification processes (Stevenson and Cole, 1999). In practise C: N ratios ranging from 14:1 (Møller *et al.*, 1995) up to 560:1 (Hoyle *et al.*, 1995) have been proposed as 'suitable' or 'optimal' for biodegradation.

In some instances, when intrinsic nutrient levels are already adequate for biodegradation, nutrient amendments have no significant effect on remediation rates (Margesin and Schinner, 1997). Other studies, including those by Bossert and Bartha (1984), Fayad and Overton (1995) Manilal and Alexander (1995), and Raymond *et al.* (1976), found that biodegradation can even be inhibited by nutrient additions. Different nutrient levels or amendments result in a range of degradation rates due to the intimate relationship between nutrient and water concentrations in the soil matrix. Nutrients are known to become toxic to soil microbiota at high osmotic potentials (Walworth *et al.*, 1997), so it is important to not only maintain sufficient N and P (and possibly other micronutrients), but to ensure that soil moisture is also adequate. Walworth *et al.* suggested reporting nutrient concentrations as a function of soil water rather than the more commonly cited concentration relative to dry soil weight. This will allow better comparisons of the effects that nutrient additions have on microbial mineralisation of hydrocarbons in different studies, from a range of environments, under a variety of management regimes. Walworth *et al.* also noted that soil type was an important factor influencing water holding capacity and thus nutrient concentration in the soil water.

In their studies on the effects of nutrients on the bioremediation potential of Arctic microbes, Braddock *et al.* (1997) showed that for a range of nutrient amendments between 1666 and 6666 mg N kg-soil-H₂O⁻¹ (recalculated to quoted water contents) the lowest nutrient concentration of 1666 mg N kg-soil-H₂O⁻¹, which equated to 50 mg N kg dry soil⁻¹, yielded the fastest rate of mineralisation. Similarly, Walworth *et al.* recommended nutrient amendments of *ca* 2000 mg N kg-soil-H₂O⁻¹, irrespective of the concentration of hydrocarbon contamination in the soil, and they found that much higher N concentrations could limit degradation. If the nutrient amendments used by Mohn and Stewart (2000) in their radiometric microcosm study are expressed in terms of N per unit of water, then in Arctic soil amendments of *ca* 11 200 mg N kg-soil-H₂O⁻¹ were found to be inhibitory to alkane mineralisation. Similarly, Durant *et al.* (1997) determined that even quite low levels of nutrient additions can be inhibitory to contaminant mineralisation when low nutrient concentrations are not the main limitation to biodegradation. They found that an 85 mg N kg-soil-H₂O⁻¹ amendment in coal-tar-contaminated sand inhibited the degradation of naphthalene because of competition by Fe²⁺ in the sand during oxidation.

Clearly, getting the right nutrient-water balance is of major importance when considering remediation of petroleum contaminated soils (Riser-Roberts, 1998). This is especially relevant in terrestrial Antarctica where liquid water is a scarce resource. Polar deserts typically have extremely low humidity and precipitation and water retention is further limited by the poor water holding capacities that characterise many Antarctic soils (Campbell *et al.*, 1994). In some instances the water balance is further compromised by unusually high salt contents that characterise many Antarctic soils (Kennedy, 1993).

In this Chapter radiometric microcosm experiments and gas chromatography (GC) are used to determine the biodegradation of aliphatic hydrocarbons under a range of nutrient concentrations and moisture contents in soils from Old Casey Station. To further explore the relevance of expressing nutrients relative to soil water, rather than dry soil weight, treatments in which water was varied relative to constant nutrient-soil concentrations are compared, and in which nutrients were varied relative to constant soil water. The reduction in total aliphatic hydrocarbons and changes in geochemical indices that are sensitive to biodegradation were used as tracers to help elucidate the role of nutrients and water in biodegradation.

4.2 Methods

4.2.1 Rationale

As there are currently no published studies that have quantified the effects of nutrient-water-soil interactions on biodegradation of hydrocarbons in Antarctic soils, this study was designed to test if the parameters that had been shown to be significant for alkane mineralisation in Arctic soils were also important in Antarctic soils. While contaminated Arctic soils have fundamental differences in composition, texture and thermal regimes from the Antarctic soils, it was decided to examine the effects of nitrogen and water on petroleum mineralisation as these are major limiting factors in Arctic soils. To examine whether the petroleum degradation in contaminated soil at Old Casey Station is limited by nutrients and water, biodegradation across a range of concentrations from no additions, to very high nutrient or water amendments were examined.

To allow comparison between these experiments and the previous study into the effect of temperature on bioremediation in petroleum contaminated soil from Antarctica (Chapter 3), the microcosm experiments described here were prepared as previously described. This study was divided into several tests as shown in Table 4.1. Fresh soil (soil II) was collected from the same site that was investigated in Chapter 3. Soil from the temperature experiment from 2 years previously (Chapter 3 – soil I) was also included to check whether there were significant differences between the two experimental batches. The soil used within Chapter 3 (soil I) was stored in a sealed glass jar for *ca* 2 years at -18°C prior to use in the current study. The main focus of this Chapter is the investigation of the effect of changing water and nutrient concentrations on soil II (Table 4.1). Three main investigations were carried out: no nutrient amendments, water amended treatments with constant C: N ratios, and varied C: N ratios with constant water contents. The microcosms ranged from the unamended nutrient and water contents of 85 mg N kg-soil-H₂O⁻¹, up to *ca* 28 000 mg N kg-soil-H₂O⁻¹ by the addition of dry NH₄Cl. The N: P ratio was fixed at 16:1 for all amended treatments by the addition of K₂HPO₄, and water contents ranged from 9.5 to 39.8% by weight. Phosphorus is sparingly soluble in most soil water systems and it is much more difficult to over fertilize soils with phosphorus (Stevenson and Cole, 1999), hence nutrient amendments relative to N concentration are the main variable of concern.

Table 4.1 Microcosm conditions used to test the effects of water and nutrient additions on the mineralisation of ^{14}C -octadecane and degradation of the aliphatic components of SAB at 10°C. Nitrogen concentration was estimated by summing natural and added N. The C:N ratio was calculated from an initial hydrocarbon concentration of 15 000 ppm. Repeat microcosm data are from Chapter 3; A sub-sample of soil I was incubated as part of the previous study for 45 days and a different sub sample was incubated as part of these experiments for 95 days. Treatments indicated with an asterisk are shown twice on the table.

	Number of Replicates	Water (wt %)	Added Nitrogen (mg N kg soil ⁻¹)	Total Nitrogen (mg N kg-soil-H ₂ O ⁻¹)	C: N	Sterilization
3.1 Controls						
Chem. Inhib.	4	19.9 (± 0.8)	189.9	535.0 (± 23.9)	64: 1	HgCl
Heat killed	4	25.1 (± 5.3)	189.9	437.3 (± 99.8)	64: 1	HgCl + Autoclaved
3.2 Repeat microcosm experiment using soil I after 2 years storage						
Soil I	3	13.6	58.3	420	185: 1	-
3.4 Unamended						
Water removed	3	9.5	-	95	127: 1	-
Field	3	10.5	-	85	127: 1	-
3.5 Water amended treatments with constant nutrients						
Low	3	9.9	189.9	2012	64: 1	-
Medium	7	10.5	189.9	1710	64: 1	-
High	2,1	28.6, 39.8	189.9	697, 508	64: 1	-
3.6 Nutrient amended treatments with constant water						
Unamended*	3	10.5	-	85	127: 1	-
Low	3	10.5	173.3	1570	70: 1	-
Medium*	7	10.5	189.9	1710	64: 1	-
High	3	10.5	3244	27944	4: 1	-

4.2.2 Site characterization

The soil used in this experiment was collected from a contaminated site at Old Casey Station near the old workshop/powerhouse (Chapter 1, locations WS6 and WS7 of Deprez *et al.*, 1994; 1999). The soil was collected in the 2000-01 austral summer, sieved

to 5 mm into a 20 L metal container, then frozen at -18°C and returned to Australia for analysis. All experimentation was completed within 12 months of soil collection.

The background concentration of nitrogen and phosphorus in the initial homogenised bulk soil was determined in triplicate. Organic nitrogen was determined by Flow Injection Analysis (FIA) after Kjeldahl extraction (sulphuric acid digestion). Inorganic nitrogen was determined after extraction with 2M KCl. The total nitrogen, which is the sum of the two fractions, was 10.3 ± 0.6 mg N kg dry soil⁻¹. Average phosphorus, also determined after Kjeldahl digestion, was 28.3 ± 2.1 mg P kg dry soil⁻¹. The average soil pH at Old Casey Station is 7.6 ± 0.9 (n=161: method H+ 4-86 APHA *et al.*, 1999).

4.2.3 Hydraulic properties of the soil

Gravimetric moisture contents were determined by the change in weight after drying at 105°C for 24 hours. Saturated hydraulic conductivity (K_{sat}) was determined in both hydrocarbon contaminated and cleaned soil. The hydrocarbon contamination was removed from *ca* 500 g of soil by soxhlet extraction over 8 hours using 1:1 acetone: ethylether. After extraction, the soil was transferred to a wide mouth beaker and left in the fume cupboard to dry.

K_{sat} was determined by the constant head method (Klute and Dirksen, 1986). Degassed, distilled water was used as the test fluid as it was considered to most closely resemble snow melt. The hydraulic conductivity columns were packed to a bulk density (P_b) of 1.95 g cm⁻³; the tests were conducted isothermally at 20°C. The average K_{sat} of the contaminated soil was 13.88 ± 4.51 (n = 30) cm day⁻¹ compared with 4.56 ± 2.45 cm day⁻¹ for the cleaned soil. Such increases in K_{sat} have been shown in hydrocarbon contaminated soils from the Arctic due to changes in particle aggregation and pore space

distribution (White and Coutard, 1999; White and Williams, 1999), and this is a factor that might affect remediation design (Rike *et al.*, 2003).

4.2.4 Microcosm preparation

A full description of the microcosm preparation is given in Section 3.2.3. In brief, 850 g of soil II was thawed at 4°C overnight. It was then homogenised and kept on ice while each microcosm was prepared. ^{14}C -octadecane was added to the soil as a surrogate to trace *in situ* mineralisation. Squalane, a large multiple branched alkane which is known to be resistant to microbial degradation (Watkinson and Morgan, 1990), was also added to act as a biodegradation internal standard for GC analysis. The 850 g of soil received 0.87 mg (63.14 μCi) of ^{14}C -octadecane (150 700 dpm g^{-1} of soil) and 78 mg squalane kg^{-1} . Sub-samples were taken for the determination of dry weight and petroleum hydrocarbon concentration. The initial aliphatic hydrocarbon concentration in the test soil was *ca* 15 000 mg kg dry soil $^{-1}$, of which *ca* 82 mg kg dry soil $^{-1}$ was octadecane. Thus the ^{14}C -octadecane amounted to *ca* 1% of the total octadecane in the soil.

Thirty three microcosms were prepared to study nine different concentrations of N and P by varying the amount of nutrient added or the water content, as shown in Table 4.1. The ratio of N and P additions was held constant in all microcosms at 16:1. Each microcosm consisted of *ca* 20 g of the prepared soil in a biometer flask (Bellco, New Jersey) with 10 mL of 1 M NaOH in the trap. All microcosms were incubated at 10°C. Several sterile controls were included to quantify abiotic loss of the hydrocarbons. Chemically inhibited controls were prepared by adding *ca* 3 mL of saturated HgCl solution to the soil. Heat-killed controls were prepared with *ca* 3 mL saturated HgCl

solution per microcosm which were then autoclaved at 121°C for 20 min. The controls were also incubated at 10°C.

The microcosms were sampled every 12 hours for the first two weeks and thereafter every Monday, Wednesday and Friday. In Chapter 3, *ca* 3.3×10^{-4} % of the total isotope added to each control microcosm was recovered in the dreschel bottle CO₂ traps after actively purging with fresh air (see Figure 3.1). Negligible ¹⁴CO₂ was expected in the headspace of each flask at any time and thus aeration was supplied to the microcosms by opening the flasks for a brief period during sampling to allow the microcosms to equilibrate with the surrounding atmosphere to ensure oxygen supply was not limiting to hydrocarbon mineralisation. Mineralised ¹⁴C-octadecane was measured on a 2250CA Tri-Carb Packard Liquid Scintillant Analyser as previously described in Section 3.2.3.

4.2.5 Hydrocarbon analysis of the soil

At the end of the experiments 1000 µg nonacosane (C₂₉H₆₀) dissolved in hexane was added to 10 g of soil from each microcosm for hydrocarbon quantification. The aliphatic hydrocarbons were extracted by solvents and separated on a silica-alumina column as described previously (Section 3.2.4). Aliphatic fractions were analysed using a Varian 3410 GC fitted with a septum-equipped programmable injector and flame ionisation detector. Analyses were performed using a 50 m non-polar methyl-silicone-fused silica capillary column (HP-1, 0.32 mm internal diameter, 0.23 µm film thickness) with helium as the carrier gas. All samples were run at 40°C for 1 min then ramped to 120°C at 30°C min⁻¹ then to 310°C at 4°C min⁻¹ and then held for 15 min. Estimates of total fuel concentrations were approximated by the sum of all the GC-resolved peaks and the

unresolved complex mixture in the aliphatic fraction normalised to the known concentration of the *n*-C₂₉ internal standard. Squalane was used as a conservative tracer.

4.3 Results

4.3.1 Control microcosms

Both heat killed and chemically inhibited controls were used in this experiment to account for the abiotic loss of hydrocarbons. The use of cytotoxic chemicals to sterilise controls is often not totally effective because tolerant microbes are commonly found in contaminated sites. While autoclaving is a more effective sterilization procedure, it could potentially promote hydrocarbon volatilization (*cf.* Figure 3.3). There was only a slightly higher isotope recovery in the NaOH of the heat killed controls ($0.39 \pm 0.26\%$) than the chemically inhibited controls ($0.16 \pm 0.10\%$); thus the control data shown in Figure 4.1A represents an average of the isotope recoveries in both the heat killed and chemically inhibited microcosms. There was a $13.4 \pm 3.2\%$ average reduction in total aliphatics in both the heat killed and chemically inhibited control microcosms (Figure 4.1B, Table 4.2), with no statistically significant difference ($p < 0.05$) between the two types of control microcosms. The abiotic reduction in aliphatic hydrocarbons was attributed to loss of the volatile diesel compounds in the range of nonane – dodecane; there was very little isotope recovery in the NaOH trap during the 95 days incubation period indicating an absence of biological degradation. Also, because biodegradation indices such as *n*-C₁₇: pristane did not change appreciably in the control samples (Figure 4.1C), the radiometric data for the microcosm treatments reflected biodegradation and not evaporation. By using both types of controls it can be concluded that there was

insignificant biological mineralisation in the abiotic controls during the incubation period.

Table 4.2 Gas chromatography results for pre and post incubation (95 days at 10°C) microcosm soils. Soil I did not contain squalane and thus these indices can not be calculated. Results are the average values and 1s of replicates shown in Table 4.1. Isoprenoids are abbreviated as pristane, pr; phytane, ph and squalane, sq.

Nitrogen concentration (mg N kg soil-H ₂ O ⁻¹)	Total aliphatic hydrocarbons (mg kg dry soil ⁻¹)	Resolved fraction (%)	pr: ph	<i>n</i> -C ₁₇ : pr	<i>n</i> -C ₁₈ : ph	<i>i</i> -C ₁₃ : sq	<i>i</i> -C ₁₄ : sq	<i>i</i> -C ₁₅ : sq
Pre soil II	14183 ± 1414	51.3 ± 5.1	11.1 ± 1.2	1.5 ± 0.0	8.8 ± 0.9	1.3 ± 0.1	2.7 ± 0.2	1.7 ± 0.1
Pre soil I	15559 ± 2721	55.6 ± 0.1	10.0 ± 0.2	1.1 ± 0.0	6.0 ± 0.1	NA	NA	NA
85	8251 ± 1679	52.1 ± 2.6	10.1 ± 0.2	1.4 ± 0.0	8.0 ± 0.2	0.7 ± 0.2	1.8 ± 0.3	1.0 ± 0.2
95	9391 ± 1331	51.8 ± 2.4	10.9 ± 0.6	1.4 ± 0.0	8.8 ± 0.5	0.8 ± 0.1	2.0 ± 0.2	1.2 ± 0.0
420	7817 ± 906	50.6 ± 3.8	10.5 ± 0.8	0.8 ± 0.0	4.5 ± 0.4	NA	NA	NA
508	12783	47.6	11.7	1.1	8.6	1.1	2.8	1.6
697	11235 ± 1725	48.4 ± 3.2	11.3 ± 1.7	1.1 ± 0.0	6.3 ± 0.5	1.0 ± 0.1	2.5 ± 0.2	1.5 ± 0.1
1570	6284 ± 1870	41.7 ± 2.8	10.3 ± 0.6	0.8 ± 0.3	4.9 ± 1.6	0.5 ± 0.2	1.8 ± 0.5	1.1 ± 0.2
1710	7992 ± 2953	49.2 ± 3.1	10.9 ± 0.7	1.2 ± 0.1	7.0 ± 0.1	0.7 ± 0.0	2.4 ± 0.2	1.3 ± 0.1
2012	8575 ± 409	47.2 ± 0.9	10.9 ± 0.6	1.2 ± 0.1	7.0 ± 0.3	0.7 ± 0.1	2.2 ± 0.2	1.3 ± 0.2
27944	10442 ± 296	53.8 ± 1.8	11.6 ± 0.4	1.4 ± 0.0	9.4 ± 0.4	0.9 ± 0.1	2.2 ± 0.1	1.2 ± 0.0
heat killed controls	12057 ± 1120	53.1 ± 3.2	11.6 ± 0.3	1.4 ± 0.0	9.4 ± 0.4	1.0 ± 0.0	2.5 ± 0.0	1.5 ± 0.0
Chem. Inhib. controls	12674 ± 749	49.2 ± 3.1	10.8 ± 1.2	1.4 ± 0.0	8.6 ± 0.9	1.1 ± 0.0	2.5 ± 0.1	1.5 ± 0.1

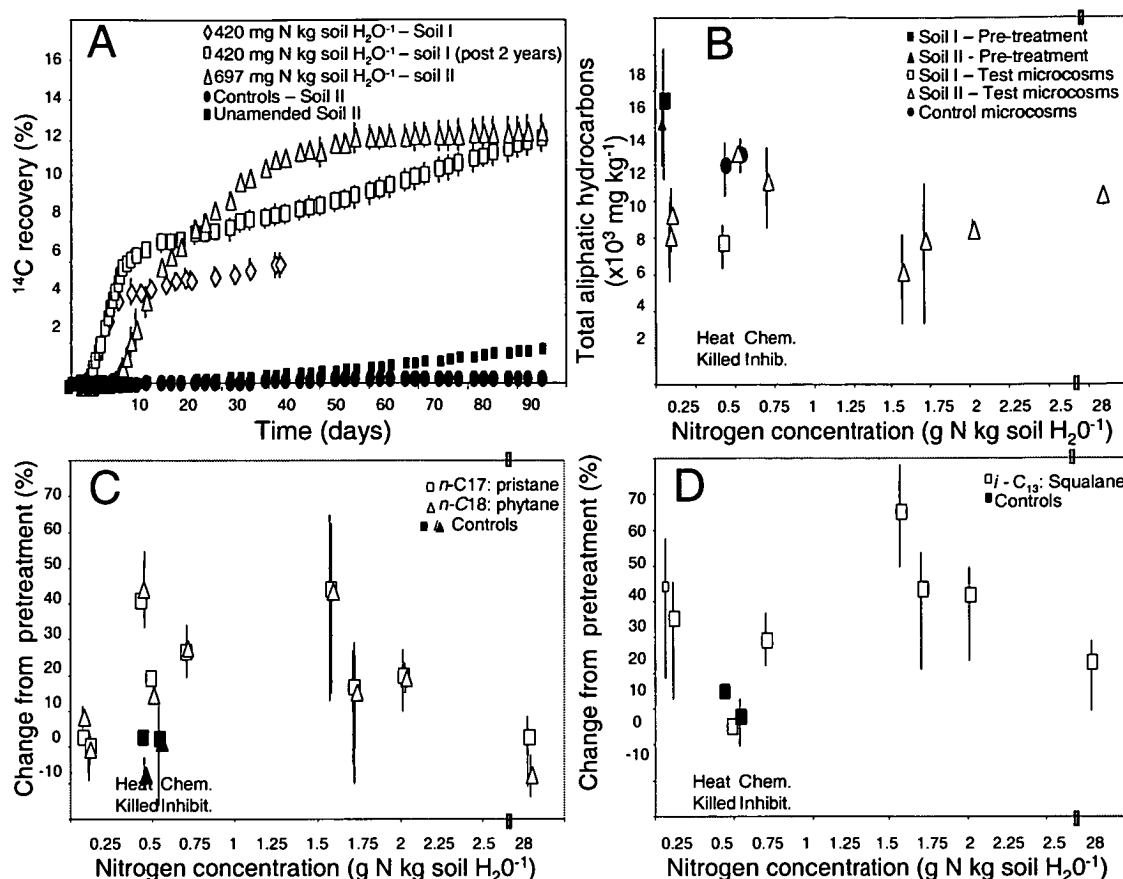


Figure 4.1 Panel A- percentage of ^{14}C -octadecane mineralised to $^{14}\text{CO}_2$ in Antarctic soils treated with *ca* 500 mg N kg-soil- H_2O^{-1} incubated at 10°C for 95 days. The 420 mg N kg-soil- H_2O^{-1} microcosms (diamond symbols) is reproduced from Chapter 3. Control data represents the average of both heat killed and chemically inhibited (sterile) control microcosms (closed circle symbols) and unamended controls (closed square symbols). All symbols represent the average of the number of replicates shown in Table 4.1 and error bars represent 1s. Panel B- total aliphatic hydrocarbon concentration, normalised to squalane, in the pre-treatment, and after 95 days incubation at 10°C for the control and treatment microcosm soils. Points are an average of data from microcosms in each treatment. Error bars (1s) are shown, data also present in Table 4.2. Panel C- percentage change from pre-treatment soil of two common biodegradation ratios ($n\text{-C}_{17}$: pristane and $n\text{-C}_{18}$: phytane). Error bars (1s) are shown, data also present in Table 4.2. Panel D- percentage change from pre-treatment soil of an evaporation ratio ($i\text{-C}_{13}$: squalane). Note that the 420 mg N kg-soil- H_2O^{-1} microcosm data are not present as these microcosms did not contain squalane. Error bars (1s) are shown, data also present in Table 4.2.

4.3.2 Repeat microcosm experiment using soil I after 2 years storage

Storing soil I for two years at -18°C after adding the ^{14}C tracer slightly increased the total amount of isotope recovered as $^{14}\text{CO}_2$. In the initial temperature experiment (Chapter 3) the lag phase took 3 days and the exponential mineralisation rate was $4.03 \pm 0.2 \times 10^{-10}$ mmol octadecane kg-dry-soil $^{-1}$ day $^{-1}$, which was similar to the 2.7 day lag phase and $4.6 \pm 0.1 \times 10^{-10}$ mmol octadecane kg-dry-soil $^{-1}$ day $^{-1}$ mineralization rate after two years storage (Table 4.3). The final amount of total aliphatic hydrocarbon that was mineralised also increased slightly (Figure 4.1A). Small increases in total isotope recovery as $^{14}\text{CO}_2$ after storage occurred largely because the exponential phase lasted longer. It is possible that there were sufficient evaporative losses of the light, short chain hydrocarbons during repeated sample handling reducing the availability of the more bioavailable carbon sources in the microcosms (discussed further below).

Table 4.3 First order mineralisation rate half-lives $T_{1/2}$, and zeroth order mineralisation rates of ^{14}C -octadecane to $^{14}\text{CO}_2$ in soil microcosms at different N loadings between the time intervals indicated. The lag was estimated from the time delay required for the best-fit zeroth order function. The microcosms indicated by an asterisk did not exhibit a plateau phase of ^{14}C -octadecane mineralisation. At these concentrations, first order rates were calculated as the average time for the evolution from 10 % to 100 % of the total $^{14}\text{CO}_2$.

Nitrogen concentration (mg N kg soil-H ₂ O ⁻¹)	Average isotope recovery as $^{14}\text{CO}_2$ after 95 days (%)	$T_{1/2}$ (days)	Rate (mmol (kg dry soil) $^{-1}$ day $^{-1}$) $\times 10^{-11}$	Time Interval (days)	Lag (days)
85*	1.46 ± 0.18	4354.6 ± 99	1.05 ± 0.02	20-76	14 ± 2.2
95*	1.85 ± 0.05	3306.5 ± 114	0.86 ± 0.02	25-90	5.4 ± 2.4
420	12.2 ± 0.54	70.3 ± 4	46.02 ± 0.78	4.2-10.2	4.2 ± 0.5
508	8.4	328.61	20.55 ± 1.47	8.2-25	7.6
697	12.6 ± 0.69	225.1 ± 0.22	22.52 ± 0.97	8.7-32	9.2 ± 0.3
1570*	15.3 ± 4.68	345.7 ± 3.6	10.47 ± 0.47	15-69	11.5 ± 3.4
1710*	9.22 ± 2.75	606.4 ± 84	8.30 ± 0.15	8.7-50	8.5 ± 1.5
2012*	10.07 ± 1.03	489.5 ± 63	8.44 ± 0.10	9-62	10.8 ± 1.0
27944*	0.92 ± 0.68	4056.8 ± 271	1.00 ± 0.21	50-95	43.9 ± 9.4

4.3.3 Differences between soil I and soil II

^{14}C -octadecane mineralisation was significantly different in the two different soils (I and II), which otherwise had similar contamination histories and concentrations and were sampled from the same site, and were incubated under similar experimental conditions. The average amount of isotope that was recovered as $^{14}\text{CO}_2$ from soil I from the first set of experiments conducted at 10°C was *ca* 6% after 42 days. These microcosms had N concentrations of *ca* 420 mg N kg-soil- H_2O^{-1} (Chapter 3, Figure 4.1). The most similar nitrogen contents used for soil II were treatments which contained 508 and 697 mg N kg-soil- H_2O^{-1} with 7.56 and $11.15 \pm 0.04\%$ isotope recovery after 42 days. The lag was considerably shorter for soil I compared to soil II indicating that the factor that controls the lag is an intrinsic property of the soil. It is unclear whether this is an abiotic or a biological function or both, but the results for soil I analysed in this study indicate that the different lags were not a function of the experimental design.

A comparison of the exponential mineralisation rates for the two types of soils with most similar nutrient-water concentrations (420 and 508 mg N kg-soil- H_2O^{-1}) revealed that the zeroth order mineralisation rate in soil I was significantly greater than in soil II ($4.6 \pm 0.1 \times 10^{-10}$ and $2.1 \pm 0.1 \times 10^{-10}$ mmol octadecane kg dry-soil $^{-1}$ day $^{-1}$ respectively). These differences in mineralisation rates and lag phases in the two soils mostly likely attributable to differences in microbial density and community structure but could also be caused by the inherent variability within microcosms studies. The two soils were collected from the same location and thus have similar geological properties, contaminant type and concentration. However, soil I does have a slightly more biodegraded signature when compared with soil II (see for example *n*- C_{17} : pristane, Table 4.1, discussed below). A shorter lag would make sense in this case as the

microbiota in this soil show signs of higher petroleum degrading activity and thus are able to capitalise on the change to a more suitable nutrient soil water regime. The reduction in short-chain hydrocarbon concentrations, which are more biodegradable than octadecane, may decrease the lag phase.

4.3.4 Unamended soil

Mineralisation of ^{14}C -octadecane in the unamended microcosms ($10.3 \pm 0.6 \text{ mg N kg dry soil}^{-1}$ corresponding to 85 and $95 \text{ mg N kg-soil-H}_2\text{O}^{-1}$) had extended lag phases of 14 and 5.4 days respectively and low total isotope recoveries ($< 2\%$, Table 4.3). When the two microcosm sets did eventually reach the exponential mineralisation phase, the rate of mineralisation was still considerably slower than mineralisation in any of the amended treatments, except for the very high nutrient amended microcosms.

There was a *ca* 40 and 35% reduction in total aliphatic hydrocarbons in the 85 and $95 \text{ mg N kg-soil-H}_2\text{O}^{-1}$ treatments respectively (Figure 4.1B). The $n\text{-C}_{17}$: pristane and $n\text{-C}_{18}$: phytane biodegradation ratios shown in Figure 4.1C are not significantly different from the pre-treatment soil, while ratios known to be sensitive to evaporation, such as $i\text{-C}_{13}$: squalane, exhibited *ca* 40% differences (Table 4.2, Figure 4.1D). This implies that the reduced total aliphatics is through volatilisation and not bioremediation in the 85 and $95 \text{ mg N kg-soil-H}_2\text{O}^{-1}$ treatments.

4.3.5 Water amended treatments with constant nutrient-soil ratio

Four sets of replicated microcosms were all amended with *ca* $190 \text{ mg N kg dry soil}^{-1}$ but with water contents that ranged from 9.9 to 39.8% (Table 4.1). These amendments yielded nutrient concentrations in soil-water of 508 , 697 , 1710 and $2012 \text{ mg N kg-soil-H}_2\text{O}^{-1}$. Variations in nutrient soil water compositions across this range did not

produce significant differences in the total amount of isotope recovered after 95 days incubation (8.4 to 12.6 %), or in the length of the lag phase (7.6 to 10.8 days; Table 4.3). However, significantly faster zeroth order mineralisation rates (*ca* 20×10^{-11} mmol octadecane kg-dry-soil⁻¹ day⁻¹) were found in the microcosms with high water contents of about 30-40%. Ironically the high water content microcosms did not show a significant reduction in total aliphatic hydrocarbons compared to the abiotic controls (Figure 4.1B), and showed less total reductions than the unamended microcosms described in Section 4.3.4 above. I suspect that water saturation of the soils in these microcosms acted as a barrier that hindered evaporation of the more volatile hydrocarbons into the microcosm headspace. These “high water content” microcosms had the least change in the *i*-C₁₃: squalane ratio (*ca* 15%, see Figure 4.1A and Figure 4.1D) which is indicative that the hydrocarbons in these flasks were least affected by evaporation.

4.3.6 Nutrient amended treatments with constant water-soil ratio

To further explore the relevance of expressing N relative to soil water rather than dry soil weight, several treatments were prepared by fixing the unamended water content at 10.5% and varying N amendments between 0 and 3244 mg N kg dry soil⁻¹. Nutrient concentrations in soil water ranged from the unamended nutrient 85 mg N kg-soil-H₂O⁻¹, also described in Section 4.3.5, through to 27 944 mg N kg-soil-H₂O⁻¹ (Table 4.1). The microcosms with 173 mg N kg soil⁻¹ or 1570 mg N kg-soil-H₂O⁻¹ showed the highest zeroth order mineralisation rate (10.47×10^{-11} mmol octadecane kg-dry-soil⁻¹ day⁻¹) and the shortest half life (346 days), and ¹⁴C-octadecane mineralisation remained in the exponential phase throughout the trial. This treatment also had the least residual total

aliphatic hydrocarbon concentration (Figure 4.1B) and showed the greatest change in biodegradation ratios (Figure 4.1C).

Unamended soil with nutrient concentrations of only 85 mg N kg-soil-H₂O⁻¹ showed an extended lag phase (14 days), a long half life (4354 days) and low zeroth order mineralisation rate (see Section 4.3.4 and Table 4.3). At 27 944 mg N kg-soil-H₂O⁻¹, mineralisation was very initially slow, with a lag phase of over 42 days. This lag response exceeded the lag in the soil that received no nutrient amendments. High nutrient amendments (4:1 C: N ratio) greatly inhibited hydrocarbon biodegradation in this soil.

4.4 Discussion

4.4.1 *Nutrients, water and biodegradation*

Natural biomineralisation of petroleum hydrocarbons at 10°C in unamended soil from Old Casey Station is limited by low nitrogen concentrations. Unamended microcosm treatments had no more than 85 mg N kg-soil-H₂O⁻¹ and at these concentrations total mineralisation was almost 10 times less than the greatest total mineralisation in mid-range nutrient amended treatments. However, when the soil was amended to near the Redfield nutrient target (27 944 mg N kg-soil-H₂O⁻¹, 4:1 C:N) hydrocarbon mineralisation was severely inhibited. Applying all the nutrients required for complete hydrocarbon mineralization and incorporation of all carbon into biomass proved to be more toxic to micro-organisms than even the chemically inhibited controls used in these experiments. Walworth *et al.* found similar results for coarsely textured soil in the Arctic, and it is not surprising that the sandy soil used in this study was sensitive to over fertilization because of its limited water holding capacity. Suggestions made by

Walworth *et al.* (1997) that the optimum nitrogen fertilization for a sandy matrix may be as low as 100 mg N kg dry soil⁻¹ are probably also realistic estimates for the soils around Old Casey Station.

In terms of understanding the relationship between nutrients, soil and pore-water, the general utility of expressing nutrient loads relative to pore-water rather than on a dry mass basis is confirmed. There were statistically significant differences ($p < 0.05$) between exponential mineralisation rates for a range of nutrient-water concentrations for which the nutrients on a dry soil mass basis were approximately the same, at about 180 mg N kg dry soil⁻¹. The greatest mineralisation extent or shortest hydrocarbon half lives occurred at concentrations of between about 508 and 2012 mg N kg-soil-H₂O⁻¹. The fastest first order rates occurred in samples at the lower end of the range, although the greatest extent of mineralisation of ¹⁴C-octadecane and the most depleted *n*-C₁₇: pristane and *n*-C₁₈: phytane ratios occurred in the microcosm that contained 1570 mg N kg-soil-H₂O⁻¹. It is unclear whether the fast first order rates in the 508 and 697 mg N kg-soil-H₂O⁻¹ microcosms occurred because the nutrient-soil-water concentrations were more favourable, or because the water contents were more favourable. The optimal water content for hydrocarbon mineralisation in these soils has yet to be investigated. For remediation at the site, however, it probably is more significant that the microcosms with 1570 mg N kg-soil-H₂O⁻¹ and 10% water content did not enter the plateau stage of mineralisation even after 95 days. It is also likely that greater water contents would lead to O₂ limitation in soils around Old Casey Station (cf. Huesemann and Truex, 1996).

4.4.2 Strengths and weaknesses of the microcosm approach to site assessment

Radiolabelled microcosm tracer studies accurately quantify biological mineralization of ¹⁴C-tracers, usually through three stages of growth. As such it is useful for exploring

which factors influence the duration of the lag phase, the rate and duration of the exponential phase, and the onset of the plateau phase. It should be noted that laboratory radiometric studies are always artefactual and should be interpreted with caution. Fuels are complex mixtures of compounds and the different components are not equally bioavailable. Although the maximum ^{14}C -octadecane mineralisation of 15.3% that occurred at $1570 \text{ mg N kg-soil-H}_2\text{O}^{-1}$ after 95 days incubation at 10°C was relatively low, octadecane is one of the heavier alkanes within SAB, and is less bioavailable than lighter alkanes (Chapter 2, Atlas, 1981). The extent of ^{14}C -octadecane mineralisation to $^{14}\text{CO}_2$ is likely to underestimate the amount of degradation occurring in a soil contaminated by SAB. Also, the soil from Old Casey Station used in these microcosms was highly contaminated with more than $15\,000 \text{ mg fuel kg}^{-1}$. With so much contaminant to degrade, the absolute recoveries of the radiometric tracer are going to be small over a short time frame. These outcomes are similar to those reported by Whyte *et al.* (1999) who showed that high initial hydrocarbon concentration reduced the amounts of $^{14}\text{CO}_2$ recovered, with only 15% $^{14}\text{CO}_2$ recovered with an initial TPH of $26\,900 \text{ mg kg dry soil}^{-1}$ compared to 35% at $200 \text{ mg kg dry soil}^{-1}$. Of importance from an experimental perspective are the timing and relative magnitudes of changes in mineralization with successive manipulations of environmental variables. Although alternative approaches using gas chromatography provide a definitive measure of the amount of contaminant degraded, it is often difficult to isolate the effects of evaporation from biodegradation, and evaporation of light diesel is likely to be much more prevalent in microcosms than in field conditions. Using indices such as $n\text{-C}_{17}$: pristane or $i\text{-C}_{13}$: pristane (or squalane) which are sensitive to either biodegradation or evaporation may provide some insight, but this approach is not practical in replicated time course

experiments which are required in investigations of the parameters that most affect biodegradation and which could be manipulated to promote bioremediation in the contaminated site.

When used in conjunction, chromatographic and radiometric approaches enabled some understanding of the nutrient-water-soil parameters that influence the rate of petroleum degradation at low temperatures. Although a degree of caution is required when extrapolating the results from laboratory experiments to the conditions at a field site, or when predicting the outcomes of remediation actions, a number of testable procedures and remediation recommendations can be made for the soils at Old Casey Station from this study.

4.4.3 Implication for nutrient amended remediation at Old Casey Station

The results for hydrocarbon mineralisation in unamended soils from Old Casey Station support the field evidence of long term persistence of hydrocarbons in these soils and that intrinsic remediation at this site is very slow with contaminant concentrations still exceeding 15 000 mg fuel kg⁻¹ after *ca* 15 years. Apart from temperature limitations (Chapter 3), nutrient and water availability limits the potential for biodegradation. From the nutrient amended treatments described here, it is apparent that a *ca* 10-fold increase in the overall biodegradation rate would be possible by amending soils at Old Casey Station, if appropriate temperatures can be maintained. However, *in situ* remediation will still be relatively slow and might take of the order of 5 years or more to reduce contaminant levels to an acceptable level of less than 2000 ppm (Table 7.3, Snape *et al.*, 2003).

From the results described here, and similar studies by Walworth and co-workers (1997) from the Arctic, it is apparent that coarse textured soils are prone to over

fertilization. It is encouraging that enhanced degradation occurs across a broad range of nutrient-water concentrations; the difficulty for treating the highly contaminated cryic soils, such as those found at Old Casey Station, is maintaining nutrient soil water balance in the optimal window for a protracted period. This is because the soil water status is highly variable and nitrate is easily soluble, with reports of as much as half of applied nitrate lost from the soil through deep drainage (Stevenson and Cole, 1999). Whilst this means that nitrogen applied at the surface will be transported down the soil profile to where the bulk of the hydrocarbon contamination resides, nitrogen that is not utilised will undergo offsite dispersal where it could cause detrimental effects in the catchment downstream. It also means that nutrient amendments would need to be applied often and in small doses, which will be difficult and costly in remote sites such as those in Antarctica. Also soils that undergo freeze-thaw cycles on a regular basis will continually change its free-water content and thus its nutrient-water concentration.

The study by Macnaughton *et al.* (1999), while not primarily focused on the effects of nutrients on hydrocarbon degradation, found that the addition of 2 kg of NaNO_3 to a 4 x 9 m sand-beach plot in an experimental oil spill had beneficial effects. The addition was not made in a single dose, but rather gradually, as a *ca* 400 mg N kg-soil- H_2O^{-1} solution, which possibly explains why their high total nutrient addition had no inhibitory effects. Similarly Swannel *et al.* (1999) found that the addition of 1.5 kg NaNO_3 in a weekly dose of 21 mg N kg-soil- H_2O^{-1} to a pebble beach in Wales enhanced biodegradation. Both of these studies were conducted on sandy beaches and constant small nutrient additions kept the concentrations of nutrients in the range required for microbial mineralisation of petroleum hydrocarbons.

If halotolerant microbes constituted a minority of the microbiota in soil from Old Casey Station, then the long lag phase in the microcosms amended with 27 944 mg N kg-soil-H₂O⁻¹ used in this investigation may explain the eventual exponential growth after an extended lag phase in the microcosms. At this nitrogen concentration, slow microbial community response was expected as, according to Walworth *et al.*, the osmotic potential would be toxic to the majority of the microbial population. The recovery of mineralisation rates at this concentration after an extended period of incubation can be explained by either the development of a halotolerant microbial population or an eventual reduction in the ammonium concentration. It is more probable that halotolerant microbes were present in low numbers in the initial microbial population and took over 43 days to reach adequate numbers for measurable mineralisation to occur. As it was not possible to derive a mineralisation rate at this nutrient concentration as the plateau phase was not reached, the slow rate of mineralisation at this nutrient concentration was similar to the rate in the unamended soil and suggests that bioremediation of the Old Casey Station site at this nutrient concentration would be protracted. As high concentrations of nutrients in the soil-water phase markedly affect the hydrocarbon mineralisation rate, controlled release nutrients (CRNs) are potentially of great benefit for bioremediation in cold regions (Snape *et al.*, 2003). Not only do they avoid over fertilisation in the short term, but single applications could maintain nutrients in the optimal window irrespective of water content or stage in the seasonal thaw cycle. Unfortunately the emphasis on application recommendations for CRNs are still based on providing enough nutrients to remediate the total contaminant load, rather than maintaining the best possible conditions in the soil. Quantifying nutrient release coupled to biological demand at low temperatures requires

further research. Preliminary results from an *in situ* field trial at Old Casey Station at the same site as the soils studied here yielded substantially faster hydrocarbon degradation than the rate of natural attenuation in the field (Snape *et al.*, 2003). As with the experiments described here, the field trials utilized indigenous micro-organisms and the natural summer thaw cycle. After 3 years, nutrient amended treatments degraded the most hydrocarbon to produce near surface concentrations that have reduced from ~20 000 to less than 2000 mg fuel kg soil⁻¹ (Snape *et al.*, 2003).

4.5 Conclusions

Soil collected from a site at Old Casey Station that was contaminated over 15 years ago still remains highly contaminated with more than 15 000 mg fuel kg soil⁻¹. Addition of ¹⁴C-octadecane to otherwise unamended microcosms at 10°C for 95 days indicated that hydrocarbon mineralisation in these soils is strongly limited by low nutrient concentrations. Unamended soil had long lag times (~ 10 days), low exponential mineralization rates (*ca* 1 x10⁻¹¹ mmol ¹⁴C-octadecane kg-dry-soil⁻¹ day⁻¹), and a low extent of mineralisation (<2%). Mineralization results for a range of nutrient and water amended treatments indicated that the addition of nutrients to soil, up to a point, greatly increased the overall rate of biodegradation. Nutrient water concentrations in the range 420 to 2012 mg N kg-soil-H₂O⁻¹ had the shortest lag times for mineralisation, and the fastest exponential mineralisation rates. The highest nutrient water concentration in this range did not reach a plateau phase, even after 95 days, and showed the greatest overall ¹⁴C-octadecane mineralisation of any of the treatments.

However, high nutrient water concentrations of 27 944 (~3 g N kg dry soil⁻¹) produced long mineralisation lag times of more than 42 days, slow exponential mineralization rates, and a very low overall extent of mineralisation. Such high nutrient

loads clearly inhibited biodegradation in this soil, and confirm observations made by Walworth *et al.* that over fertilization can inhibit hydrocarbon mineralisation during remediation of cold region soils.

One surprising observation from a comparison between the results described here and from Chapter 3, concerns differences in lag phases between two very similar soil samples. Two samples taken 2 years apart from the same site and that had similar contamination histories and geological properties, yielded quite different lag and mineralization profiles. These differences were not a function of the experimental design, but are probably related to localised differences in microbial density and community structure.

The experimental approach using the ^{14}C -octadecane tracer usefully followed mineralization through several stages of $^{14}\text{CO}_2$ evolution. As such the technique provides valuable insight into how manipulating environmental variables might influence the duration of the lag phase, the rate and duration of the exponential phase, and the timing of the onset of the plateau phase. Unlike the previous work (Chapter 3), several treatments did not culminate in a plateau phase of growth.

A supplementary approach using gas chromatography supported the observations from the radiometric time course experiment with regard to the effect of nutrient and water amendments on biodegradation. Indices or ratios of hydrocarbon compounds that are known to be sensitive to either biodegradation or evaporation, such as *n*-C₁₇: pristane and *i*-C₁₃: pristane/ squalane, confirmed that much higher rates of degradation were possible if nutrients were added to the soil in the concentration range 508-1570 mg N kg-soil-H₂O⁻¹. However, evaporation of hydrocarbons in the limited amount of soil in the biometer flasks proved to be a significant process by which the original contaminant

was lost, especially for the lighter compounds in SAB. Such evaporative losses were much greater than could be theoretically achieved during *in situ* remediation and this places a limitation on how analogous these experiments are to the site at Old Casey Station. Nevertheless, the results from both geochemical approaches indicate that a 10-fold increase in biodegradation in contaminated Old Casey Station soils might be achievable at appropriate temperatures through careful nutrient-water management. The high petroleum contaminant concentrations that reside in the soil, coupled with other environmental limitations, such as low temperatures and high hydraulic conductivities, mean that a considerable nutrient and water load will be required for total degradation if remediation is purely to take place *in situ*. The technical challenge now is to design a nutrient delivery system that is capable of maintaining relatively low nutrient water concentrations in a dynamic hydrological system, probably for a protracted period spanning several summer seasons. The overall feasibility and relatively long treatment time involved with *in situ* remediation needs to be balanced against the much higher costs and greater environmental risks associated with *ex situ* treatments that involve heating or venting.

Chapter 5

Numerical modelling of ^{14}C mineralisation data

5.1 Introduction

5.1.1 *Microbial kinetic rate equations*

Zero or first order chemical reaction kinetics are often used to describe the mineralisation of organic compounds in soil microcosms studies (Chang and Alvarezcohen, 1996; Grundy *et al.*, 1996; Moyer *et al.*, 1996; Lahvis *et al.*, 1999). As the rate of contaminant mineralisation is influenced by both biological (enzymatic reactions) and physical (diffusion, absorption and solubility) processes (Alexander, 1999a), zero and first order kinetics are often too simplistic to adequately describe the three phases of microbial mineralisation (lag, exponential and plateau) that often occur in microcosm studies. To mathematically describe organic carbon mineralisation data, non-linear mineralisation regressions are often attempted (Scow *et al.*, 1986; Nuck and Federle, 1996; Helweg *et al.*, 1998; Reffstrup *et al.*, 1998).

Brunner and Focht (1984) proposed a three-half-order model to describe the mineralisation of organic compounds specifically in soil. There are two forms of this model depending on the microbial growth rate (linear or exponential). The Brunner and Focht (1984) model has been used to describe the mineralisation kinetics of a variety of chemicals, such as di (2-ethylhexyl) phthalate and *n*-dodecylbenzene sulfonate (Dörfler *et al.*, 1996), pyrimidine 2-c-14 rimsulfuron (Metzger *et al.*, 1999), mecoprop and isoproturon (Helweg *et al.*, 1998) and atrazine (Grigg *et al.*, 1997), and the effect of changing environmental conditions on mineralisation (Dörfler *et al.*, 1996). It has been shown that the exponential form of the model best approximates mixed culture soil microcosms (Brunner and Focht, 1984; Scow *et al.*, 1986; Dörfler *et al.*, 1996; Nuck and

Federle, 1996). Brunner and Focht (1984) suggested that the growth of microbes in soil is limited by the desorption and diffusion of substrate and nutrient from the soil matrix and by the prevalence of microbial growth on soil surfaces; when biomass exceeds the soil surface available for attachment, linear growth results. The linear and exponential forms of the model are shown in Equations 5.1 and 5.2 respectively.

$$P = S_0 \left(1 - e^{-k_1 t - \left(\frac{k_2 t^2}{2} \right)} \right) + k_0 t \quad (5.1)$$

Equation 5.1 Brunner and Focht (1984) three-half order linear growth model.

$$P = S_0 \left(1 - e^{-k_1 t - \frac{E_0}{\mu} (e^{\mu t} - 1)} \right) + k_0 t \quad (5.2)$$

Equation 5.2 Brunner and Focht (1984) three-half order exponential growth model.

In these equations, P is the concentration of the product, S_0 approximates the initial substrate concentration, k_1 is the first order rate co-efficient, t is time, k_2 is a constant in units of reciprocal time squared, k_0 is the zero order rate co-efficient, E_0 is the initial biomass growth rate and μ is the non-linear exponent of growth.

Negative k_0 and k_2 values may result when the Brunner and Focht (1984) model is applied to mineralisation studies using octadecane (Ferguson *et al.*, 2003), phenol, aniline and nitrilotriacetic acid (Scow *et al.*, 1986). The k_2 parameter is a proxy for the initial degradative capacity of the microcosms and thus a negative value cannot conform to reality. Brunner and Focht (1984) mentioned that this parameter could be set to zero, thus eliminating that part of the formula. A null k_2 is used to describe situations in which no microbial growth occurs. Interpretation of negative k_0 values (k_0 represents the mineralisation of the less available fraction of the substrate) is also not logical as it

would indicate an increase in substrate concentration in the microcosms over time. When both k_2 and k_o are bounded to zero, poor fitting results are produced (Ferguson *et al.*, 2003).

Trefry and Franzmann (2003) addressed these issues by extending the Brunner and Focht three-half order model to include terms that further characterize the initial lag phase. Trefry and Franzmann (2003) found that lagged production curves were best described by a delayed onset of the mineralisation process, whilst the biomass growth phase conformed well to the Brunner and Focht exponential model. The Trefry and Franzmann extensions can be applied to either the linear or exponential microbial growth rate of the Brunner and Focht three-half order model. The linear and exponential forms of the Brunner and Focht (1984) model with Trefry and Franzmann (2003) extensions are shown in Equation 5.3, and Equation 5.4 respectively.

$$P(t) = S_0 \left(1 - e^{-k_1 t - \left(\frac{k_2 t^2}{2} \right)} \right) + k_0 \left(t - \frac{\sqrt{\pi}}{2} v \operatorname{erf}(t/v) \right) \quad (5.3)$$

Equation 5.3 Trefry and Franzmann (2003) model with linear biomass growth.

$$P(t) = S_0 \left(1 - e^{-k_1 t - \frac{E_0}{\mu} (e^{\mu t} - 1)} \right) + k_0 \left(t - \frac{\sqrt{\pi}}{2} v \operatorname{erf}(t/v) \right) \quad (5.4)$$

Equation 5.4 Trefry and Franzmann (2003) model with exponential biomass growth.

In these equations, P is the cumulative product, S_0 approximates the initial substrate concentration ($\text{mg } ^{14}\text{C-octadecane kg}^{-1}$), k_1 is the first order rate co-efficient (describing substrate consumption independent of growth) (d^{-1}), t is time (d), k_2 is a constant in units of reciprocal time squared (characterising the linear biomass growth rate and has been used as an indicator of growth or increased degradative capacity of mixed cultures), k_0 is the zero-order rate co-efficient describing the plateau phase (represents the rate of indigenous mineralization or the mineralisation of the ^{14}C that was initially incorporated into biomass and mineralisation of less available fractions of the substrate) ($\text{mmol } ^{14}\text{C-octadecane g soil}^{-1} \text{ d}^{-1}$) and, for the exponential model, E_0 is the initial biomass growth rate (d^{-1}), and μ represents the non-linear exponent of growth (d^{-1}). In both Equations 5.3 and 5.4, v is a lag phase parameter (units of time) that governs the smooth variations of indigenous mineralisation from zero at early time, to k_0 at large time. In Equation 5.3 and Equation 5.4, erf is the error function (Abramowitz and Stegun, 1964). Equations 5.3 and 5.4 take the form of a sum of two terms. The first terms represent production from a notional “highly bioavailable” fraction of the substrate that is metabolised quickly by a rapidly growing (linear growth rate for Equation 5.3, exponential growth rate for Equation 5.4) microbial population. The second term, which is common to both equations, represents production from a “less bioavailable” fraction of the substrate that becomes the dominant source of production as the highly bioavailable fraction is depleted.

5.1.2 Temperature- dependent rate models

The effects of temperature on mineralisation rate can also be described by regression models. Unlike the previously discussed rate equations, regression models, such as the Arrhenius (1889) and the Ratkowsky (1983) models, describe the

temperature-dependence of the rate. The simplest of these regression models utilise the Arrhenius equation (e.g. Pelletire *et al.*, 1999). When applied to first order rate reactions the Arrhenius model (1889) requires the determination the first order rate co-efficient (k_1) as shown in Equation 5.5. In Equation 5.5, C_o is the initial concentration of a reactant added to the microcosms (^{14}C -octadecane in the microcosms presented in Chapter 3), C_t is the concentration of a product produced at time t ($^{14}\text{CO}_2$ in the microcosms presented in Chapter 3).

$$k_1 = \ln\left(\frac{C_o - C_t}{C_o}\right) \quad (5.5)$$

Equation 5.5 First-order rate kinetics (k_1)

The Arrhenius equation is shown in Equation 5.6 where, k_1 is the first order rate co-efficient calculated by Equation 5.5. Ea is the activation energy in J mol^{-1} and can be considered as a measure of the effect of temperature on biological activity in microcosms studies. R is the universal gas constant ($8.34 \text{ J K}^{-1} \text{ mol}^{-1}$) and T is temperature in Kelvin.

$$\ln k_1 = -\frac{Ea}{RT} + \ln A \quad (5.6)$$

Equation 5.6 Arrhenius (1889) equation

Ratkowsky *et al.* (1982; 1983) proposed a more complex model to describe the effect of temperature on microbial growth. The Ratkowsky model recognised that activation energy decreases as temperature increases, whereas the Arrhenius model assumes that the activation energy is constant at different temperatures. The Ratkowsky model has been previous used to with mixed cultures to describe the effect of temperature on denitrification in a Quebec cropped soil (Pelletire *et al.*, 1999). In the Ratkowsky model

(1983) shown in Equation 5.7, r is the growth rate or the reciprocal of time required to achieve a level of growth (or a surrogate measure of growth), b is the regression coefficient (described by the slope of the regression line below the optimal growth temperature), and c is a fitting parameter for data above the optimal growth temperature, T is temperature, T_{min} and T_{max} are the minimum and maximum growth temperatures respectively (conceptual temperatures of no metabolic significance but at which the equation predicts that the generation time is infinite).

$$\sqrt{r} = b(T - T_{min}) \left(1 - e^{c(T - T_{max})}\right) \quad (5.7)$$

Equation 5.7 Ratkowsky (1983) bacterial growth rate model

5.2 Results and discussion

5.2.1 *Modelling the effect of temperature on microbial mineralisation of ¹⁴C-octadecane*

5.2.1.1 *Arrhenius*

The Arrhenius model when applied to the mineralisation data for ¹⁴C-octadecane at different temperatures did not describe the data well. The assumptions behind the Arrhenius model, namely that biological mineralisation rates would approximate the effect of temperature on a chemical reaction across the entire temperature range investigated was too simplistic. The Arrhenius plots for the mineralisation rate co-efficients found within the temperature microcosms described in Chapter 3 are shown in Figure 5.1. The mineralisation rates used in the comparison were the mineralisation rates during exponential microbial growth from all microcosms except the microcosms incubated at 28°C. The growth rates are nominally labelled in Figure 5.1 as either psychrotrophic or mesophilic depending on what was postulated as the dominant

bacterial population during the exponential growth rate (Chapter 3). A change in the microbial population in the 28°C microcosms from a psychrotrophic to a mesophilic-dominated population was postulated in Chapter 3. The initial mineralisation rate at 28°C was ascribed to a psychrotrophic microbial population, while the rate during the exponential phase was attributed to a mesophilic microbial population (discussed further below). The rate co-efficients for the -2°C microcosms were not included in the best-fit estimate of the Arrhenius model for the psychrotrophic microcosms as free water is required for microbial growth. The Arrhenius model supports the finding that the rate of microbial mineralisation of ^{14}C -octadecane increases with increasing temperatures and supports the hypothesis of both psychrotrophic and mesophilic populations within the contaminated soil at Old Casey Station (Chapter 3). The activation energies (E_a , Equation 5.6) for octadecane mineralisation for both the psychrotrophic and mesophilic bacterial populations were estimated from the slope of the Arrhenius plots (Figure 5.1). Unsurprisingly, increasing temperature had a greater effect on the octadecane mineralisation rate by mesophiles ($E_a = 97.8 \text{ J mol}^{-1}$ octadecane) than it had on the mineralisation rates by psychrotrophs ($E_a = 65.2 \text{ J mol}^{-1}$ octadecane).

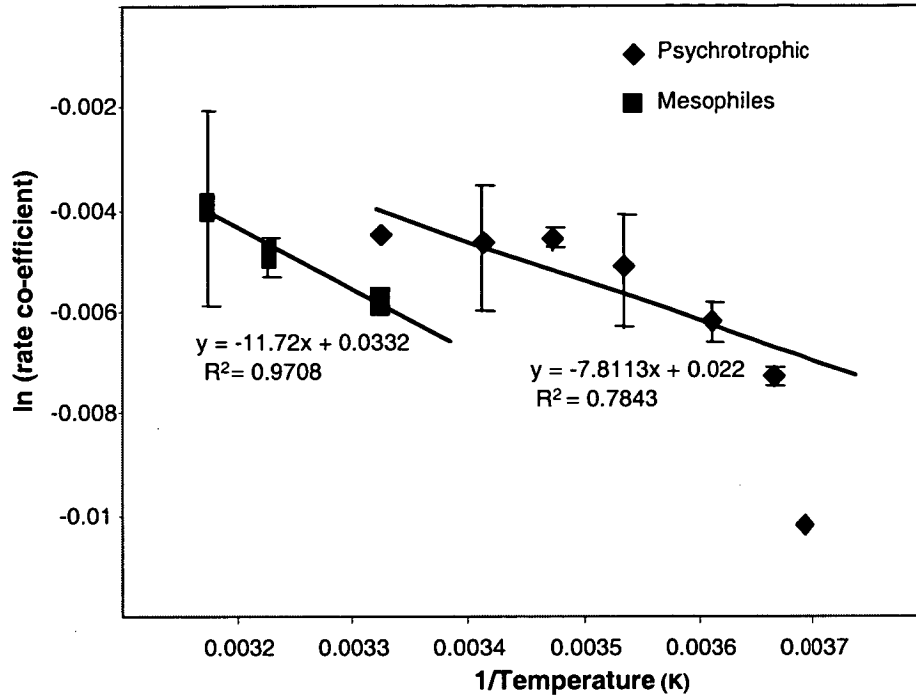


Figure 5.1 Arrhenius plot of the natural log of the first order rate co-efficient (k , Equation 5.5) for $^{14}\text{CO}_2$ production from ^{14}C -octadecane in the microcosms presented in Chapter 3. Mineralisation rates were calculated from the exponential phase of growth except for the 28°C microcosms which is shown twice (lag and exponential mineralisation rates are shown). Microcosms grown from -2 to 28°C are nominally labelled as psychrotrophic, while mesophilic microcosms are from 28 to 42°C . Error bars ($2s$) are shown.

5.2.1.2 Ratkowsky

The best-fit parameter estimates from the Ratkowsky (1983) model when applied to the mineralisation rates from the temperature-microcosms data from Chapter 3 are shown on Figure 5.2. As in Figure 5.1, the mineralisation rate co-efficient for the 28°C microcosms are shown twice to represent both a psychrotrophic and mesophilic bacterial populations. Unfortunately, there were not enough data points to attempt fitting the Ratkowsky model (1983) to the mesophilic data; it is impossible to fit a function with four parameters to a data set with three points. The best-fit estimates for the Ratkowsky model applied to the psychrotrophic microcosm did not produce a well-fitting solution.

The most likely explanation for the poor fit is that the Ratkowsky model (1983) was developed for axenic cultures. An extensive change in microbial community structure, as distinct from an increase in total numbers, might explain the large errors associated with fitting the temperature-microcosm mineralisation data to the model.

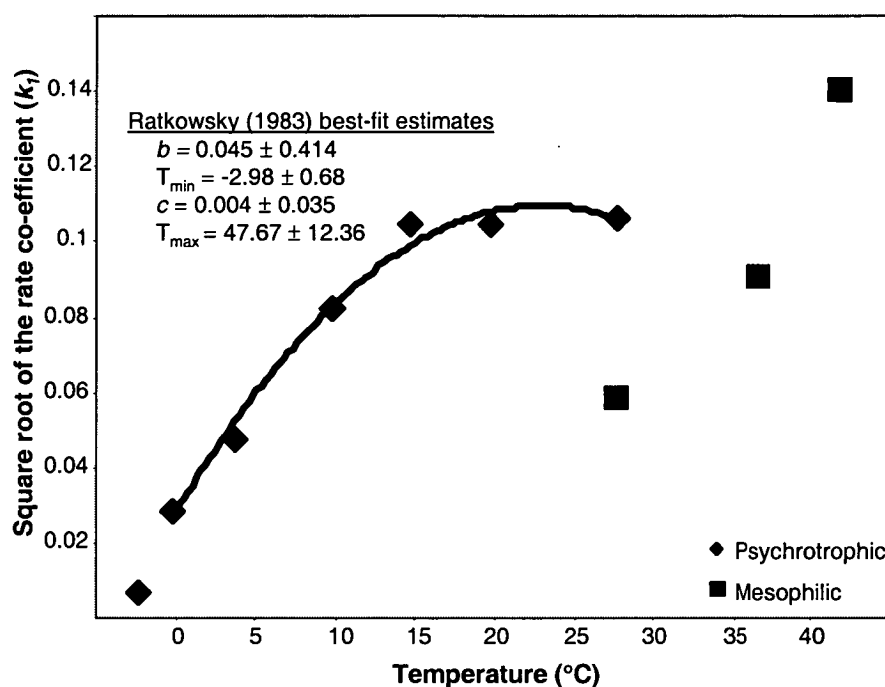


Figure 5.2 Ratkowsky (1983) plot and best-fit estimates when applied to the ^{14}C -octadecane mineralisation rates (-2°C to 28°C) from Chapter 3.

5.2.1.3 Three-half order models

Although previous mineralisation studies have found a good approximation for their data using the three-half order Brunner and Focht model, Trefry and Franzmann (2003) showed that the exponential form of their extended model provided a more realistic production curve, especially for results with an initial lag in mineralisation, such as occurred in the microcosms described in Chapter 3 and Chapter 4. It was decided to apply both the exponential and linear forms of the Trefry and Franzmann extended model to the data from Chapter 3 for comparison. The k_1 parameter was set to zero for

all microcosms to ensure that the model best-fit estimates conformed to reality (see Section 5.1.1 for the justification of this simplification). The best-fit parameter estimates of both models, gained with a least-squares objective function with an all-parameter nonlinear regression algorithm, are presented in Figure 5.3, Table 5.1 and Table 5.2. Differences between the best-fit parameter estimates for the two growth models were subtle and as the exponential model resulted in tighter confidence intervals only the curves and data for the exponential growth model are shown in Figure 3.2. Best-fit residuals for the two growth models were comparable for the temperature-microcosm results, with the linear model doing slightly better at 4, 15, 20 and 28°C. At 42°C, the $^{14}\text{CO}_2$ production replicates are widely spaced, and the best-fit curve simply follows the average of the replicates. For this reason, undue emphasis should not be placed on the fitted kinetic parameter values for these microcosms, especially those parameters that describe the long-term production of $^{14}\text{CO}_2$ (i.e. S_0 and k_0). It is not the purpose of this study to recommend or reject production curve models based on the regression results. Rather, two lagged models were applied to the temperature-microcosm data to show that the two sets of regressed parameter estimates and confidence intervals are comparable and robust.

Table 5.1 Results of nonlinear regressions on the production curves for different temperatures, with ideal linear microbial growth ($\lambda = 0$) and non-ideal (Gaussian) mineralisation. S_0 and the root-mean-square regression residual R are expressed in units of $\text{mg } ^{14}\text{C-octadecane}/(\text{kg soil})$ converted to $^{14}\text{CO}_2$, k_0 in units of $\text{mmol } ^{14}\text{C-octadecane}/(\text{g soil})/\text{day}$, k_2 in units of d^{-2} , and v in units of days. Confidence intervals are expressed at the 95% level.

T °C	S_0 ($\times 10^{-8}$)	k_0 ($\times 10^{-9}$)	k_2	v	R ($\times 10^{-9}$)
4	5.2 ± 3.0	0.9 ± 1.4	0.0066 ± 0.01	8.5 ± 70	5.7
10	6.4 ± 2.9	0.6 ± 0.2	0.041 ± 0.019	3.3 ± 69	5.1
15	6.4 ± 4.0	1.2 ± 0.1	0.088 ± 0.031	2.8 ± 38	2.9
20	7.1 ± 1.3	1.5 ± 0.1	0.11 ± 0.027	1.8 ± 9.9	3.0
28	5.5 ± 1.3	4.3 ± 0.2	0.18 ± 0.096	0.6 ± 3.7	8.8
37	0.2 ± 33	9.1 ± 0.8	0.15 ± 4.8	8.8 ± 6.2	24
42	52 ± 190	0.25 ± 17	0.006 ± 0.007	13 ± 7300	110

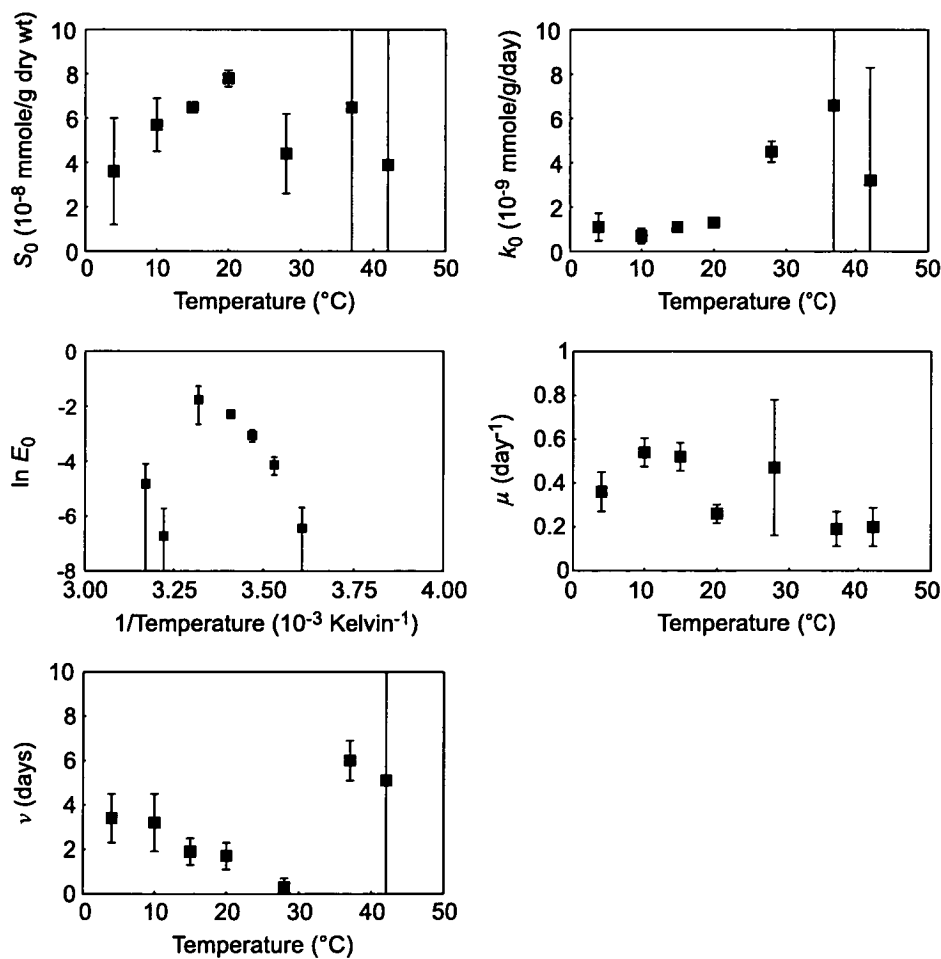


Figure 5.3 Temperature dependence of the exponential growth rate model parameters. Best-fit estimates are shown, together with standard errors

Table 5.2 Results of non-linear regressions on the production curves for different temperatures, with ideal exponential microbial growth ($\lambda = 0$) and non-ideal (Gaussian) mineralisation. S_0 and the root-mean-square regression residual R are expressed in units of mg ^{14}C -octadecane/(kg soil) converted to $^{14}\text{CO}_2$, k_0 in units of mmol ^{14}C -octadecane/(g soil)/day, E_0 and μ in units of d^{-1} , and v in units of days. Confidence intervals are expressed at the 95% level. ^a Estimated value.

T °C	S_0 ($\times 10^{-8}$)	k_0 ($\times 10^{-9}$)	E_0	μ	v	R ($\times 10^{-9}$)
4	3.6 ± 5.3	1.1 ± 1.4	0.002 ± 0.004	0.36 ± 0.18	3.4 ± 2.2	5.8
10	5.7 ± 2.8	0.7 ± 0.8	0.016 ± 0.010	0.54 ± 0.12	3.2 ± 2.5	4.4
15	6.5 ± 0.4	1.1 ± 0.1	0.046 ± 0.018	0.52 ± 0.13	1.9 ± 1.2	3.7
20	7.8 ± 0.8	1.3 ± 0.2	0.10 ± 0.025	0.26 ± 0.08	1.7 ± 1.3	4.3
28	4.4 ± 3.8	4.5 ± 1.0	0.17 ± 0.14	0.46 ± 0.7	0.3 ± 0.5	10
37	6.5 ^a	6.6 ± 11	0.001 ± 0.002	0.19 ± 0.15	6.0 ± 1.5	23
42	3.9 ^a	3.2 ^a	0.008 ± 0.016	0.20 ± 0.18	5.1 ± 19	110

A thorough examination of the best-fit estimates of the Trefry and Franzmann (2003) model parameters allows an insight into the *in situ* properties of the contaminated site and associated changes in the microbial population during SAB mineralisation. One of the strengths of the model is that all three phases of $^{14}\text{CO}_2$ production in the temperature-mineralisation experiments are well described by the model parameters. The model accomplishes this by partitioning the substrate into a highly bioavailable fraction, and a less bioavailable fraction. The k_0 and v parameters describe production from the less bioavailable fraction of the isotope, while S_0 , k_2 , E_0 and μ describe production from the highly bioavailable fraction.

5.2.1.3.1 Mineralisation of less bioavailable fraction

The k_0 and v parameters are common to both growth forms of the extended model (Equation 5.3 and 5.4). The two growth rate models gave similar best-fit results for k_0 , although the linear form had tighter confidence intervals at respective growth temperatures. The k_0 parameter, which describes the long-term production rate from the less bioavailable fraction of substrate, and is assumed to be related to the amount of ^{14}C

incorporated into biomass (Nuck and Federle, 1996) although other processes that affect the bioavailability of ^{14}C -octadecane are expected to influence k_0 (Trefry and Franzmann, 2003). The k_0 parameter was approximately constant at lower temperatures but increased in the microcosms incubated at and above 28°C. The confidence interval for k_0 at 42°C is large for the linear growth form of the model (Table 5.1) and was too large to estimate in Table 5.2. This increase in the k_0 parameter could be related to the postulated change in microbial species composition. If there was a growing mesophilic population in the higher temperature microcosms, the mesophilic population would have had to increase significantly for detectable mineralisation to occur. A growing population requires more of the available carbon sources to be utilised in the construction of cellular material rather than in energy production. The increase in k_0 could equally be due to the increased bioavailability of the tracer due to its melting; the melting point of octadecane is 28.2°C (Weast, 1995).

For the lag parameter, ν , the exponential growth model gives appreciably better confidence intervals than the linear growth model, even though the estimated values are similar. In general the lag parameter is highest at low and at high temperatures (see Figure 3.2), and declines to near zero at 28°C. It is noted that the 90% lag time is approximately 1.5 ν for a Gaussian lag function (Trefry and Franzmann, 2003). Within the Trefry and Franzmann extended model, the lag parameter is used to delay action of the mineralisation term. As the Gaussian lag function starts at zero and asymptotes towards one, the 90% lag time is an estimate of the time at which the mineralisation is 90% of maximum rate (e.g. at 4°C the best fit estimate for ν is 3.4 d, therefore the mineralisation rate is 90% after $3.4 \times 1.5 = 5.1$ days).

The ^{14}C -octadecane mineralisation results from the 28°C microcosms, like the other mid-range temperature microcosm, did not exhibit a lag phase, but differed in that mineralisation rate did not plateau (Figure 3.2). This might be due to the increased bioavailability of octadecane at temperatures above its melting point of 28.2°C (Weast, 1995). It is widely recognised that hydrocarbons are more bioavailable as liquids (Wodzinski and Coyle, 1974). The decrease in the $n\text{-C}_{17}$: pristane and $n\text{-C}_{18}$: phytane biodegradation ratios, shown in Figure 3.3B, at and above 28°C indicates increased biodegradation. This increased biodegradation may be due to a change in the physical state of alkanes. Using radiolabeled hexadecane, Whyte *et al.* (1999) found an increased rate of hydrocarbon degradation in microcosms incubated at 23°C compared with those incubated at 5°C. They surmised that 23°C is the optimal temperature for cold-regions bioremediation as it utilised the increased bioavailability of the hydrocarbons without inhibiting the activity of the indigenous microbes. Their microcosm results appear similar to the mid-range temperature microcosms described here, in which the rate of mineralisation plateaued after *ca* 15 days.

Another possible explanation for the change in the latter part of the ^{14}C -octadecane mineralisation curve shown in Figure 3.2 might result from a change in the structure of the microbial community responsible for the mineralisation of the ^{14}C -octadecane (as might have occurred in the high range temperature microcosms; Chapter 3). As 28°C supports the growth of mesophilic and psychrotrophic microbes, a change in the community structure, from a psychrotrophic to a mesophilic-dominated population, would not have been as fast at this temperature as it might have been in the higher temperature microcosms.

5.2.1.3.2 Mineralisation of the highly bioavailable fraction

Having considered the k_0 and ν parameters, the remaining model parameters describe the kinetics of the short-lived production from the highly bioavailable substrate fraction. These parameters are S_0 and k_2 (linear growth rate model) and S_0 , E_0 and μ (exponential growth rate model). In considering the S_0 parameter, it is plausible to think of it as an indicator of the initial bioavailable concentration of substrate. It must be remembered that S_0 is a mathematical fitting function and thus is only an theoretical estimate of the initial bioavailable substrate concentration. Again, both growth models resulted in similar best-fit estimates, although the exponential model gave slightly tighter confidence intervals. It was expected that S_0 would remain steady up to 28°C and then increase at temperatures above this due to the ^{14}C -octadecane being in a liquid phase in those microcosms. The exponential growth rate form of the model did result in fairly stable S_0 results until 20°C, after which S_0 decreased. Again, the confidence limits on the 42°C microcosm results are too large for safe interpretation of those results. Similar behaviour was seen for S_0 in the linear form of the model.

In the linear form of the model, the k_2 parameter characterises the linear biomass growth rate and thus is an indicator of the degradative capacity of the microcosms. The best-fit estimates for k_2 increased with temperature until 37°C when it began to decline rapidly (Table 5.2). This is consistent with the notion of faster microbial process rates near optimal growth temperatures or psychrotrophic population die off. In the exponential model, the growth rate is determined by the initial rate parameter, E_0 , and an exponent μ . Best-fit estimates for E_0 were found to conform to an Arrhenius thermodynamic relation for temperatures above 0°C (Arrhenius, 1889) (see Figure 5.3). The Arrhenius model normally used in microbial contexts to describe the relationship of the natural log of the first order mineralisation co-efficient to the reciprocal of the

temperature (Section 5.2.1.1, Pelletire *et al.*, 1999). In this case, it is used to describe the natural log of the best-fit E_0 parameter instead. The Arrhenius equation for E_0 holds for the microcosms between 4 and 28°C. The 37 and 42°C results do not fit on this line. The initial microbiota in all of the microcosms would be the same, and it has been assumed that it was dominated by psychrotrophic species. As stated in Chapter 3, Antarctic microbes tend to be psychrotrophic and generally have a T_{opt} of around 25°C and a T_{max} below ~37°C. It is logical to assume that the initial growth rate of these psychrotrophic microbes would obey the Arrhenius equation, having a faster growth rate (and thus E_0), at higher temperatures until such point that their T_{opt} was reached. Incubation temperatures above the T_{opt} will result in a dramatic decrease in the growth rate. The increase of E_0 at 42°C as compared to 37°C might be due to the postulated mesophilic species, which would have a higher growth rate at 42°C than at 37°C. Interestingly the growth rate exponent μ was approximately constant throughout the set of microcosms. Thus, μ is largely unaffected by temperature and may be characteristic of the population/soil milieu from Old Casey Station.

Time-dependent production rates of $^{14}\text{CO}_2$ from ^{14}C -octadecane from the two bioavailable fractions can be derived from Equations 5.3 and 5.4. In these Equations, the first term represents the cumulative production from the highly bioavailable fraction, and the second gives the cumulative production from the less bioavailable fraction. The production rate from either fraction is obtained simply by differentiating the appropriate term with respect to time. Figure 5.4 shows rates from the highly bioavailable fraction. For both growth models, fitted curves yielded production rates with peak values that increased with temperature, and which were achieved at times that decreased with temperature. The total production from the bioavailable fraction also tended to increase

with increasing temperature up to 20°C (Table 5.3). In the exponential model, this relationship is linear ($r = 0.987$). This linearity is surprising as a sharp increase in the bioavailable fraction was expected as the temperature approached the melting point of the octadecane. The reason for the decrease of the highly bioavailable fraction at 28°C is unknown.

Table 5.3 Temperature dependence of the total $^{14}\text{CO}_2$ production from the highly bioavailable fraction.

Microcosm Temperature (°C)	Total $^{14}\text{CO}_2$ Production (10^{-8} mmol/g dry wt)	
	Linear model	Exponential Model
4	5.2	6.4
10	3.6	6.5
15	6.5	7.8
20	5.8	7.1
28	5.5	4.4

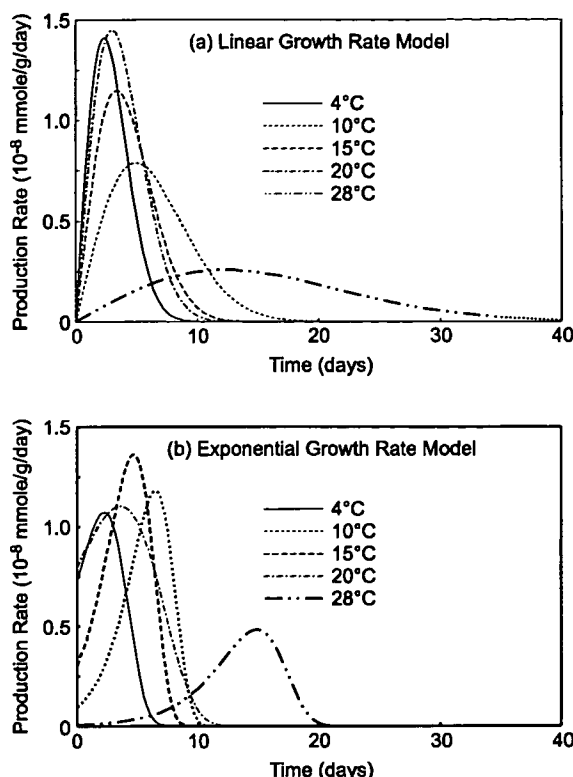


Figure 5.4 Production rate curves calculated using best-fit parameters for the two growth models, based on the highly bioavailable fraction of the label.

5.2.2 Modelling the effect of nitrogen and water on microbial mineralisation of ¹⁴C-octadecane

The best fit estimates for the modified three-half order model of Trefry and Franzmann (2003) for the microcosms that reached a plateau stage of growth in Chapter 4 (soil II), viz. the microcosms from Chapter 3 (Soil I - 420 mg N kg-soil-H₂O⁻¹), are given in Table 5.4. Soil I had the faster rate of mineralisation of the less bioavailable (incorporated) fraction of the radiometric tracer (k_0) but a slower rate of biomass growth (E_0). This indicates that soil I had a faster rate of microbial population turnover than soil II, and that numbers of hydrocarbon degrading microbes were increasing at a faster rate in soil II.

Table 5.4 Results of nonlinear regression on the production curves for different nutrient concentrations, with ideal exponential microbial growth ($\lambda=350$ or 0) and non-ideal (Gaussian) mineralisation. S_o are expressed in units of mg ^{14}C -octadecane kg soil $^{-1}$ converted to $^{14}\text{CO}_2$, k_o in units of ^{14}C -octadecane kg-soil $^{-1}$ d $^{-1}$, E_o and μ are in units of d $^{-1}$ and ν in units of days.

Nitrogen concentration (mg N kg-soil-H ₂ O $^{-1}$)	S_o (x 10 $^{-8}$)	k_o (x 10 $^{-11}$)	E_o	μ	ν
420	5.7	70.00	0.0160	0.54	77
508	9.8	15.6	0.1512	0.0072	390
697	16	6	0.0792	0.0048	445

In Section 5.2.4, the μ parameter, which is the non linear exponent of growth, was found to be largely unaffected by temperature and it was concluded that μ might be a characteristic of the microbial population or soil milieu from Old Casey Station. In the nutrient and water amended experiments described in Chapter 4, it was found that the μ parameter is roughly inversely proportional to nutrient concentration through the range 420-697 mg N kg-soil-H₂O $^{-1}$, suggesting that nutrients are a major factor limiting microbial growth rate in this soil.

5.3 Conclusion

The fitting of empirical kinetic models to data is undertaken to assist *a posteriori* analysis rather than to describe from first principles the type of reactions involved within the microcosms. Empirical fitting of the microcosm mineralisation results from Chapter 3 and Chapter 4 to the Trefry and Franzmann (2003) kinetic model provided useful estimates of the temperature and nutrient concentration dependence of key microbial population parameters. The availability of these functions raises the possibility of applying the production curves to obtain quantitative estimates of *in situ* remediation efficiencies under the seasonal thermal cycles at Old Casey Station.

The Trefry and Franzmann (2003) extended three-half order model logically described the three phases of isotope recovery in the microcosm experiments that reached a plateau phase of isotope recovery in both Chapter 3 and Chapter 4. By examining the effects of temperature and nutrient concentration on the best-fit estimates of the 5 model parameters it was possible to assess the importance of various factors, such as changing microbial community structure and tracer solubility. Unfortunately the model is not intuitive and requires that the microcosms reach the plateau phase of growth. Nevertheless, the model does provide a predictive framework to allow comparison of mineralisation under a range of environmental conditions.

Chapter 6

Effect of temperature on the soil microbial ecology: implications of high-temperature remediation

6.1 Introduction

Development of petroleum-hydrocarbon remediation strategies often involves treatability studies (Stevenson and Cole, 1999) to assess the potential for *in situ* microbial biodegradation of the contaminant (Chapter 3 and Chapter 4). Optimization of a bioremediation strategy typically includes the identification and characterisation of factors that limit or possibly enhance the activity of contaminant-degrading microbiota. In Antarctica the major limitations include low temperatures with corresponding low microbial activity (Chapter 3, Morita, 1992; Nedwell, 1999), poor water holding capacity of the soils and low soil nutrient contents (Chapter 4). Another potential limitation that may also affect engineered bioremediation strategies concerns the distribution, abundance and type of microorganisms in the contaminated soil, especially those that can effectively degrade petroleum hydrocarbons at medium to high temperatures. In remote cold regions where achieving a high level of remediation-efficiency is essential to keeping cost manageable, understanding the microbial community responsible for hydrocarbon degradation throughout different remediation treatments is the first step towards optimising the growth condition for the dominant contaminant-degrading organisms.

It was shown in Chapter 3 that biodegradation of SAB in Antarctic soil is positively correlated with temperature (between -2 and 42°C), with the fastest rate of mineralisation found at the highest temperature tested (Figure 3.2). The high rate of mineralisation above 37°C was unexpected as Antarctic microbes tend to be psychrotrophic (Franzmann, 1996; Aislabie *et al.*, 2000; Panicker *et al.*, 2002). As there

was a relatively long lag phase before the high rates of mineralisation at these elevated temperatures, it was postulated in Chapter 3 that a mesophilic component of the microbial population was initially minor, but after incubation at mesophilic temperatures they could be responsible for the bulk of the petroleum mineralisation. In this model, numerically minor or rare components in the microbiota would have resided in the soil at temperatures well outside temperatures most favourable for their growth. When given appropriate nutrient and water amendments, and exposed to higher temperatures, they increased greatly in numbers, possibly at the expense of psychrotrophic members of the microbial community that commonly dominate the microbiota of Antarctic soils (Line, 1988).

A mesophilic hydrocarbon degrading microbial population occurring in Antarctic contaminated sites opens the potential for utilising engineered remediation strategies that involve soil heating. As the Antarctic Treaty prohibits the introduction of non-indigenous biota (Lewis Smith, 1996), bioaugmentation with non-indigenous Antarctic organisms is not an option for contaminated sites in Antarctica. Moreover, in other cold regions such as Alaska, commercial bioaugmentation products are often less effective than the autochthonous hydrocarbon degrading microbiota (Filler *et al.*, 2001). Hence the presence of indigenous mesophilic organisms is essential if higher-temperature bioreactor or heated biopile-type treatments are to be considered for remediation strategies for hydrocarbon-contaminated Antarctic soils.

The analysis of microbial community structure and density is a challenge and current techniques have serious limitations (Head *et al.*, 1998; Powell *et al.*, 2003). Culture based methods, such as most probable number (MPN) counts or the Biolog system only detect between 0.1 - 10% of the total microbial community (Garland and Mills, 1991).

Another widely-used technique is phospholipid fatty acid (PLFA) analysis. This technique does not provide definitive identification of species composition and the PLFA profile can change depending of the physiological state of the microbial community (Ourisson *et al.*, 1979), and experimental test variables such as temperature can change the PLFA signature without a concurrent change in microbial community structure (Nichols *et al.*, 1997). DNA methods such as denaturing gradient gel electrophoresis (DGGE) also have limitations including gel and PCR biases (Powell *et al.*, 2003) and, in complex communities, often it is only the major species that are detected (Muyzer and Smalla, 1998). Colony hybridization and PCR amplification have previously been used to screen contaminated soils for the presence of the catabolic genes required for hydrocarbon degradation (Whyte *et al.*, 2001). Emerging molecular technologies, such as microarrays (Zhou, 2003), functional gene expression (Watanabe and Hamamura, 2003), and stable isotope (Pelz *et al.*, 2001; Manefield *et al.*, 2002; Pombo *et al.*, 2002; Adamczyk *et al.*, 2003) techniques allude to the possibility of linking the members within a microbial community to a particular metabolic function, and thus the isolation and characterisation of the microbe(s) responsible for environmentally significant contaminant removal. Unfortunately these techniques are still in their infancy; with numerous technical nuisances to overcome before their wide spread application in contaminated site assessments. As no single technique allows for the identification and characterisation of the key microbial elements responsible for the bulk of hydrocarbon degradation within a contaminated site, we are reliant on a combination of culture-dependent, molecular, chemical and physiological approaches.

This study aims to gain an understanding of the microbial community changes within Antarctic petroleum hydrocarbon contaminated soils when incubated at different

temperatures. The cause of maximal hydrocarbon mineralisation at $\geq 42^{\circ}\text{C}$ (Chapter 3), significantly above previously reported optimum growth temperature for microbes in cold soils (Franzmann, 1996; McCammon *et al.*, 1998; Smith *et al.*, 2000), is further investigated here. Degradation of the entire aliphatic hydrocarbon envelop was traced by GC-FID analysis. MPN and DGGE analyses were used to assess changes in the microbial community structure. The dominant culturable hydrocarbon degrading bacteria were then isolated and characterised by their PLFA and 16S rRNA gene sequences. The identification and characterisation of a hydrocarbon degrading microbial population from the spill site in Antarctica is an important first step in optimising growth conditions so that a cost-effective engineered remediation strategy can be developed that is suitable for this challenging polar environment.

6.2 Methods

6.2.1 Site history, contaminants, experimental rationale and set-up

To be consistent with our previous experiments (Chapter 3 and Chapter 4) soil from the Old Casey Station spill was also used in this experiment. Seventy kilograms of petroleum-contaminated soil was sieved to 5 mm in the 1998-99 summer season as part of a long-term field bioremediation trial (Snape *et al.*, 2003), and a sub-sample of that soil is used here. Frozen soil (-18°C) was returned to Australia for these experiments.

Microcosms were prepared as previously described in Chapter 3, except that radiolabelled tracer was not added. In summary, *ca* 1300 g of soil was thawed at 4°C overnight. It was then mixed and kept on ice. Nutrients were added as NH_4Cl and K_2PO_4 , and moisture content was adjusted to the levels used in our previous experiments

(i.e. *ca* 420 mg N kg-soil-H₂O⁻¹ and 14% gravimetric water content) (Chapter 4). Squalane was added to act as an internal standard for the GC analyses.

Each microcosm consisted of *ca* 70 g soil in 100 mL hexane-rinsed Schott bottles with Teflon-lined caps. They were successfully incubated in triplicate at 4, 10 and 42°C. Chemically inhibited control microcosms were prepared from a 450 g sub-sample of the soil to which 2.25 g HgCl₂ was added. Control microcosms were incubated in triplicate at 4°C and 42°C. Subsamples of the initial soil (with and without HgCl₂) were taken for MPN, DGGE and GC analyses.

Approximately 1 g of soil was subsampled for MPN analysis with a further 10 g taken for GC analysis. Samples were taken from the control and test microcosms on days 5, 7, 20, 30 and 40. All sub samples for DGGE and GC analyses were frozen at -18°C until analysed, while MPNs were inoculated within 30 minutes of sample collection.

6.2.2 Hydrocarbon analysis

Aliphatic hydrocarbons were extracted from the soil and separated on a silica-alumina column as described previously in Chapter 3. In brief, the aliphatic fractions were analysed using a Varian 3410 GC fitted with a septum-equipped programmable injector and flame ionisation detector. Analyses were performed using a 50 m non-polar methyl-silicone-fused silica capillary column (HP-1, 0.32 mm internal diameter, 0.23 µm film thickness) and helium as the carrier gas. All samples were run at 35°C for 1 min then ramped to 120°C at 30°C min⁻¹ then to 310°C at 4°C min⁻¹ and then held for 15 min. Total aliphatic hydrocarbon concentrations were determined from the sum of all the GC-resolved peaks and the unresolved complex mixture (UCM) in the aliphatic fraction normalised against the added nonacosane (C₂₉H₆₀; Sigma) extraction standard.

6.2.3 *Microbial population enumeration and isolation*

Heterotrophic and hydrocarbon degrading bacteria were enumerated from each treatment using microtitre MPN methods. Hydrocarbon degrading bacteria were enumerated using a tailored version of the Brown and Braddock (1990) sheen-screen MPN method. An initial dilution of *ca* 1 g soil in 10 mL basal hydrocarbon medium (Atlas and Parks, 1997) was used for a 6 tube MPN, with seven 1: 10 serial dilutions in a 96 well microtitre plate. After serial dilution, 5 μ L of filter-sterilised SAB was applied to the surface of the medium in each well. The last row of tubes contained only medium and SAB as an un-inoculated control. Microtitre plates were incubated for up to 30 days and examined every 5 days. Tubes were scored as positive if the hydrocarbon sheen-screen was disrupted. Heterotrophic bacteria were enumerated in a similar manner except half strength Tryptone Soya Broth (TSB) was used instead of hydrocarbon degrading medium and SAB. Positive growth at each dilution was indicated by turbidity. Heterotrophic microtitre plates were incubated for ten days. All microtitre plates were incubated at the same temperature as the associated microcosms.

Dominant hydrocarbon degrading bacteria were isolated at the end of the experiment from each microcosm on the above basal hydrocarbon medium with the addition of 15 g agar L⁻¹. A streak-plate from the most dilute positive MPN well was incubated at the associated temperature for 14 days. The dominant colony types from each plate were sub-cultured three times to ensure purity. Microbes were preserved at -18°C in 2 mL sterile glycerol (10%). Student t-tests were undertaken to assess the statistical significance ($p < 0.05$) of the observed changes in the hydrocarbon signatures and in most probable numbers of organisms within the contaminated soil throughout the incubation periods.

6.2.4 Soil microbial community composition

DGGE was used to assess overall changes in the soil microbial community in each microcosm. Analyses were performed as previously described (Powell *et al.*, 2003) on soil before and after the 40 days of incubation. Briefly, primers 357FC (CGC CCG CCG CGC CCC GCG CCC GGCCCG CCG CCC CCG CCC CCC TAC GGG AGG CAG CAG) and 907R (CCG TCA ATT CCT TTG AGT TT) were used to amplify a fragment of the 16S rRNA gene using Advantage 2 Taq (Clontech). DDGE was performed using the D-Code Universal Mutation Detection System (Bio-Rad) with a denaturing gradient of 30-65% (where 100% denaturant is 7 M urea and 40% formamide). Gels were run at 80 V for 16 h at 60°C in 1 x TAE (40 mM Tris, 20 mM sodium acetate, 1 mM EDTA). Gel photographs were scanned using the UTHSCSA ImageTool program (University of Texas Health Science Centre, USA). The banding pattern was transformed into a presence/absence matrix for statistical analysis using the Primer5 (Plymouth Marine Laboratory, UK) multivariate statistical package.

6.2.5 Identification of hydrocarbon degrading isolates

Bacterial cultures of the dominant culturable organisms were identified by their 16S rRNA gene sequences. Colonies were suspended in 0.3 mL saline EDTA with 50 µL 10% SDS. After gentle mixing, 0.3 mL of 24: 1 chloroform: isoamylalcohol was added. This emulsion was centrifuged at 10 000 x g for 5 min and the aqueous phase removed to a clean tube. The crude DNA was further purified using the Prep-a-gene kit (Bio-Rad). A fragment of the 16S rRNA gene was amplified using HotStar Mastermix (Qiagen) using the primers 519F (CAG CMG CCG CGG TAA TAC) and 1492R (TAC GGY TAC CTT GTT ACG ACT T). The PCR product was sequenced with the BigDye Terminator Ready Reaction mix and the 519F primer. Sequences were compared to the

GenBank database using BLAST searches (<http://www.ncbi.nlm.nih.gov/blast>). The most similar sequences in GenBank were downloaded and aligned against each cultures sequence. A phylogenetic tree was constructed using DNADIST and NEIGHBOR from the PHYLIP package (Felsenstein, 1995).

6.2.6 *Extraction and identification of fatty acids from pure cultures*

Fatty acids were extracted, saponified and methylated according to the Sherlock Microbial Identification System procedure (MIDI). Briefly, cultures were grown on TSBA plates at either 4, 10 or 42°C until sufficient biomass developed. A small scoop of cell material was added to 1 mL 15% w/v KOH in methanol: milliQ water (1:1) in a screw-capped test tube at 100°C for 30 min to extract lipids, and to free any fatty acids from other lipid components by base hydrolysis. Two millilitre of a methanol: 6 M HCl (11:13) mixture was added to convert the fatty acids to their corresponding fatty acid methyl esters (FAMES). After addition of 1 mL milliQ, the FAMES were extracted with 3 x 1.8 mL of hexane: CH₂Cl₂ (4:1) The solvent was removed under a stream of dry nitrogen, and the residue treated with bis(trimethylsilyl)trifluoroacetamide (BSTFA) in order to convert any hydroxy fatty acids to their corresponding trimethylsilyl ethers. Excess BSTFA was removed under a stream of nitrogen, and the FAMES were taken up in 200 – 500 µL CH₂Cl₂ for injection into the GC.

GC analysis was carried out using a HP5890 gas chromatograph fitted with a split/splitless injector maintained at 250°C (run in the splitless mode) and a flame ionisation detector (320°C). The capillary column used was a HP 2 Ultra (50 m x 0.32 mm inner diameter x 0.17 µm film thickness), and the carrier gas helium. The head pressure was 60 kPa. Samples were injected with the oven temperature at 50°C, which was maintained for 1 minute. The temperature was then increased at a rate of 30°C min⁻¹ to

150°C, then by 2°C min⁻¹ to 250°C and finally by 5°C min⁻¹ to 300°C, which was maintained for 15 minutes. Individual FAMES were identified by comparison of their retention times to laboratory standards. For identification of unknown FAMES, and FAMES for which the retention time did not give an unambiguous identity, samples were injected into a GC-mass spectrometer system that provided further information about the structure of the compounds. Finally, the locations of the double bonds in the monounsaturated acids were determined unequivocally by reaction with dimethyl disulfide according to the method of Nichols *et al.* (1986).

Fatty acids were identified by the number of carbon atoms, the number of double bonds and the position of the unsaturation from the aliphatic end, where as the position of methyl and hydroxy groups were numbered from the carboxyl end of the molecule (e.g., 18:1ω9). The prefixes or suffixes *c*, *t*, *i*, *a*, *cy*, Me, and OH denote cis- and trans-stereochemistry around double bonds, iso- and anteiso- methyl branching, and the presence of a cyclopropane ring, a mid-chain methyl group and a hydroxy group within the carbon chain. In line with standard nomenclature, the positions of double bonds are numbered from the aliphatic end of molecule, and the positions of hydroxy and mid-chain methyl groups from the carboxyl end. The statistical significance of differing fatty acid compositions were assessed with a Bray-Curtis similarity matrix after square root transformation using the Primer5 (Plymouth Marine Laboratory, UK) multivariate statistical package.

6.3 Results and discussion

6.3.1 *Hydrocarbon concentrations throughout the experiment*

The initial concentration of aliphatic hydrocarbon (Figure 6.1A) in the microcosms were similar to the aliphatic hydrocarbon concentration in the microcosm that were used previously to test the effect of temperature on hydrocarbon mineralisation rates in these soils (Chapter 3). Likewise, there was no significant decrease in the total aliphatic hydrocarbon concentration in any of the chemically inhibited control microcosms after 40 days incubation, although there was considerable heterogeneity between samples (Figure 6.1A). For this reason there was no statistically significant reduction in total aliphatic hydrocarbons in any of the test microcosms.

Evaporative loss of hydrocarbon is indicated by a change in the ratio of light to heavier isoprenoids that are resistant to biodegradation (Chapter 2 Wang and Fingas; 2003a; Snape *et al.*, Submitted). Up to about 85% evaporative loss of SAB can be quantified from the *i*-C₁₃: pristane ratio and thus it has been proposed as the most sensitive index to indicate evaporative loss in environmental samples (Snape *et al.*, Submitted). The percent change in the *i*-C₁₃: pristane ratio from the initial soil is shown in Figure 6.1B. Statistically significant volatilisation of the light hydrocarbons from the microcosms would be indicated by a 33% change in the *i*-C₁₃: pristane ratio from the initial soil ratio (0.94 ± 0.15); but no significant volatilisation occurred in any of the control or test microcosms in this study.

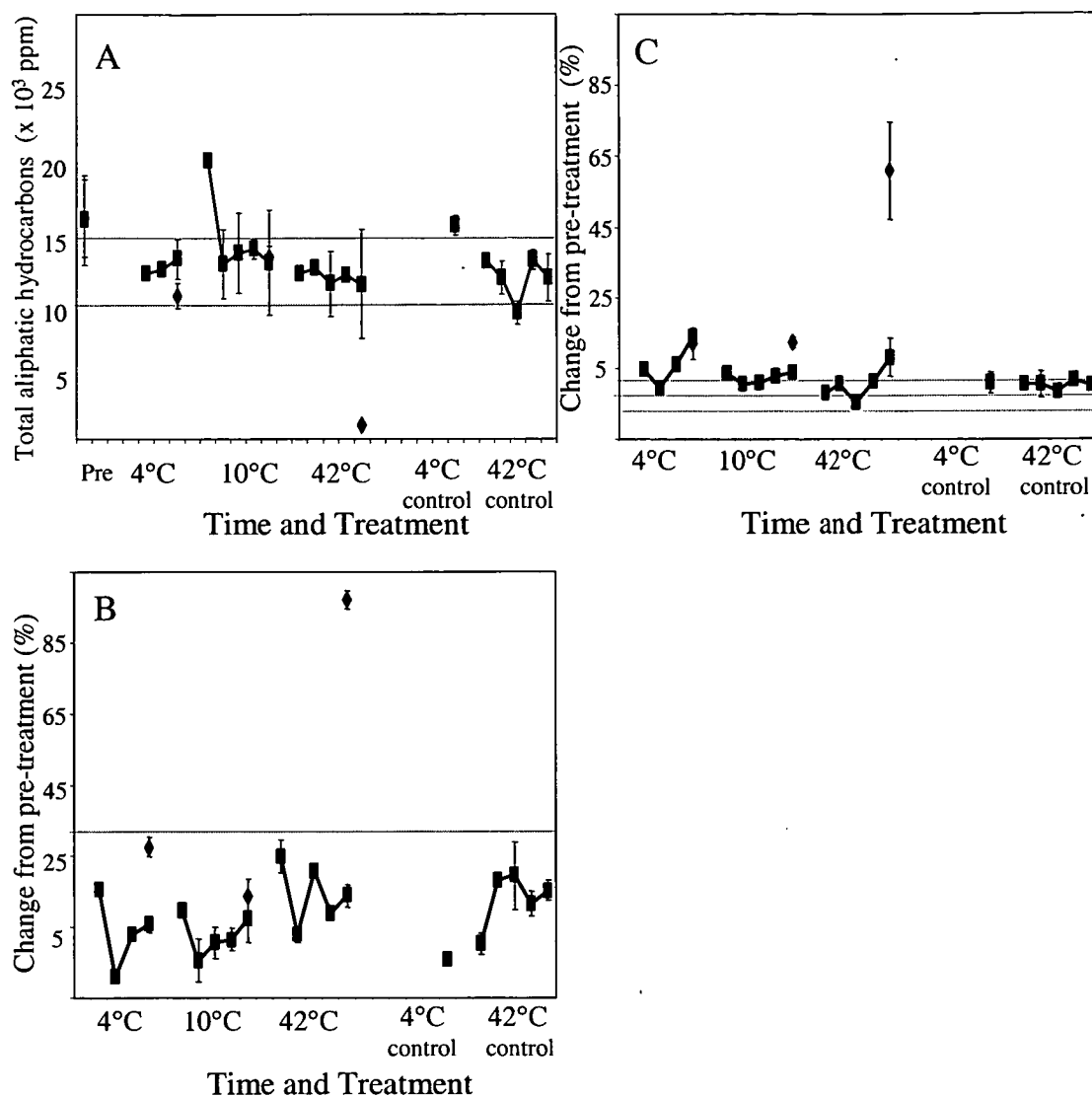


Figure 6.1 Total aliphatic hydrocarbon concentration (Panel A) and the change from the initial (pre-treatment) for both evaporation (Panel B; *i*-C₁₃: pristane) and biodegradation (Panel C; *n*-C₁₇: pristane). Square symbols represent the data from this experiment; data from Chapter 3 are shown for comparison (diamond symbols). Error bars in panels A-C represent one standard deviation of the microcosm replicates at each time point, and the change required for statistical differences according to student t-test are indicated by a broken line on these panels.

Biodegradation of hydrocarbon mixtures is indicated by a decrease in the ratio of a straight chain *n*-alkane to an isoprenoid with a similar vapour point as the *n*-alkane, such as *n*-C₁₇: pristane (Chapter 2 Prince, 1993; Wang and Fingas, 2003a; Snape *et al.*, Submitted). Both molecules undergo similar abiotic weathering such as evaporation, but the straight chain alkanes are more biodegradable (Atlas, 1981). The percent change in *n*-C₁₇: pristane ratio from the initial soil is shown in Figure 6.1C. The *n*-C₁₇: pristane ratio appears to be less affected by sample heterogeneity than the *i*-C₁₃: pristane ratio, as statistically significant biodegradation is indicated by a 3% or greater change from the initial soil ratio (1.11 ± 0.02). The addition of HgCl₂ appears to effectively halt the microbial degradation of the aliphatic petroleum hydrocarbons as no change in the *n*-C₁₇: pristane ratio was detected in any of the chemically treated control microcosms. Significant biodegradation eventually occurred in all of the test microcosms, with significant aliphatic hydrocarbon mineralisation observed after 30 days in the 4°C microcosms, whereas 40 days were required in the 10 and 42°C microcosms before the *n*-C₁₇: pristane ratios became significantly lower. The extended lag prior to biodegradation at 42°C was expected as an extended lag phase in ¹⁴C-octadecane mineralisation was previously observed in soil from this site (Chapter 3).

6.3.2 *Bacterial abundance*

The bacterial abundance as estimated by MPN was highly variable, resulting in high standard deviations in each microcosm and at each time of sample collection (Table 6.1). This is a widely recognised limitation of the technique. The addition of HgCl₂ effectively halted microbial population growth. The initial culturable heterotrophic microbial population (between 1.7×10^5 g⁻¹ at 4°C and 6.1×10^5 g⁻¹ at 10°C) was similar to

numbers of culturable heterotrophs observed in this soil ($1.38 \times 10^5 \text{ g}^{-1}$ at 4°C : Chapter 7). Numbers are lower than occur at uncontaminated sites around the Casey region (9×10^7 to $1 \times 10^9 \text{ g}^{-1}$ by epifluorescence microscopy (Beyer *et al.*, 2001) and, $1 \times 10^7 \text{ g}^{-1}$ by MPN analysis (Bowman *et al.*, 2003)). Such a range of bacterial abundances has been observed in other Antarctic hydrocarbon-contaminated soil environments. For sites in the Ross Dependency, Aislabe *et al.* (1998) enumerated between $1.1 \times 10^3 \text{ g}^{-1}$ and $5.8 \times 10^7 \text{ g}^{-1}$ total heterotrophs by plate counts, and up to $1.7 \times 10^7 \text{ g}^{-1}$ hydrocarbon degrading microbes by MPN analysis. Likewise, Delille (2000) showed that soil in four contaminated site in the Terra Adélie land area contain between 10^8 and 10^9 g^{-1} total heterotrophs and between 10^3 and 10^6 g^{-1} hydrocarbon degraders.

Table 6.1 Numbers of heterotrophic and hydrocarbon degrading bacterial numbers as determined by MPN (cells per g dry soil⁻¹). Mean and standard deviation (1s) are shown. NG is no cells recovered in the MPN medium.

Time (days)	Controls 4 & 42°C	SAB as sole carbon source			Growth on TSB		
		4°C	10°C	42°C	4°C	10°C	42°C
0	NG	$9.3 \times 10^3 \pm 8.1 \times 10^3$	$1.4 \times 10^3 \pm 1.2 \times 10^3$	$2.8 \times 10^3 \pm 2.8 \times 10^3$	$1.7 \times 10^5 \pm 8.1 \times 10^3$	$6.1 \times 10^5 \pm 1.4 \times 10^5$	$1.6 \times 10^2 \pm 2.9 \times 10^2$
		$7.7 \times 10^5 \pm 3.8 \times 10^5$	$2.8 \times 10^5 \pm 1.6 \times 10^5$	NG	$3.7 \times 10^7 \pm 2.0 \times 10^7$	$8.7 \times 10^7 \pm 5.2 \times 10^7$	$4.2 \times 10^6 \pm 3.0 \times 10^6$
5	NG	$7.0 \times 10^6 \pm 3.8 \times 10^6$	$9.9 \times 10^5 \pm 1.2 \times 10^6$	NG	$3.5 \times 10^7 \pm 3.2 \times 10^7$	$2.2 \times 10^7 \pm 8.1 \times 10^6$	$7.2 \times 10^6 \pm 6.3 \times 10^6$
		$8.3 \times 10^5 \pm 2.3 \times 10^5$	$4.6 \times 10^7 \pm 4.3 \times 10^7$	NG	$7.6 \times 10^6 \pm 1.0 \times 10^6$	$2.2 \times 10^7 \pm 2.5 \times 10^7$	$8.4 \times 10^6 \pm 1.6 \times 10^5$
8	NG	$7.1 \times 10^2 \pm 1.1 \times 10^6$	$1.9 \times 10^7 \pm 1.1 \times 10^7$	NG	$4.1 \times 10^7 \pm \pm 2.7 \times 10^7$	$2.1 \times 10^7 \pm 3.5 \times 10^6$	$2.3 \times 10^7 \pm 1.6 \times 10^7$
		$1.3 \times 10^4 \pm 6.5 \times 10^3$	$1.8 \times 10^7 \pm 2.5 \times 10^7$	NG	$1.9 \times 10^7 \pm 1.9 \times 10^7$	$2.1 \times 10^7 \pm 1.8 \times 10^7$	$3.9 \times 10^7 \pm 1.9 \times 10^7$
20	NG						
30	NG						
40	NG						

The total bacterial population increased by two orders of magnitude to $1.2 \times 10^8 \text{ g}^{-1}$ dry soil after 10 days incubation in our microcosms, which is attributed largely to the addition of nutrients (*cf.* Chapter 4). The culturable psychrotrophic bacterial population then decreased and remained stable at *ca* $7 \times 10^7 \text{ g}^{-1}$ dry soil. Ringelberg *et al.* (2001) also showed a sharp increase in biomass (measured by total PLFA concentration in soil)

during the bioremediation of polyaromatic hydrocarbons. After 2 months biomass levels decreased which they ascribed to a natural progression of biological mechanisms (i.e., parasitism and predation).

Initially the mesophilic bacterial population (those growing at 42°C) was a minor component of the total population (*ca* 0.2%) and this component increased exponentially in the first 5 days of the experiment and then continued to increase steadily throughout the rest of the experiment (*ca* 35% after 40 days incubation). While the culturable mesophilic bacteria recovered on TSB increased throughout the experiment, culturable hydrocarbon degrading bacteria at 42°C could only be enumerated in the initial soil (2.8×10^3 g dry soil⁻¹). However, as it was possible to isolate bacteria at 42°C on basal media with hydrocarbons as a sole carbon source, culturable hydrocarbon degraders were present in the microcosms, but at very low numbers, or required surfaces for growth.

The average culturable hydrocarbon degrading bacteria at 4°C were *ca* 7% of the total culturable heterotrophic bacteria over the entire 40 days incubation, with the highest proportion of hydrocarbon degrading bacteria occurring after 20 days. At 10°C hydrocarbon-degrading bacteria were more dominant in the assemblage, averaging *ca* 60% of the number of culturable heterotrophs.

6.3.3 Microbial community structure

Changes within the microbial community were investigated by DGGE analysis and by isolation and characterisation of the dominant hydrocarbon degrading bacteria at each temperature. A photograph of the DGGE gels is shown in Figure 6.2. The Figure also shows the banding pattern of three microcosms that were incubated at 28°C, but due to

equipment failure these microcosms were not considered further. The banding pattern in each DGGE gel was recorded as a presence-absence matrix then transformed into a similarity matrix using Bray-Curtis transformation and plotted as a non-metric multi-dimensional scaling (MDS) ordination plot (Figure 6.3). Differences between groups were tested by an analysis of similarity (ANOSIM) (Table 6.2).

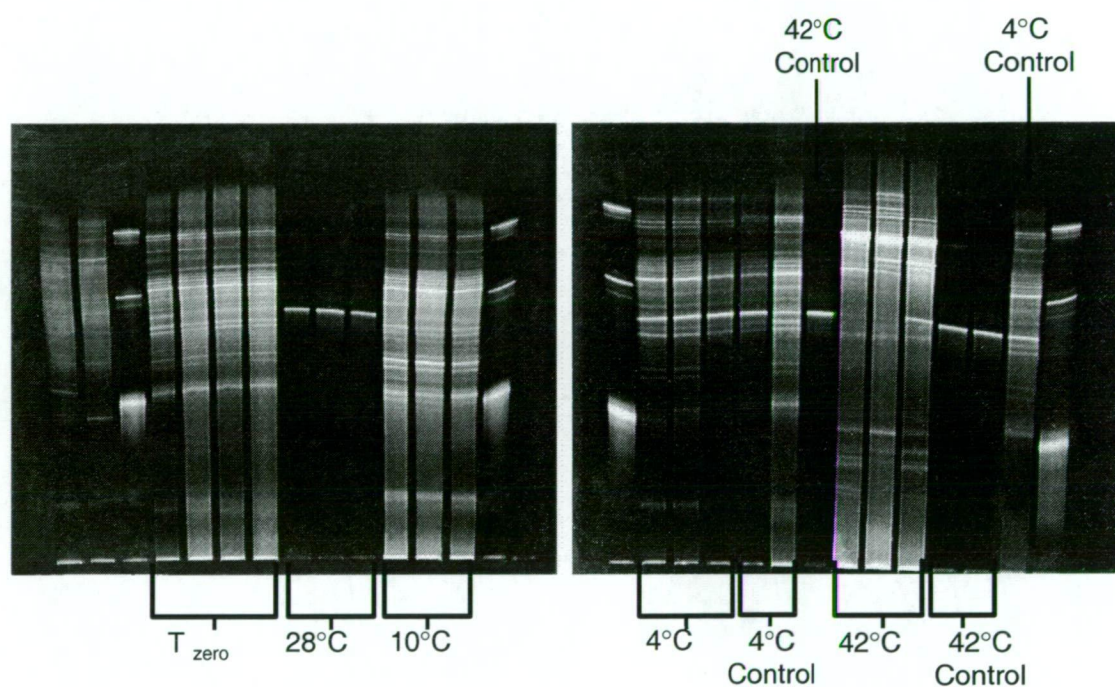


Figure 6.2 Photographs of the DGGE gels from the analysis of the triplicate soil microcosms. The outside lanes (unlabelled) on each gel are a standard DNA control mix used within our laboratory. The DNA from the initial soil (T_{zero}) and after 40 days incubation; lanes are labelled with the incubation temperature.

The addition of $HgCl_2$ to the soil did not alter the banding pattern in the initial pre-treatment soil, with all four initial replicates (two with and two without $HgCl_2$ addition) exhibiting the same banding pattern. These four initial replicates were combined as one treatment for further statistical analysis. The DGGE banding pattern in

all of the 42°C control microcosms contained only a single band. This same band also occurred in all of the 28°C microcosm after it was accidentally heated to 90°C for three days due to thermostat failure (Figure 6.2). The HgCl₂ was added to inhibit microbial activity throughout the experiment, and a correlation between mercury concentration and reduced complexity in species community composition has been found previously (Pennanen, 2001; Casucci *et al.*, 2003). The combination of increased temperature (42°C) and chemical treatment or extremely high temperatures (90°C) reduced the total soil microbial community complexity to a single band in the PCR-DGGE analysis. It is also possible that this single band represents a spore forming microbe(s). Treatments which are highly different from other treatments may skew multivariate MDS analysis and for this reason the 42°C chemically inhibited controls were removed from the data set to allow detailed examination of the subtle difference in the other treatments (Table 6.2).

There were significant shifts in the microbial community within the 4°C chemically inhibited controls. There are two factors which could contribute to the changes within the microbial community within the 4°C chemically inhibited controls. Either the HgCl₂ did not completely inhibit microbial activity at 4°C, or the combined effect of temperature and mercury allowed preservation of some, but not all of the DNA, which could be subsequently amplified by PCR.

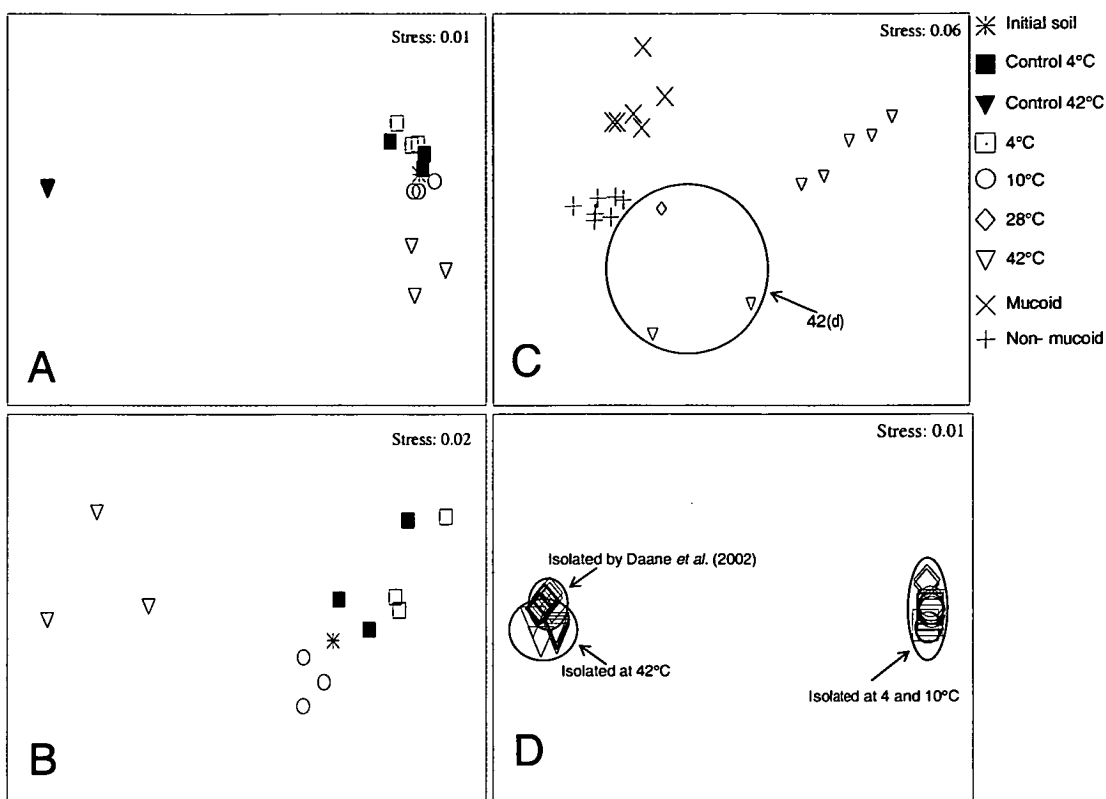


Figure 6.3 Panels A and B are MDS ordination plots showing the relative similarities in the DGGE banding pattern between initial soil, incubated treatment and control microcosms. Panel A is the complete data set, while Panel B has the 42°C control microcosms removed as they contained only one band and were completely dissimilar to all of the other patterns. The initial soil with and without HgCl₂ exhibited the same banding pattern and thus were combined for further statistical analysis. Panel C and D show the MDS ordination plots of the relative similarity of the FAME data. In Panel C mucooid and non-mucooid isolates are from Daane *et al.* (2002). The acids identified in this study and not by the MIDI system as used by Daane *et al.* (2002) have been grouped to form ‘other’ in the multivariate statistical analysis. Panel D is the MDS based the temperature the isolates were incubated at before FAME analysis.

The ANOSIM of the DGGE banding pattern showed that the soil incubated at 4°C contained a microbial population that was not significantly different to the population in the 4°C controls, but was significantly different from the microbial population in the initial soil (Table 6.2). The change in the microbial community in the 4°C control microcosms compared to the initial soil was not expected. While the *in situ* soil

temperature at Old Casey Station is close to 4°C (Chapter 3, Appendix 10.3) nutrients amendments to the microcosms may have caused the change in the microbial community in the 4°C treatment microcosms.

Table 6.2 Pair-wise ANOSIM of the DGGE banding patterns with initial control and test soil combined but excluding the 42°C controls. R statistic is a measure of similarity (0 is maximum similarly while 1 is maximum dissimilarly) while the significance level is the percent of instances the observed pattern occurs during random permutations. Each treatment and control consisted of three replicates, while the initial soil represents four treatments. Ten and 2.9 % are the best achievable statistic level with 3 x 3 or 3 x 4 replicates compared respectively.

Pair-groups	R	Significance
	Statistic	Level %
Control 4°C, 42°C	1.000	10
Control 4°C, 4°C	0.074	50
Control 4°C, 10°C	0.593	10
Control 4°C, Initial	0.630	2.9
42°C, 4°C	1.000	10
42°C, 10°C	1.000	10
42°C, Initial	1.000	2.9
4°C, 10°C	0.981	10
4°C, Initial	0.889	2.9
10°C, Initial	0.778	2.9

6.3.4 Dominant hydrocarbon degrading isolates

There was no growth detected in the hydrocarbon degrading MPN at 42°C after 40 days (Table 6.1). The cultures were obtained by directly plating a 1: 10 soil dilution onto hydrocarbon containing agar plates. The 4 and 10°C cultures were obtained from the highest MPN dilution that showed hydrocarbon degradation. The strains clustered into two groups based on their 16S rRNA gene sequence (Figure 6.4). One group contained the bacteria isolated from the 4 and 10°C microcosms, while the other group contained the isolates from the microcosms incubated at 42°C. The 4 and 10°C isolates clustered with *Pseudomonas spp.*, with no apparent distinctions between these cultures.

Pseudomonas spp. are ubiquitous and many strains degrade hydrocarbons (Eriksson *et al.*, 2001; Belhaj *et al.*, 2002; Kahng and Nam, 2002; Rahman *et al.*, 2002; Roy *et al.*, 2002). Strains 4(f), 10(b) and 10(c) were the most similar to each other, with 16S rRNA gene sequence fragments greater than 98% sequence identity.

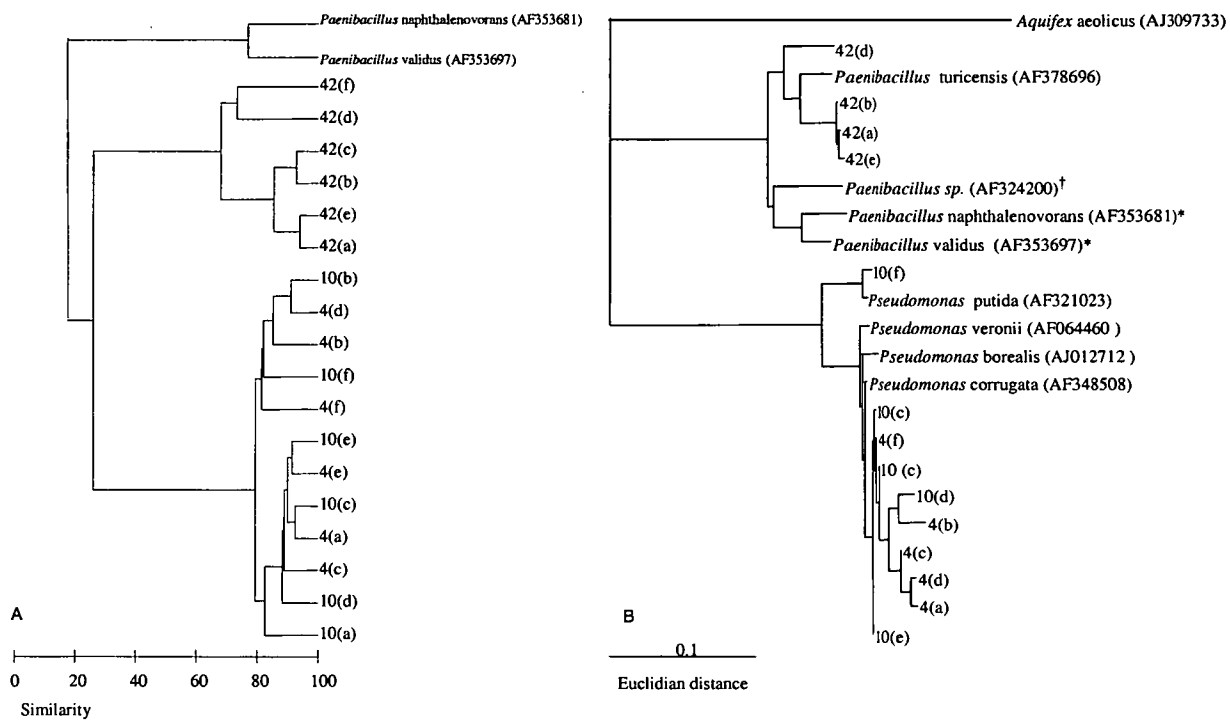


Figure 6.4 Panel A shows the similarities between the isolates FAME. The tree was constructed after square-root Bray-Curtis transformation and cluster analysis (group-average linkages). Temperatures indicated after the isolate designations specify the temperature at which the isolates were regrown to investigate the effect of temperature on FAME composition. Panel B is a phylogenetic tree based on partial 16S rRNA gene sequences. Isolates are designated according to incubation temperature and isolate designation, (e.g. 4°C isolate b is 4(b)). Reference sequences are shown with GenBank accession numbers. Isolates indicated by an asterisk were isolated by Daane *et al.* (2002) and isolates with a cross were from Antarctica (Christner *et al.*, 2001).

16S rRNA gene sequences of the cultures that dominated the culturable hydrocarbon degraders at 42°C were most similar to *Paenibacillus turicensis* (Bosshard *et al.*, 2002). *Paenibacillus* strains with the ability to degrade petroleum hydrocarbons have been previously found in contaminated soil from the Czech Republic (Meyer *et al.*, 1999) and in salt marshes in Brooklyn, NY (Daane *et al.*, 2001; Daane *et al.*, 2002). Daane *et al.* (2002) isolated two *Paenibacillus spp.* with differing colony morphology, being either mucoid or non-mucoid in nature. A representative of each of these strains is included in Figure 6.3 and Figure 6.4. All of the *Paenibacillus spp.* isolated by Daane *et al.* (2002) were grown under mesophilic conditions. In Antarctica, *Paenibacillus spp.* have been isolated from soil from Cape Evans, Ross Island (Wery *et al.*, 2003), and associated with particulates within the accreted ice from above Lake Vostok (Christner *et al.*, 2001). Both previous Antarctic *Paenibacillus spp.* isolates were 98.5% similar to each other. However, the 42°C isolates in this study clustered separately from the Lake Vostok isolate (AF324200).

The major phospholipids obtained from the hydrocarbon degrading cultures are listed in Table 6.3. The MDS ordination plot based on the FAME composition (Figure 6.3) also indicated that the cultures cluster into mesophilic and psychrotrophic groups. The ANOSIM demonstrated that the strains isolated at 42°C were significantly different from cultures obtained from the 4°C or 10°C microcosms, but cultures obtained from the 4 and 10°C microcosms were similar (Table 6.4). The two types of *Paenibacillus spp.* isolated by Daane *et al.* (2002) were also significantly different from each other and the *Paenibacillus spp.* isolated in this study. Cluster analysis of the FAME compositions of the cultures produced the same groupings as the phylogenetic tree (Figure 6.4).

Isolate	Acid (percent of total acids detected)																			18:1 ω7c	Others
	10:0 2OH	12:0 3OH	12:0 2OH	14:0	14:0 2OH	i14:0	15:0	i15:0	a15:0	16:0	i16:0	16:0 3OH	16:1 ω7c	16:1 ω7t	16:1 ω11c	i17:0	a17:0	cy17:0	18:0		
4(a)	4.2	1.0	-	-	-	-	-	-	-	23.9	-	-	54.4	-	-	-	-	-	1.1	15.3	0.1
4(b)	0.7	0.3	-	-	0.1	-	-	-	-	21.7	-	-	54.0	0.2	-	-	-	0.2	0.3	22.6	-
4(c)	0.6	0.5	-	-	-	-	-	-	-	27.7	-	-	53.3	0.1	-	-	-	-	1.2	16.4	0.2
4(d)	2.0	0.8	-	0.1	-	-	-	-	-	23.4	-	-	56.8	0.2	-	-	-	0.1	0.6	16.0	-
4(e)	1.0	0.8	-	-	-	-	-	-	-	24.6	-	-	57.8	0.2	-	-	-	-	0.9	14.8	-
4(f)	2.7	0.4	-	-	-	-	-	-	-	20.9	-	-	51.9	0.2	-	-	-	0.2	0.1	23.6	-
10(a)	0.2	1.0	-	-	-	-	-	-	-	27.3	-	-	48.3	-	-	-	-	-	2.3	20.9	-
10(b)	1.7	0.6	-	-	-	-	-	-	-	19.8	-	-	58.1	0.3	-	-	-	-	1.0	18.5	-
10(c)	8.2	0.8	-	-	-	-	-	-	-	21.3	-	-	53.6	0.2	-	-	-	-	0.8	15.1	-
10(d)	1.6	0.9	-	-	-	-	-	-	-	35.6	-	-	50.9	-	-	-	-	-	2.0	8.9	-
10(e)	2.2	0.9	-	-	-	-	-	-	-	26.0	-	-	50.0	0.2	-	-	-	-	2.9	17.8	-
10(f)	3.0	0.9	-	-	0.1	-	-	-	-	18.4	-	0.3	49.4	0.2	-	-	-	-	1.4	26.2	-
42(a)	-	-	-	2.9	-	-	0.6	2.2	11.8	60.3	9.8	-	-	-	-	2.9	7.1	-	-	-	2.4
42(b)	-	-	-	2.6	-	0.6	0.7	7.1	23.3	39.7	10.6	-	-	-	-	4.5	6.6	-	-	-	4.3
42(c)	-	-	-	3.2	-	0.5	1.7	5.4	18.0	45.6	10.8	-	-	-	-	4.4	6.9	-	-	-	3.5
42(d)	-	-	-	0.5	-	2.0	1.3	38.0	37.4	3.0	5.9	-	-	-	-	4.4	6.0	-	-	-	1.5
42(e)	-	-	-	3.1	-	-	0.9	1.8	9.7	67.4	8.0	-	-	-	-	2.0	4.5	-	-	-	2.6
42(f)	-	-	-	1.5	-	5.6	1.3	10.1	13.4	6.5	18.9	-	-	-	-	11.5	26.0	-	-	-	5.2
Isolate – incubation temperature																					
4(a) - 4	1.3	4.4	1.4	0.5	0.4	-	-	-	-	19.2	-	0.2	47.8	1.7	-	-	-	0.3	0.1	22.3	0.5
4(a) - 10	0.2	4.1	1.2	0.3	0.4	-	-	-	-	21.4	-	0.1	41.6	4.5	-	-	-	0.4	0.2	25.6	-
4(a) - 28	1.1	6.9	1.9	0.3	1.3	-	-	-	-	36.1	-	1.1	23.6	1.0	-	-	-	11.0	0.8	13.2	1.6
4(f) -4	0.2	1.3	2.2	0.2	-	-	-	-	-	26.5	-	0.1	50.1	1.9	-	-	-	0.1	0.1	17.2	-
4(f) -10	0.3	1.4	2.8	0.2	0.1	-	-	-	-	18.0	-	0.2	45.7	4.3	-	-	-	0.5	0.1	26.2	0.1
4(f) - 28	0.4	1.9	4.4	0.5	1.2	-	-	-	-	41.1	-	0.8	24.7	0.8	-	-	-	11.0	0.4	11.5	1.2
42(d) - 28	-	-	-	2.0	-	1.0	1.4	17.5	35.3	18.8	6.7	-	-	-	4.8	4.9	5.2	-	0.1	-	2.2
42(d) - 42	-	-	-	0.4	-	0.2	1.1	13.0	27.7	16.7	12.3	-	-	-	0.3	12.6	15.0	-	0.2	-	0.6

Table 6.3. Whole-cell fatty acid compositions (% of total) of the dominant hydrocarbon degrading bacteria isolated from each microcosm. Isolates are labelled according to incubation temperature, microcosm replicate and isolate. All isolates were grown on TSA Individual fatty acids which comprised less than 0.1% of the totals were combined into the other acid column, which includes: 12:0, 14:0 3OH, i16:1ω10c, 17:0, i17:1ω11c, a17:1ω11c, 17:1ω12c.

Table 6.4. Pair-wise ANOSIM of the isolated FAME composition including FAME composition of mucoid and non-mucoid isolates from Danne *et al.* (2002). Groups indicate the temperature the bacteria were isolated at (or colony morphology). R statistic is a measure of similarity (0 is maximum similarity while 1 is maximum dissimilarity) while the significance level is the percent of instances the observed pattern occurs during random permutations.

Groups	R Statistic	Significance Level %
non-mucoid, mucid	0.923	0.1
4°C, non-mucoid	1.000	0.1
10°C, non-mucoid	1.000	0.1
42°C, non-mucoid	0.677	0.2
4°C, mucoid	1.000	0.2
10°C, mucoid	1.000	0.2
42°C, mucoid	0.696	0.2
4°C, 10°C	0.059	27.7
10°C, 42°C	1.000	0.2
4°C, 42°C	1.000	0.2

To verify that the differences in the FAME composition was caused by differing species composition and not to the effect of growth conditions, two psychrotrophic strains (4(a), and 4(f)) and one mesophilic strain (42(d)) were investigated further. Each strain was subcultured and incubated at 4, 10, 28 and 42°C. After 30 days, there was no growth of the mesophilic microbe at 4 and 10°C and the psychrotrophic cultures did not grow at 42°C. The FAME compositions of the cultures, grown at different temperatures are shown in Table 6.3 and a MDS ordination plot based on incubation temperature is shown in Figure 6.3D. The 4°C cultures had a marked increase in the 16:0 and cy17:0 and a decrease in 16:1ω7c when grown at 28°C. An increase in cy17:0 could indicate that these bacteria are psychrophilic as cyclopropyl fatty acid concentrations are known to be increased with growth outside the bacteria's optimal growth temperature (Guckert *et al.*, 1986). Conversely, increased cyclopropyl fatty acids have also been observed in the FAMEs composition of the *Halomonadaceae* family when they are in the stationary phase (Franzmann and Tindall, 1990) as compared to the exponential growth phase

(Skerratt *et al.*, 1991). When the 42°C culture was grown at 28°C there was a general trend towards shorter chain length fatty acids and a decrease in the unsaturated acids, which is consistent with increasing membrane fluidity at lower temperature. However, while significant changes in the FAME composition in the three strains occurred with different incubation temperature, these changes were minor compared to the differences between the psychrotrophic and mesophilic strains (Table 6.5). When grown at 42°C, 42(d) was 77.8% similar (Bray-Curtis similarity with square-root transformation) to PR-N13 (a non-mucoid *Paenibacillus spp.*) described in Daane *et al.* (2002). When it was grown at the same temperature (28°C) as the strains in Daane *et al.* (2002) the similarity increased to 89.3%.

Table 6.5. Pair-wise ANOSIM of the isolated FAME composition including FAME composition of mucoid and non-mucoid isolates from Danne *et al.* (2002) grown at 28°C. Groups indicate the temperature the isolates were grown at before phospholipid extraction. R statistic is a measure of similarity (0 is maximum similarity while 1 is maximum dissimilarity) while the significance level is the percent of instances the observed pattern occurs during random permutations.

Groups	R Statistic	Significance Level %
4°C, 10°C	-0.021	51.7
4°C, 28°C	0.834	0.1
4°C, 42°C	1.000	0.1
10°C, 28°C	0.848	0.1
10°C, 42°C	1.000	0.1
42°C, 28°C	0.526	0.3

6.3.5 Implications

In Chapter 5 the production of $^{14}\text{CO}_2$, from the treatability studies presented in Chapter 3 and Chapter 4, was used to model microbial mineralisation of ^{14}C -octadecane through three growth phases (lag, exponential and plateau) using an extended three-half order kinetic model (Trefry and Franzmann, 2003). From a treatability perspective it would be ideal to reduce the length of the lag phase and increase the rate and duration of

the exponential phase by delaying the onset of the plateau phase. It was previously postulated that the change in biodegradation parameters strongly influenced the microbial population dynamics by selecting for a sub-component of the microbial population, in response to changing environmental conditions (high nutrients, high temperatures, good water availability). In the study presented in this Chapter two distinct microbial communities developed under differing thermal regimes. Enumeration of the mesophilic and psychrotrophic microbial communities supports the hypothesis of a changing hydrocarbon-degrading microbial population within Antarctic soil incubated under mesophilic conditions. The culturable mesophilic population required more than 20 days before entering the exponential growth phase in this experiment. In the initial radiometric experiment the lag phase at 42°C lasted for 10 days before measurable mineralisation occurred (Chapter 3). The apparent longer lag phase in this study could be due to the difference in sensitivities between measuring the production of $^{14}\text{CO}_2$ and enumerating indicator organisms. Although the influence of slightly different starting constraints cannot be excluded either (*cf.* Chapter 3 and Chapter 4). Sonderkamp *et al.* (2001) found that the dominant component of bacterial population in a hydrocarbon contaminated site is not necessarily responsible for hydrocarbon degradation. The mesophilic microbial population capable of growth on basal medium with SAB as a sole carbon source was below the level of detection (*ca* 90 microbes g dry soil⁻¹) in our soil. This makes it difficult to detect a potentially important component of the microbial community for implementation of bioremediation in Antarctic soil.

One of the technical limitations of this type of study is relating microbiota composition (MPN, DGGE and FAME) to biodegradation. I was unable to detect the mesophilic hydrocarbon degrading population by MPN analysis in this study, but after

40 days the number of mesophilic bacteria capable of growth on TSB increased exponentially while the psychrotrophic bacterial numbers remained approximately stable. The *Paenibacillus spp.* were only recovered on solid medium. Further work is required to validate the growth parameters and hydrocarbon degrading ability of these isolates. It is also possible that the microbe(s) responsible for the ^{14}C -octadecane mineralisation in the initial treatability study are not culturable (Garland and Mills, 1991).

There was no significant difference in the number of bands detected by DGGE in either the mesophilic or psychrotrophic microcosms. While the number of bands detected by DGGE analysis did not significantly change from the initial soil in the incubated microcosms, the banding pattern within the soil at each temperature was significantly different after 40 days incubation. Juck *et al.* (2000) postulated that hydrocarbon contamination has the potential to increase bacterial diversity in Arctic soil which otherwise have limited carbon sources. The results from this study indicate that engineered bioremediation treatments will also substantially change the soil microbial ecosystem. Given that the effective treatment season in Antarctica is only 6-10 weeks, the period most favourable to microbial growth, the challenge for scientists is to rapidly develop the optimal growth requirements for the hydrocarbon degrading population. One potential way to avoid a lengthy lag period, for example, might be to culture indigenous hydrocarbon degrading microorganisms for subsequent reintroduction.

6.4 Conclusions

The identification of a bacterial population capable of rapidly mineralising hydrocarbons at 42°C in an Antarctic hydrocarbon contaminated site opens the possibility of utilising high temperature engineered site remediation strategies. For

bioremediation in Antarctica allochthonous organisms can not be used as the Antarctic Treaty prohibits the introduction of non-indigenous biota. While *Paenibacillus spp.* was putatively identified as a hydrocarbon degrading mesophilic bacteria, further work is required to categorically prove its ability to degrade petroleum hydrocarbons and to determine the optimal growth temperature range of this species. Significant shifts in the soil microbial community when the soil was incubated at constant temperature and with nutrient amendments indicates that engineered remediation strategies will result in further disturbance to the *in situ* microbial population. It is hoped that emerging technologies, such as ^{13}C imaging techniques, will allow the investigation of the biochemical pathway of the degradation process to reduce the long lag phase that is currently observe for high temperature treatments of petroleum contaminated soils.

Chapter 7

In situ Chemical Oxidation (ICO)

7.1 Introduction

Bioremediation of the large volume of petroleum contaminated soil at Old Casey Station will be logistically and technically difficult (Kerry, 1993). Recalcitrant components of fuels, such as dibenzothiophenes, polycyclic aromatic hydrocarbons (PAH), and compounds found in the unresolved complex mixture (UCM) will not be readily degraded during bioremediation (Alexander, 1999b; Watson *et al.*, 2002). Although *in situ* and on site bioremediation is possible in Antarctica (e.g. Snape *et al.*, 2003), factors such as low temperatures (Chapter 3), seasonally frozen soil, difficulties maintaining an adequate nutrient concentration (Chapter 4), poor water holding capacity (Section 4.2.3) and a difficult working environment mean that bioremediation of some spills may take many years to reach environmentally benign concentrations.

In situ chemical oxidation (ICO) offers the potential of a complementary remediation strategy that could deliver fast efficient results and avoid many of the drawbacks associated with bioremediation. This technology involves introducing reactive chemicals directly into contaminated soil or other media, such as waste waters, to oxidise organic contaminants to carbon dioxide and water, or transform them to other environmentally harmless compounds, such as inorganic salts (Riser-Roberts, 1998). ICO has been used to treat a range of organic contaminants through an aggressive and reportedly non-specific chemical oxidation process (Pignatello, 1992; Kakarlar and Watts, 1997; McKinzi and Dichristina, 1999). The most common ICO treatments include Fenton's reagent, hydrogen peroxide and hypochlorite (Yin and Allen, 1991).

Fenton's reagent has received the most attention in the literature and has been used in the remediation of a range of highly recalcitrant organic pollutants, including petroleum

hydrocarbons (Moran *et al.*, 1998; Watts *et al.*, 2000), hexadecane (Watts and Stanton, 1999), atrazine (Arnold *et al.*, 1995), aromatic compounds (Martens and Frankenberger, 1995; Casero *et al.*, 1997; Lunar *et al.*, 2000), dioxins (Kao and Wu, 2000) and chlorinated solvents (McKinzi and Dichristina, 1999; Yeh *et al.*, 2002). The Fenton's process is well documented (Walling, 1975) and involves production of hydroxyl radicals from the iron (II)-catalysed decomposition of hydrogen peroxide (Equation 7.1). The hydroxyl radicals are highly reactive, with a relative reactivity of 2.06 (Anon, 1998), and may be scavenged by another molecule of Fe^{2+} (Equation 7.2), or react with organic contaminants through electrophilic addition to alkenes or aromatic rings, and hydrogen abstraction with saturated compounds (Equation 7.3 and Equation 7.4 respectively) (Walling, 1975).



Equation 7.1-7.4 Stoichiometric reactions involved in the Fenton's Process

Ferrous sulphate ($FeSO_4$) is typically used for the iron (II) catalyst source in Fenton's reactions, but the subsequent hydroxyl radical formation is so rapid that the hydroxyl radicals react quickly with organic contaminants and the reactive hydroxyl radicals are consumed close to the point of application (Dorfman and Adams, 1973). The application of hydrogen peroxide (relative reactivity of 1.31 (Anon, 1998)) without an iron catalyst produces slower rates of hydroxyl radical formation which allows greater subsurface

infiltration and is known to treat a range of organics including phenols, aldehydes and organic acids (Chambers *et al.*, 1991). Fenton-like processes occur by utilising naturally occurring mineral irons, such as goethite and hematite (Yeh *et al.*, 2003). Indeed, hydrogen peroxide application has been found to degrade up to 97% of trichloroethylene (TCE) contamination in aquifer sand with ~ 0.2 wt % naturally occurring iron oxyhydroxides (Yeh *et al.*, 2003). Therefore, it is likely that the natural iron levels in soils around Old Casey Station, which have dithionate-citrate extractable iron levels in the range of ~ 0.1 – 0.8 wt % (Beyer *et al.*, 2001), should be sufficient to produce a Fenton-like process through the application of H₂O₂.

Although hypochlorites have received little attention for *in situ* treatment purposes due to the risk of forming chlorinated organic compounds (such as chloroform), which may be more toxic than the original contaminants (Riser-Roberts, 1998), they have long been used in the water and wastewater treatment field for disinfection purposes and to remove organic compounds (Chambers *et al.*, 1991). Most commonly in a sodium form, hypochlorite acts as a chlorinating agent and is strongly oxidising, with a relative reactivity of 1.10 (Anon, 1998).

Site hydrogeological characteristics, such as subsurface porosity, hydraulic conductivity and pH need be considered when implementing ICO. In soil with naturally high levels of organic matter, the oxidants may be scavenged by non-contaminant organics which reduces the efficiency of the remedial action (Zappi *et al.*, 2000). However, Antarctic soil tends to have low total organic carbon (TOC), sometimes with concentrations of less than 0.1% (Aislabie *et al.*, 2001; Burkins *et al.*, 2001), and are unlikely to interfere with the effectiveness of ICO remediation in most cases. Other general safety and environmental issues include chemical handling, production of

volatile organic compounds, toxic by-products, and the increase in water solubility and mobility of degraded products (Chambers *et al.*, 1991).

The aim of this study is to investigate the feasibility of using ICO as a remediation strategy. Possible uses of ICO technology include incorporation with bioremediation techniques and immediate implementation for small-scale petroleum spills to limit contaminant migration and sorption to soils. While shown to be effective in oxidising a wide range of contaminants in laboratory studies and in *ex situ* batch reactors (e.g. Huling *et al.*, 2000; Chen *et al.*, 2001; Yeh *et al.*, 2003), field trials of ICO to remediate contaminated soils in polar-regions have not previously been reported but have been identified as a possible petroleum spill management option (Aislabie *et al.*, 2004).. To investigate the effectiveness of using various chemical oxidative treatments (Fenton's reagent, Fenton-like process and sodium hypochlorite) to remediate petroleum hydrocarbon contaminated soil in Antarctica, two concurrent field trials were undertaken. An open-plot small-scale field trial (with plots of $\sim 1 \text{ m}^3$) was conducted to test the initial effectiveness of the treatments, evaluate ICO penetration distance, and determine the short-term effect on physical soil characteristics (temperature, pH and moisture). A smaller semi-enclosed box-plot trial (with plots of $\sim 0.1 \text{ m}^3$) was undertaken to monitor microbial ecosystem recovery and to investigate if ICO treatment increased the biodegradability of a Special Antarctic Blend (SAB) diesel fuel.

7.2 Materials and methods

7.2.1 Field trials

The soil used in these experiments was from the contaminated site at Old Casey Station near the old workshop/ powerhouse (Chapter 1, locations WS6 and WS7 of Deprez *et al.*, 1994; 1999).

The chemical treatments in both trials were kept similar to allow inter-trial comparisons (Table 7.1). The chemicals were prepared immediately prior to use in these experiments and were slowly applied to the surface of each plot or box using a watering can to avoid pooling. Surface application of chemicals was used in both trials because contamination is known to be <1 m deep. The semi-enclosed box-plot trial was carried out to study the effectiveness of the various ICO treatments while limiting the effects of contaminant flux. The experimental tins were partially isolated from the surrounding environment to limit migration of the contaminant into and out of the experimental system. The experimental tins were monitored over three years to observe ecosystem recovery. Unfortunately several treatments could not be sampled at various times as boxes did not thaw. The semi-enclosed box-plot trial forms part of a longer term field trial into the feasibility of various site remediation strategies for use in Antarctica. Only the results relating to the use of ICO technology are presented in this thesis. Preliminary results from this long-term field trial show that bioremediation can reduce hydrocarbon concentrations to below 2000 mg fuel kg⁻¹ with the addition of nutrients and water within 36 months (see figure 3, Snape *et al.*, 2003).

Table 7.1 Summary of the chemical treatments applied to the soil from the semi-enclosed box-plot and open-plot small-scale implementation ICO field trials. The semi-enclosed box-plot experiment was established in duplicate, composites samples from 4 separate locations within each plot in the open-plot small-scale field trial was taken at each time Asterisks indicate where only single samples were obtained. Treatments were applied in the open-plot small-scale field trial on days 1 and 14.

Treatment	Chemicals added	Chemical concentration (%)	Volume added (L per plot)	Time interval of samples obtained
<i>Semi-enclosed box-plot</i>				
Control	None	-	0	Pre, 12m, 15m
Fenton	FeSO ₄ / H ₂ O ₂	30	0.25 / 0.5	3d, 12m, 15m, 24m*
Peroxide	H ₂ O ₂	30	0.5	3d*, 12m, 15m
High NaHOCl	NaHOCl	12.50	0.5	3d, 12m, 15m, 24m*
<i>Open-plot small-scale field trial</i>				
Control	None	-	0	Pre, 7d, 23d, 36d
Fenton	FeSO ₄ / H ₂ O ₂	30	5 / 5	Pre, 7d, 23d, 36d
Peroxide	H ₂ O ₂	30	5	Pre, 7d, 23d, 36d
High NaHOCl	NaHOCl	12.50	5	Pre, 7d, 23d, 36d
Low NaHOCl	NaHOCl	6.25	5	Pre, 7d, 23d, 36d

7.2.1.1 Open-plot small-scale field trial

For the open-plot small-scale ICO field trial, five 1 m³ test plots were established (Figure 7.1). Chemical treatments were applied twice (see Table 7.1). Treatments were applied on days 1 and 24, while the plots were sampled on days 0 (pre-treatment), 7, 23, and 36. Samples were collected at depth intervals of 20-50 mm and 100-150 mm. Each sample was a composite from 4 separate locations within the plot, at least 100 mm from the plot boundary, to provide representative material at each sampling time and depth and avoid cross-over from adjacent plots. The control plot remained untreated. The soil was analysed for temperature, pH, gravimetric water content, hydrocarbon concentration by a photo ionisation detector (PID; miniRAE Classic, Raesystems) and gas chromatography (GC). Surface soil temperature was also monitored throughout the application of chemical treatments.

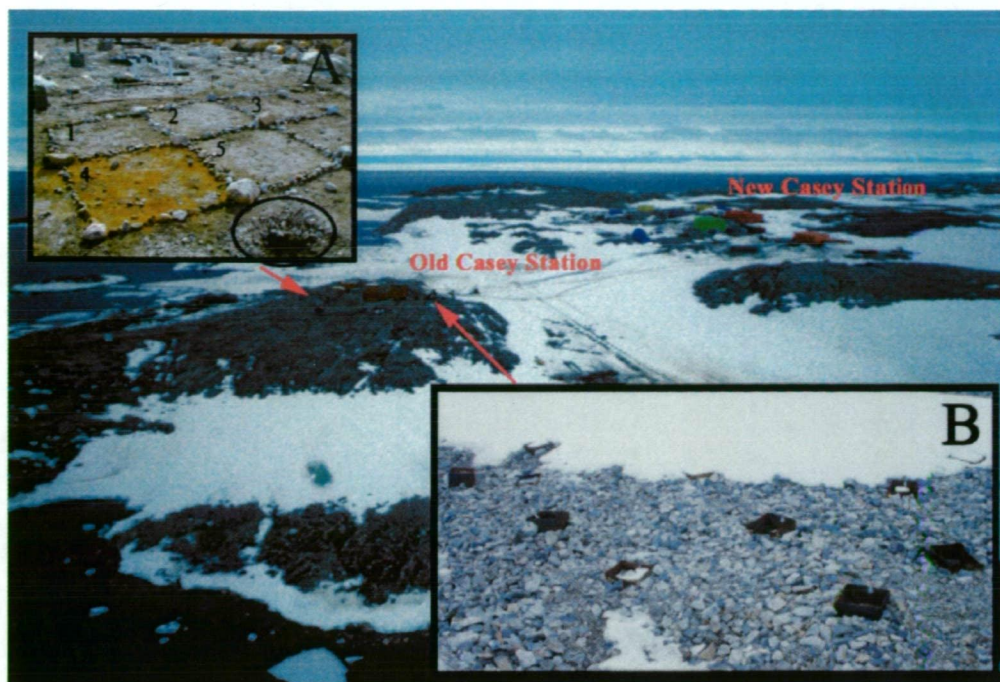


Figure 7.1 Photographs of the Casey region and experimental plots. Panel A is the small-scale open-plot field trial. Plots are 1 high NaHOCl; 2 Control; 3 low NaHOCl; 4 Fentons and 5 H₂O₂. Soil for the semi-enclosed box-plot was collected from the lower right hand corner of the insert (circled) and panel B shows the semi-enclosed box-plots.

7.2.1.2 Semi-enclosed box-plot

The semi-enclosed box-plot comprised sieved (<5.0 mm) homogenised soil from the spill site, placed in 8 hexane-cleaned metal containers (ca 250 (w) x 250 (l) x 350 (d) mm) with perforated bottoms to allow free drainage and prevent soil saturation. The metal boxes were then buried in a way that ensured a similar aspect and micro-climate as the nearby contaminated site (Figure 7.1). In this way, contaminant migration could be controlled. Six pre-treatment samples (ca 20 g) for chemical and microbial analysis were taken randomly. ICO treatments and control tins were established in duplicate (Table 7.1). Chemical treatments were applied once, except to the control tins, and all tins were sampled from the 10-30 mm depth interval for petroleum hydrocarbon analysis and

microbial counts at 3 days, 12 and 15 months; those that were thawed were also sampled at 24 months (Table 7.1).

7.2.2 *Chemical analysis*

Volatile petroleum hydrocarbon contamination was semi-quantified using a PID. Unsieved subsurface soil samples (*ca* 200 g) were collected into airtight plastic bags for PID analysis. The bags were sealed to achieve the maximum headspace possible and agitated briefly before being allowed to equilibrate with the head space for *ca* 2 min. The PID probe was inserted into the headspace, with readings taken as an average over 1 min.

The aliphatic fraction of SAB was extracted from sieved soil by solvents and separated on a silica-alumina column prior to analysis using a Varian 3410 GC. The GC was fitted with a septum-equipped programmable injector and a flame ionisation detector, as previously described in Section 3.2.4. Analyses were performed using a 50 m non-polar methyl-silicone-fused silica capillary column (HP-1, 0.32 mm internal diameter, 0.23 μm film thickness) with helium as the carrier gas. All samples were run at 35°C for 1 min, then ramped to 120°C at 30°C min⁻¹, then to 310°C at 4°C min⁻¹ and finally held for 15 min. The quantity of fuel was approximated by the sum of all the GC-resolved peaks and the UCM in the aliphatic fraction, normalised against an added internal squalane (Sigma) extraction standard.

Soil moisture content and pH were measured in accordance to standard methods (APHA *et al.*, 1999). Soil temperature was measured at the time of soil sampling and during the application of chemical treatments. The statistical significance of the results was determined with t-tests.

7.2.3 *Microbial measurements*

Total heterotrophic and hydrocarbon degrading bacteria were enumerated from each treatment in triplicate using adapted microtitre most probable number (MPN) methods. Total hydrocarbon degrading bacteria were enumerated in triplicate using a tailored version of the Wrenn and Venosa (1996) MPN method. An initial soil dilution of *ca* 0.13 g soil: 1 g Bushnell-Haas mineral salt broth (Difco) was used for a 4 tube MPN, with seven 1: 5 serial dilutions in a 96 well microtitre plate. After serial dilution, 5 µL of filter-sterilised SAB was applied to the surface of the Bushnell-Haas broth. The last row of tubes contained only Bushnell-Haas broth and SAB as a negative growth control. After 10 days incubation at 4°C, 50 µL of 3% iodonitrotetrazolium violet (Sigma) solution was added to each of the microtitre tubes and re-incubated overnight. Positive tubes were scored based on the formation of a red precipitate. Total heterotrophic bacteria were also enumerated in triplicate in a similar manner except half strength tryptone soya broth was used instead of Bushnell-Haas broth and SAB. Positive tubes were indicated by turbidity. Total heterotrophic microtitre plates were incubated at 4°C for seven days.

7.3 Results

7.3.1 *Open plot small-scale field trial*

7.3.1.1 *General observations*

No significant change in the pH was found in the untreated (control), or NaHOCl treated soil. Fenton's reagent was the only treatment to significantly alter soil pH, where surface pH was reduced from 9.3 to 3.8 during the first application of chemicals and from 7.2 to 4.6 during the second application (Table 7.2). However, the soil pH

reduction was a temporary effect as a rebound in pH was observed in the period between the two treatments, from 3.8 back to 7.2. A slight pH reduction deeper in the soil profile also occurred with Fenton's reagent application, although without the rebounding effect. The pattern of pH reduction and rebound, albeit to a lesser degree, was seen at both surface and depth with the hydrogen peroxide treatment.

Soil temperatures before and after the addition of all oxidative treatments (data not shown) only changed for the Fenton's application where soil surface temperatures increased from *ca* 8°C before treatment to between 35 and 60°C. Minor changes in the soil and air temperatures at the time of sampling are consistent with natural variations rather than the effects of chemical treatments.

There was a general loss of moisture from the soil during the trial period, except in the surface of the Fenton's reagent plot. At the start of the trial, the average soil moisture content was $9.1 \pm 0.9\%$ and there was no significant difference between moisture at the surface and at depth (Table 7.2). At the end of the experimental period, average soil moisture content (excluding the surface Fenton application plot) was $5.8 \pm 1.5\%$, but 11.5% at the surface of the Fenton's plot. The overall decrease in soil moisture was attributed to natural drainage during the summer; it is possible that the Fenton's reagent affected the hydraulic characteristics of the surface soil (discussed below).

Table 7.2 Soil parameters and chemical results for the open-plot small-scale trial. Arrows indicate before and after oxidant treatment. Unk represented unknown values as the samples were lost in transit. Air and soil temperature at time of samplings varied between -3.8 and -0.5°C and 1.8 and 13°C respectively.

Treatment		Moisture (%)	pH	Volatile hydrocarbons (ppm)	Aliphatic hydrocarbons (ppm x10 ³)
<i>Application One (Pre-treatment → day 7)</i>					
Control	(<5cm)	8.5 → 6.5	8.4 → 8.6	19 → 33	17 → 19
Control	(10-15cm)	8.2 → 7.0	8.0 → 7.9	85 → 82	18 → 23
Fenton	(<5cm)	10.1 → 12.6	9.3 → 3.8	35 → 12	24 → 14
Fenton	(10-15cm)	10.0 → 9.4	8.8 → 8.4	120 → 117	18 → 25
Peroxide	(<5cm)	10.6 → 7.5	9.4 → 8.6	40 → 18	17 → 9
Peroxide	(10-15cm)	9.3 → 8.5	8.6 → 8.3	95 → 96	29 → 33
NaHOCl	(high - <5cm)	7.7 → 8.9	9.4 → 9.9	19 → 35	20 → 17
NaHOCl	(high 10-15cm)	8.6 → 8.4	8.7 → 8.8	142 → 60	21 → 23
NaHOCl	(low - <5cm)	8.5 → 8.5	9.0 → 9.8	44 → 19	22 → 13
NaHOCl	(low 10-15cm)	9.2 → 8.3	8.3 → 8.5	110 → 81	31 → 30
<i>Application Two (Day 23 → 36)</i>					
Control	(<5cm)	7.4 → 3.0	8.5 → 8.2	18 → 14	25 → unk
Control	(10-15cm)	6.6 → 5.0	7.8 → 7.7	75 → 41	20 → 25
Fenton	(<5cm)	11.7 → 11.5	7.2 → 4.6	58 → 13	18 → 16
Fenton	(10-15cm)	8.3 → 7.3	8.1 → 8.2	80 → 61	23 → 27
Peroxide	(<5cm)	8.7 → 5.0	8.8 → 8.2	75 → 12	18 → 17
Peroxide	(10-15cm)	7.5 → 4.6	8.6 → 8.2	87 → 57	34 → 30
NaHOCl	(high - <5cm)	6.9 → 6.3	9.7 → 9.7	9 → 13	15 → unk
NaHOCl	(high 10-15cm)	9.0 → 7.3	8.8 → 9.1	50 → 35	17 → 20
NaHOCl	(low - <5cm)	8.7 → 7.1	9.5 → 9.6	18 → 15	17 → 14
NaHOCl	(low 10-15cm)	8.4 → 6.6	8.5 → 8.7	153 → 48	27 → 26

7.3.1.2 Hydrocarbon characterisation

Volatile hydrocarbons as measured by PID were highly variable within plots, reflecting small scale heterogeneity. No correlation between soil or air temperature and volatile hydrocarbon concentration (Pearson product moment correlation coefficients <0.3, p<0.05) was found. Nevertheless, higher initial hydrocarbon concentrations in each plot occurred in the deep soil rather than at the surface (Table 7.2), the average initial PID hydrocarbon concentration was 27.9 ± 11.9 ppm at the surface, and 101.3 ±

24.0 ppm at depth. This is consistent with the known hydrocarbon distribution at this site (Revill *et al.*, 1998; Snape *et al.*, In Prep).

The addition of 6.25% NaHOCl was the only treatment to significantly reduce the volatile hydrocarbon concentration (surface only) at day 7, with a *ca* 69% reduction. There was a significant increase in the surface hydrocarbon concentration in both the Fenton's and the H₂O₂ plots and at depth with 6.25% NaHOCl at day 23. By day 36, the volatile hydrocarbon concentration was only significantly reduced from the initial concentration with the application of both 6.25 and 12.5 % NaHOCl.

After ICO application PID results reveal that both the Fenton's and the hydrogen peroxide treatments followed the reduce-rebound effect seen in the pH values, with a significant increase in volatile hydrocarbon concentrations between the two applications of chemical treatments (Table 2). Fenton's treatment initially reduced the volatile hydrocarbon concentration from 35 to 12 ppm, which then rebounded to 58 ppm. Hydrogen peroxide treatment also reduced the initial concentration from 40 to 18 ppm, which then rebounded to 75 ppm. The significant increase in surface concentrations may indicate that these treatments increased volatile contaminant mobility. If volatile contaminant reduction from the elevated concentration on day 23 is considered, then both Fenton's and H₂O₂ treatments cause a significant reduction of 78 and 83 % respectively.

In contrast with the PID results, GC analysis in the pre-treatment plots showed no significant difference in the initial total aliphatic hydrocarbon concentrations between the soil at surface and depth (Table 7.2). This difference is attributed to the loss of PID-measurable volatile hydrocarbons from the surface, but where loss of the total hydrocarbon envelope is highly restricted to all but the very surface soil (see also Kang

and Oulman, 1996). In general, there was no significant decrease in total aliphatic concentrations with the application of the oxidative chemicals, except with the 6.25 % NaHOCl treatment. For the hydrogen peroxide treatment, hydrocarbon concentrations significantly increased at the surface after the first addition (day 7) and at depth on days 7 and 23.

Ratios indicative of the early stages of biodegradation, such as *n*-alkane / isoprenoid (Chapter 2, Humphrey *et al.*, 1987; Prince, 1993; Wang and Fingas, 2003a), showed no change indicating that biological activity was minimal during the experiment (data not shown). Ratios indicative of evaporation, such as light isoprenoid to pristane (Chapter 2' Revill *et al.*, 1998; Snape *et al.*, 2003), indicate that evaporation only occurred with the application of NaHOCl (both concentrations) and only at depth. Surprisingly, no significant decrease was observed in the more volatile compounds with the application of both Fenton's reagent and hydrogen peroxide, instead there was a significant increase in the more volatile compounds at depth in these plots.

7.3.2 *Semi-enclosed box-plot*

The application of oxidative treatments did not alter the total aliphatic hydrocarbon concentration when the treatments were initially applied (Table 7.3). Fenton's reagent reduced the hydrocarbon concentration by *ca* 60% after 12 months and concentrations remained steady at levels of *ca* 7000 ppm. Hydrogen peroxide did not reduce the hydrocarbon concentration relative to the controls. The hydrocarbon concentration in the NaHOCl treatment tins appears to be gradually decreasing, although it took over 15 months for this to be statistically significant from the controls.

Table 7.3 Average results for the geochemical and microbial analysis of the soil from the semi-enclosed box-plot ICO trial. Pr is pristane. MPNs are in most probable number of microbes per g dry soil⁻¹. Percentage hydrocarbon degrading bacteria of total heterotrophic bacteria are shown in parentheses in the hydrocarbon degraders column. Some samples were not collected because the soil was frozen. ND is Not Detected, detection limit of MPN method was 0.03×10^3 microbes g⁻¹. Standard deviation (1s) are shown ($n=2$). Biodegradation data from Snape *et al.* (2003) are shown for comparison ($n=4$).

Time	Chemical results			MPN ($\times 10^3$)	
	Total aliphatic (ppm)	<i>n</i> -C ₁₇ : pr	<i>i</i> -C ₁₃ : pr	Total heterotrophs	Hydrocarbon degraders (%)
<i>Control</i>					
Pre-treatment	10 200 \pm 1200	1.24 \pm 0.02	0.66 \pm 0.30	138 \pm 96	80 \pm 52 (58)
3 days	-	-	-	137 \pm 265	3.9 \pm 4 (2.8)
12 months	8000 \pm 1100	1.22 \pm 0.01	0.44 \pm 0.10	418 \pm 358	30 \pm 15 (7.2)
15 months	8400 \pm 1100	1.16 \pm 0.00	0.41 \pm 0.07	-	-
24 months	-	-	-	208 \pm 229	33 \pm 20 (16)
36 months	-	-	-	278 \pm 421	32 \pm 36 (12)
<i>Fenton's</i>					
3 days	12 000 \pm 1200	1.24 \pm 0.01	0.41 \pm 0.08	ND	ND
12 months	6500 \pm 600	1.22 \pm 0.01	0.38 \pm 0.01	ND	ND
15 months	7700 \pm 1400	1.23 \pm 0.01	0.43 \pm 0.02	-	-
24 months	6800	1.24	0.35	ND	ND
36 months	-	-	-	1652 \pm 1730	0.4 \pm 0.02 (<0.1)
<i>H₂O₂</i>					
3 days	9600	1.25	0.7	ND	ND
12 months	9300 \pm 2600	1.23 \pm 0.01	0.46 \pm 0.01	ND	ND
15 months	8100 \pm 900	1.14 \pm 0.08	0.40 \pm 0.02	-	-
24 months	-	-	-	1934 \pm 2169	1369 \pm 1996 (71)
36 months	-	-	-	787 \pm 4000	35 \pm 35 (4.4)
<i>NaHOCl</i>					
3 days	9500 \pm 3000	1.26 \pm 0.01	0.74 \pm 0.13	ND	ND
12 months	7900 \pm 1600	1.26 \pm 0.03	0.44 \pm 0.01	ND	ND
15 months	6700 \pm 700	1.20 \pm 0.03	0.37 \pm 0.01	-	-
24 months	6000	1.21	0.27	ND	0.04 \pm 0.00
36 months	-	-	-	983 \pm 1371	742 \pm 931 (76)
<i>Bioremediation</i>					
Pre	23 000 \pm 2600	1.11 \pm 0.03	0.96 \pm 0.20	-	-
3 weeks	14 000 \pm 1000	0.93 \pm 0.02	0.70 \pm 0.16	-	-
12 months	7800 \pm 420	0.12 \pm 0.04	0.51 \pm 0.04	-	-
15 months	4900 \pm 600	0.04 \pm 0.01	0.17 \pm 0.02	1400 \pm 2200	9.0 \pm 13 (0.64)
36 months	1300 \pm 700	0.02 \pm 0.00	0.02 \pm 0.01	160 000 \pm 130 000	1.2 \pm 0.3 (<0.1)

Ratios thought to be good indicators of the early stages of biodegradation did not change for any ICO treatment, for example, *n*-C₁₇: pristane was 1.22 ± 0.03 for all treatments and controls during the 24 months of geochemical monitoring. However, ratios known to be sensitive to evaporation appear to indicate evaporative loss with the *i*-C₁₃: pristane ratio changing from 0.66 ± 0.06 to 0.39 ± 0.06 . This evaporation occurred in the 12-24 month period in all the treatments except the Fenton's treatment. Fenton's treatment appears to have promoted evaporation at the time of application, with *i*-C₁₃: pristane decreasing to 0.44 ± 0.08 within 3 days. This is possibly the result of the heat produced during the exothermic Fenton's reaction.

7.3.2.1 Microbiota

The soil initially contained 1.38×10^5 total culturable microbes g⁻¹ of which SAB degraders consisted *ca* 60% of the population (Table 7.2). The sieving and homogenising process did not alter the total microbial community. However, the homogenising process also appeared to decrease the SAB-degrading population to below 5% of the total culturable microbiota. After 12 months, SAB degrading and total cultivable microbial numbers increased in the control plots, with the SAB degrading population recovering to *ca* 40% of the total population. After which, the SAB degrading microbial population remained roughly stable at 40% and with total heterotrophic microbes declining towards pre-treatment levels.

The application of Fenton's reagent had a disastrous effect on the microbial community, reducing it to below detectable levels within three days of chemical application. It took a further three years before microbial growth was detected again. However, after 3 years total cultivable microbial numbers had increased to *ca* 1200% of pre-treatment levels, but contained less than 0.02% hydrocarbon degrading microbes.

Antarctic ecosystems are slow to recover from perturbation (Gore *et al.*, 1999) and thus may explain the extended recovery time after treatment with Fenton's reagent. The cause of the relative paucity of hydrocarbon degraders is more enigmatic, and will be discussed below.

NaHOCl treatment also severely reduced the microbial community to below detectable levels. After two years, only *ca* 40 microbes g⁻¹ SAB degrading microbes were detected. But by the next season, total microbial numbers recovered to *ca* 700% of pre-treatment levels (9.83 x 10⁵ total culturable microbes g⁻¹) and contained *ca* 75% hydrocarbon degrading microbes.

The application of hydrogen peroxide had the least severe effect on the microbial community. The total microbial population was below detection level for one year and then returned to over 1400% of the pre-treatment level by the end of 3 years. After 24 months hydrocarbon degrading microbes consisted of *ca* 70% of the total microbial community. This result is not surprising considering that H₂O₂ has been used as an oxygen source for microbes in bioremediation applications (Riser-Roberts, 1998).

7.4 Discussion

7.4.1 Chemical penetration and subsurface transport

With surface application the infiltration and dispersion of reactive chemicals is critical. The rate of organic contaminant oxidation by hydroxyl radicals, reportedly between 10⁷ and 10¹⁰ M⁻¹ s⁻¹, is limited by their rates of diffusion (Haag and Yao, 1992; Watts *et al.*, 2000). At this rate, it has been found that hydroxyl radicals are quickly consumed close to the point of chemical application (Yeh *et al.*, 2003) making it difficult to deliver the hydroxyl radicals to the contaminant. The rate of hydroxyl radical

formation with Fenton's reaction is optimised with acidic conditions, and thus this study used near neutral conditions in the hope that the rate of the hydroxyl radical quenching would be reduced, thus allowing deeper infiltration.

If pH and soil temperature are an indirect indicator of organic contaminant oxidation, the pH reduction and dramatic temperature increase in the surface layer in the Fenton's treatments indicates limited chemical penetration into the soil. It is likely that the majority of the hydroxyl radicals were formed and rapidly consumed at the surface. Only slight effects were seen with the hydrogen peroxide treatment; surface pH changed from 9.4 to 8.2 but temperature remained constant. A Fenton-like process probably occurred at a slower rate and with deeper hydroxyl radical penetration than with the Fenton's treatment. Experimental studies by Yeh *et al.* (2003) found that hydroxyl radicals penetrated up to 10 cm when using a surface application of a Fenton-like process in a sand column, and in their experiment the contaminants (trichloroethylene) were oxidized to this depth.

The observed decrease in soil moisture in the small-scale open-plot trial was most likely a natural effect as mineral soils, such as those around Old Casey Station, readily dry out towards the end of summer. It is unknown why there was an increase in soil moisture at the surface of the Fenton's plot, but this could be related to changes in hydraulic characteristics by the formation of iron oxyhydroxide precipitates. These were clearly visible in the soil after the Fenton's treatment (Figure 7.1) and other studies have reported that oxide precipitates can clog subsurface pore spaces (e.g. Yin and Allen, 1991), thereby reducing hydraulic conductivity and limiting drainage. It is also feasible that the exothermic reaction caused a melting of the underlying permafrost which increased moisture content.

7.4.2 Limitations and implication of ICO treatment of hydrocarbon contaminated soil in polar-regions

ICO has been recommended as a potential remediation strategy for contaminated sites, where very rapid contaminant reduction is desired, or where excavation is not feasible, such as in building basements (e.g. Moran *et al.*, 1998). However, extensive soil heating similar to the response to Fenton's reagent observed here could affect permafrost integrity and have serious engineering implications (Seligman, 2000). Exothermic reactions in frozen soils are also likely to melt underlying permafrost, and drive contaminants downwards making any subsequent remediation efforts harder. There is also the risk of increasing the areal extent of contamination by melting the soil-contaminant matrix. Once melted, contaminants are free to migrate off site, potentially into sensitive ecosystems.

At Old Casey Station, if ICO treatments were conducted at the start of summer, contaminant mobilisation would be exacerbated as thawing of the active layer would occur before the bulk of the summer snow melt. If application were later in the season, when the soil is relatively dry, the effect would be to melt the underlying permafrost, pushing the active layer beyond its normal lower limit.

Possible limitations to ICO treatment efficiency include low temperature (Yin and Allen, 1991), pH (Zappi *et al.*, 2000) and soil sorption/matrix effects (Chen *et al.*, 2001). However, Yeh *et al.* (2002) were able to degrade chlorophenol at near neutral pH, and Watts and Stanton (1999) were able to oxidize hexadecane in a sorbed-soil system.

The lack of a significant reduction in hydrocarbon concentrations from Fenton's reagent and hydrogen peroxide treatment in this study is somewhat surprising (Figure 7.2 and Table 7.3). The ability of Fenton's reagent to oxidise organic contaminants is

well known, and the natural iron concentration in the soil from Old Casey Station is likely to be adequate for the Fenton-like processes to occur with hydrogen peroxide application.

The old age of the spill at Old Casey Station may be a reason for the lack of hydrocarbon destruction from ICO treatment found in this study as contaminants are strongly sorbed to sediment particles. Oxidation is much more rapid and effective when contaminants are in the dissolved phase (Yin and Allen, 1991), and so organics bound to solids must first desorb into subsurface pore water to be degraded. This study used an 8.8M H₂O₂ solution which may not have been strong enough to overcome the sorption of hydrocarbon contamination at this site. However, Kakarla and Watts (1997) were able to overcome the sorption of hexadecane by using 15 M H₂O₂. In a separate study, more than 99% of petroleum hydrocarbons were removed, including those in the soil-sorbed state, by using a 1: 1 ratio of H₂O₂ and Fe³⁺ (Watts and Dilly, 1996). Other work has found that direct degradation of contaminants sorbed to soil particles occurs, albeit at a slower rate (Yin and Allen, 1991).

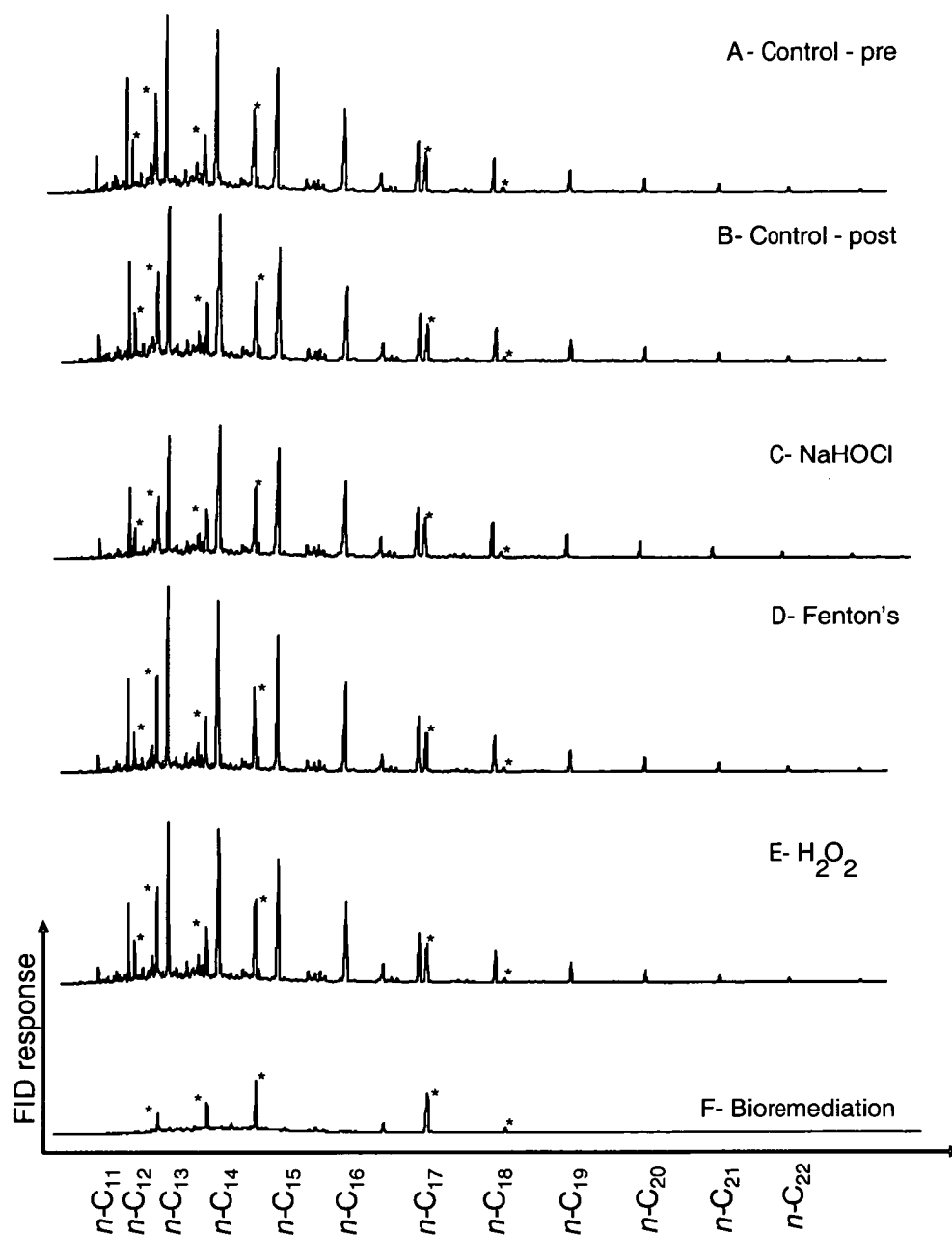


Figure 7.2 GC trace of the aliphatic fraction of neat SAB with normal and isoprenoid alkanes labelled. Insert A and B is the GC trace extracted from the control tins pre and post 15 months respectively. The remain aliphatic contamination 2 years after treatment with 6.25% NaHOCl and Fentons are shown in Insert C and Insert D respectively. Insert E shows the remaining aliphatic hydrocarbon contamination 15 months after treatment with hydrogen peroxide, while Insert F shows the contamination after 3 years of bioremediation treatment (Snape *et al.*, 2003). Acyclic isoprenoids are indicated with an asterisk.

The large increase in microbial numbers found in this study several years after the addition of oxidative treatments is an interesting observation. It is likely that the microbial populations are recycling carbon and other nutrients from the pre-treatment microbial community. This is supported by the dramatic decrease in the proportion of hydrocarbon degrading microbes in the population. It is also possible that a decrease in hydrocarbon contaminant concentrations would occur with microbial community recovery. The NaHOCl treatment of the semi-enclosed box-plot trial had the highest number of hydrocarbon degrading bacteria after three years and a corresponding significant reduction in hydrocarbon concentrations compared to the no-treatment controls. The severe reduction in the microbial communities is probably a combined result of the strong oxidative conditions, the heat produced during the exothermic reactions, and possibly the acidic conditions produced during the Fenton's and Fenton-like process.

Regardless of the mechanism for the lack of hydrocarbon oxidation, significant reduction in the contaminant load was not found within either of the experiments with the use of ICO treatments. However, in a related investigation on the same soil using bioremediation, the hydrocarbon concentrations in the semi-enclosed box-plot trial were reduced to $< 2000 \text{ mg fuel kg soil}^{-1}$, well below Australian site remediation guidelines (figure 3, Snape *et al.*, 2003: see also Figure 7.2F).

7.5 Conclusions

Although the promise of a technology which delivers fast acting, complete contaminant removal is highly attractive and worthy of investigation, it was shown in this study that a surface application of oxidative chemicals to remediate long-term petroleum hydrocarbon contaminated soil is not effective. Of more concern was

evidence that it was also highly destructive to the fragile Antarctic soil microbiota. The exothermic Fenton's reaction could also promote increased contaminant dispersal through soil heating and melting of the underlying permafrost. Furthermore, strong oxidative chemicals have significant occupational risks associated with their use. While the use of chemical oxidation has previously been found to be highly effective in the remediation of recalcitrant organic contamination, unfortunately it can not be recommended for use in Antarctica based on the results found in this study. Preliminary results from a long-term field trial indicate that bioremediation may reduce hydrocarbon contamination concentration to environmentally benign levels, without the potential risks associated with ICO treatments.

Chapter 8

Conclusions

Through a detailed site characterisation of a petroleum contaminated at Old Casey Station it is apparent that natural attenuation or off-site treatments are not viable remediation options for Antarctica. Two on-site technologies, involving biological and chemical treatments were identified for further consideration. The safety issues concerning implementation of chemical oxidation plus those factors which could limit treatment efficacy in the Antarctic Environment were investigated. The influence of low temperature, low nutrients, highly variable seasonally water availability, poor water holding capacity that could potentially limit bioremediation and the effect of treatment on the microbial consortium were also explored.

To examine the premise that low temperatures will inhibit attempts to bioremediate petroleum contaminated soils in Antarctica, the effects of temperature on the hydrocarbon mineralisation rate were quantified. ^{14}C -labelled octadecane was added to nutrient amended microcosms that were incubated over a range of temperatures between -2 and 42°C. A positive correlation between temperature and mineralisation rate was found; with the fastest rates occurring in samples incubated at the highest temperatures. At temperatures below or near the freezing point of water there was a virtual absence of mineralisation. High temperatures (37 and 42°C) and the temperatures just above the freezing point of water (4°C) showed an initial mineralisation lag period, then a sharp increase in the mineralisation rate before a protracted plateau phase. Mineralisation at temperatures between 10 and 28°C had no initial lag phase. The high rate of mineralisation at 37 and 42°C was surprising, as most continental Antarctic microorganisms described thus far have an optimal temperature for growth of between

20 and 30°C and a maximal growth temperature <37°C. One possible explanation of this result is that two distinct microbial populations could be involved, naturally occurring psychrotrophs, and higher temperatures (e.g. 42°C) mesophiles. To test this hypothesis, a series of nutrient amended microcosm studies, were conducted at 4, 10, 28 and 42°C. Sample heterogeneity resulted in no statistically significant reduction in total aliphatic hydrocarbons during 40 days of incubation, but ratios that are indicative of biodegradation, such as *n*-C₁₇: pristane, indicate that biodegradation occurred. Nutrient amendments increased the culturable psychrotrophic bacterial population (4 and 10°C), which peaked after 10 days incubation ($1.3 \times 10^8 \text{ g}^{-1}$ dry soil), before decreasing to and remaining stable at *ca* $7 \times 10^7 \text{ g}^{-1}$ dry soil. Growth of a mesophilic bacterial population (42°C) remained in lag phase for *ca* 20 days but after 40 days consisted *ca* 40% of the culturable bacterial population. Multivariate statistical analysis of denaturing gradient gel electrophoresis banding patterns indicated significant differences between microbial communities in Antarctic soil after incubation at the different temperatures. Dominant culturable hydrocarbon degrading bacteria were isolated at each temperature. Based on the isolates' 16S rRNA gene sequences, the dominant hydrocarbon degraders at 4 and 10°C were identified as *Pseudomonas spp.*, and the dominant hydrocarbon degraders from 42°C were identified as *Paenibacillus spp.* Fatty acid methyl ester profiles of the cultures were consistent with these identifications. The results from this experiment indicate that high temperature bioremediation treatments will substantially change the soil microbial ecosystem. Moreover, an increase in the effective-remediation period each summer may be achieved through the re-introduction of cultured-autochthonous mesophilic hydrocarbon degrading microbes into *in situ* mesophilic remediation treatment cells prior to the commencement of the treatment.

To optimise nutrient amendments for the remediation of the long-term hydrocarbon-contaminated site at Old Casey Station in Antarctica, the effects of nitrogen (and phosphorus) amendments on microbial mineralisation using radiometric microcosm experiments and gas chromatography were investigated. Hydrocarbon mineralisation at nine different inorganic nitrogen concentrations (ranging from 85 to over 27 000 mg N kg-soil-H₂O⁻¹) was monitored over 95 days incubation at 10°C. Total ¹⁴C-octadecane mineralisation increased with increasing nutrient concentration peaking in the range 1000 -1600 mg N kg-soil-H₂O⁻¹. The microcosms with the lowest and highest concentrations of N had extended lag phases of over 12.5 days prior to significant mineralisation. Gas chromatographic analysis of the aliphatic components of Special Antarctic Blend (SAB) diesel in the contaminated soil showed good agreement with the ¹⁴C-octadecane mineralisation outcomes. Ratios of *n*-C₁₇: pristane and *n*-C₁₈: phytane indicated that low nutrient concentrations rather than water were the main limiting factor for biodegradation of hydrocarbons in the soil collected from Old Casey Station when incubated at 10°C. However, because the soils from this site are characterised by low water holding capacities, it would be difficult to maintain optimal nutrient concentrations during full scale treatment, and thus the use of a controlled release nutrient is being considered as a nutrient source in the bioremediation of SAB-contaminated Antarctic soils.

The microbial mineralisation of the ¹⁴C-octadecane within microcosm treatability studies can be described with three-half order kinetic rate equations and the temperature-dependence of the rate of mineralisation with the use of regression models. The Trefry and Franzmann (2003) extended three-half order model logically described the three phases of ¹⁴CO₂ production in the treatability experiments investigating the

effect of temperature and nutrient concentration, in the microcosms that reached a plateau phase of $^{14}\text{CO}_2$ production. By examining the effects of temperature and nutrient concentration on the best-fit estimates of the model parameters it was possible to assess the importance of various factors, such as changing microbial community structure and tracer solubility. The best-fit estimates for the regression models, such as the Ratkowsky and Arrhenius models, did not produce a well-fitting solution when applied to the microcosms investigating the effect of temperature. The most likely explanation for the poor fit is that these models were developed for axenic cultures or simple chemical reactions. An extensive change in microbial community structure, as distinct from an increase in total numbers, might explain the large errors associated with fitting the temperature-microcosm mineralisation data to the Ratkowsky model. The availability of these functions raises the possibility of applying the production curves to obtain quantitative estimates of *in situ* remediation efficiencies under the seasonal thermal cycles at Old Casey Station

In situ chemical oxidation (ICO) was identified as an alternative potential technology for the remediation of the petroleum hydrocarbon contaminated sites in Antarctica. ICO involves introducing reactive chemicals to contaminated soils so that organics such as petroleum hydrocarbons are oxidised to environmentally innocuous compounds. Two field trials were undertaken to evaluate the feasibility of using a surface application of these oxidative treatments (Fenton's reagent, hydrogen peroxide and sodium hypochlorite) to remediate the petroleum contaminated soil at Old Casey Station. The results showed that the ICO technology used at this site, where contamination occurred over a decade ago, did not significantly reduce petroleum hydrocarbon concentrations and would likely hinder biodegradation through the destruction of subsurface microbial

communities. Further treatment testing and optimisation is required before ICO would be an effective remediation strategy for petroleum contaminated sites in Antarctica. However, the near complete destruction of subsurface microbiota, coupled with a discoloured orange soil residue and soil heating, mean that other more environmentally sensitive techniques such as bioremediation are a preferred treatment methodology.

This study has gone some ways to the development of an integrated model for bioremediation of petroleum contaminated soils in Antarctica. Through the use of diagnostic ratios and microcosm treatability studies a number of limitations, such as low temperature and nutrient concentrations, have been determined. Furthermore, it was shown in that a surface application of oxidative chemicals is not effective and highly destructive to the soil microbiota. The results from this study indicate that further work into controlled release nutrients and/ permeable reactive barriers as possible remediation technologies for cold regions is required. Emerging microbial technologies, which offer the possibility of isolation and characterisation of the microbe(s) responsible for environmentally significant contaminant removal such as stable isotope labelling, offer further potential for the optimisation of site remediation.

Chapter 9

References

- Abramowitz, M., Stegun, I. A., 1964. Handbook of Mathematical Functions. Dover Publications, New York.
- Adamczyk, J., Hesselsoe, M., Iversen, N., Horn, M., Lehner, A., Nielsen, P. H., Schlöter, M., Roslev, P., Wagner, M., 2003. The isotope array, a new tool that employs substrate-mediated labeling of rRNA for determination of microbial community structure and function. *Applied and Environmental Microbiology*. 69(11), 6875-6887.
- Aislabie, J., McLeod, M., Fraser, R., 1998. Potential for biodegradation of hydrocarbons in soil from the Ross Dependency, Antarctica. *Applied Microbiology and Biotechnology*. 49(2), 210-214.
- Aislabie, J., Foght, J. M., Saul, D., 2000. Aromatic hydrocarbon-degrading bacteria from soil near Scott Base, Antarctica. *Polar Biology*. 23(3), 183-188.
- Aislabie, J., Fraser, R., Duncan, S., Farrell, R. L., 2001. Effects of oil spills on microbial heterotrophs in Antarctic soils. *Polar Biology*. 24(5), 308-313.
- Aislabie, J. M., Balks, M. R., Foght, J. M., Waterhouse, E. J., 2004. Hydrocarbon spills on Antarctic soils: Effects and management. *Environmental Science and Technology*. 38(5), 1265-1274.
- Alexander, M., 1999a. Sorption. In: Alexander, M., (Eds.). *Biodegradation and Bioremediation*. Academic Press, San Diego, pp. 117-134.
- Alexander, M., 1999b. *Biodegradation and bioremediation*. Academic Press, San Diego.
- ANARE news, 1990. No 63. Australian Antarctic Division, Kingston, Tasmania, pp. 31.
- Anon, 1997. Expedited site assessment tools for underground storage tank sites: A guide for regulators. EPA 510-B-97-001. United States Environmental Protection Agency, Washington.
- Anon, 1998. Field application of *in Situ* remediation technologies: Chemical oxidation. EPA 542-R-98-008. United States Environmental Protection Agency, Washington, pp. 1-31.
- Anon, 2003. SW-846 On-line test methods for evaluating solid wastes. Physical/chemical methods (<http://www.epa.gov/epaoswer/hazwaste/test/main.htm>). United States Environmental Protection Agency.
- APHA, AWWA, WEF, 1999. Standard methods for examination of water & wastewater. American Public Health Association, New York.

Arnold, S. M., Hickey, W. J., Harris, R. F., 1995. Degradation of atrazine by Fenton's reagent: condition optimization and product quantification. *Environmental Science and Technology*. 29(8), 2083-2089.

Arrhenius, S., 1889. Über die reaktionsgeschwindigkeit bei der inversion von rohrzucker durch säuren. *Zeitschrift fuer Physikalische Chemie (Munich)*. 4, 226-248.

ATCM, 1985. Annex to Recommendation XIII-8. Site of Special Scientific Interest (SSSI) No. 17, Clark Peninsula, Budd Coast, Wilkes Land. In: *Facilitation of scientific research: Sites of Special Scientific Interest (SSSI) Nos. 9-21 Interim Guidelines: Additional Sites*.

Atlas, R. M., Bartha, R., 1972. Biodegradation of petroleum in sea water at low temperatures. *Canadian Journal of Microbiology*. 18, 1851-1855.

Atlas, R. M., 1981. Microbial degradation of petroleum hydrocarbons: An environmental perspective. *Microbiological Reviews*. 45(1), 180-209.

Atlas, R. M., Boehm, P. D., Calder, J. A., 1981. Chemical and biological weathering of oil from the *Amoco Cadiz* oil spillage, within the littoral zone. *Estuarine, Coastal and Marine Science*. 12, 589-608.

Atlas, R. M., Parks, L. C., 1997. *Handbook of microbiological media*. CRC Press, Boca Raton.

Bagrii, Y. I., 1995. Advances in the chemistry of adamantane. *Petroleum Chemistry*. 35(3), 205-209.

Bej, A. K., Saul, D., Aislabie, J., 2000. Cold-tolerant alkane-degrading *Rhodococcus* species from Antarctica. *Polar Biology*. 23(2), 100-105.

Belhaj, A., Desnoues, N., Elmerich, C., 2002. Alkane biodegradation in *Pseudomonas aeruginosa* strains isolated from a polluted zone: identification of *alkB* and *alkB*-related genes. *Research in Microbiology*. 153(6), 339-344.

Bence, A. E., Kvenvolden, K. A., Kennicutt II, M. C., 1996. Organic geochemistry applied to environmental assessments of Prince William Sound, Alaska, after the *Exxon Valdez* oil spill- a review. *Organic Geochemistry*. 24(1), 7-42.

Berekaa, M. M., Steinbuchel, A., 2000. Microbial degradation of the multiply branched alkane 2,6,10,15,19,23-hexamethyltetracosane (squalane) by *Mycobacterium fortuitum* and *Mycobacterium ratisbonense*. *Applied and Environmental Microbiology*. 66(10), 4462-4467.

Beyer, L., Sorge, C., Blume, H.-P., Schulten, H.-R., 1995. Soil organic matter composition and transformation in gelic histosols of coastal continental Antarctica. *Soil Biology and Biochemistry*. 27(10), 1279-1288.

- Beyer, L., Blume, H.-P., Sorge, C., Schulten, H.-R., Erlenkeuser, H., Schneider, D., 1997. Humus composition and transformations of a pergelic cryohemist of coastal Antarctica. *Arctic and Alpine Research*. 29(3), 358-365.
- Beyer, L., Bölter, M., 1998. Formation, ecology, and geography of cryosols of an ice-free oasis in Coastal East Antarctica near Casey Station (Wilkes Land) [Review]. *Australian Journal of Soil Research*. 37(1), 209-244.
- Beyer, L., Bölter, M., 1999. Formation, ecology, and geography of cryosols of an ice-free oasis in Coastal East Antarctica near Casey Station (Wilkes Land) [Review]. *Australian Journal of Soil Research*. 37(1), 209-244.
- Beyer, L., Bölter, M., Seppelt, R. D., 2000. Nutrient and thermal regime, microbial biomass, vegetation of Antarctic soils in the Windmill Islands region of East Antarctica (Wilkes Land). *Arctic, Antarctica and Alpine Research*. 32(1), 30-39.
- Beyer, L., White, D. M., Bölter, M., 2001. Soil organic matter composition, transformation, and microbial colonisation of Gelic Podzols in the coastal region of East Antarctica. *Australian Journal of Soil Research*. 39(3), 543-563.
- Blume, H.-P., Beyer, L., Bolter, M., Erlenkeuser, H., Kalk, E., Kneesch, S., Pfisterer, U., Schneider, D., 1997. Pedogenic zonation in soils of the Southern Circum-Polar region. *Advances in GeoEcology*. 30, 69-90.
- Boehm, P. D., Steinhauer, M. S., Green, D. R., Fowler, B., Humprey, B., Fiest, D. L., Cretney, W. J., 1987. Comparative fate of chemically dispersed and beached crude oil in subtidal sediments of the arctic nearshore. *Artic*. 40(Supp 1), 133-148.
- Bonham, C. D., 2002. Selection of hydrocarbon variables to assess reduction of residual oil on nutrient enriched beaches. *Applied Mathematics and Computation*. 126(2-3), 361-376.
- Bossert, I., Bartha, R., 1984. *Petroleum microbiology*. Macmillan Publishing Company, New York.
- Bosshard, P. P., Zbinden, R., Altwegg, M., 2002. *Paenibacillus turicensis* sp. nov., a novel bacterium harboring heterogeneities between 16S rRNA genes. *International Journal of Systematic and Evolutionary Microbiology*. 52(6), 2241-2249.
- Bowman, J. P., McCammon, S. A., Gibson, J. A. E., Robertson, L., Nichols, P. D., 2003. Prokaryotic metabolic activity and community structure in Antarctic continental shelf sediments. *Applied and Environmental Microbiology*. 69(5), 2448-2462.
- Braddock, J. F., Ruth, M. L., Catterall, P. H., Walworth, J. L., McCarthy, K. A., 1997. Enhancement and inhibition of microbial activity in hydrocarbon-contaminated Arctic soils: Implications for nutrient-amended bioremediation. *Environmental Science and Technology*. 31(7), 2078-2084.

- Bragg, J. R., Prince, R. C., Harner, E. J., Atlas, R. M., 1994. Effectiveness of bioremediation for the *Exxon Valdez* oil spill. *Nature*. 368, 413-418.
- Brook, T. R., Stiver, W. H., Zytner, R. G., 2001. Biodegradation of diesel fuel in soil under various nitrogen addition regimes. *Soil and Sediment Contamination*. 10(5), 539-553.
- Brown, E. J., Braddock, J. F., 1990. Sheen screen, a miniaturized most-probable-number method for enumeration of oil-degrading microorganisms. *Applied and Environmental Microbiology*. 56(12), 3895-3896.
- Brunner, W., Focht, D. D., 1984. Deterministic three-half-order kinetic model for microbial degradation of added substrates in soil. *Applied and Environmental Microbiology*. 47(1), 167-172.
- Burkins, M., Virginia, R., Wall, D., 2001. Organic carbon cycling in Taylor Valley, Antarctica: quantifying soil reservoirs and soil respiration. *Global Change Biology*. 7(1), 113-125.
- Campbell, I. B., Claridge, G. G. C., Baks, M. R., 1994. The effect of human activities on moisture content of soils and underlying permafrost from the McMurdo Sound region, Antarctica. *Antarctic Science*. 6(3), 307-314.
- Casero, I., Sicilia, D., Rubio, S., Perez-Bendito, D., 1997. Chemical degradation of aromatic amines by Fenton's reagent. *Water Research*. 31(8), 1985-1995.
- Casucci, C., Okeke, B. C., Frankenberger, W. T., 2003. Effects of mercury on microbial biomass and enzyme activities in soil. *Biological Trace Element Research*. 94(2), 179-191.
- Cavanagh, J. E., Juhasz, A. L., Nichols, P. D., Franzmann, P. D., McMeekin, T. A., 1995. Analysis of microbial hydrocarbon degradation using TLC-FID. *Journal of Microbiological Methods*. 22, 119-130.
- Chambers, C. D., Willis, J., Giti-Pour, S., Zieleniewski, J. L., Rickabough, J. F., Mecca, M. I., Pasin, B., Simms, R. C., Sorensen, D. L., Sim, J. L., McLean, R., Mahmood, R., Dupont, R. P., Wagner, K., 1991. *In situ* treatment of hazardous waste-contaminated soils. Noyes Data Corporation, Park Ridge, N.Y.
- Chang, H. L., Alvarezcohen, L., 1996. Biodegradation of individual and multiple chlorinated aliphatic hydrocarbons by methane-oxidizing cultures. *Applied and Environmental Microbiology*. 62(9), 3371-3377.
- Chen, G., Hoag, G. E., Chedda, P., Nadim, F., Woody, B. A., Dobbs, G. M., 2001. The mechanism and applicability of *in situ* oxidation of trichloroethylene with Fenton's reagent. *Journal of Hazardous Materials*. 87(1-3), 171-186.

- Cho, Y. G., Rhee, S. K., Lee, S. T., 2000. Effect of soil moisture on bioremediation of chlorophenol-contaminated soil. *Biotechnology Letters*. 22(11), 915-919.
- Christner, B. C., Mosley-Thompson, E., Thompson, L. G., Reeve, J. N., 2001. Isolation of bacteria and 16S rDNAs from Lake Vostok accretion ice. *Environmental Microbiology*. 3(9), 570-577.
- Clark, C. J., 2003. Field detector evaluation of organic clay soils contaminated with diesel fuel. *Environmental Forensics*. 4(3), 167-173.
- COMNAP, 1999. An assessment of environmental emergencies arising from activities in Antarctica. Antarctic Treaty XXIII Consultative meeting, pp. 1-9.
- Daane, L. L., Harjono, I., Zylstra, G. J., Häggblom, M. M., 2001. Isolation and characterization of polycyclic aromatic hydrocarbon-degrading bacteria associated with the rhizosphere of salt marsh plants. *Applied and Environmental Microbiology*. 67(6), 2683-2691.
- Daane, L. L., Harjono, I., Barns, S. M., Launen, L. A., Palleroni, N. J., Häggblom, M. M., 2002. PAH-degradation by *Paenibacillus* spp. and description of *Paenibacillus naphthalenovorans* sp. nov., a naphthalene-degrading bacterium from the rhizosphere of salt marsh plants. *International Journal of Systematic and Evolutionary Microbiology*. 52, 131-139.
- Delille, D., 2000. Response of Antarctic soil bacterial assemblages to contamination by diesel fuel and crude oil. *Microbial Ecology*. 40(2), 159-168.
- Delille, D., Pelletier, E., 2002. Natural attenuation of diesel-oil contamination in a subantarctic soil (Crozet Island). *Polar Biology*. 25(9), 682-687.
- Deprez, P. P., Arens, M., Locher, H., 1994. Identification and preliminary assessment of contaminated sites in the Australian Antarctic Territory. 1. Casey Station. Australian Antarctic Division, Hobart.
- Deprez, P. P., Arens, M., Locher, H., 1999. Identification and assessment of contaminated sites at Casey Station, Wilkes Land, Antarctica. *Polar Record*. 35(195), 299-316.
- Dörfler, U., Haala, R., Matthies, M., Scheunert, I., 1996. Mineralization kinetics of chemicals in soils in relation to environmental conditions. *Ecotoxicology and Environmental Safety*. 34(3), 216-222.
- Dorfman, L. M., Adams, G. E., 1973. Reactivity of the hydroxyl radical in aqueous solutions. U.S. National Bureau of Standards, Washington.
- Durant, N. D., Jonkers, C. A. A., Bouwer, E. J., 1997. Spatial variability in the naphthalene mineralization response to oxygen, nitrate, an orthophosphate amendments in MCP aquifer sediments. *Biodegradation*. 8, 77-86.

- Eriksson, M., Ka, J. O., Mohn, W. W., 2001. Effects of low temperature and freeze-thaw cycles on hydrocarbon biodegradation in Arctic tundra soil. *Applied and Environmental Microbiology*. 67(11), 5107-5112.
- Fayad, N. M., Overton, E. B., 1995. A unique biodegradation pattern of the oil spilled during the 1991 Gulf war. *Marine Pollution Bulletin*. 30(4), 239-246.
- Felsenstein, J., 1995. PHYLIP v.3.57c (phylogenetic inference program package). University of Washington, Seattle, WA.
- Ferguson, S. H., Franzmann, P. D., Snape, I., Revill, A. T., Trefry, M. G., Zappia, L. R., 2003. Effects of temperature on mineralisation of petroleum in contaminated Antarctic terrestrial sediments. *Chemosphere*. 52(6), 975-987.
- Ferguson, S. H., Powell, S. M., Snape, I., Gibson, J. A. E., Franzmann, P. D., Submitted. Changes in microbial ecology within petroleum hydrocarbon contaminated site treatability (microcosm) studies. *FEMS Microbiology Ecology*.
- Filler, D. M., Lindstrom, J. E., Braddock, J. F., Johnson, R. A., Nickalaski, R., 2001. Integral biopile components for successful bioremediation in the Arctic. *Cold Regions Science and Technology*. 32(2-3), 143-156.
- Filler, D. M., Barnes, D. L., 2003. Technical procedures for recovery and evaluation of chemical spills on tundra. *Cold Regions Science and Technology*. 37(2), 121-135.
- Fiore, S., Zanetti, M. C., Genon, G., 2003. Experimental study of the pH influence on the transport mechanisms of phenols in soil. *Annali Di Chimica*. 93(5-6), 595-605.
- Foght, J. M., Semple, K., Gauthier, C., Westlake, D. W. S., Blenkinsopp, S., Sergy, G., Wang, Z., Fingas, M., 1999. Effect of nitrogen source on biodegradation of crude oil by a defined bacterial consortium incubated under cold, marine conditions. *Environmental Technology*. 20, 839-849.
- Franzmann, P. D., Tindall, B. J., 1990. A Chemotaxonomic Study of Members of the Family *Halomonadaceae*. *Systematic and Applied Microbiology*. 13(2), 142-147.
- Franzmann, P. D., 1996. Examination of Antarctic prokaryotic diversity through molecular comparisons. *Biodiversity and Conservation*. 5(11), 1295-1305.
- Franzmann, P. D., Patterson, B. M., Power, T. R., Nichols, P. D., Davis, G. B., 1996. Microbial biomass in a shallow, urban aquifer contaminated with aromatic hydrocarbons: analysis by phospholipid fatty acid content and composition. *Journal of Applied Bacteriology*. 80, 617-625.
- Garland, J. L., Mills, A. L., 1991. Classification and characterization of heterotrophic microbial communities on the basis of patterns of community-level sole-carbon-source utilization. *Applied and Environmental Microbiology*. 57(8), 2351-2359.

Gill, R. A., Robotham, P. W. J., 1989. Composition, source and source identification of petroleum hydrocarbons and their residues. In: Green, J. Trett, M. W., (Eds.). *The fate and effects of oil in freshwater*. Elsevier, New York, pp. 11-40.

Gore, D. B., Revill, A. T., Guille, D., 1999. Petroleum hydrocarbons ten years after spillage at a helipad in Bunger Hills, East Antarctica. *Antarctic Science*. 11(4), 427-429.

Gough, M. A., Rhead, M. M., Rowland, S. J., 1992. Biodegradation studies of unresolved complex mixtures of hydrocarbons: model UCM hydrocarbons and the aliphatic UCM. *Organic Geochemistry*. 18(1), 17-22.

Grice, K., Alexander, R., Kagi, R. I., 2000. Diamondoid hydrocarbon ratios as indicators of biodegradation in Australian crude oils. *Organic Geochemistry*. 31, 67-73.

Grigg, B. C., Assaf, N. A., Turco, R. F., 1997. Removal of atrazine contamination in soil and liquid systems using bioaugmentation. *Pesticide Science*. 50(3), 211-220.

Grundy, S. L., Bright, D. A., Dushenko, W. T., Reimer, K. J., 1996. Weathering and dispersal of polychlorinated biphenyls from a known source in the Canadian Arctic. *Environmental Science and Technology*. 30(9), 2661-2666.

Guckert, J. B., Hood, M. A., White, D. C., 1986. Phospholipid ester-linked fatty-acid profile changes during nutrient deprivation of vibrio-cholerae- increases in the trans cis ratio and proportions of cyclopropyl fatty-acids. *Applied and Environmental Microbiology*. 52(4), 794-801.

Guichard, A., 1999. Alternative energy systems for polar regions (ASAC 2181). Australian Antarctic Division - SnoWhite Metadata (<http://www-aadc.aad.gov.au/metadata/>)

Guille, D., Revill, A. T., Bowman, J. P., 1997. Long-term fate of petroleum contamination at Casey Station, Antarctica. Australian Antarctic Division, Hobart, pp. 1-69.

Gustafson, J. B., Tell, J. G., Orem, D., Association of American Railroads., United States. Air Force., Total Petroleum Hydrocarbon Criteria Working Group., 1997. Selection of representative TPH fractions based on fate and transport considerations. Amherst Scientific Publishers, Amherst, Mass.

Haag, W. R., Yao, C. C. D., 1992. Rate constants for reactions of hydroxyl radicals with several drinking water contaminants. *Environmental Science and Technology*. 26(5), 1005-1013.

Head, I. M., Saunders, J. R., Pickup, R. W., 1998. Microbial evolution, diversity, and ecology: A decade of ribosomal RNA analysis of uncultivated microorganisms. *Microbial Ecology*. 35, 1-21.

- Helweg, A., Fomsgaard, I. S., Reffstrup, T. K., Sorensen, H., 1998. Degradation of mecoprop and isoproturon in soil influence on initial concentration. *International Journal of Environmental Analytical Chemistry*. 70(1-4), 133-148.
- Hoyle, B. L., Scow, K. M., Fogg, G. E., Darby, J. L., 1995. Effect of carbon:nitrogen ratio on kinetics of phenol biodegradation by *Acinetobacter Johnsonii* in saturated sand. *Biodegradation*. 6, 283-293.
- Huesemann, M. H., Truex, M. J., 1996. The role of oxygen diffusion in passive bioremediation of petroleum contaminated soils. *Journal of Hazardous Materials*. 51, 93-113.
- Huling, S. G., Arnold, R. G., Sierka, R. A., Jones, P. K., Fine, D. D., 2000. Contaminant adsorption and oxidation via Fenton reaction. *Journal of Environmental Engineering-ASCE*. 126(7), 595-600.
- Humphrey, B., Boehm, P. D., Hamilton, M. C., Norstrom, R. J., 1987. The fate of chemically dispersed and untreated crude oil in Arctic benthic biota. *Arctic*. 40(Supp 1), 149-161.
- Humphrey, B., Owens, E. H., Sergy, G. A., 1992. The Fate and Persistence of Stranded Crude Oil: A Nine-year Overview from the BIOS Project, Baffin Island, NWT, Canada. EPS 3/SP/4. Environment Canada, Ottawa.
- Juck, D., Charles, T., Whyte, L. G., Greer, C. W., 2000. Polyphasic microbial community analysis of petroleum hydrocarbon-contaminated soils from two northern Canadian communities. *FEMS Microbiology Ecology*. 33(3), 241-249.
- Kahng, H. Y., Nam, K., 2002. Molecular characteristics of *Pseudomonas rhodesiae* strain KK1 in response to phenanthrene. *Journal of Microbiology and Biotechnology*. 12(5), 729-734.
- Kakarlal, P. K. C., Watts, R. J., 1997. Depth of Fenton-like oxidation in remediation of surface soil. *Journal of Environmental Engineering-ASCE*. 123(1), 11-17.
- Kang, S. H., Oulman, C. S., 1996. Evaporation of petroleum products from contaminated soils. *Journal of Environmental Engineering-ASCE*. 122(5), 384-387.
- Kao, C. M., Wu, M. J., 2000. Enhanced TCDD degradation by Fenton's reagent preoxidation. *Journal of Hazardous Materials*. 74(3), 197-211.
- Karl, D. M., 1989. Petroleum degradation by microorganisms: Initial results from the *Bahia Paraiso* oil spill. *Antarctic Journal of the United States*. 24(5), 170-172.
- Karl, D. M., 1992. The grounding of the *Bahia Paraiso*: Microbial ecology of the 1989 Antarctic oil spill. *Microbial Ecology*. 24, 77-89.

Kennedy, A. D., 1993. Water as a limiting factor in the Antarctic terrestrial environment: A biogeographical synthesis. *Arctic and Alpine Research*. 25(4), 308-315.

Kennicutt II, M. C., 1990. Oil spillage in Antarctica. *Environmental Science and Technology*. 24(5), 620-624.

Kennicutt II, M. C., Sweet, S. T., Fraser, W. R., Stochton, W. L., Culver, M., 1991. Grounding of the *Bahia Paraiso* at Arthur Harbor, Antarctica. 1. Distribution and fate of oil spill related hydrocarbons. *Environmental Science and Technology*. 25(3), 509-518.

Kerry, E., 1993. Bioremediation of experimental petroleum spills on mineral soils in the Vestfold Hills, Antarctica. *Polar Biology*. 13, 163-170.

Klute, A., Dirksen, C., 1986. Hydraulic conductivity and diffusivity: Laboratory methods. In: Klute, A., (Eds.). *Methods of soil analysis. Part 1. Physical and mineralogical methods*. Soil science society of America Inc., Madison, pp. 687-734.

Lahvis, M. A., Baehr, A. L., Baker, R. J., 1999. Quantification of aerobic biodegradation and volatilization rates of gasoline hydrocarbons near the water table under natural attenuation conditions. *Water Resources Research*. 35(3), 753-765.

Lewis Smith, R. I., 1996. Introduced plants in Antarctica: potential impacts and conservation issues. *Biological Conservation*. 76(2), 135-146.

Line, M. A., 1988. Microbial-flora of some soils of Mawson Base and the Vestfold Hills, Antarctica. *Polar Biology*. 8(6), 421-427.

Loynachan, T. E., 1978. Low temperature mineralization of crude oil in soil. *Journal of Environmental Quality*. 7(4), 494-500.

Lunar, L., Sicilia, D., Rubio, S., Pérez-Bendito, D., Nickel, U., 2000. Degradation of photographic developers by Fenton's reagent: condition optimization and kinetics for metol oxidation. *Water Research*. 34(6), 1791-1802.

Macnaughton, S. J., Stephen, J. R., Venosa, A. D., Davis, G. A., Chang, Y. J., White, D. C., 1999. Microbial population changes during bioremediation of an experimental oil spill. *Applied and Environmental Microbiology*. 65(8), 3566-3574.

Manefield, M., Whiteley, A. S., Griffiths, R. I., Bailey, M. J., 2002. RNA stable isotope probing, a novel means of linking microbial community function to Phylogeny. *Applied and Environmental Microbiology*. 68(11), 5367-5373.

Manilal, V. B., Alexander, M., 1995. Factors affecting the microbial degradation of phenanthrene in soil. *Applied Microbiology and Biotechnology*. 35, 401-405.

Manzoni, M., 1992. Environmental hazards in Antarctica and man's impact on the Antarctic environment. In: Francesco, F., (Eds.). *International environmental law for Antarctica*. Giuffr e, Milano, pp. 53-92.

Margesin, R., Schinner, F., 1997. Bioremediation of diesel-oil-contaminated alpine soils at low temperatures. *Applied Microbiology and Biotechnology*. 47, 462-468.

Margesin, R., Schinner, F., 2001. Bioremediation (natural attenuation and biostimulation) of diesel-oil-contaminated soil in an alpine glacier skiing area. *Applied and Environmental Microbiology*. 67(7), 3127-3133.

Martens, D. A., Frankenberger, W. T., 1995. Enhanced degradation of polycyclic aromatic hydrocarbons in soil treated with an advanced oxidative process - Fenton's reagent. *Journal of Soil Contamination*. 4(2), 1-16.

McCammon, S. A., Innes, B. H., Bowman, J. P., Franzmann, P. D., Dobson, S. J., Holloway, P. E., Skerratt, J. H., Nichols, P. D., Rankin, L. M., 1998. *Flavobacterium hibernum* sp. nov., a lactose-utilizing bacterium from a freshwater Antarctic lake. *International Journal of Systematic Bacteriology*. 48, 1405-1412.

McFarland, M. J., Sims, R. C., 1991. Thermodynamic framework for evaluating PAH degradation in the subsurface. *Groundwater*. 29(6), 885-896.

McKinzi, A. M., Dichristina, T. J., 1999. Microbially driven Fenton reaction for transformation of pentachlorophenol. *Environmental Science and Technology*. 33(11), 1886-1891.

Melick, D., 1991. Casey Fuel Spill - Initial Environment Report. Australian Antarctic Division, Hobart.

Metzger, L. O. Y., Munier-Lamy, C., Belgy, M. J., Andreux, F., Chone, T., Védry, J. C., 1999. A laboratory study of the mineralization and binding of ¹⁴C labelled herbicide rimsulfuron in a rendzina soil. *Chemosphere*. 39(11), 1889-1901.

Meyer, S., Moser, R., Neef, A., Stahl, U., Kämpfer, P., 1999. Differential detection of key enzymes of polyaromatic-hydrocarbon-degrading bacteria using PCR and gene probes. *Microbiology-Uk*. 145(8), 1731-1741.

Møller, J., Gaarn, H., Steckel, T., Wedebye, E. B., Westermann, P., 1995. Inhibitory effects on degradation of diesel oil in soil-microcosms by a commercial bioaugmentation product. *Bulletin of Environmental Contamination and Toxicology*. 54, 913-918.

Mohn, W. W., Stewart, G. R., 2000. Limiting factors for hydrocarbon biodegradation at low temperature in Arctic soils. *Soil Biology and Biochemistry*. 32(8-9), 1161-1172.

Mohn, W. W., Radziminski, C. Z., Fortin, M. C., Reimer, K. J., 2001. On site bioremediation of hydrocarbon-contaminated Arctic tundra soils in inoculated biopiles. *Applied Microbiology and Biotechnology*. 57(1-2), 242-247.

Moran, B. V., Babaian, P., Young, C. P., 1998. Use of hydrogen peroxide as remedial additive for petroleum contaminated soils. In: (Eds) *Annual conference on contaminated soils* University of Massachusetts, 19-22 October.

Morita, R. Y., 1992. Low temperature environments. In: Lederberg, J., (Eds.). *Encyclopaedia of Microbiology*. Academic Press, New York, pp. 625-637.

Moyer, E. E., Ostendorf, D. W., Richards, R. J., Goodwin, S., 1996. Petroleum hydrocarbon bioventing kinetics determined in soil core, microcosm and tubing cluster studies. *Groundwater Monitoring and Remediation*. 16(1), 141-153.

Muyzer, G., Smalla, K., 1998. Application of denaturing gradient gel electrophoresis (DGGE) and temperature gradient gel electrophoresis (TGGE) in microbial ecology. *Antonie Van Leeuwenhoek*. 73, 127-141.

Nadkarni, R. A., 2000. Guide to ASTM test methods for the analysis of petroleum products and lubricants. ASTM, West Conshohocken, PA.

Nedwell, D. B., 1999. Effect of low temperature on microbial growth: lowered affinity for substrates limits growth at low temperature. *FEMS Microbiology Ecology*. 30(2), 101-111.

NEPC, 1999. National Environmental Protection Measure (Assessment of Site Contamination). National Environmental Protection Council, Adelaide.

Nichols, D. S., Brown, J. L., Nichols, P. D., McMeekin, T. A., 1997. Production of eicosapentaenoic and arachidonic acids by an antarctic bacterium: response to growth temperature. *FEMS Microbiology Letters*. 152, 349-354.

Nichols, P. D., Guckert, J. B., White, D. C., 1986. Determination of monounsaturated fatty acid double-bond position and geometry for microbial monocultures and complex consortia by capillary GC-MS of their dimethyl disulphide adducts. *Journal of Microbiological Methods*. 5(1), 49-55.

NOSID, 2001. National oil on the sea database. AGSO, Canberra.

Nuck, B. A., Federle, T. W., 1996. Batch test for assessing the mineralization of C-14-radiolabeled compounds under realistic anaerobic conditions. *Environmental Science and Technology*. 30(12), 3597-3603.

Olson, J. J., Mills, G. L., Herbert, B. E., Morris, P. J., 1999. Biodegradation rates of separated diesel components. *Environmental Toxicology and Chemistry*. 18(11), 2448-2453.

Oudot, J., Merlin, F. X., Pinvidic, P., 1998. Weathering rates of oil components in a bioremediation experiment in estuarine sediments. *Marine Environmental Research*. 45(2), 113-125.

- Ourisson, G., Albrecht, P., Rohmer, M., 1979. The hopanoids. Palaeochemistry and biochemistry of a group of natural products. *Pure and Applied Chemistry*. 51, 709-729.
- Panicker, G., Aislabie, J., Saul, D., Bej, A. K., 2002. Cold tolerance of *Pseudomonas* sp. 30-3 isolated from oil-contaminated soil, Antarctica. *Polar Biology*. 25(1), 5-11.
- Pelletire, F., Prévost, D., Laliberté, G., van Bochove, E., 1999. Seasonal response of denitrifiers to temperature in a Quebec cropped soil. *Canadian Journal of Soil Science*. 79(4), 551-556.
- Pelz, O., Chatzinotas, A., Andersen, N., Bernasconi, S. M., Hesse, C., Abraham, W. R., Zeyer, J., 2001. Use of isotopic and molecular techniques to link toluene degradation in denitrifying aquifer microcosms to specific microbial populations. *Archives of Microbiology*. 175(4), 270-281.
- Pennanen, T., 2001. Microbial communities in boreal coniferous forest humus exposed to heavy metals and changes in soil pH - a summary of the use of phospholipid fatty acids, Biolog ® and ³H-thymidine incorporation methods in field studies. *Geoderma*. 100(1-2), 91-126.
- Pignatello, J. J., 1992. Dark and photoassisted Fe³⁺- catalyzed degradation of chlorophenoxy herbicides by hydrogen peroxide. *Environmental Science and Technology*. 26(5), 944-951.
- Poland, J. S., Riddle, M. J., Zeeb, B. A., 2004. Contaminants in the Arctic and the Antarctic: a comparison of sources, impacts, and remediation options. *Polar Record*. 39(211), 369-384.
- Pombo, S. A., Pelz, O., Schroth, M. H., Zeyer, J., 2002. Field-scale ¹³C-labeling of phospholipid fatty acids (PLFA) and dissolved inorganic carbon: tracing acetate assimilation and mineralization in a petroleum hydrocarbon-contaminated aquifer. *FEMS Microbiology Ecology*. 41(3), 259-267.
- Powell, S. M., Bowman, J. P., Snape, I., Stark, J. S., 2003. Microbial community variation in pristine and polluted nearshore Antarctic sediments. *FEMS Microbiology Ecology*. 45, 135-145.
- Prince, R. C., 1993. Petroleum spill bioremediation in marine environments. *Critical Reviews in Microbiology*. 19(4), 217-242.
- Prince, R. C., Owens, E. H., Sergy, G. A., 2002. Weathering of an Arctic oil spill over 20 years: the BIOS experiment revisited. *Marine Pollution Bulletin*. 44(11), 1236-1242.
- Rahman, K. S. M., Thahira-Rahman, J., Lakshmanaperumalsamy, P., Banat, I. M., 2002. Towards efficient crude oil degradation by a mixed bacterial consortium. *Bioresource Technology*. 85(3), 257-261.

- Raoux, C., Bayona, J. M., Miquel, J. C., Teyssie, J. L., Fowler, S. W., Albaiges, J., 1999. Particulate fluxes of aliphatic and aromatic hydrocarbons in near-shore waters to the northwestern Mediterranean Sea, and the effect of continental runoff. *Estuarine Coastal and Shelf Science*. 48(5), 605-616.
- Ratkowsky, D. A., Olley, J., McMeekin, T. A., Ball, A., 1982. Relationship between temperature and growth rate of bacterial cultures. *Journal of Bacteriology*. 149(1), 1-5.
- Ratkowsky, D. A., Lowry, R. K., McMeekin, T. A., Stokes, A. N., Chandler, R. E., 1983. Model for bacterial culture growth rate though out the entire biokinetic temperature range. *Journal of Bacteriology*. 154(3), 1222-1226.
- Raymond, R. L., Hudson, J. O., Jamison, V. W., 1976. Oil degradation in soil. *Applied and Environmental Microbiology*. 31, 522-535.
- Redfield, A. C., Ketchum, B. H., Richards, F. A., 1963. The influence of organisms on the composition of seawater. In: Hill, M. N., (Eds.). *The Sea*. Wiley, New York, pp. 26-77.
- Reffstrup, T. K., Sorensen, H., Helweg, A., 1998. Degradation of mecoprop at different concentrations in surface and sub-surface soil. *Pesticide Science*. 52(2), 126-132.
- Reid, D., 1999. Petroleum contamination at Old Casey Station. Australian Antarctic Division, Hobart, Personal Communication
- Revill, A. T., Guille, D., Snape, I., 1998. Petroleum contamination at Casey Station, Antarctica. Part 2: chemical constraints on transport, weathering and biodegradation. CSIRO, Marine, Hobart, Tasmania, Personal Communication
- Rike, A. G., Haugen, K. B., Børresen, M., Engene, B., Kolstad, P., 2003. *In situ* biodegradation of petroleum hydrocarbons in frozen Arctic soils. *Cold Regions Science and Technology*. 37(2), 97-120.
- Ringelberg, D. B., Talley, J. W., Perkins, E. J., Tucker, S. G., Luthy, R. G., Bouwer, E. J., Fredrickson, H. L., 2001. Succession of phenotypic, genotypic, and metabolic community characteristics during in vitro bioslurry treatment of polycyclic aromatic hydrocarbon-contaminated sediments. *Applied and Environmental Microbiology*. 67(4), 1542-1550.
- Riser-Roberts, E., 1998. Remediation of petroleum contaminated soils: biological, physical, and chemical processes. Lewis Publishers, Boca Raton.
- Robson, J. N., Rowland, S. J., 1988. Biodegradation of highly branched isoprenoid hydrocarbons - a possible explanation of sedimentary abundance. *Organic Geochemistry*. 13(4-6), 691-695.

Roy, S., Hens, D., Biswas, D., Kumar, R., 2002. Survey of petroleum-degrading bacteria in coastal waters of Sunderban Biosphere Reserve. *World Journal of Microbiology and Biotechnology*. 18(6), 575-581.

Scow, K. M., Simkins, S., Alexander, M., 1986. Kinetics of mineralisation of organic compounds at low concentrations in soils. *Applied and Environmental Microbiology*. 51(5), 1028-1035.

Seligman, B. J., 2000. Long-term variability of pipeline-permafrost interactions in north-west Siberia. *Permafrost and Periglacial Processes*. 11(1), 5-22.

Shepherd, D., 1999. Meteorology data from Casey Station (current) (300017), Antarctica 1989 ongoing, surface measurements. Australian Antarctic Division - SnowWhite Metadata (<http://www-aadc.aad.gov.au/metadata/>)

Skerratt, J. H., Nichols, P. D., Mancuso, C. A., James, S. R., Dobson, S. J., McMeekin, T. A., Burton, H., 1991. The phospholipid ester-linked fatty acid composition of members of the family *Halomonadaceae* and genus *Flavobacterium*: A chemotaxonomic guide. *Systematic and Applied Microbiology*. 14, 8-13.

Smith, M. C., Bowman, J. P., Scott, F. J., Line, M. A., 2000. Sublithic bacteria associated with Antarctic quartz stones. *Antarctic Science*. 12(2), 177-184.

Smith, R. I. L., 1990. Plant community dynamics in Wilkes Land, Antarctica. *Proceedings Japanese National Institute of Polar Research*. 3, 229-244.

Smith, R. I. L., 1996. Introduced plants in Antarctica: potential impacts and conservation issues. *Biological Conservation*. 76(2), 135-146.

Snape, I., Riddle, M. J., Pitt, K., 2000. *Proceedings of the 9th SCALOP Symposium*. Tokyo, Japan.

Snape, I., Riddle, M. J., Stark, J. S., Cole, C. M., King, C. K., Duquesne, S., Gore, D. B., 2001. Management and remediation of contaminated sites at Casey Station, Antarctica. *Polar Record*. 37(202), 199-214.

Snape, I., Gore, D. G., Cole, C. M., Riddle, M. J., 2002. Contaminant dispersal and mitigation at Casey Station: An example of how applied geoscience research can reduce environmental risks in Antarctica. *The royal society of New Zealand Bulletin*. 35, 641-648.

Snape, I., Ferguson, S. H., Revill, A. T., 2003. Constraints on rates of natural attenuation and *in situ* bioremediation of petroleum spills in Antarctica. In: Nahir, M., Bigger, K. Cotta, G. (Eds) *Assessment and remediation of contaminated sites in Arctic and cold climates* (ARCSACC) Edmonton, Canada, May 4-6.

- Snape, I., Ferguson, S. H., Harvey, P., Revill, A. T., In Prep. Chemical constraints on natural attenuation of fuel spills at Casey Station, Antarctica. *Chemosphere*.
- Snape, I., Ferguson, S. H., Harvey, P., Revill, A. T., Submitted. Chemical constraints on natural attenuation of fuel spills at Casey Station, Antarctica. *Chemosphere*.
- Sonderkamp, S., Vomberg, A., Schmitz, C., Faßbender, U., Klinner, U., 2001. Interactions between bacterial populations during degradation of lubricant base oil. *FEMS Microbiology Ecology*. 38, 97-104.
- Speight, J. G., 2001. Handbook of petroleum analysis. Wiley-Interscience, New York.
- Stevenson, F. J., Cole, M. A., 1999. Cycles of soil: carbon, nitrogen, phosphorus, sulfur, micronutrients. Wiley, New York.
- Swannell, R. P. J., Mitchell, D., Lethbridge, G., Jones, D., Heath, D., Hagley, M., Jones, M., Petch, S., Milne, R., Croxford, R., Lee, K., 1999. A field demonstration of the efficacy of bioremediation to treat oiled shorelines following the Sea Empress incident. *Environmental Technology*. 20(8), 863-873.
- Trefry, M. G., Franzmann, P. D., 2003. An extended kinetic model accounting for non-ideal microbial substrate mineralisation in environmental samples. *Geomicrobiology Journal*. 20(2), 113-129.
- Tumeo, M. A., Wolk, A. E., 1994. Assessment of the presence of oil-degrading microbes at McMurdo station. *Antarctic Journal of the United States*. 29, 357-377.
- Tumeo, M. A., Cummings, M. A., 1996. Subsurface soil temperature measurements at McMurdo Station, Antarctica. *Antarctic Journal of the United States*. 31(2), 268-272.
- Vincent, W. F., Quesada, A., 1997. Microbial niches in the polar environment and the escape from UV radiation in non-marine habitats. In: Battaglia, B., Valencia, J. Walton, W. H., (Eds.). *Antarctic communities. Species, structure and survival*. University Press, Cambridge, pp. 388-395.
- Walling, C., 1975. Fenton's reagent revisited. *Accounts of Chemical Research*. 8, 125-131.
- Walworth, J. L., Wooldard, C. R., Braddock, J. F., Reynolds, C. M., 1997. Enhancement and inhibition of soil petroleum biodegradation through the use of fertilizer nitrogen: An approach to determining optimum levels. *Journal of Soil Contamination*. 6(5), 465-480.
- Wang, Z., Fingas, M., 1997. Developments in the analysis of petroleum hydrocarbons in oils, petroleum products and oil-spill-related environmental samples by gas chromatography. *Journal of Chromatography A*. 774, 51-78.
- Wang, Z., Fingas, M., Blenkinsopp, S., Sergy, G., Landriault, M., Sigouin, L., Foght, J., Semple, K., Westlake, D. W. S., 1998. Comparison of oil composition changes due to

biodegradation and physical weathering in different oils. *Journal of Chromatography A*. 809(1), 89-107.

Wang, Z., Fingas, M., Page, D. S., 1999. Oil spill identification. *Journal of Chromatography A*. 843, 369-411.

Wang, Z., Fingas, M. F., 2003a. Development of oil hydrocarbon fingerprinting and identification techniques. *Marine Pollution Bulletin*. 47(9-12), 423-452.

Wang, Z. D., Fingas, M., Sergy, G. A., 1995. Chemical characterization of crude oil residues from an Arctic beach by GC/MS and GC/FID. *Environmental Science and Technology*. 29, 2622-2631.

Wang, Z. D., Fingas, M., 2003b. Fate and identification of spilled oils and petroleum products in the environment by GC-MS and GC-FID. *Energy Sources*. 25(6), 491-508.

Watanabe, K., 2002. Linking genetics, physiology and ecology: An interdisciplinary approach for advancing bioremediation. *Journal of Bioscience and Bioengineering*. 94(6), 557-562.

Watanabe, K., Hamamura, N., 2003. Molecular and physiological approaches to understanding the ecology of pollutant degradation. *Current Opinion in Biotechnology*. 14(3), 289-295.

Watkinson, R. J., Morgan, P., 1990. Physiology of aliphatic hydrocarbon-degradation microorganisms. *Biodegradation*. 1, 79-92.

Watson, J. S., Jones, D. M., Swannell, R. P. J., van Duin, A. C. T., 2002. Formation of carboxylic acids during aerobic biodegradation of crude oil and evidence of microbial oxidation of hopanes. *Organic geochemistry*. 33(10), 1153-1169.

Watts, R. J., Dilly, S. E., 1996. Evaluation of iron catalysts for the Fenton-like remediation of diesel contaminated sediments. *Journal of Hazardous Materials*. 51, 209-224.

Watts, R. J., Stanton, P. C., 1999. Mineralization of sorbed and NAPL-phase hexadecane by catalyzed hydrogen peroxide. *Water Research*. 33(6), 1405-1414.

Watts, R. J., Haller, D. R., Jones, A. P., Teel, A. L., 2000. A foundation for the risk-based treatment of gasoline-contaminated soils using modified Fenton's reactions. *Journal of Hazardous Materials*. 76(1), 73-89.

Weast, R. C., 1995. *CRC Handbook of Chemistry and Physics*. CRC Press.

Wellington, E. M. H., Berry, A., Krsek, M., 2003. Resolving functional diversity in relation to microbial community structure in soil: exploiting genomics and stable isotope probing. *Current Opinion in Microbiology*. 6(3), 295-301.

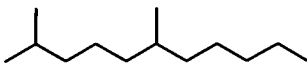
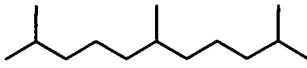
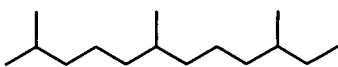
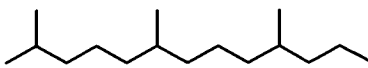
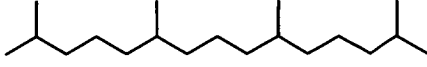
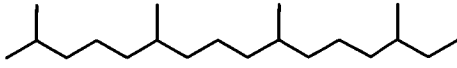
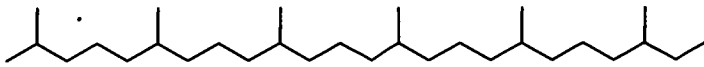
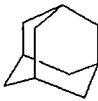
- Wery, N., Gerike, U., Sharman, A., Chaudhuri, J. B., Hough, D. W., Danson, M. J., 2003. Use of a packed-column bioreactor of isolation for divers protease-producing bacteria from Antarctic soil. *Applied and Environmental Microbiology*. 69(3), 1457-1464.
- Westlake, D. W. S., Jobson, A., Phillippe, R., Cook, F. D., 1974. Biodegradability and crude oil composition. *Canadian Journal of Microbiology*. 20, 915-928.
- White, T. L., Coutard, J. P., 1999. Modification of silt microstructure by hydrocarbon contamination in freezing ground. *Polar Record*. 35(192), 41-50.
- White, T. L., Williams, P. J., 1999. The influence of soil microstructure on hydraulic properties of hydrocarbon-contaminated freezing ground. *Polar Record*. 35(192), 25-32.
- Whittaker, M., Pollard, S. J. T., Risdon, G., 1999. The fate of heavy oil wastes in soil microcosms II: a performance assessment of source correlation indices. *The Science of the Total Environment*. 226(1), 23-34.
- Whyte, L. G., Greer, C. W., Inniss, W. E., 1996. Assessment of the biodegradation potential of psychrotrophic microorganisms. *Canadian Journal of Microbiology*. 42, 99-106.
- Whyte, L. G., Hawari, J., Zhou, E., Bourbonnière, L., Inniss, W. E., Greer, C. W., 1998. Biodegradation of variable chain length alkanes at low temperatures by a psychrotrophic *Rhodococcus* sp. *Applied and Environmental Microbiology*. 64(7), 2578-2584.
- Whyte, L. G., Bourbonnière, L., Bellerose, C., Greer, C. W., 1999. Bioremediation assessment of hydrocarbon-contaminated soils from the high Arctic. *Bioremediation Journal*. 3(1), 69-79.
- Whyte, L. G., Goalen, B., Hawari, J., Labbe, D., Greer, C. W., Nahir, M., 2001. Bioremediation treatability assessment of hydrocarbon-contaminated soils from Eureka, Nunavut. *Cold Regions Science and Technology*. 32(2-3), 121-132.
- Wigger, J. W., Torkelson, B. E., 1997. Petroleum hydrocarbon fingerprinting - numerical interpretation developments. In: (Eds) *4th Annual International Petroleum Environmental Conference* San Antonio, Texas, September 23-26.
- Wilkniss, P., Chiang, E., 1990. Fuel spill clean up in the Antarctic. *Antarctic Journal of the United States*. 25(4), 3-10.
- Wodzinski, R. S., Coyle, J. E., 1974. Physical state of phenanthrene for utilization by bacteria. *Applied Microbiology*. 27(6), 1081-1084.
- Woolard, C. R., White, D. M., Walworth, J. L., Hannah, M. E., 1999. Magnitude and variability of biogenic interference in cold regions soils. *Journal of Cold Regions Engineering*. 13(3), 113-120.

- Wrenn, B. A., Venosa, A. D., 1996. Selective enumeration of aromatic and aliphatic hydrocarbon degrading bacteria by a most-probable-number procedure. *Canadian Journal of Microbiology*. 42(3), 252-258.
- Yang, X., Glasser, H., Stoelting, R., Barden, M., Mickelson, G., Delwiche, J., Alvarez, G., 1997. Natural attenuation demonstration in Wisconsin. In: Alleman, B. C. Leeson, A. (Eds) *In situ and on site bioremediation*, Vol. Vol 1 Battelle Press, New Orleans, 28 April- May1.
- Yeh, C. K. J., Kao, Y. A., Cheng, C. P., 2002. Oxidation of chlorophenols in soil at natural pH by catalyzed hydrogen peroxide: the effect of soil organic matter. *Chemosphere*. 46(1), 67-73.
- Yeh, C. K. J., Wu, H. M., Chen, T. C., 2003. Chemical oxidation of chlorinated non-aqueous phase liquids by hydrogen peroxide in natural sand systems. *Journal of Hazardous Materials*. 96(1), 29-51.
- Yin, Y., Allen, H. E., 1991. *In situ* chemical treatment. TE-99-01. Groundwater Remediation Technology Analysis Center, Pittsburgh, pp. 1-82.
- Zappi, M., White, K., Hwang, H. M., Bajpai, R., Qasim, M., 2000. The fate of hydrogen peroxide as an oxygen source for bioremediation activities within saturated aquifer systems. *Journal of the Air and Waste Management Association*. 50(10), 1818-1830.
- Zhou, J., 2003. Microarrays for bacterial detection and microbial community analysis. *Current Opinion in Microbiology*. 6, 288-294.
- ZoBell, C. E., 1973. Bacterial degradation of mineral oils at low temperatures. In: Ahearn, D. G. Meyers, S. P., (Eds.). *The microbial degradation of oil pollutants*. Louisiana State Univeristy, Baton Rouge, pp. 153-161.

Chapter 10

Appendix

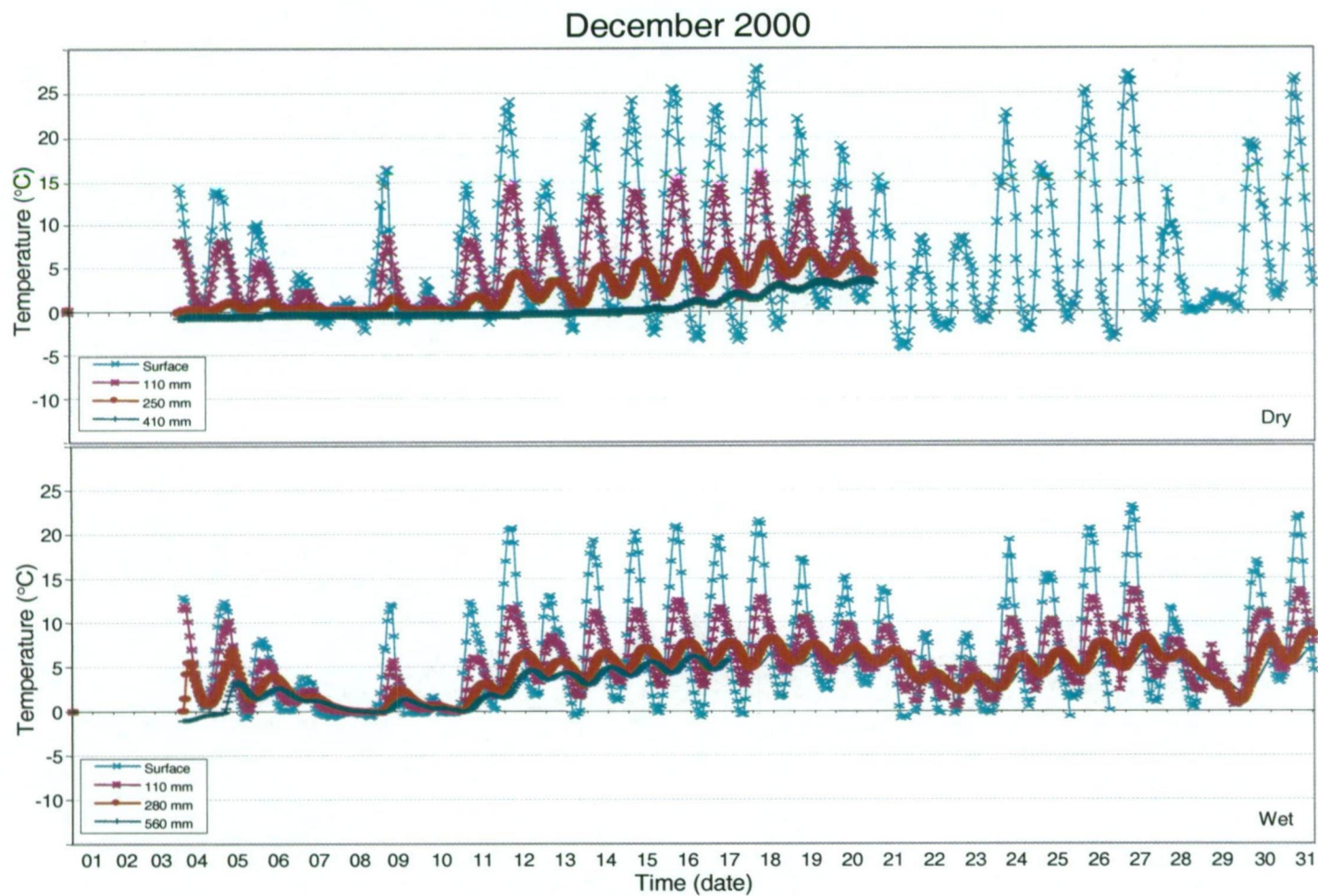
10.1 Structure of several hydrocarbons present in SAB or used as standards

Hydrocarbon	Molecular formula	Structure
<i>i</i> -C ₁₃ (2,6-dimethylundecane)	C ₁₃ H ₂₈	
<i>i</i> -C ₁₄	C ₁₄ H ₃₀	
<i>i</i> -C ₁₅ (Farnesane)	C ₁₅ H ₃₂	
<i>i</i> -C ₁₆	C ₁₆ H ₃₄	
Pristane	C ₁₉ H ₄₀	
Phytane	C ₂₀ H ₄₂	
Squalane	C ₃₀ H ₆₂	
Adamantane	C ₁₀ H ₁₆	

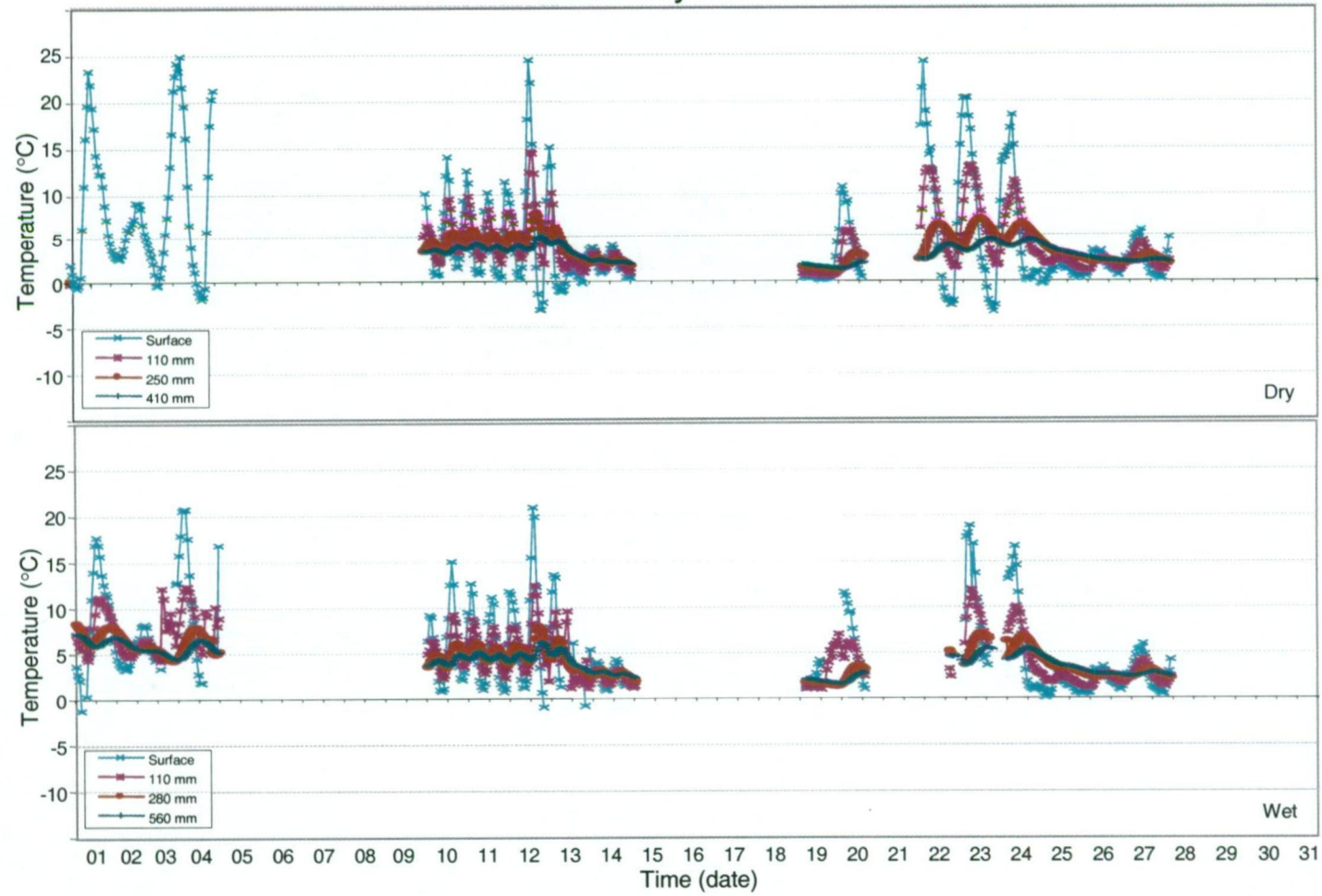
10.2 Chemical composition of SAB – historical data

Refinery Date analysed	Geelong 21-Apr-95	Geelong 4-May-95	Kwinana 1-Aug-97	Kwinana 18-Apr-98	Kwinana 15-Aug-01
Aliphatic Groups	ppm	ppm	ppm	ppm	ppm
C ₆ -C ₁₀	18600	48500	110000	67500	76400
C ₁₁ -C ₁₅	135000	239000	789000	592000	803000
C ₁₆ -C ₂₀	<10	3360	27100	24700	33400
C ₂₁ -C ₃₀	<10	442	-	-	6770
C ₃₁ -C ₄₀	<10	<10	-	-	-
EPA Priority polyaromatic hydrocarbons					
Naphthalene	3520	584	5210	5280	10200
Fluorene	35.1	85.2	97.9	39.7	235
Phenanthrene	45.3	10.5	<10	<10	<10
Anthracene	10.4	<10	<10	<10	<10
Alkylated polyaromatic hydrocarbons					
C1-Naphthalene isomers	16500	4000	18300	18000	29000
C2-Naphthalene isomers	17500	6750	7860	16700	22200
C3-Naphthalene isomers	650	1550	2690	4390	5420
C4-Naphthalene isomers	91.9	776	506	537	755
C5-Naphthalene isomers	<10	<10	<10	<10	<10
C6-Naphthalene isomers	<10	<10	<10	<10	<10
C1-Acenaphthene isomers	<10	<10	<10	11	<10
C2-Acenaphthene isomers	17.7	62.9	<10	11	<10
C1-Acenaphthylene isomers	<10	<10	46.7	11	<10
Biphenyl Compounds					
Biphenyl	1150	233	354	259	1280
C1-Biphenyl isomers	81.9	44.8	332	355	1010
C2-Biphenyl isomers	55	81.5	199	151	649
C3-Biphenyl isomers	<10	59.4	24.1	36	283
C4-Biphenyl isomers	<10	<10	<10	11	-
Mono Aromatics					
Benzene	<10	<10	387	155	<10
Toluene	187	334	820	363	278
Ethylbenzene	<10	<10	725	397	281
Xylene isomers	235	153	5870	4430	2330
C3-Alkylated benzene isomers	3580	654	5750	24200	13000
C4-Alkylated benzene isomers	4640	1470	9260	45300	28800
C5-Alkylated benzene isomers	3790	1350	4830	20700	25900
C6-Alkylated benzene isomers	2240	922	<10	9770	1820
C7-Alkylated benzene isomers	1250	771	<10	2460	459
Styrene	<10	<10	<10	<10	<10
Indan	507	<10	474	468	374
C1-Indan isomers	1370	<10	5150	3460	2990
C2-Indan isomers	<10	<10	<10	7970	347
C3-Indan isomers	<10	<10	<10	6890	<10

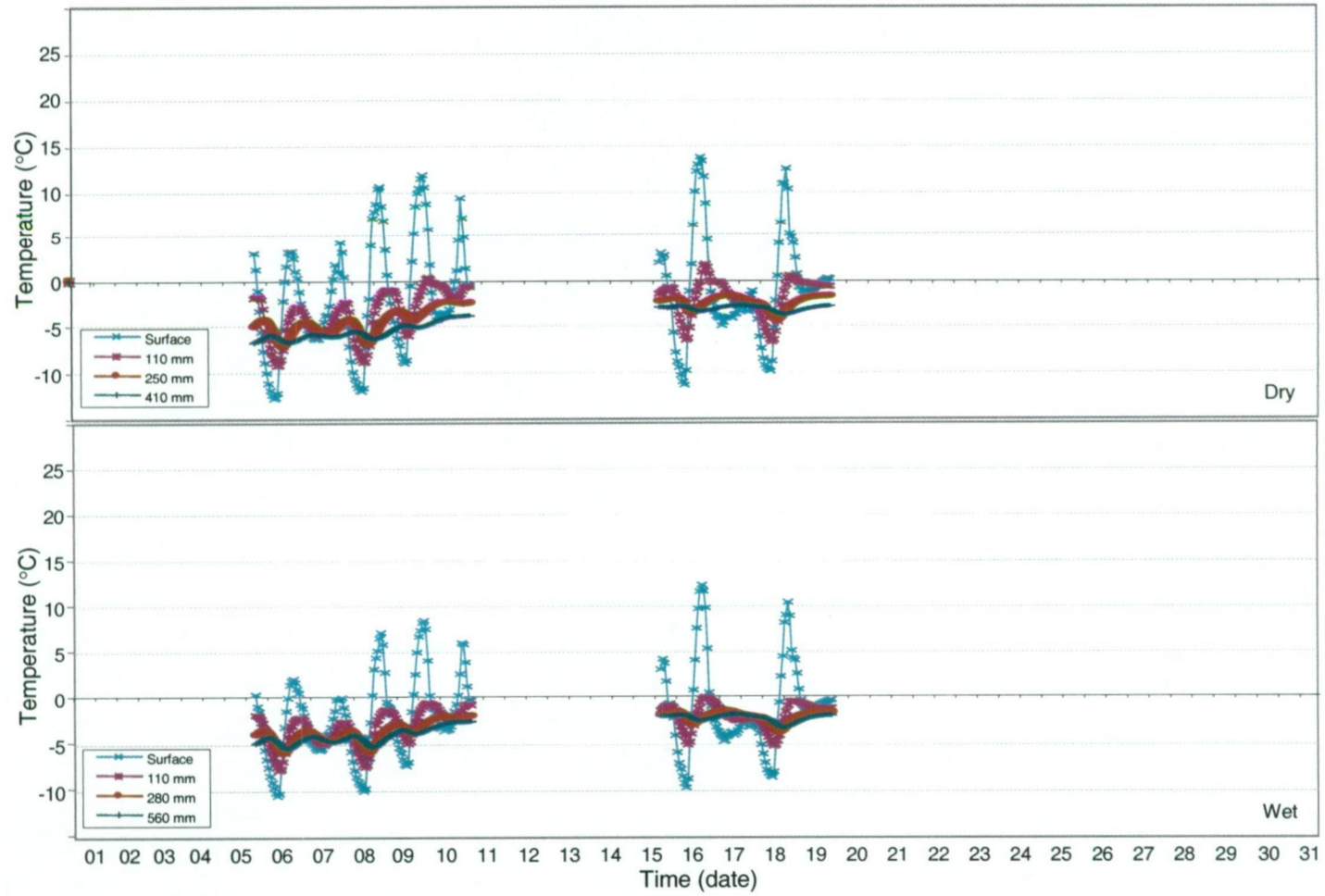
10.3 Soil temperature profiles from Old Casey Station



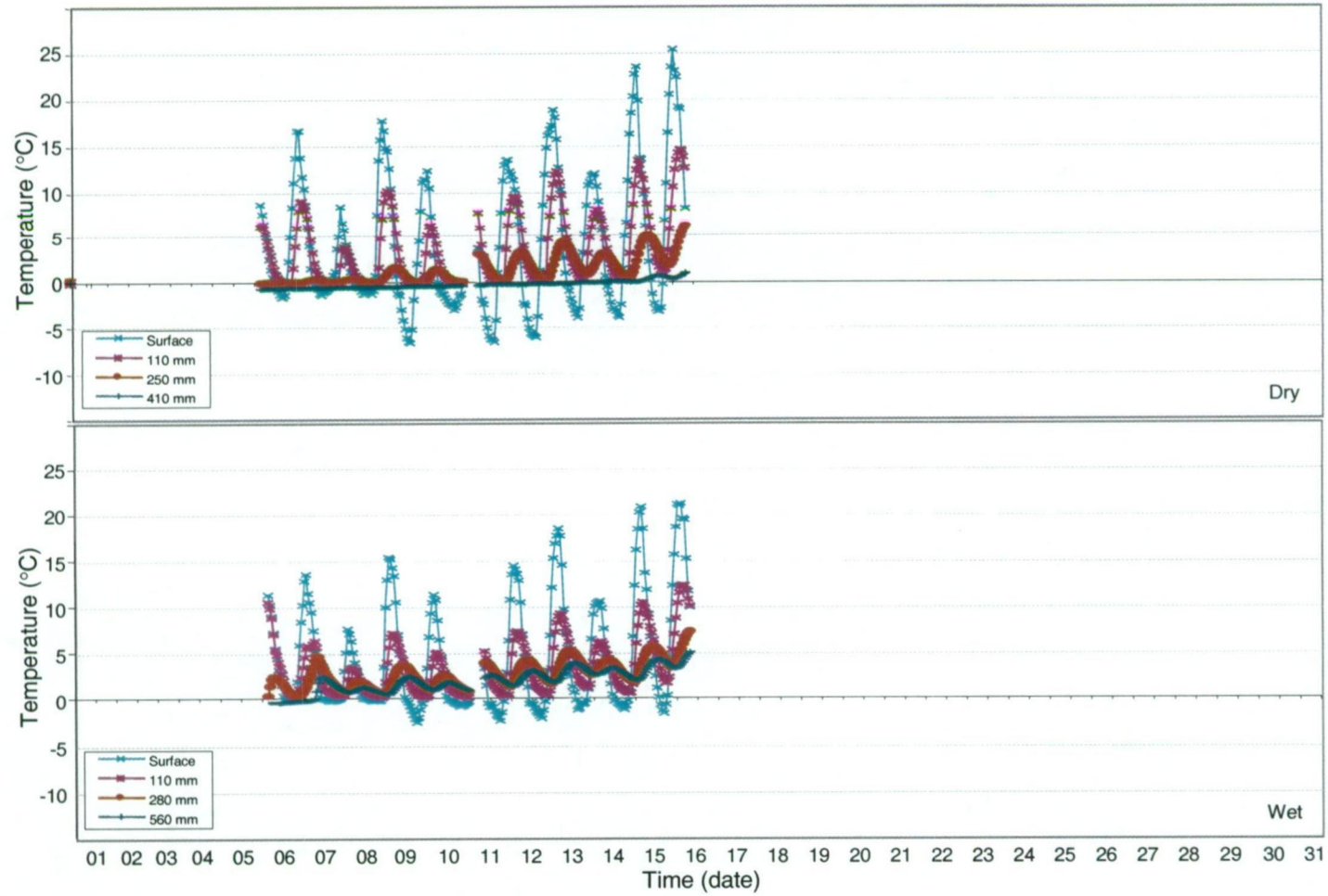
January 2001



November 2001



December 2001



*I could perhaps like other have astonished you
with strange improbable tales;
But I rather chose to relate plain matter of fact
in the simplest manner and style;
Because my principal design was to inform you,
and not amuse you.*

**Jonathon Swift
Gulliver's Travels**

This page intentionally left blank